Fouling Indices for Quantification of Natural Organic Matter Fouling and Cleaning in Ceramic and Polymeric Membrane Systems

by
Mohammad Alresheedi, B.A.Sc., M.A.Sc.

A thesis submitted to the Faculty of Graduate and Postdoctoral Affairs in partial fulfilment of the requirements for the degree of

Doctor of Philosophy
in
Environmental Engineering*

Department of Civil and Environmental Engineering
Carleton University
Ottawa, Ontario
Canada

*The Doctor of Philosophy in Environmental Engineering program is a joint program with the University of Ottawa administered by the Ottawa-Carleton Institute for Environmental Engineering

Abstract

Polymeric membranes have emerged as an economically effective treatment option to produce drinking water. More recently, ceramic membranes are raising interest in this field due to their unique physical properties, which may prove to be important in moving towards more robust and sustainable drinking water treatment methods. However, the loss of membrane permeability as a result of natural organic matter (NOM) fouling remains one of the biggest challenges for sustainable polymeric and ceramic membranes operation. A key challenge in membrane system is to understand how operating pressure and water temperature may impact fouling and subsequent cleaning in relationship to NOM. Further there is limited data to ascertain if ultrafiltration (UF) polymeric and ceramic systems will respond in similar or different manners to NOM fouling which then further impacts how respective systems need to be cleaned.

Fouling indices have been developed by means of simple, short, empirical filtration tests to assess the fouling potential of membrane feed water. The modified ultrafiltration fouling index (MFI-UF) is a standard test that is used to estimate a fouling index value that gives a general indication about the treatability of feed water or the need for pretreatment prior to a membrane unit. Unlike the MFI-UF, the unified membrane fouling index (UMFI) is used to quantify fouling a membrane is subjected to (i.e. reversible vs. irreversible), which provide different data on fouling. However, different approaches in fouling assessment may suggest that direct comparison lack context which lead to some disconnect between predicted and actual fouling in the field. Thus, the applicability of the MFI-UF to be effectively used in complement with the UMFI to predict NOM fouling under changes in

filtration conditions needs to be examined with both ceramic and polymeric membranes systems.

In addition, due to the superior chemical resistance of ceramic membranes, the utilization of high cleaning pH 12 solutions in a single, stepwise, or combined approach with sodium hypochlorite (NaOCl) and sodium hydroxide (NaOH) and ozone (O_3) clean in place (CIP), which are not recommended with polymeric membranes, could highlight an advantage to ceramic membranes in drinking water applications for irreversible NOM fouling control.

The research showed that all NOM types exhibited higher MFI-UF values, and therefore, higher fouling propensity as pressure increased from 1 to 3 bars and water temperature decreased from 35°C to 5°C indicating the effect of pressure and temperature on the MFI-UF fouling prediction. The NOM fouling potential order was consistent at different temperature which was the highest for the NOM mixture and proteins (BSA) followed by alginate and lastly humic acid. The MFI-UF normalization model was useful in estimating the fouling potential away from standard testing conditions (2 bar and 20°C). Therefore, MFI-UF values measured at standard testing conditions can be altered to actual filtration conditions by adjusting for the pressure and viscosity terms in the MFI-UF equation.

While the MFI-UF was impacted by operational conditions, variation in feed water temperature in polymeric and ceramic membrane systems demonstrated negative impacts on NOM fouling and cleaning. NOM fouling increased as water temperature decreased from 20°C to 5°C while fouling decreased as temperature increased from 20°C to 35°C.

The UMFI analysis showed that irreversible NOM fouling ratios increased at cold water condition (5 °C), along with decreased in backwash and chemical cleaning effectiveness of both membrane types. The UMFI results obtained in the polymeric and ceramic UF systems demonstrated useful fit with the MFI-UF prediction for establishing NOM fouling trend and order with temperature. Therefore, utilizing the MFI-UF is useful to monitor changes in NOM fouling behavior with temperature to achieve long-term operational sustainability.

Under an equivalent fouling and cleaning conditions, NOM fouling order of a ceramic UF membrane was found to be similar to their polymeric counterparts in the following order: the NOM mixture > BSA > alginate+Ca^{+2} > alginate-Ca^{+2} > humic acid, suggesting that both membranes are susceptible to fouling by proteins. Ceramic membranes, however, demonstrated better performance in terms of backwashing, thus, lower irreversible fouling highlighting the ease of integration of ceramic membranes into drinking water applications. Chemical cleaning of a ceramic UF membrane using O_3 CIP for 1 hour at a ratio of 0.50 mgO_3/mgC demonstrated higher reduction of irreversible fouling of hydrophobic (humic acid) and hydrophilic (alginate) NOM fractions and lower sensitivity to water quality conditions compared to 4 hours cleaning using single, stepwise, or combined use of NaOCl and NaOH CIP. Since the ceramic membrane is quite robust, it allows for some creativity regarding fouling mitigation techniques, particularly backwashes and chemical cleaning.

Acknowledgements

I wholeheartedly want to express my gratitude to my supervisor Dr. Onita Basu. Her support and understanding, both academically and personally, have made this long journey less arduous and more rewarding. Her support from start to finish, encouragement and exceptional guidance throughout this research project has been a constant source of motivation.

I wish to express my deep and sincere gratitude to Dr. Benoit Barbeau for his guidance and contribution to this research as well as providing me with excellent laboratories for conducting my research. My deepest appreciation goes to Mireille Blais and all the technicians at the CREDEAU laboratories at Polytechnique, Montréal, for their excellent assistance. There are too many names to list but a huge thank you to everyone in the Dr. Barbeau research group both past and present.

I also would like to thank all the faculty and staff in the Department of Civil and Environmental Engineering at Carleton University, especially Dr. Marie Tudoret, for her constant availability to provide help and advice in the laboratory. I am very grateful to all my colleagues in the Dr. Basu research group for their cooperative manner and wonderful support.

I give special thanks to Geoff Seatter and Kerwin Lewis for their help with installation of the automated membrane filtration system. Their patience and countless efforts to explain

the operation of solenoid valves, resistors, arduino board, etc., are much appreciated. Thank you.

I would like to thank summer students, Bia Pereira and Marina Guimarães for their assistance during portions of the experiments.

I would like to express my appreciation for the love and support of my family and friends. Their unconditional understanding and encouragement during this research project have motivated me to keep fighting but without struggling.

I would also like to acknowledge and thank all the members of my thesis defense committee. Thank you for your time and contributions.

This research was funded by the Saudi Arabia Ministry of Education (MOE) and Natural Sciences and Engineering Research Council of Canada (NSERC).

Table of Contents

List of Tables

List of Figures

List of Appendices

List of Acronyms

Alginate - Ca^{+2}	Alginate without calcium
Alginate + Ca^{+2}	Alginate with calcium
ANOVA	Analysis of variance
ASTM	American Society for Testing and Materials
BAC	Biological activated carbon
BDOC	Biodegradable dissolved organic carbon
BSA	Bovine serum albumin
CA	Cellulose acetate
CEB	Chemical enhanced backwash
CIP	Clean in place
CRBD	Completely randomized block design
CWF	Clean water flux
DBPs	Disinfection by-products
DI	Deionized water
DOC	Dissolved organic carbon
EDTA	Ethylenediaminetetraacetic acid
EPA	Environmental Protection Agency
EPS	Extracellular polymer substances
FEEM	Fluorescence excitation and emission matrix
GLM	Generalized linear model
HAA	Haloacetic acids
HCl	Hydrochloric acid
ID	Inside diameter
kDa	Kilodaltons
LMH	Liter per membrane area per hour
LPM	Liter per minute
MBR	Membrane bio reactor
MF	Microfiltration

$MFI_{0.45}$	Modified fouling index
MFI-UF	Modified ultrafiltration fouling index
$MFI\text{-}UF_{exp}$	Experimental modified ultrafiltration fouling index
$MFI\text{-}UF_{nor}$	Normalized modified ultrafiltration fouling index
$MFI\text{-}UF_{pr}$	Predicted modified ultrafiltration fouling index
MGD	Million gallon per day
MW	Molecular weight
MWCOs	Molecular weight cut offs
NaOCl	Sodium hypochlorite
NaOCl/NaOH	NaOCl followed by NaOH
NaOCl+NaOH	Combined NaOCl and NaOH
NaOH	Sodium hydroxide
NaOH/NaOCl	NaOH followed by NaOCl
NF	Nanofiltration
NOM	Natural organic matter
NTU	Nephelometric turbidity unit
O_3	Ozone
OD	Outside diameter
PAN	Polyacrylonitrile
PES	Polyethersulfone
POC	Particulate organic carbon
PS	Polysulfone
PVDF	Polyvinylidene fluoride
R_c	Cake layer resistance
R_{cir}	Chemically irreversible fouling resistance
R_{cr}	Chemically reversible fouling resistance
R_f	Total fouling resistance
R_{hir}	Hydraulically irreversible fouling resistance
R_{hr}	Hydraulically reversible fouling resistance
RIS	Resistance in series

R_m	Intrinsic membrane resistance
RO	Reverse osmosis
SDI	Silt density index
SDS	Sodium dodecyl sulfate
SEM	Scanning electron microscopy
SMPs	Soluble microbial products
SUVA	Specific ultraviolet absorbance
THM	Trihalomethane
TMP	Transmembrane pressure
TOC	Total organic carbon
UF	Ultrafiltration
UMFI	Unified membrane fouling index
$UMFI_{cir}$	Chemically irreversible fouling index
$UMFI_{cr}$	Chemically reversible fouling index
$UMFI_f$	Total unified fouling index
$UMFI_{hir}$	Hydraulically irreversible fouling index
$UMFI_{hr}$	Hydraulically reversible fouling index
UVA_{254}	Ultraviolet absorbance
Vs	Specific filtered water volume

Chapter 1

Introduction and Research Objectives

1.1 Statement of problem

The application of polymeric membranes has gained wide acceptance as an effective technology in drinking water treatment. More recently, ceramic membranes are raising interest in this field due to their unique physical properties, which may prove to be important in moving towards more robust and sustainable drinking water treatment methods. The main advantages of ceramic membranes over polymeric membranes lies in their superior mechanical, thermal, and chemical stability, which make them ideal for industrial applications that deal with challenging water conditions such as in food and beverage production (Vasanth et al., 2013; Zhou et al., 2010). These characteristics can also prove valuable in drinking water treatment applications due to the higher fluxes and backwash pressures that can be applied, and robustness against aggressive chemical cleaning conditions. Unfortunately, a current major limitation preventing their widespread use over polymeric membranes in drinking water treatment is cost. However, the cost of production due to technological advances has started to decrease and their higher capital cost may be compensated by lower operating costs due to higher permeabilities and longer lifetimes (Lee et al., 2014; Freeman and Shorney-Darby, 2011; Lehman and Liu, 2009). As a result, ceramic membranes are becoming cost-competitive for full-scale operations and may potentially become the more economical alternative to polymeric membranes.

Fouling is the major challenge for successful implementation of both polymeric and ceramic membranes in water filtration. Fouling can decrease membrane separation,

increase operating costs, and ultimately decreases the lifetime of the membrane. Previous studies on membrane fouling have provided valuable insights on the major foulants present during the filtration of natural waters. This includes natural organic matter (NOM), inorganic substances, particulate/colloids matter, and microbiological compounds (Guo et al., 2012; Zularisam et al., 2006). Among these foulants, fouling by NOM such as humic acids, proteins and polysaccharide-like substances, is one of the greatest challenges in membrane-based drinking water processes (Hashino et al., 2011; Katsoufidou et al., 2010; Sioutopoulos et al., 2010; Xiao et al., 2009). Currently, the study of NOM fouling and cleaning in water treatment was almost exclusively focused on polymeric membranes, while less research were conducted with ceramic membranes.

First of all, it is necessary to investigate the NOM fouling characteristics of ceramic membranes compared to polymeric membranes under equivalent operational conditions. The results would suggest any similarities and differences in NOM fouling mechanisms between the two membrane types. The identification of the dominant contributing resistances and relative contribution of the resistances would influence the cleaning strategy for different membrane materials. Therefore, research into the impacts of NOM fouling on ceramic membranes is needed to better clarify if and how it fouls differently than the more common polymeric membranes in drinking water treatment. To truly understand NOM fouling it is important to clarify the ease of use of fouling indices, water temperature influences, and cleaning regimes. The sections below briefly outline the needs of research in these various membrane areas.

While NOM is generally understood to be a significant contributor to membrane fouling, the methods for analysis and prediction have also been developing over time. A great deal of effort has been made to understand the nature of the membrane fouling, develop fouling predication and quantification methods, and improve the filtration performance. Fouling prediction focuses on the utilization of fouling index methods, such as the silt density index (SDI), modified fouling index ($MFI_{0.45}$), and modified ultrafiltration fouling index MFI-UF, to assess the fouling potential of feed water and/or pretreatment efficiency prior to membrane systems. These tests are typically performed under specific standard conditions of filtration mode, membrane materials, pressure, and temperature. Fouling quantification focuses on the application of resistance in series (RIS) and unified membrane fouling index (UMFI) methods for identifying the reversible and irreversible fouling nature in an operating system. Fouling mechanisms describe how fouling occurs whether on the membrane surface, within the membrane pores, or a combination of both. Fouling characteristics focus more on identifying the operational conditions and foulant properties that play an important role in fouling during membrane filtration. Polymeric membranes have been almost exclusively dealt with in current fouling research although the same cannot be said for ceramic membranes.

Fouling indices have been developed by means of simple, short, empirical filtration tests to quantify the level or degree of membrane fouling. The $MFI_{0.45}$ method is one of the most commonly used method for assessing the fouling potential of membrane feed water. This standardized method uses a 0.45μm flat sheet microfiltration (MF) membrane and typically performed at constant standard testing conditions of pressure and temperature. Water

temperature changes seasonally and over filtration cycle of membrane systems. Thus, the actual capacity of the MFI testing and the normalization model to predict NOM fouling at non-standard testing conditions need to be clarified. Moreover, although few researchers used a flat sheet ultrafiltration (UF) membrane with the MFI testing with RO systems (Jeong and Vigneswaran, 2015; Rodriguez et al., 2015), the application of the MFI-UF method proposed by Boerlage et al. (2002), utilizing a 13 kDa hollow fiber UF membrane, for NOM fouling prediction has not been researched in the past. Full-scale membrane systems are typically operated under conditions that are not similar to the MFI-UF testing conditions and designed with different polymeric or ceramic membrane materials. Thus, these characteristics can have significant impacts on evaluating the fouling potential of feed water, specifically if NOM is the main source of fouling.

Water temperature is another key design parameter that influence fouling and cleaning of membrane systems. Previous research on the impact of water temperature on fouling has been conducted with high pressure nanofiltration (NF) and reverse osmosis systems (RO) with temperature greater than 20°C and more focused on the solution diffusivity but not on changes in membrane fouling and cleaning with temperature (Zhao and Zou, 2011; Jin et al., 2009). In fact, little to no research exists that investigate water temperature effect on low pressure membranes systems. More specifically, the changes in the hydraulically and chemically irreversible and reversible fouling indices with temperature for low pressure polymeric and ceramic membrane systems need to be examined to better determine potential changes in backwash and chemical cleaning regimes for irreversible fouling control. Additionally, the actual capacity of the MFI-UF to be effectively used with the

UMFI for NOM fouling prediction with polymeric and ceramic membranes under changes in water temperature condition needs more research. Thus, it is necessary to examine how water of different fouling indices affects polymeric and ceramic membranes in terms of fouling and cleaning efficiency. This type of research is important in order to optimize the membrane performance and ultimately reduce the treatment costs.

Chemical cleaning is an integral part of membrane systems operation. The main goal of chemical cleaning is to reduce membrane fouling, particularly irreversible fouling. The characteristics of feed water and compatibility of membrane materials influence the selection of a cleaning agent (Regula et al., 2014). Studies addressing the impacts of different cleaning parameters of sodium hypochlorite (NaOCl) and sodium hydroxide (NaOH) for cleaning polymeric membranes have shown that chemical concentration and cleaning sequence impact the cleaning efficiency and membrane physical structure (Puspitasari et al., 2010; Hilal et al., 2005;). High concentration of chemicals can oxidize membrane polymers and cause swelling of membrane fibers, thus, shortening the membrane lifetime (Puspitasari et al., 2010; Arkhangelsky et al., 2007). Moreover, frequent cleaning can cause changes in membrane functional groups and surface properties (Wang et al., 2018). Thus, polymeric membranes are typically restricted to lower pH and chlorine concentration conditions. Unlike polymeric membranes, ceramic membranes have superior chemical resistance allowing much more aggressive cleaning approaches without risk of damaging membrane integrity (Lee et al., 2014). Therefore, utilization of high pH cleaning in a single or stepwise approach with the NaOCl and NaOH solutions can be beneficial for

controlling irreversible fouling of ceramic membranes for drinking water treatment applications. However, little to no research in this area.

Ozone (O_3) cleaning is another option to cleaning of ceramic membranes that is not available to polymeric membranes. The use of O_3 as a pretreatment or with the backwash step with ceramic membranes for the treatment of natural waters has shown to reduce membrane fouling (Zhang et al., 2013; Kim et al., 2008; Sartor et al., 2008). However, limited to no research exists that investigate O_3 CIP cleaning with respect NOM fouling control compared to conventional cleaning chemicals (i.e., NaOCl and NaOH) with ceramic membranes. A comprehensive chemical cleaning study allows for identifying cleaning methodologies that control irreversible fouling of ceramic membranes, which can ultimately translate into a reduction in ceramic membranes operation costs due to the minimization of chemicals or treatment required.

1.2 Research objectives and scope

The objectives of this research are to assess the fouling response of NOM under various operating conditions and with both polymeric and ceramic membrane systems. To evaluate the capacity of the MFI-UF method in predicting NOM fouling under changes in operating conditions. Further to assess the MFI-UF effectiveness for use in complement with the UMFI with polymeric and ceramic membrane systems under changes in water temperature conditions. Moreover, this research presents side-by-side evaluation of fouling and chemical cleaning of ceramic and polymeric membranes using model NOM solutions. The specific objectives of this research were to:

1) To assess the MFI-UF method in predicting the fouling potential of various NOM fractions commonly found in surface water sources under changes in pressure and water temperature conditions. Further to propose an empirical model that can be used to extend its useful application range for fouling studies.

2) To investigate the effects of feed water temperature on NOM fouling and cleaning of polymeric and ceramic UF membrane systems. Identify the temperature impacts on irreversible and reversible fouling ratios using the UMFI index method. Determine the capacity of the MFI-UF to be effectively used with the UMFI for predicting NOM fouling for the polymeric and ceramic UF under changing temperature conditions.

3) To quantitatively compare NOM fouling and cleaning of a tubular ceramic UF and hollow fiber polymeric UF membranes. To elucidate differences in NOM reversible and irreversible fouling mechanisms with the two membrane types.

4) To evaluate chemical cleaning regimes of a tubular ceramic UF membrane using O_3 CIP and conventional cleaning chemicals (NaOCl or NaOH) in controlling irreversible fouling by hydrophilic and hydrophobic NOM fractions. Assess the application of O_3 CIP cleaning in comparison to a single, stepwise, or combined chemical cleaning approach using NaOCl and/or NaOH.

1.3 Thesis structure

The thesis is divided into five main stages; generally, each stage builds upon the previous. The chapters were written in journal article format; with Chapters 3, 4, 5, 6, and 7 each representing one research article.

Chapter 1: introduces the research statement and specific objectives of the research presented.

Chapter 2: is a background section that covers general information that is relevant to the research.

Chapter 3 (Published): presents the results of the first stage, which investigates the application of the MFI-UF index methods with NOM under variable testing conditions. The capacity of the MFI-UF to predict NOM fouling away from standard testing conditions was examined using regression models.

Chapter 4 (Published): presents the results of the second stage, which evaluates the impact of water temperature on fouling and cleaning behavior of a submerged polymeric UF membrane. Different model NOM solutions were used and the changes in irreversible and reversible fouling ratios with temperature were quantified using the UMFI method. Chemical cleaning of NOM was assessed for more insights into the impact of temperature on membrane resistance and permeability recoveries. The MFI-UF method was used to

predict the fouling potential of different NOM components with temperature and its correlation with the UMFI was examined.

Chapter 5 (Submitted): presents the results of the third stage, which investigates the impact of water temperature on fouling and cleaning behavior of a tubular ceramic UF membrane. A mixture of different NOM solutions was used and the changes in irreversible to reversible fouling ratios with temperature were quantified using the UMFI method and fluorescence excitation and emission matrix (FEEM) analysis. The application of the MFI-UF method for use with ceramic membranes in complement with the UMFI analysis was assessed with the NOM mixture solution.

Chapter 6 (Published): presents the results of the fourth stage, which compares fouling and cleaning behaviors of a ceramic and polymeric UF membranes with different NOM components. Membranes performance was evaluated using the RIS method, for respective differences in reversible and irreversible fouling mechanisms, NOM retention, carbon balance, and FEEM analysis of backwash and chemical wash water.

Chapter 7 (Submitted): presents the results of the final stage, which examines chemical cleaning of a tubular ceramic UF membrane using O_3 in comparison to conventional cleaning chemicals (NaOCl and NaOH). Hydrophobic and hydrophilic NOM solutions were used, and the cleaning efficiency was assessed using the UMFI method and carbon balance of chemical wash water.

Chapter 8: summarizes the research work with a focus on significant conclusions and contributions and potential future work.

1.4 Articles summary and authors contribution

Article 1: Application of MFI-UF Fouling Index with NOM Fouling under Various Operating Conditions

Authors: Mohammad T. Alresheedi[1], Onita D. Basu[1]

Published: Journal of Desalination and Water Treatment

Mohammad T. Alresheedi: First Author, Corresponding Author

Onita D. Basu: Second Author

[1] Department of Civil and Environmental Engineering, Carleton University, 1125 Colonel by Drive, Ottawa, ON, K1S 5B6.

Authors contribution:

Author 1: Mohammad T. Alresheedi

- Designed and performed the experiments
- Collected the data
- Performed data analysis
- Wrote the paper

Author 2: Dr. Onita D. Basu

- Contributed to experimental design and data analysis
- Contributed to the paper writing

Article 2: Investigation into the Temperature Effect on NOM Fouling and Cleaning in Submerged Polymeric Membrane Systems

Authors: Mohammad T. Alresheedi[1], Onita D. Basu[1]

Published: Journal of Desalination and Water Treatment

Mohammad T. Alresheedi: First Author, Corresponding Author

Onita D. Basu: Second Author

[1] Department of Civil and Environmental Engineering, Carleton University, 1125 Colonel by Drive, Ottawa, ON, K1S 5B6.

Authors contribution:

Author 1: Mohammad T. Alresheedi

- Designed and performed the experiments
- Collected the data
- Performed data analysis
- Wrote the paper

Author 2: Dr. Onita D. Basu

- Contributed to experimental design and data analysis
- Contributed to the paper writing

Article 3: Effects of Feed Water Temperature on Irreversible Fouling of Ceramic Ultrafiltration Membranes

Authors: Mohammad T. Alresheedi[1], Onita D. Basu[1]

Submitted to: Journal of Separation and Purification Technology

Mohammad T. Alresheedi: First Author, Corresponding Author

Onita D. Basu: Second Author

[1] Department of Civil and Environmental Engineering, Carleton University, 1125 Colonel by Drive, Ottawa, ON, K1S 5B6.

Authors contribution:

Author 1: Mohammad T. Alresheedi

- Designed and performed the experiments
- Collected the data
- Performed data analysis
- Wrote the paper

Author 2: Dr. Onita D. Basu

- Contributed to experimental design and data analysis
- Contributed to the paper writing

Article 4: Comparisons of NOM Fouling and Cleaning of Ceramic and Polymeric Membranes during Water Treatment

Authors: Mohammad T. Alresheedi[1], Benoit Barbeau[2], Onita D. Basu[1]

Published: Journal of Separation and Purification Technology

Mohammad T. Alresheedi: First Author, Corresponding Author

Benoit Barbeau Second Author

Onita D. Basu: Third Author

[1] Department of Civil and Environmental Engineering, Carleton University, 1125 Colonel by Drive, Ottawa, ON, K1S 5B6.

[2] Department of Civil, Geological and Mining Engineering, Polytechnique, C.P. 6079 Succursale Centre-Ville, Montreal, QC, H3C 3A7.

Authors contribution:

Author 1: Mohammad T. Alresheedi

- Designed and performed the experiments
- Collected the data
- Performed data analysis
- Wrote the paper

Author 2: Dr. Benoit Barbeau

- Contributed to experimental design and data analysis
- Contributed to the paper writing

Author 3: Dr. Onita D. Basu

- Contributed to experimental design and data analysis
- Contributed to the paper writing

Article 5: Chemical Cleaning of Ceramic Ultrafiltration Membranes – Ozone versus Conventional Cleaning Chemicals

Authors: Mohammad T. Alresheedi[1], Onita D. Basu[1], Benoit Barbeau[2]

Submitted to: Journal of Chemosphere

Mohammad T. Alresheedi: First Author, Corresponding Author

Onita D. Basu: Second Author

Benoit Barbeau Third Author

[1] Department of Civil and Environmental Engineering, Carleton University, 1125 Colonel by Drive, Ottawa, ON, K1S 5B6.

[2] Department of Civil, Geological and Mining Engineering, Polytechnique, C.P. 6079 Succursale Centre-Ville, Montreal, QC, H3C 3A7.

Authors contribution:

Author 1: Mohammad T. Alresheedi

- Designed and performed the experiments
- Collected the data
- Performed data analysis
- Wrote the paper

Author 2: Dr. Onita D. Basu

- Contributed to experimental design and data analysis
- Contributed to the paper writing

Author 3: Dr. Benoit Barbeau

- Contributed to experimental design and data analysis
- Contributed to the paper writing

Chapter 2

Literature Review

The main goal of all water treatment technologies is to remove pollutants that can pose health risks. Natural surface water and ground water sources are impacted by different sources of contamination such as seasonal precipitation and surrounding industrial and agricultural activities. Therefore, most water sources can contain dissolved and suspended contaminants that are harmful to human health. The Environmental Protection Agency (EPA) categorized drinking water contaminants into chemical and microbiological. Chemical contaminants include organic and inorganic compounds, heavy metals, disinfection by-products, and micro pollutants, such as pharmaceuticals and personal care products. Microbiological contaminants include coliform bacteria, E. coli, giardia, cryptosporidium, and viruses. The use of polymeric membranes in drinking water treatment has been commonly accepted as an effective technology to remove most of the chemical and microbiological contaminants. More recently, ceramic membranes have gained considerable attention in the drinking water industry due to their robustness and unique mechanical, thermal, and chemical properties. Among all water contaminants, the presence of natural organic matter (NOM) in source water and their removal are critical issues in the operation of water treatment systems specifically membrane processes. The presence of NOM in source water is known to significantly contribute to the poor production efficiency of membranes in terms of separation performance and permeate flux. This chapter presents background information and discussion on NOM characterization, NOM fouling and cleaning, and their removals using membrane processes, with a focus on low pressure polymeric and ceramic microfiltration (MF) and ultrafiltration (UF) membranes for

drinking water treatment applications. The literature discussion is mainly on that material which is not included in other chapters since each chapter already contains a literature review that is relevant to that specific set of objectives and experimental results. Cited references are in the list of references at the end of the thesis.

2.1 Natural Organic Matter (NOM)

2.1.1 Characteristics of NOM in water

NOM is a complex matrix of organic compounds and a key component in aquatic environments. NOM is derived both from the breakdown of terrestrial plants and as the by-product of bacteria and algae. It consists of a range of compounds with a wide variety of chemical compositions, molecular size, molecular weight, and structure. NOM found in natural waters can be categorized into two categories: hydrophobic and hydrophilic components. The hydrophobic part, known as humic substances, represents up to 50% of total organic carbon (TOC) in most water. Hydrophobic NOM is rich in aromatic carbon, phenolic structures, and conjugated double bonds (Zularisam et al., 2006). Hydrophilic NOM contains a higher proportion of aliphatic carbon such as carbohydrates, sugars, and amino acids (Guo et al., 2012; Zularisam et al., 2006). The presence of NOM in water bodies is not known to have any direct effects on human health; however, it has significant impacts on many aspects of water treatment including performance of treatment processes, chemical usage, and the biological stability of the water. NOM can affect water properties such as color, taste, and odor. NOM can react with disinfectants used in water treatment, such as chlorine, and produce undesirable disinfection by-products (DBPs) such as trihalomethane (THM) and haloacetic acids (HAA), which are known to be carcinogenic

to humans (Trang et al., 2012; Shao et al., 2011; Lowe and Hossain, 2008). NOM can also impact the treatment process design such as coagulation and disinfection by increasing coagulant and disinfectant dose requirements (Matilainen et al., 2011). Therefore, NOM removal is essential to meet stricter drinking water treatment regulations and overcome problems with water quality.

Membrane processes are considered reliable option for NOM removal during drinking water treatment. In fact, NOM has been identified as a major foulant during membrane filtration, which causes more fouling than any other water constituents due to its adsorptive capacity on the membrane surface (Shao et al., 2011; Zularisam et al., 2006). The presence of NOM in water is believed to be responsible for the reduction in membrane productivity during operation and shortening the lifetime of the membrane unit. NOM fractions that have been linked to fouling of polymeric MF and UF membranes as humic acids, protein, and polysaccharides substances (Wang X. et al., 2018; Hashino et al., 2011; Katsoufidou et al. 2010; Sioutopoulos et al. 2010). However, it is not clear which fraction of NOM is the dominant foulant. Some studies reported that humic acid is the fraction of dissolved organics that caused severe fouling due to adsorption (Xiao et al, 2012; Shao et al., 2011; Zularisam et al., 2011); whereas other studies found that protein is the dominant organic fraction in membrane fouling (Liu et al., 2011; Henderson et al., 2008). Recent studies have reported that sodium alginate had a significant contribution to fouling than humic acid and protein during surface water treatment (Katsoufidou et al., 2010). It is clear that humic, proteins, and polysaccharides NOM fractions are the main contributor to membrane fouling.

2.1.2 Measurements of NOM in water

Characterization of NOM in terms of quantity and composition are useful for NOM optimal removal. In practice, NOM is usually represented by the measurement of total organic carbon (TOC), adsorption of UV-light (UVA_{254}), and/or specific ultraviolet absorbance (SUVA). TOC is composed of two carbon fractions: dissolved organic carbon (DOC) and particulate organic carbon (POC). DOC is the carbon fraction remaining in a sample after filtering the sample through a 0.45 μm filter whereas POC is the carbon fraction in particulate form that is retained by a 0.45 μm filter. UVA_{254} analysis in drinking water treatment is important to understand the composition of NOM in the source water. It is commonly used to provide insight into the aromatic compound (unsaturated double-bond) such as humic acid that can produce color and contribute to the formation of DBPs during water treatment (Zularisam et al., 2006). Normally, any wavelength from 220 to 280 nm has been considered to be the most appropriate for NOM measurements (Matilainen et al., 2011). The wavelengths are believed to identify different chromophores of NOM. For example, absorbance at 220 nm is associated with both the carboxylic and aromatic chromophores, whereas, absorbance at 254 nm is typical for the aromatic groups, such as humic acids. SUVA can be defined as the ratio of UV to DOC and is reported as (L/mg-cm). It provides insight into the hydrophobicity and biodegradability of NOM in water in which higher SUVA value indicates the presence of NOM with high aromaticity (i.e. humic substances) and lower biodegradability. Previous studies reported that SUVA of NOM from natural water is in the range of 2 to 4 L/mg-m (Zularisam et al., 2006).

Another advanced approach for the characterization of NOM is the measurements of

fluorescence excitation and emission matrix (FEEM). FEEM is a method in which the analyte molecules are excited by irradiation at a certain wavelength and the emitted radiation is measured at wavelengths range from 200 nm to 500 nm (Matilainen et al., 2011; Zepp et al., 2004). The specific excitation and emission wavelengths are the characteristics of a particular molecular conformation, called fluorophore. These fluorophores are helpful in describing the structural compositions of NOM in water (Bieroza et al., 2010; Zhang et al., 2008; Uyguner et al., 2007; Zepp et al., 2004). FEEM has received increased attention in the drinking water treatment, particularly due to its advantages such as rapid and sensitive characterization of NOM, no sample preparation is required, and the potential for online monitoring of NOM treatability (Markechova, et al., 2013; Matilainen et al., 2011).

Various studies have demonstrated the usefulness of FEEM for drinking water treatment. For example, Gone et al. (2009) used fluorescence intensities to evaluate the coagulation-flocculation process efficiency for removing dissolved organic carbon (DOC). Aluminium sulphate (alum) was used as coagulant and DOC residual and fluorescence intensities were acquired. The results illustrated a linear relationship between DOC removal and fluorescence intensities. Decrease in fluorescence peaks for each raw and treated water was correlated well with measured DOC removal ($R^2 \approx 0.90$). The study recommended the use of fluorescence spectroscopy as an analytical technique for DOC removal efficiency in water treatment. Baghoth et al. (2011) also found that coagulation significantly reduced fluorescence intensities of humic-like as well as those of the tyrosine-like components, hence, resulting in a high DOC removal. The change of the fluorescence peaks before and

after coagulation was also used to evaluate the performance of coagulation process at different pH levels (Bieroza et al., 2011; Bieroza et al., 2010). Moreover, FEEM analysis was used to investigate the characteristics of DOC for the formation of DBPs (Hao et al., 2012; Pifer and Fairey, 2012). Results indicated good correlation between the measured fluorescence intensities and the DBPs concentration in water ($R^2 \approx 0.85$). In addition, fluorescence analysis can provide insights into the composition of NOM responsible for fouling during membrane filtration and that cause short and/or long-term impact on membrane performance. Peldszus et al. (2011) used FEEM analysis to identify water constituents responsible for reversible and irreversible fouling of ultrafiltration (UF) membrane and the effect of biofiltration pre-treatment on membrane fouling. Protein-like substances were found to highly correlate with irreversible fouling of the UF membrane. It was suggested that fouling transition from reversible to irreversible fouling was dependent on feed water composition and operating time. Direct biofiltration reduced the protein-like fluorescence peaks indicating the removal of protein from the membrane feed water, thus, reduced the irreversible fouling.

2.2 Membrane Filtration Processes for Drinking Water Treatment

The main goal of membrane filtration is to act as a physical barrier, allowing some constituents to pass through the membrane while blocking the passage of others. In membrane filtration, the water is pushed through a semi-permeable membrane. The water that passes through the membrane is called permeate or filtrate while the water remaining on the feed side is called retentate. The movement of materials across a membrane requires a driving force such as gradients in concentration or pressure across the membrane.

Membrane processes commonly used in drinking water treatment applications use pressure as the driving force. There are four types of pressure driven membrane processes: MF, UF, NF and RO. MF and UF, known as low-pressure membranes, are commonly used to remove suspended particles, a fraction of NOM, and microbes such as viruses, E. coli, giardia, and cryptosporidium. NF and RO, known as high-pressure membranes, are commonly employed to remove NOM, DBPs and dissolved ions such as salt. The distinction between all types of membranes is typically based upon the molecular weight cut off (MWCO) or pore size. MWCO is typically defined as molecular weight of a solute that has a 90% rejection coefficient for a given membrane (Van der Bruggen et al., 2003). The characteristics of pressure driven membranes are summarized in Table 2.1.

Table 2.1- Pressure driven membranes (Adapted from Bruggen et al., 2003)

	MF	**UF**	**NF**	**RO**
Pore size (MWCO)	0.1- 10 μm (> 100,000 Da)	0.01-0.1 μm (1000 – 100,000 Da)	1 – 2 nm (200 – 400 Da)	< 1 nm (50 – 200 Da)
Applied pressure, psi (bar)	1.5 – 30 (0.1 – 2)	1.5 – 75 (0.1 – 5)	45 – 300 (3 – 20)	75 – 1800 (5 – 120)
Rejection	algae, protozoa Particles/turbidity bacteria,	Dissolved organic matter, Particles, viruses	Dissolved organic matter, ions, particles	Dissolved organic matter, ions, particles
Application	Surface water/ Groundwater	Surface water/ Groundwater	Groundwater/ Brackish water	Seawater Desalination

For water treatment applications, membranes are constructed from organic (polymeric) or inorganic (ceramic) materials. Polymeric membranes largely dominate the application of membrane filtration in drinking water treatment. These types of polymeric membrane

materials can be classified into two categories: hydrophilic polymers such as cellulose acetate (CA) and polysulfone (PS), and hydrophobic membranes such as polyethersulfone (PES), polyvinylidene fluoride (PVDF), and polyacrylonitrile (PAN). Polymeric membranes have low cost and can be manufactured in different configurations such as hollow fibers, flat sheet, spiral-wound, and tubular. However, in general they have low resistance against aggressive chemical cleaning conditions (i.e. pH > 11) cleaning agents (i.e. chlorine) and low stability at high temperature and high pressure (Regula et al., 2014). In addition, due to their surface hydrophobicity, polymeric membranes were reported to have higher tendency to foul which limits their use without proper pretreatment or surface modification (Shao et al., 2011; Wei et al., 2006).

Ceramic membranes are composed of inorganic materials and are available as metal oxides such as aluminium oxide or alumina (α-Al_2O_3 and γ- Al_2O_3), zirconium dioxide (ZrO_2), titanium dioxide (TiO_2), and silicon carbide (SiC). These types of membranes have an asymmetric structure, where there is a distinct transition between the dense filtration layer and the support structure, and multi-channel elements. Ceramic membranes are commonly manufactured in flat sheet or tubular configurations. These types of membranes are known for their superior mechanical, chemical, and thermal properties compared to polymeric membranes (Lee and Kim, 2014; Xia et al., 2013). Mechanical stability allows for higher fluxes, higher backwash pressures, and longer life span. The high chemical resistance allows for higher concentrations and longer exposure times to chemicals and the operation at higher pH conditions (i.e., pH > 11). Thermal stability allows for operation at high water temperatures. However, ceramic membranes currently impose higher capital costs

compared to polymeric membranes which has thus far largely limited their use to industrial applications (e.g., food and beverage, oil and gas produced waters) (Vasanth et al., 2013; Zhou et al., 2010). However, due to their inherent operational advantages, the use of ceramic membrane for drinking water treatment is expected to grow over the next years.

2.3 Membrane Fouling: Source, Mechanism, and Assessment

2.3.1 Fouling source

Fouling is a common yet serious problem in drinking water treatment using membrane processes. Membrane fouling can be defined as the accumulation of unwanted feed impurities (e.g. particulates, colloidal matters, organic and inorganic materials, and microorganisms) on the membrane surface or within membrane pores. The adverse effects of fouling include decrease in the efficiency of separation performance (i.e., low rejection), decrease in permeate flux, and increase in transmembrane pressure (TMP). These effects can eventually impact the economics of membrane processes by increasing the frequency of cleaning and energy requirements. Previous studies have demonstrated that membrane fouling is influenced by the membrane properties (i.e. hydrophobicity, surface charge and MWCO), source water composition, and mode of operation (Kenari and Barbeau, 2016; Guo et al., 2012; Sentana et al., 2011; Shao et al., 2011). Among these factors, water composition plays an important role in fouling. Previous studies on fouling have classified membrane foulants into four categories as shown in Table 2.2. These foulants can cause either reversible or irreversible fouling. The loss in membrane performance due to reversible fouling can be restored through appropriate physical cleaning methods (i.e. backwashing and air scour) and chemical cleaning (using chemical agents). On the other

hand, irreversible fouling cannot be removed through physical and chemical cleaning methods and the membrane must go through extensive chemical cleaning or to be replaced.

Table 2.2- Classification of membrane foulants (Adapted from Guo et al., 2012)

Source of Foulant	Example	Fouling Mechanism
Organics	organic compounds (e.g. humic and proteins)	Adsorption, pore blocking
Inorganics	Inorganic compounds (e.g. calcium and silica)	Precipitate onto the membrane surface (scaling)
Colloids	organic or inorganic colloids	Cake formation, pore blocking
Biological Organisms	Algae, bacteria	Biofouling (biofilm formation)

2.3.2 Fouling mechanism

Over the past decades, researchers have identified several filtration models known as blocking law models that describe the relation between flux, TMP, and fouling during membrane filtration. Blocking models describe four main mechanisms of fouling: cake formation, intermediate blocking, standard blocking, and complete blocking (Blankert et al., 2006; Hermia, 1982). Fouling due to cake formation is based on the assumption that particles that are larger than the membrane pore size are retained due to cake formation on the membrane surface. Other particles will tend to deposit on the cake layer which will eventually increase the filtration resistance. In the intermediate blocking model, large and small particles tend to deposit on previously deposited particles or can narrow membrane pores. Standard blocking occurs when particles smaller than membrane pore size deposit on the internal membrane pores. Complete blocking is based on the assumption that particles tend to block the membrane pores by sealing the pores completely (Guo et al., 2012). Figure 2.1 illustrates different membrane fouling mechanisms.

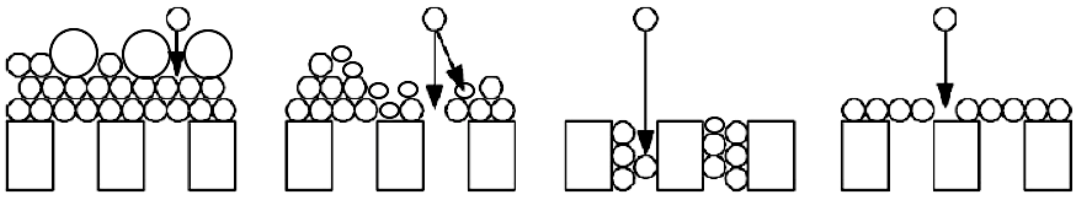

(A) **(B)** **(C)** **(D)**

Figure 2.1 – Illustration of membrane fouling mechanisms (blocking models): **(A)** Cake formation, **(B)** Intermediate blocking, **(C)** Standard blocking, **(D)** Complete blocking. Adapted from Blankert et al. (2006).

2.3.3 Fouling assessment

2.3.3.1 Resistance in series (RIS)

During membrane filtration, foulants in source water can cause either reversible and/or irreversible fouling resistance. The RIS method, Equation 2.1, (Crittenden et al., 2005), is commonly applied to estimate each contributing fouling resistance using operational data such as flux, pressure, and temperature.

$$J = \frac{\Delta P}{\mu R_t} = \frac{\Delta P}{\mu (R_m + R_{hr} + R_{cr} + R_{cir})} \qquad \text{Equation (2.1)}$$

Where J is the filtration flux (m/s); Δp is the applied transmembrane pressure (psi); μ is the water viscosity (kg/m.s); and R_t is total resistance (m^{-1}). R_t is a function of the intrinsic membrane resistance (R_m); hydraulically reversible resistance (R_{hr}) that can be removed by backwash, and hydraulically irreversible resistance (R_{hir}) that resist backwash. R_{hir} can be divided into chemically reversible resistance (R_{cr}) which can be removed by chemical

cleaning, and chemically irreversible resistance (R_{cir}) which cannot be removed by chemical cleaning. The later resistant is undesirable as it causes long term loss in membrane permeability and shorten the lifetime expectancy of the membrane unit. R_{hr} and R_{hir} are calculated by collecting flux and pressure data before and immediately after backwash respectively; whereas R_{cr} and R_{cir} are calculated by collecting flux and pressure data before and after chemical cleaning, respectively.

2.3.3.2 Unified membrane fouling index (UMFI)

The UMFI model, Equation 2.2 (Huang et al., 2008) has been introduced as a method for calculating reversible and irreversible fouling based on the relation between the normalized specific flux and specific permeate volume.

$$\frac{1}{J_S'} = 1 + (\text{UMFI}) \text{x } V_S \qquad \text{Equation (2.2)}$$

Where:

J_S': is the normalized specific flux, Js' = $(J/P)/(J_0/P_0)$, (unitless)

V_S: is the specific permeate volume (m^3/m^2)

UMFI: is an estimate of the extent of fouling (m^{-1}).

During membrane filtration, the UMFI is divided into different fouling indices as shown in Equation 2.3.

$$\text{UMFI}_f = \text{UMFI}_{hr} + \text{UMFI}_{hir} = \text{UMFI}_{hr} + \text{UMFI}_{cr} + \text{UMFI}_{cir} \qquad \text{Equation (2.3)}$$

Where:

UMFI_f: is the total fouling resistance index (m^{-1})

$UMFI_{hr}$: is hydraulically reversible fouling resistance index (removable by backwash, m^{-1})

$UMFI_{hir}$: is hydraulically irreversible fouling resistance index (remained after backwash, m^{-1}). $UMFI_{hir}$ can be divided into $UMFI_{cr}$ and $UMFI_{cir}$.

$UMFI_{cr}$: is chemically reversible fouling resistance index (removable by chemical cleaning, m^{-1})

$UMFI_{cir}$: is chemically irreversible fouling resistance index (remained after chemical cleaning, m^{-1}).

Each fouling index is calculated as following: $UMFI_f$ represents the slope of the $1/J_S'$ versus V_S data from the start to end of filtration. $UMFI_{hir}$ represents the slope of the $1/J_S'$ versus V_S data after the backwash step. $UMFI_{hr}$ is the difference between $UMFI_f$ and $UMFI_{hir}$. $UMFI_{cir}$ represents the slope of the $1/J_S'$ versus V_S data the chemical cleaning step. $UMFI_{cr}$ is the difference between $UMFI_{hir}$ and $UMFI_{cir}$.

2.3.3.3 Fouling indices

Membrane fouling is an inevitable problem impairing all membrane processes. Over the past several years, researchers have developed fouling prediction methods that can be employed to assess the fouling tendency of membrane feed water. The silt density index (SDI), modified fouling index ($MFI_{0.45}$), and modified ultrafiltration fouling index (MFI-UF) methods have been proposed subsequently (ASTM, 2014; Boerlage et al., 2002; Schippers and Verdouw, 1980). These short filtration tests are used to estimate a fouling index value that give a general indication about the treatability of feed water or the need for pretreatment prior to the membrane unit.

2.3.3.3.1 Silt density index (SDI)

The SDI measurement is performed according to a standard method (ASTM-D4189 – 07/2014). The feed water is pumped into a flat sheet MF membrane with a pore size of 0.45μm in dead-end filtration mode at a constant pressure of 2 bar (30 psi) and constant water temperature of 20 °C. The SDI is a time based test in which the plugging rate of a membrane filter (P) is estimated by measuring the time required to collect the first 500mL of filtrate sample at the beginning of filtration (t_i) and the time needed for collecting a second 500mL of filtrate sample (t_f), usually after 5, 10, or 15 minutes of filtration (T). The SDI value can be calculated using Equation 2.4 (ASTM, 2014). A schematic representation of the SDI setup is shown in Figure 2.2.

$$SDI = \frac{\%P}{T} = \frac{(1-\frac{ti}{tf}) \times 100}{T} \qquad \text{Equation (2.4)}$$

The SDI value represents the expected percentage of flux decline per minute of filtration for a specific membrane system. In general, feed water with the SDI value < 3 %/min would result in lower fouling rates and consider suitable for membrane feed without pretreatment. For feed water having an SDI value > 3 %/min, it is preferable to be pretreated prior to the membrane process in order to control fouling (Koo et al., 2012). The common pretreatment methods include flocculation, PAC adsorption, ozonation, and/or media filtration.

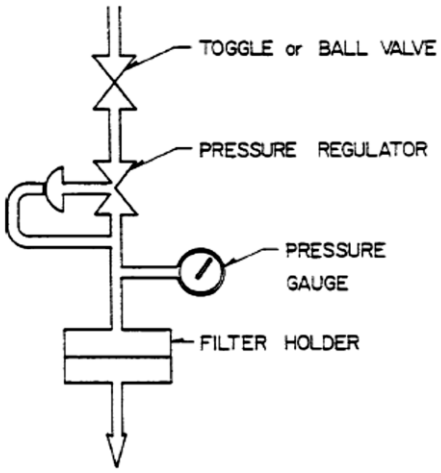

Figure 2.2 - SDI setup (adapted from ASTM-D4189 – 07/2014)

Previous research and field observations have reported major drawbacks of the SDI measurement. Lack of a correlation between the concentration of particles in water and the SDI value estimated. some membrane plants experienced severe fouling when receiving feed water of a low SDI value (i.e. low fouling potential) whereas water with low turbidity had high SDI values (Rachman et al., 2011; Burashid and Hussain, 2004; Ando et al., 2003). Severe colloidal fouling problems were observed in a RO membrane treating feed water with an SDI < 1 %/min (Yiantsios et al., 2005). RO permeate with turbidity around 0.06 NTU have an SDI around 2%/min (Rachman et al., 2011). In addition, the SDI test is based on a comparison between two flow rates at two different times, which are at the beginning and at the end of filtration. Thus, the distinction between different fouling mechanisms, (i.e. pore blocking and cake filtration) is not considered during testing. As a consequence of the lack of a filtration model supporting the calculation of the SDI, the predictability of the fouling rate by the SDI is questionable (Koo et al., 2012). The lack of agreement between SDI operational conditions and membranes may also result in an overestimation or underestimation of the fouling potential of feedwater. The SDI testing

was also found to be influenced by the membrane resistance and pore size (Habib et al., 2013; Alhadidi et al., 2011; Rachman et al., 2011). In addition, while the SDI test is mainly used as an indicator of particulates and colloids fouling, other water quality attributes such as NOM also contribute to fouling, which leads to some of disconnect between predicted SDI values and actual observed fouling in the field. Theoretically, water filtered with MF and UF membranes would achieve better quality of permeate whereby the SDI usually should be < 3 %/min. However, Mosset et al. (2008) study found that NOM fouling had occurred in the membrane system despite the fact that a low value of SDI (i.e., SDI_{15} of 2%/min) was obtained upon pretreatment with UF membrane. From these studies, the reliability of the SDI to predict NOM fouling under changes in testing conditions is questionable.

2.3.3.3.2 Modified fouling index ($MFI_{0.45}$)

The $MFI_{0.45}$ is determined using the same equipment setup for the SDI (refer to Figure 2.2), however is performed differently which results in different data on fouling. The volume of filtered water is recorded at an interval of 30 seconds over a 15 minutes filtration period (ASTM, 2016; Schippers and Verdouw 1980). Equation 2.5 can be used to calculate the $MFI_{0.45}$. Where t is the filtration time (s); V is permeate produced (m^3); ΔP is the pressure (bar); μ is the viscosity of water (kg/m s); A is the membrane area (m^2); R_m is the membrane resistance (m^{-1}); α is the specific cake resistance (m/kg); and C_b is the bulk concentration (kg/m^3). The $MFI_{0.45}$ is defined as the slope of the inverse flow rate (t/V) versus permeate volume (V).

$$\frac{t}{V} = \frac{\mu R_m}{\Delta P A} + \left(\frac{\mu C_b \alpha}{2 \Delta P A^2}\right) V = \frac{\mu R_m}{\Delta P A} + (MFI)\, V \qquad \text{Equation (2.5)}$$

Unlike the SDI, the $MFI_{0.45}$ is based on observations that different fouling mechanisms occur during testing (Boerlage et al 2002; Schippers and Verdouw, 1980). The $MFI_{0.45}$ graph (Figure 2.3) is divided into three regions. The first region represents membrane pore blocking by particles. The second region represents cake formation while the third region represents cake formation with compression. The $MFI_{0.45}$ is the slope of the line in the second region considering that cake formation is the dominant fouling mechanism during filtration. Feed water having an $MFI_{0.45}$ between 0-10 s/L^2 is acceptable for membrane feed (Koo et al., 2012). However, the $MFI_{0.45}$ value was found to be dependent on the membrane filter pore size. Schippers and Verdouw, (1980) found that the $MFI_{0.45}$ value for river water increased with decreasing membrane pore size from 0.8 – 0.05 μm. The increase of $MFI_{0.45}$ was attributed to the presence of smaller colloids in the river water. Therefore, the $MFI_{0.45}$ was found to be unable to account for small colloids. Lower $MFI_{0.45}$ values were obtained for the membrane with 0.45 μm pore size or higher due to its failure to capture the smaller particles (Schippers and Verdouw, 1980). In addition, the measurement method of $MFI_{0.45}$ is relatively more complicated than the SDI test. MFI involves a more complex test analysis, whereby the value of $MFI_{0.45}$ could only be obtained by plotting a graph and estimating the slope of the linear region which represents the $MFI_{0.45}$. That is why SDI testing is usually conducted by operators on site (Koo et al., 2013).

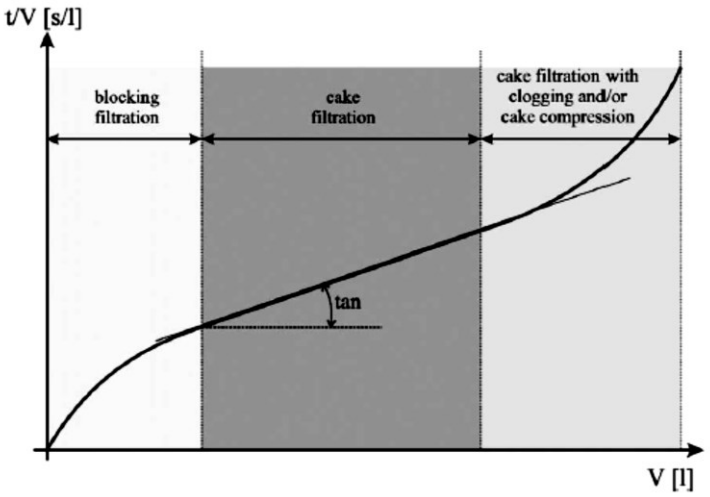

Figure 2.3 - Ratio of filtration time and filtrate volume (t/V) as a function of filtrate volume (V), (adapted from Boerlage et al., 2003)

2.3.3.3.3 Modified ultrafiltration fouling index (MFI-UF)

As previously noted, the SDI and $MFI_{0.45}$ are the most widely applied methods to measure the fouling potential of feedwater. The two methods use specific membranes with pore size of 0.45 µm but are performed differently. However, researchers have observed that smaller particles (i.e. <0.45 µm) contribute to membrane fouling (Boerlage et al., 2002; Schippers and Verdouw,1980). It was hypothesized that these particles limit the ability of SDI and $MFI_{0.45}$ in predicting fouling rate during membrane operation. Boerlage et al. (2002) developed a MFI utilizing a UF membrane (MFI-UF) to incorporate the fouling of smaller particles (i.e. <0.45 µm). The MFI-UF is determined by pumping feed water into a PAN hollow fiber UF membrane with molecular weight cutoff (MWCO) of 13 kDa in dead-end filtration mode at constant pressure of 2 bar and constant water temperature of 20 °C (Boerlage et al., 2003; Boerlage et al., 2002). A typical MFI-UF setup is shown in Figure 2.4.

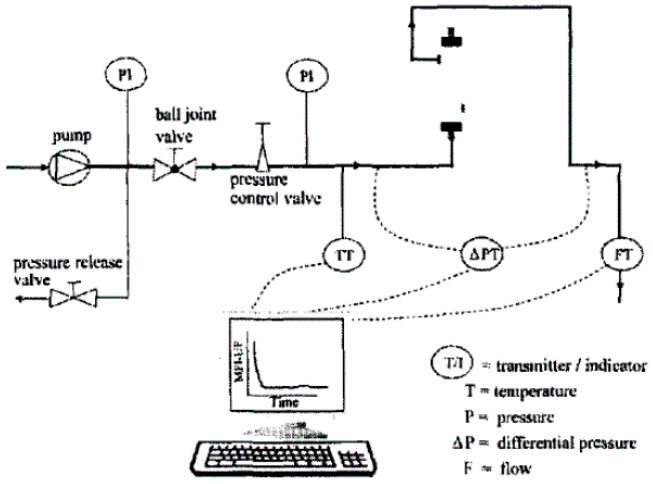

Figure 2.4 - MFI-UF equipment (adapted from Boerlage et al., 2002)

Similar to the $MFI_{0.45}$, the MFI-UF value is determined graphically by plotting the inverse of the flow rate (t/V) versus cumulative filtered water volume (V), (refer to Figure 2.3). The slope of the line in the second region (cake filtration region) is the MFI-UF. Feed water having an MFI-UF < 3000 s/L^2 is equivalent to SDI < 3 %/min, which is acceptable for membrane feed (Boerlage et al., 2003; Boerlage et al., 2002). The effectiveness of the MFI-UF in predicting the fouling potential of RO processes was assessed using different hollow fiber UF membranes with different pore sizes (1 to 100 kDa). The values of the MFI-UF reported were 400-1400 times greater than the corresponding SDI and $MFI_{0.45}$ due to the retention of smaller particles by the UF membrane (Boerlage et al., 2002). A PAN 13 kDa UF membrane was proposed as the most promising reference membrane for the MFI-UF testing (Boerlage et al., 2002; Boerlage et al., 2003).

The utilization of the MFI-UF for assessing the fouling propensity has been carried out in recent studies with high pressure RO systems (Jeong and Vigneswaran, 2015; Ju et al.,

2015; Rodriguez et al., 2015; Villacorte et al., 2015; Taheri et al., 2013; Sim et al., 2011). For example, the MFI-UF was used to assess particulate and biofouling potential for RO membranes (Jeong and Vigneswaran, 2015; Rodriguez et al., 2015). Moreover, MFI-UF was applied to assess fouling potential of algae (Villacorte et al., 2015). Other studies (Ju et al., 2015; Taheri et al., 2013), investigated the influence of inorganic silica and calcium colloids on the MFI-UF fouling index for seawater RO systems. It should be noted that in the above studies, a flat sheet UF membrane was used which was different than the hollow fiber (13 kDa) PAN membrane proposed by Boerlage et al. (2003). Thus, the filtration configuration and rejection mechanism differ. In fact, to date, little to no research exists on the ability of the MFI-UF to predict NOM fouling for low pressure polymeric and ceramic membrane systems under changes of membrane process conditions, which is necessary for expanding the MFI-UF application for NOM fouling prediction.

2.4 Water Contaminants Removal Using Polymeric and Ceramic Membranes

2.4.1 Polymeric membranes applications in drinking water treatment

Polymeric MF and UF membrane processes have gained considerable acceptance in the drinking water industry over the past decades, and have demonstrated excellent capabilities for removal of particles, turbidity, microorganisms such as giardia and cryptosporidium and a certain amount of NOM. In fact, it is well known that various NOM fractions such as humic acids, proteins, and polysaccharides substances are the main contributors to polymeric membranes fouling during water treatment (Tian et al., 2013; Hashino et al., 2011; Katsoufidou et al., 2010; Xiao et al., 2009; Katsoufidou et al., 2007; Yuan and Zydney, 2000). Yuan and Zydney (2000) studied humic acid fouling during MF and found

that humic acid was responsible for the initial stage of fouling. Furthermore, the fouling mechanism was substantially due to deposition and internal pore adsorption. Van de Ven et al., (2008) study found that the irreversible fouling resistance of the alginate increased during filtration and showed an adverse impact on membrane permeability. This can be supported by Sioutopoulos et al. (2010) who investigated alginate and humic acid fouling of a PAN membrane. Alginate resulted in a greater drop in membrane permeability than humic acid. The cake resistance of alginate and humic acid was found to increase with increasing alginate concentration. This was similar to findings by Katsoufidou et al. (2010) who found that the cake resistance of the alginate and humic acid mixture was much closer to the cake resistance of alginate alone. Xiao et al. (2009) study reported that the adsorption of protein to a PVDF membrane was much lower than the adsorption of humic acid. This was not the case in the Hashino et al. (2011) study that reported higher protein fouling with hydrophobic membranes. Tian et al. (2013) study showed that humic acid alone resulted in higher fouling than when humic acid was filtered together with a protein. From these studies, it is clear that different NOM compositions contribute differently to fouling of different polymeric membranes.

Other applications of MF and UF membranes in water treatment include microbial removal by physical sieving which is considered as the major mechanism of removal of giardia and cryptosporidium and other microbes. The pore sizes for MF and UF used in water treatment processes is lower in magnitude than the size of protozoan cysts (4-15 μm), therefore, it has been generally accepted that MF and UF can provide complete removal of all protozoan cysts. Studies have demonstrated that MF and UF membranes provide log removals of

giardia and cryptosporidium ranging from 99 to 99.9999% (2–6 log removal) (Fiksdal and Leiknes, 2006; Betancourt and Rose, 2004). However, biofouling remains as one of the biggest issue using polymeric MF and UF membranes in water treatment applications (Henderson et al., 2008).

2.4.2 Ceramic membranes applications in drinking water treatment

Ceramic membranes, which are made of inorganic materials, are a rapidly emerging technology due to many advantages over polymeric membranes. Ceramic membranes are superior in their mechanical and chemical characteristics, which allows for higher fluxes and backwash pressures as well as aggressive cleaning approaches without risk of damaging membrane integrity (Lee and Kim, 2014; Pendergast and Hoek, 2011). These advantages would potentially increase the operational life expectancy of ceramic membranes and decrease the cleaning and replacement requirements. The downside of ceramic membranes is the high capital costs compared to polymeric membranes which have limited the use of polymeric membranes to industrial applications that deal with challenging and high polluted waters (Vasanth et al., 2013; Zhou et al., 2010). However, due to their inherent operational advantages, the implementation of ceramic membranes for drinking water production is increasing. For example, in the United States (US), 2.5 MGD and 10 MGD plants are being designed in California and Colorado respectively (Freeman and Shorney-Darby, 2011). In Japan, over 50 ceramic membrane systems have been constructed (Freeman and Shorney-Darby, 2011; McAliley and D'Adamo, 2009). In the Middle East, ceramic membranes have been implemented as pretreatment step for NF/RO systems in desalination plants (Dramas and Groue, 2013; Hamad et al., 2013).

Several studies have applied ceramic membranes for water treatment. For example, Konieczny et al. (2006) used coagulation and ceramic MF processes to treat water containing 7 and 10 mg C/L of humic acids. Two 19- channel ceramic membranes with pore sizes of 0.1 and 0.2 μm respectively, composed of a monolithic support layer of TiO_2/Al_2O_3 and an active layer of ZrO_2/TiO_2 were used. The membrane filtration process was operated using a cross flow configuration at constant pressure. The removal of TOC by coagulation alone, ceramic MF alone and a combination of coagulation and MF processes were investigated. Ceramic MF membrane showed a complete removal of TOC (i.e. 100%) compared to coagulation alone. However, a significant flux decline due to organic adsorption and pore blocking was observed when using MF process alone. The use of coagulation prior to the MF process showed significant improvements in fouling reduction and flux. It was suggested that performance by MF alone is not suitable for optimal operation, and when used with pre-coagulation, it can be improved with stable fluxes. This can be supported by studies (Meyn et al., 2012; Meyn et al., 2008; Lehman et al., 2007) that showed a combination of coagulation and ceramic MF processes was effective in improving DOC removal and maintaining a stable membrane operation.

A number of studies (Fan et al., 2014; Guo et al. 2013; Lehman and Liu, 2009; Kim et al., 2008) have used ozonation process prior to ceramic membranes and this is in part due to the fact that ceramic membranes have superior resistance to strong oxidants. Kim et al. (2008) investigated the effects of three ozone dosages (1.5, 5.5 and 9.5 g/m^3), cross-flow velocities (0.11, 0.47, and 0.88 m/s) and TMP (0.68, 1.36, and 2.03 bar) on the performance of tubular ceramic UF membrane composed of α-Al_2O_3 and TiO_2. The ceramic membrane

system was used to treat lake water with average TOC concentration of 11.8 mg/L under a cross flow mode. A significant improvement in permeate fluxes was observed at higher ozone dosage and cross-flow velocity and lower TMP. However, the percent removal trend of TOC across the membrane was observed to decrease with increasing ozone dosage. It was hypothesized that this was due to partial degradation of NOM to form smaller molecules that can easily pass through the membrane. Guo et al. (2013) used a flat sheet ceramic UF membrane with a pore size of 50-60 nm with ozonation and biological activated carbon filtration (BAC) to treat highly polluted river water (TOC ≈ 12-15 mg/L). Ozone dose was between 2.0–2.5 mg/L. Results showed that ceramic UF membrane was able to remove most of turbidity and suspended particulate matters (average effluent turbidity ≈ 0.14 NTU). Ozonation altered the molecular structure of organics which reduced membrane fouling and extended the membrane operation. In addition, the ozonation improved the biodegradability of organic matter, and helped the BAC process to remove up to 90% of the DOC available in the water.

Few papers have investigated the performance of ceramic membranes to treat water without pretreatment. Rubia et al. (2006) used a tubular UF ceramic membrane with a MWCO of 15 kDa to treat a 10 mg/L of synthetic humic acid solution under various pH and ionic strengths. 99% removal of DOC was obtained at pH of 7.9 and low ionic strength whereas at low pH of 2.4 and high ionic strength, the DOC removals decreased to 74%. It was concluded that the pH and the ionic strength conditions affected the filtration of humic acid by changing the properties of both the ceramic membrane surface and humic acid. Xia et al. (2013) used a 0.01 μm tubular UF ceramic membrane to treat two sources of water:

synthetic humic acid solutions (TOC of 2.78 - 9.91 mg/L) and raw lake water (TOC of 3.9 mg/L). Membrane flux decreased with increasing humic acid concentration. It was hypothesized that increasing humic acid concentration would accelerate pore blockage and particle accumulation on the membrane surface, hence, higher fouling. The removal of humic acid from the lake water was below 20% compared to the results with the synthetic humic acid solution (> 50%). This was related to differences in feed composition and molecular sizes (Xia et al., 2013).

Few published studies have compared the performance of ceramic membranes to polymeric membranes for drinking water treatment applications (Kenari et al., 2016; Lee et al. 2014; Hofs et al., 2011). It should be noted that these studies used ceramic and polymeric membranes with different characteristics (i.e., different pore size and surface area), different backwash procedures, and short filtration experiments (< 5 hours). However, the results of these studies are promising. Hofs et al., (2011) compared fouling of four ceramic (TiO_2, ZrO_2, Al_2O_3, and SiC) to a PES polymeric MF membrane. NOM and UV removals were around 30% for the ceramic membranes and between 13-25% for the polymeric membrane. The TiO_2 and SiC membranes showed the lowest TMP increase compared to the Al_2O_3, ZrO_2 and polymeric membrane. Kenari and Barbeau (2016) used ceramic and polymeric UF membranes for iron and manganese removal under changes in water chemistry. Water pH, hardness, and ionic strength had little impact on the overall iron and manganese removal efficiencies but did contribute to fouling. Physical cleaning of iron and manganese deposits was more effective for the ceramic UF membranes compared to the polymeric one. The results of the above studies have shown a great potential for the

utilization of ceramic membranes for drinking water production. However, little available research that focus on NOM fouling of ceramic membranes which is needed to better clarify if and how it fouls differently than the more common polymeric membranes in drinking water treatment.

2.5 Effect of Water Temperature on Membrane Filtration Performance

Water temperature is a key design parameter that influence membrane performance. The majority of previous studies that have examined temperature associated impacts with membranes were done with high pressure membrane systems NF and RO at temperatures greater than 20 °C or wastewater membrane bio reactor (MBR) systems (Ma et al., 2013; Van den Brink et al., 2011; Zhao and Zou, 2011; Jin et al., 2009; Mo et al., 2008). These type of studies tends to focus more on solution viscosity and solute diffusivity challenges with operation but not changes in fouling behavior. For example, Jin et al., (2009) studied the effect of temperature on humic acid fouling with RO membranes. At higher temperatures of 35°C, humic acid rejection was lower due to changes in the membrane structure and in the fraction of dissolved organic. Flux decline was higher at 15°C, but was identical at 25 and 35°C. Their study suggested that higher feed water temperature reduced energy consumption by RO system. Zhao and Zou, (2011) studied the effect of temperature on RO systems and showed that higher temperature would afford higher initial fluxes and higher water recoveries, but also caused more adverse effects on membrane scaling and cleaning. The results of Zhao and Zou (2011) are different than those reported by Jin et al. (2009), however, both studies showed the impact of temperature on RO membranes. Other studies (Ma et al., 2013; Van den Brink et al., 2011) studied the effect of temperature

variation on membrane fouling and microbial community structure in MBRs. Higher membrane fouling rates with low fouling reversibility of proteins and polysaccharides were obtained at lower temperature of 7°C compared to 25°C (Van den Brink et al., 2011). Extracellular polymer substances (EPS) and soluble microbial products (SMPs) increased with decreasing temperature, which increased membrane fouling (Ma et al., 2013).

Studies that deal with temperature effect on low pressure polymeric and ceramic membranes are very limited (Steinhauer et al., 2015). Drinking water systems have in general neglected the interplay of water temperature and fouling on low pressure membrane systems. Although one study with low pressure membrane systems found that current standards for membrane integrity testing overestimated safety design values by not taking into account temperatures below 5 °C (Farahbakhsh and Smith, 2006), highlighting the need for more research in this area. More specifically, the changes in reversible and irreversible fouling ratios with temperature for low pressure polymeric and ceramic membranes need to be identified to help control fouling and maintain membrane productivity.

2.6 Chemical Cleaning of Polymeric and Ceramic Membranes

Chemical cleaning is an integral part of the operation of membrane processes. Chemical cleaning is performed to remove foulants that are not removed by physical cleaning (i.e., backwashing). This type of fouling is referred to it as chemically reversible fouling. Membrane chemical cleaning can be performed directly by immersing the fouled membrane in the chemicals (clean-in-place (CIP)) or by cleaning in conjunction with the

backwash step (a chemical enhanced backwash (CEB)) (Shi et al., 2014). The common chemicals that are used for cleaning membranes are classified into five categories as shown in Table 2.3. The selection of a cleaning agent depends on the fouling source, compatibility of membrane materials and recommendations of membrane manufacture (Regula et al., 2014).

Table 2.3 – Classification of various cleaning chemicals (Adapted from Regula et al., 2014)

Category	Primary Foulant Targeted	Typical Chemicals	Major Function
Caustic	Organic and microbial	NaOH	Hydrolysis, solubilization
Oxidants Disinfectants	Organic and microbial	NaOCl, Ozone	Oxidation, disinfection
Acids	Scales, and inorganic deposits	Citric acid, nitric acid, hydrochloric acid	Solubilization
Chelating agents	Scales, and inorganic deposits	Citric acid, EDTA	Chelation
Surfactants	Biofilms	Surfactants, detergents	Surface Conditioning

Sodium hypochlorite (NaOCl) and sodium hydroxide (NaOH) are the most commonly used chemicals in the maintenance and recovery cleaning of membranes to restore the permeability (Shi et al., 2014). They are used to clean NOM fouling through oxidation, hydrolysis, and solubilization. Oxidation by NaOCl degrades the NOM functional groups to carboxyl and aldehyde groups, which make them more susceptible to removal (Wang X. et al., 2018). On the other hand, NaOH encourages dissolution of carboxylic and phenolic functional groups such as protein and polysaccharides (Porcelli and Judd, 2010). The

following sections provide summaries of chemical cleaning studies of polymeric and ceramic membranes with a focus on NaOCl and NaOH for NOM cleaning.

2.6.1 Polymeric membranes cleaning

Studies addressing the impacts of different cleaning parameters of NaOCl and NaOH for cleaning polymeric membranes have shown that chemicals concentration, cleaning sequence, and cleaning pH are important factors that govern the cleaning efficiency (Wang X. et al., 2018; Puspitasari et al., 2010; Ang et al., 2006; Hilal et al., 2005). Research has shown that there is an optimum concentration, above which cleaning efficiency does not improve and at times may, on the contrary, cause deterioration of membrane materials. Nigam et al. (2008) study on cleaning a UF membrane fouled with whey protein concentrate (3 wt%) found that the membrane flux recovered by 0.2% (by mass) NaOH solution was almost two times higher than that by 0.3% and 0.5% NaOH solutions. Puspitasari et al. (2010) reported that the repeated cleaning of PVDF membranes with 0.5% NaOCl was as effective as a single clean performed with 1%. Wang X. et al. (2018) found that increasing chlorine concentration from 100 to 1000 mg/l of NaOCl resulted in fast diffusion of chlorine within the fouling layer, thus, higher oxidizing capability and cleaning efficiency. However, it is commonly known that high concentration of chemicals and frequent cleaning can oxidize membrane polymers and cause swelling of membrane fibers, thus, shortening the membrane lifetime (Puspitasari et al., 2010; Arkhangelsky et al., 2007). Moreover, frequent cleaning can cause changes in polymeric membrane functional groups, physical structure, and surface properties (Wang Q. et al., 2018; Shi et al., 2014). As a

result, polymeric membranes are typically restricted to chlorine concentration < 500 ppm (Regula et al., 2014; Porcelli and Judd 2010).

Cleaning sequence is known to affect the degree of membrane permeability recovery (Porcelli and Judd, 2010). As a result, the selection of cleaning sequence is determined by the feed water composition and the type of fouling. For example, previous studies on filtration of surface water showed that caustic/acid or oxidant/acid sequence is more effective than the reverse (Liang et al., 2008; Huang et al., 2007; Kimura et al., 2004). Kimura et al., (2004) study showed that the flux recovery of a polymeric membrane fouled by polysaccharides improved with cleaning using NaOH/HCl compared to HCl/NaOH sequence. This could be explained by the effect of the charge on the membrane surface and foulants following the NaOH clean, along with swelling of both the foulant layer and the membrane at higher pH. This allows enhanced cleaning by HCl in the subsequent step (Kimura et al., 2004).

Cleaning pH is another important factor that influence the cleaning efficiency of different chemicals. Ang et al. (2006) study on EDTA and sodium dodecyl sulfate (SDS) cleaning of RO membranes fouled with alginate calcium complexes showed that the cleaning efficiency increased noticeably from 25 to 44% with increasing pH from 4.9 to 11.0 for EDTA, while there was only a slight increase for SDS at higher pH. For EDTA at pH 11.0, the alginate gel layer was broken down relatively more easily compared to lower pH, whereas no improvement in SDS cleaning at higher pH. Wang X. et al., (2018) found that increasing NaOCl pH from 5.0 to 11.0 resulted in fast diffusion of chlorine within the

fouling layer, thus, higher oxidizing capability and cleaning efficiency. However, high cleaning pH ages polymeric membranes faster by changing membrane physical structure and surface properties. (Wang Q. et al., 2018; Regula et al., 2014). Thus, polymeric membranes are typically restricted to pH 11 or lower (Regula et al., 2014).

2.6.2 Ceramic membranes cleaning

Ceramic membranes have many advantages over polymeric membranes as they are mechanically, thermally, and chemically stable (Kim et al., 2008). Most importantly, ceramic membranes have superior chemical resistivity allowing much more aggressive cleaning approaches (i.e. pH > 11 and high chemicals concentration) without risk of damaging membrane integrity (Lee et al., 2013). Moreover, utilization of high pH cleaning (i.e. pH 12 or higher) in a single or stepwise approach with the NaOCl and NaOH solutions can be beneficial for controlling irreversible fouling of ceramic membranes for drinking water treatment applications. This is usually not available for polymeric membranes as they are less resistant to high pH and/or repetitive cleaning (Wang Q. et al., 2018). Few studies exist that investigate chemical cleaning performance of ceramic membranes most of which are related to ceramic membranes application in oil, gas, and food processing industry. For example, Yin et al., (2013) found that combination of NaOCl and NaOH followed by HNO_3 was effective in cleaning ceramic UF membrane applied to desulfurization wastewater. This can be supported by Li et al., (2018) study on cleaning of ceramic UF membrane fouled by limed sugarcane juice which showed that more than 96% of flux recovery was achieved using a mixture of 1.0% NaOH and 0.5% NaOCl, followed by 0.5% HNO_3 solution.

In addition, ceramic membranes are ozone resistant, thus, the oxidation of NOM on the ceramic membrane surface can be expected, because of properties of metal oxides that form the separation layer of the membrane (Sanchez-Polo et al., 2006). The use of ozone with ceramic membranes for the treatment of natural waters has shown to reduce membrane fouling (Zhang et al., 2013; Kim et al., 2008). Ozone can oxidize NOM through a direct molecular ozone attack as well as an indirect one through: free radicals formation resulting from ozone decomposition in the bulk phase, ozone oxidation of NOM, or ozone reaction with the ceramic membrane surface (Regula et al., 2014; Van Geluwe et al., 2011). Karnik et al. (2005) found that membrane flux improved by 65% - 90% when the ceramic membrane was combined with ozonation. Other studies such as Sartor et al. (2008) and Zhang et al. (2013), reported that in situ ozonation transformed organic molecules into smaller ones and more hydrophilic, thus, less fouling. It should be noted that in the above studies, ozone is dosed in a pre-ozonation mode or with backwash step, or continuously injected into the membrane tank. However, limited research exists that investigate alternative ozone CIP cleaning regimes with respect to NOM fouling control for ceramic membranes. Furthermore, the ability to use ozone CIP with ceramic membranes may prove to have superior fouling removal versus traditional cleaning chemicals (e.g., NaOCl and NaOH) that are utilized with polymeric systems. Optimization of membrane cleaning protocols requires in depth understanding of the complex interactions between the foulant and the membrane. A more systematic approach is required to study the various aspects of fouling control. In addition, it is important to consider the economic impact of cleaning procedures, including the costs of the cleaning process itself along with the effect of the procedures on membrane lifetime and efficiency. While the majority of the current

research on chemical cleaning used polymeric membranes, little to no research exists on cleaning of ceramic membranes for drinking water treatment. Research which examines CIP methodologies with different NOM fractions is required to increase operational understanding of cleaning regimes that control irreversible fouling of ceramic membranes.

2.7 Summary of Research Needs

Fouling is the major obstacle for successful implementation of membrane processes for drinking water treatment. As discussed in this chapter, a great deal of effort has been made to understand membrane fouling in terms of mechanism, nature, prediction, and prevention. However, inconsistent results have been reported regarding the primary NOM contributor of membrane fouling and still remains to be determined by further research. The composition of NOM changes with locations, thus, it is of interest to study the impact of various NOM fractions have on membrane fouling.

The application of fouling indices such as the SDI, $MFI_{0.45}$, and MFI-UF as methods to assess NOM fouling is an area that has been frequently questioned in terms of reliability and precision. These methods are performed according to documented testing procedures to estimate an index value that is used as an indicator of the severity of fouling and not considering the typical operation of full-scale membrane systems. The ability of the MFI-UF to predict NOM fouling under changes of membrane process conditions has received little attention, which is necessary for the successful implementation of MFI-UF for NOM fouling prediction.

Fouling models based on the blocking law assume that only one fouling mechanism is controlling, this is probably not realistic. Furthermore, this approach can only be applied to one filtration cycle, while membrane systems operate with multiple filtration and backwash cycles and thus the fouling mechanisms may change from the initial cycles to subsequent cycles. The UMFI method is useful in that it does assume different fouling mechanism and quantify fouling based on foulants response to physical and chemical cleaning operations. However, different approaches in fouling assessment may suggest that direct comparison lack context. The applicability of the UMFI to be effectively used with the MFI-UF in assessing NOM fouling under changes in membrane process conditions, such as water temperature, with both polymeric and ceramic membranes needs to be clarified to help control fouling.

Ceramic membranes are an emerging technology for water treatment. Research with ceramic membranes in a drinking water context is severely limited, however, due to the potential advantages of ceramic membranes with regards to cleaning they are expected to grow in use over the next decade. It is necessary to investigate the NOM fouling characteristics of ceramic membranes to better clarify if and how it fouls differently than the more common polymeric membranes in drinking water treatment. The identification of the dominant contributing resistances would influence the cleaning strategy for different membrane materials. In addition, the robustness of ceramic membranes against rigorous chemical cleaning conditions (i.e. cleaning pH 12, ozone, etc.) may prove to be useful in controlling irreversible fouling of ceramic membranes and may be the key advantage to ease of integration of ceramic membranes into drinking water applications.

Chapter 3

Application of MFI-UF Fouling Index with NOM Fouling under Various Operating Conditions

Mohammad T. Alresheedi* and Onita D. Basu*

*Department of Civil and Environmental Engineering, Carleton University, 1125 Colonel By Drive, Ottawa, ON, K1S 5B6, Canada.

Published: Journal of Desalination and Water Treatment

Abstract

Fouling research with polymeric membranes has demonstrated that various NOM fractions contribute differentially to membrane fouling behavior. However, limited studies exist analyzing the sensitivity of the MFI-UF to be used as a tool to differentiate NOM fouling components. The results here indicate that MFI-UF is a suitable tool for assessing NOM fouling. Specifically, NOM fouling potential was in the order of organic proteins (as BSA), polymers (alginate), and humic acid, respectively. Further, a mixed solution containing BSA, alginate and humic acid fouled similarly to the BSA solution indicating the high fouling potential of organic proteins in membrane systems. The MFI-UF value was found to increase by > 30% with increasing pressure (1-3 bar) and decreasing temperature (35-5 ºC). The filtered water volume was found to correlate with the MFI-UF values indicating the dependency of the method on testing conditions. Incorporating water viscosity and pressure values against normalized conditions (20 ºC and 2 bar) with the standard MFI-UF equation was found to be useful to estimate MFI-UF values at variable operating

conditions, thus, enhances the potential application range of MFI-UF as a fouling index for NOM.

Keywords: MFI-UF; Humic acid; BSA; Sodium alginate; Temperature

3.1 Introduction

Ultrafiltration (UF) is considered a promising process for drinking water production because of its easy automation, compactness, and high removal rate of various water contaminants (Gao et al., 2011). However, one of the main challenges in membrane processes is fouling which decreases membrane efficiency in terms of flux, increases pressure requirements and cleaning frequency, and ultimately decreases the lifetime of the membrane unit (Peiris and Jaklewicz, 2013). Previous studies on membrane fouling have provided valuable insights on the major foulants during the filtration of natural waters. This includes natural organic matter (NOM), inorganic substances, particulate/colloids matter, and microbiological compounds (Guo et al., 2012; Betancourt and Rose, 2004). Among these foulants, membrane fouling by NOM is the major concern in membrane processes to treat surface water (Guo et al., 2012). The major NOM fractions that have been linked to membrane fouling were identified as humic acids, proteins, and polysaccharides like substances (Zularisam et al., 2011; Katsoufidou et al., 2010; Zazouli et al., 2010). Therefore, prevention and control of NOM fouling is essential for successful operation of membrane systems.

Over the past decades, researchers have focused their effort to develop fouling prediction methods such as the silt density index (SDI) and modified fouling index (MFI), to assess

the fouling potential of membrane feed with a goal of reducing the fouling problem. These methods are indirect estimate of fouling potential making use of microfiltration (MF) filters with pores of 0.45μm. The simplicity of these tests has led to their popularity; however, there are growing doubts about the accuracy of these tests for fouling prediction. Membranes manufacturers are frequently questioned that the filtered water does not meet the SDI/MFI values reported by the manufacturer nor the treatment requirement (Nagel et al., 1987). These observations could be attributed to the lack of agreement between fouling indices testing conditions and membrane systems. In fact, it has been proven that particles smaller than 0.45 μm are responsible for fouling of the membrane surface (Boerlage et al., 2002; Schippers and Verdoauw, 1980). Therefore, Boerlage et al (2002) developed the MFI–UF, making use of ultrafiltration (UF) membranes to count for particles <0.45 μm. The MFI–UF has been tested for seawater and used at constant pressure and constant flux (Boerlage et al., 2004; Boerlage et al., 2002). Feed water having an MFI-UF < 3000 s/L^2 is equivalent to SDI < 3 %/min, which is acceptable for membrane feed (Boerlage et al., 2002).

The utilization of the MFI-UF for assessing the fouling propensity has been carried out in recent studies. For example, Rodriguez et al. (2015) and Jeong and Vigneswaran. (2015) used the MFI-UF to assess particulate and biofouling potential for RO systems. Moreover, MFI-UF was applied to assess fouling potential of different species of bloom forming algae in marine and freshwater sources (Villacorte et al., 2015). Other studies (Ju and Hong., 2015; Taheri et al., 2013), investigated the influence of inorganic silica and calcium colloids on the MFI-UF fouling index for seawater RO systems. The MFI-UF showed

promising results with regards to assessing fouling, however, to date, the applicability of the MFI-UF testing to predict NOM fouling for low pressure membranes has received little attention.

The standardized MFI-UF test is performed under a constant pressure of 2 bar and temperature of 20 ºC. However, operating pressures and water temperatures change seasonally and over filtration cycles in membrane systems, thus developing a model away from standard conditions may extend its useful applicability. Moreover, to date, the ability of the MFI-UF to predict NOM fouling under changes of membrane process conditions has received little attention, which is necessary for the successful implementation of MFI-UF for NOM fouling prediction. Therefore, the objectives of this research are to evaluate the MFI-UF method as a tool to predict fouling of various NOM fractions commonly found in surface water sources. Further to assess the MFI-UF method under a range of pressure and temperature conditions in low pressure membrane systems and to propose empirical models that can be used to extend its useful application range for fouling studies.

3.2 Materials and Methods

3.2.1 Experimental setup and approach

The MFI-UF setup consisted of a digital gear pump (Cole Parmer: Drive No. 75211-30, Head No. 07003-04); a ball valve (Cole Parmer No. 01377-18); a pressure relief valve (Aquatrol No. 3ETU4), and a pressure regulator with gauge (Veolia No. LA512). PAN UF, hollow fiber, inside-out membrane module (Pall Corp.) was used and its characteristics are presented in Table 3.1. This UF membrane was proposed by Boerlage et al. (2002). High-

capacity precision top loading balance (Adam Equipment NBL8201e) to measure the permeate volume. A schematic representation of the MFI-UF setup is shown in Figure 3.1.

Table 3.1 - MFI-UF membranes characteristics

Membrane Type	UF - 13 kDa
Membrane Materials	PAN hollow fiber
Configuration	Inside-out
Fiber ID	0.8 mm
Fiber OD	1.4 mm
Number of Fiber	400
Membrane Area	0.2 m^2
Module Length	347 mm
Module Diameter	42 mm

The MFI-UF (constant pressure) was performed according to method described by Boerlage et al. (2002). Feed water was filtered through the UF membrane under dead-end mode, constant pressure while monitoring flux decline during the test. Permeate was collected in a tank set on the electronic balance which has an RS 232 interface with a computer in order to acquire permeate weight and filtration time data from the balance. Data were recorded every 1 minute and imported into MS Excel spread sheet with data terminal software (TeraTerm). The MFI-UF was then calculated using Equation 3.1 (Boerlage et al., 2002).

$$\frac{t}{V} = \frac{\mu R_m}{\Delta P A} + \left(\frac{\mu C_b \alpha}{2 \Delta P A^2}\right) V = \frac{\mu R_m}{\Delta P A} + MFI - UF_{exp}(V) \qquad \text{Equation (3.1)}$$

Which can be rewritten as

$$MFI - UF_{exp} = \frac{d\left(\frac{t}{V}\right)}{dV} \qquad \text{Equation (3.2)}$$

Where t is the filtration time (s); V is permeate produced (m^3); ΔP is the pressure (bar); μ is the viscosity of water (kg/m s); A is the membrane area (m^2); R_m is the membrane resistance (m^{-1}); α is the specific cake resistance (m/kg); and C_b is the particle concentration (kg/m^3). The MFI-$UF_{experimental}$ (MFI-UF_{exp}) represents the slope of the linear portion of the t/V versus V in Equation 2 (Boerlage et al., 2002). The slope of two data points from the t/V and V measurements was calculated over time and used to graph the MFI-UF as a function of filtration time (Boerlage et al., 2003; Boerlage et al., 2002). Boerlage et al. (2002) study showed that the MFI-UF value increases sharply with time during first few hours of filtration due to pore blocking then stabilizes afterwards (i.e. remains unchanged for several hours). The stabilization of the MFI-UF value was believed to be due to the occurrence of cake filtration in which the rate of increase in the filtered water volume remains constant with time. Thus, in this study, the final MFI-UF was determined by averaging the MFI-UF data in the most stable region of the MFI-UF graph (Boerlage et al., 2002). To examine the effect of testing conditions on the MFI-UF measurements, experiments were carried out under various pressure and temperature conditions. The operating pressure was varied between 1, 2, and 3 bar (15, 30, and 45 psi) whereas water temperature was varied between 5, 10, 20, 30, and 35 °C.

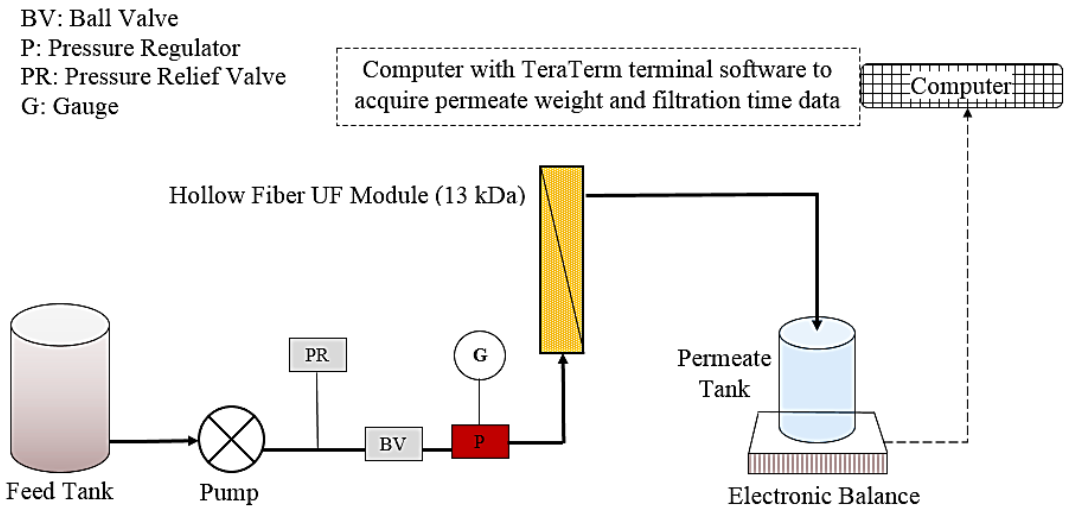

Figure 3.1- A schematic representation of the MFI-UF setup

The UF membrane was cleaned after each MFI-UF experiment. The membrane was first rinsed with DI water for approximately 30 minutes followed by chemical cleaning using sodium hypochlorite (200 ppm), which was recirculated for 60 minutes at ambient temperature followed by citric acid clean (1%). Clean water flux was measured before any experiment and calculated using Equation 3.3 (Crittenden et al., 2005) corrected to temperature of 20 °C and pressure of 2 bar (recommended by the manufacture). This was important to ensure good stability of the UF membrane before any experiment.

$$J_{20\,^{o}C} = J_m\,(1.03)^{T_{20^{o}C} - T_m} \qquad \text{Equation (3.3)}$$

3.2.2 Feed solutions

Four different synthetic feed water solutions used in this study. Humic acids (2.5 mgC/L), a protein (bovine serum albumin, BSA, 2.5 mgC/L), a polysaccharide (sodium alginate, 2.5

mgC/L), and a mixture of the three NOM models (0.83 mgC/L/each NOM model, total of 2.5 mgC/L), were used as model NOM foulants. These NOM models are commonly found in surface water and can significantly contribute to membrane fouling (Hashino et al., 2011; Katsoufidou et al., 2010). All model substances were purchased from Sigma Aldrich. A moderate hardness and alkalinity of 75 mg/L calcium carbonate ($CaCO_3$) and a low level of turbidity (5 NTU) as kaolin clay particles were included in the synthetic water matric to represent the more complex conditions of a surface water source. Previous research on fouling during surface water treatment have reported that calcium will cause the NOM particles to be less negative due to double layer compression and reduction of the electrostatic repulsion forces between particles and membrane surface, thus, increasing NOM fouling rate (Zularisam et al., 2011; Jermann et al., 2008). In addition, the presence of kaolin clay particles during filtration was reported to act as an adsorbent of NOM, thus, increasing NOM adsorption onto the membrane surface and consequently resulting in high flux decline (Jermann et al., 2008). Therefore, in this study, it was necessary to examine NOM-calcium-particles interactions in water during MFI-UF testing. This is of particular importance because the raw water characteristics may vary significantly with respect to the NOM, calcium, and particle concentrations, thus, impacting fouling estimation.

Feed solutions were prepared using DI water and were mixed using a magnetic stirrer one-day prior any experiment to ensure that materials were dissolved completely. Feed water was continuously mixed using a VWR dual speed mixer to ensure homogeneous water conditions throughout the experiment. The feed tank was insulated to maintain constant temperature throughout the testing period. An immersion heater (Cole Parmer) and a

compact chiller (LM series, Polyscience) were used to adjust the water temperature as required. Temperature and pH were monitored continuously using HACH (cat.no. 58258-00) HQd Field Case equipment. The pH of the feed was maintained around 7.5 ± 0.10.

3.2.3 Analysis

3.2.3.1 Molecular weight fractionation of NOM

The molecular weight distribution of the feed solutions, which are comprised of the respective NOM components, kaolin clay, and calcium, was determined by ultrafiltration (UF) fractionation method using a 400 mL UF stirred cell (model 8400, Amicon Inc.) and five hydrophilic regenerated cellulose membranes (Millipore, Bradford MA) with different molecular weight cut offs (MWCOs) of 1,000, 5,000, 10,000, 30,000, and 100,000 Daltons. 2 L of feed water solutions were prepared for the fractionation. The fractionation was performed sequentially by passing 400 mL of sample through the membrane with the highest MWCO to that with the lowest MWCO. Samples from permeate and retentate of particular membrane were collected and total organic carbon (TOC) was analyzed using a Tekmar Dohrmann, Phoenix 8000 TOC analyzer. Excess permeate produced by each fractionation step was used as the feed to the next membrane with a lesser MWCO. The UF fractionation method used in this study is described in detail by (Mosqueda-Jimenez et al., 2003; Kitis et al., 2002). The TOC concentration of a particular molecular weight fraction was calculated by subtracting the TOC concentration of the filtrate from one membrane from the TOC concentration of the filtrate from the membrane of the next larger nominal MWCO. After the fractionation experiments, membranes were rinsed with Milli-Q water for 60 minutes changing the water three times (i.e., every 20 minutes) and stored

in 10% by volume ethanol/water solution and kept in refrigerator at 4 °C for later use. Prior to use, the membranes were rinsed several times after which Milli-Q water was filtered through them for three times.

3.2.3.2 MFI-UF data analysis

One-way ANOVA (using the F-test) on the data collected to determine the significance of the MFI-UF measured at different pressure and temperature conditions. The mean difference between conditions was considered to be significant at a p-value of ≤ 0.05. Post ANOVA test (Tukey HSD test) was then performed to determine pair-wise comparisons between the various testing conditions.

To differentiate between pore blocking and cake filtration mechanisms during the MFI-UF testing, the combined model proposed by Ho and Zydney (2000) was used to analyze the filtration data. Four major fouling mechanisms are described as complete pore blocking (n = 2), standard blocking (n = 1.5), intermediate blocking (n = 1) and cake filtration (n = 0). A generalized equation describing the mechanisms is shown in Equation 3.4.

$$\frac{d^2t}{dV^2} = k\left(\frac{dt}{dV}\right)^n \qquad \text{Equation (3.4)}$$

Which can be rewritten as

$$\log\left(\frac{d^2t}{dV^2}\right) = \log k + n \log\left(\frac{dt}{dV}\right) \qquad \text{Equation (3.5)}$$

In which t is time (s), V is volume (L), k is blocking law filtration coefficient (units vary depending on n), and n is blocking law filtration exponent (unitless).

3.2.3.3 Modelling of the MFI-UF

Operating pressure and water temperature change seasonally and over filtration cycle time periods in membrane systems, thus, it may not be practical to alter an MFI-UF setup for different operating pressures or water temperatures. In this study, the $MFI\text{-}UF_{exp}$ calculated from the slope of the linear portion of the t/V versus V graphs (i.e. Equation 3.2) was normalized to ($MFI\text{-}UF_{nor}$) by including pressure and viscosity correction terms as shown in Equation 3.6. This was important to determine the ability of the MFI-UF to predict fouling conditions away from the standard reference conditions. The normalized model is derived from the modified fouling index (MF) model, ASTM method (2015). In addition, a general linear regression modelling (GLM) (Equation 3.7), was used to estimate the predicted MFI-UF value ($MFI\text{-}UF_{pr}$) at different conditions. The $MFI\text{-}UF_{pr}$ was utilized to establish the influence of the operating pressure and water temperature on the final MFI-UF values. The $MFI\text{-}UF_{exp}$ was then compared to the $MFI\text{-}UF_{nor}$ and $MFI\text{-}UF_{pr}$.

$$MFI\text{-}UF_{nor} = \frac{\mu_{20\ ^{o}C}}{\mu_T} \text{x} \frac{P}{P_0} \text{ x MFI} - UF_{exp} \qquad \text{Equation (3.6)}$$

$$MFI\text{-}UF_{pr} = \beta_0 + \beta_1 \text{ Pressure} + \beta_2 \text{ Temperature} \qquad \text{Equation (3.7)}$$

Where: μ_T and P are the water viscosity, operating pressure respectively. $\mu_{20\ ^{\circ}C}$, P_0, are included to normalize the MFI-UF values to the standard reference conditions of pressure

and temperature (i.e. 2 bar and 20 °C). β_0 β_1, β_2 are the intercept and regression coefficients related to the effect of pressure and temperature respectively.

3.3 Results and Discussion

3.3.1 Molecular weight distribution of feed solutions

The molecular weight distribution analysis of feed solutions (refer to Figure 3.2) indicate that the majority of the particles in the feedwater are greater than 30 kDa, and a higher percentage of particles (> 70%) are expected to be retained by the MFI UF 13 kDa membrane. Feed solutions containing BSA and NOM mixture showed higher percentage of particles in the range of > 30 kDa, thus, they are expected to cause pore blocking and have a higher MFI-UF value than the other organic fractions. The MW distribution of the humic acid and alginate feed solutions is approximately similar which indicates that the differences in fouling would be highly influenced by their chemical and material properties versus size alone. However, all four model solutions are expected to foul the membranes by cake formation, pore blockage, or a combination of both as commonly occurs in a UF membrane process.

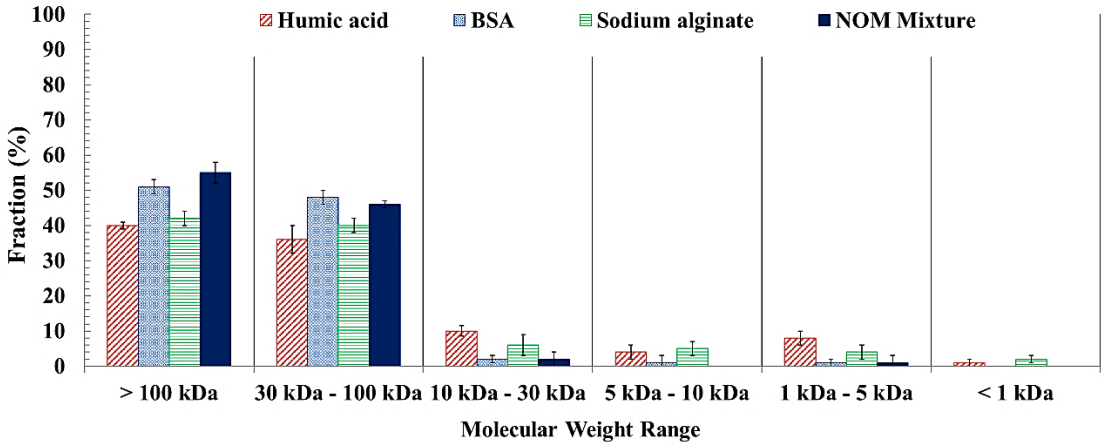

Figure 3.2- Molecular weight distribution of feed water solutions

3.3.2 Effect of variation of operating pressure and water temperature on the MFI-UF measurement to predict NOM fouling

3.3.2.1 MFI-UF measurement under variable operating pressure

In order to determine the MFI-UF values for each testing condition, the slope of two data points from the t/V and V measurements are calculated over time and used to graph the MFI-UF as a function of filtration time (Boerlage et al., 2003; Boerlage et al., 2002). Figure 3.3 is an example of the MFI-UF curves as a function of time under different operating pressures. It can be clearly seen that the MFI-UF graph in Figures 3.3A and 3.3C is divided into two regions: at the beginning of filtration (the first region), the MFI-UF increases sharply during the first 1 to 1.5 hours of filtration. This sharp increase in the MFI-UF value is due to pore blocking as indicated by Boerlage et al. (2002). The blocking law exponent (n) values were determined for each testing condition by plotting the log d^2t/dV^2 vs. log dt/dV (Figures 3.3B and 3.3D as an example) which range from 1.431 to 1.833 and from 1.772 to 2.040 for 1 bar and 3 bars, respectively. The n values are very close to 1.5-2

indicating the occurrence of standard and complete pore blocking mechanism within the first 1-1.5 hours of filtration. After 2.5-3 hours of filtration, the MFI-UF value rate change slows and then stabilizes for the duration of the test. The stabilization of the MFI-UF value is related to the occurrence of cake filtration (the second region) at which the increase in the accumulated filtered water volume remains constant with time (Boerlage et al., 2002). The n values for the cake filtration region (refer to Figures 3.3B and 3.3D as an example) are close to 0 which range from 0.014 to 0.082 and from 0.043 to 0.120 for 1 bar and 3 bars respectively. The final MFI-UF values are determined by taking the average of MFI-UF data in the most stable region in the MFI-UF curve. The MFI-UF was found to stabilize (i.e. minimum to no change) after 3-6 hours of filtration.

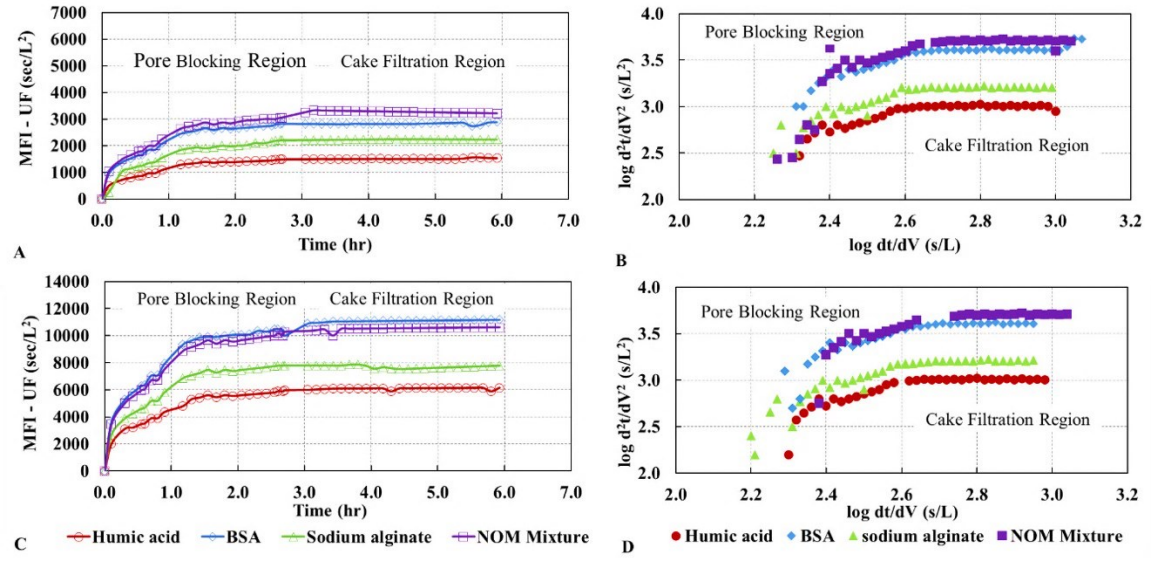

Figure 3.3 – Example of MFI-UF and filtration mechanism graphs for the NOM fractions at different pressure (T= 20 °C)

(A) MFI-UF vs time (P = 1 bar); **(B)** d^2t/dV^2 vs dt/dV curves (P = 1 bar)

(C) MFI-UF vs time (P = 3 bar); **(D)** d^2t/dV^2 vs dt/dV curves (P = 3 bar)

The MFI-UF_{exp} values (Figure 3.4) increased with increasing operating pressure. At higher operating pressure, more particles were forced towards the membrane forming a denser cake layer with lower porosity and higher resistance (Boerlage et al., 2003), hence, higher MFI-UF value. Moreover, the increase in filtration pressure led to an increase in flux which may cause compression of the cake layer and lead to higher MFI-UF value. The results from a one-way ANOVA (Appendix B, Table B1) indicate that the MFI-UF_{exp} values estimated at different pressure conditions were significant ($p < 0.05$). Post ANOVA analysis illustrates that the difference between all three pressure categories were also significant (p-values < 0.05). This indicates that MFI-UF_{exp} testing is dependent on the pressure condition and that the fouling rate of the membrane will change as pressure changes in the system; highlighting the importance of assessing fouling index values at both a reference standard condition to compare between general water system but also at operational conditions to increase the predictive power and analysis of the fouling tests.

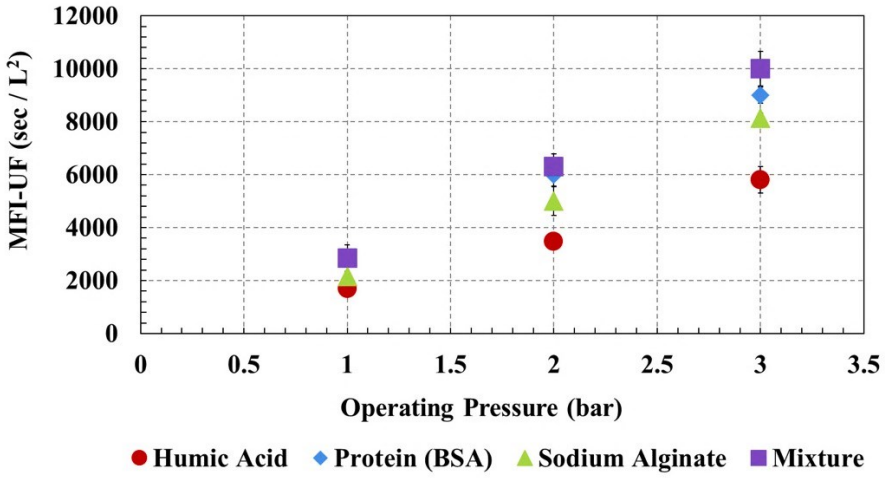

Figure 3.4 – MFI-UF_{exp} measured for various NOM fractions at different operating pressure (T = 20 °C)

Fouling potential of different feed water types predicted by the MFI-UF (constant pressure) was in the order of NOM mixture, BSA (protein), sodium alginate, and humic acid, respectively. The differences between fouling among the four types of NOM could be attributed to the molecular weight distribution (refer to Figure 3.2). Feed water solutions containing BSA and NOM mixture have higher components with molecular weight in the range of 30-100 kDa and > 100 kDa which was much larger than the MWCO of the UF membrane (13 kDa) and may therefore resulted in more pore blocking leading to higher fouling, thus, higher MFI-UF value compared to sodium alginate and humic acid. These results are also analogous to those by Hashino et al. (2011) and Katsoufidou et al. (2010) using polymeric MF and UF membranes for fouling experiments, in which humic acid had lower fouling rate compared to BSA and alginate under constant pressure filtration experiments. The MFI-UF was able to predict this fouling order which highlights the applicability of the MFI-UF for NOM fouling prediction for low pressure membranes. The NOM mixture resulted in the highest MFI-UF value. This is attributed to the complete pore blocking mechanism of the NOM mixture (n ranges between 1.833 and 2.040), refer to Figures 3.3B and 3.3D, thus, higher final MFI-UF value compared to humic acid, BSA, and alginate alone. This can be supported by molecular weight fractionation (refer to Figure 3.2), in which the NOM mixture solution has higher percentage in the size range of > 30 kDa, thus, it is expected to cause complete pore blocking to the 13 kDa UF membrane and higher MFI-UF.

3.3.2.2 MFI-UF measurement under variable water temperature

Figure 3.5 is an example of the MFI-UF curves as a function of time under different temperature conditions. It can be clearly seen that the MFI-UF graph in Figures 3.5A and 3.5C is divided into two regions: at the beginning of filtration (the first region), the MFI-UF increases sharply due to pore blocking. The blocking law exponent (n) values during the first 1-1.5 hours of filtration (refer to Figures 3.5B and 3.5D as an example) range from 1.800 to 2.060 and from 1.332 to 1.665 for 5 and 35ºC respectively. The n values are very close to 2 indicating the occurrence of pore blocking mechanism. After 2.5-3 hours of filtration, the MFI-UF value rate change slows and then stabilizes for the duration of the test indicating the occurrence of cake filtration (the second region) (Boerlage et al., 2002). The n values for the cake filtration region (refer to Figures 3.5B and 3.5D as an example) range from 0.027 to 0.130 and from 0.011 to 0.066 for 5 and 35 ºC, respectively. The final MFI-UF values are determined by taking the average of MFI-UF data in the most stable region in the MFI-UF curve. The MFI-UF was found to stabilize (i.e. minimum to no change) after 3-6 hours of filtration. The MFI-UF graphs at low water temperature (5 ºC) follow similar trend as MFI-UF graphs at high pressure (3 bar) and vice versa.

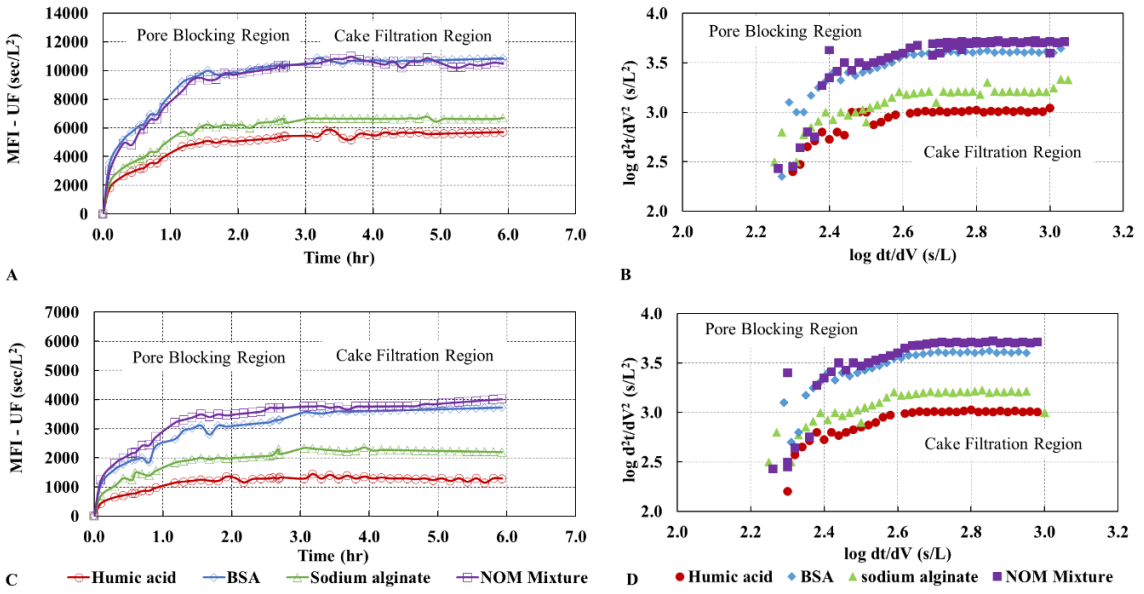

Figure 3.5 - Example of MFI-UF and filtration mechanism graphs for the NOM fractions at different temperature (P = 1 bar)

(A) MFI-UF vs time (T= 5 °C); **(B)** d^2t/dV^2 vs dt/dV curves (T= 5 °C)

(C) MFI-UF vs time (T= 35 °C); **(D)** d^2t/dV^2 vs dt/dV curves (T= 35 °C)

The $MFI\text{-}UF_{exp}$ values (Figure 3.6) decreased with increasing water temperature for all NOM solutions. NOM in cold water temperatures appears to have higher fouling potential compared to that at warmer temperatures. This could be a critical issue in predicting NOM fouling specifically in regions where there is a large seasonal variation in water temperature, as in North America and some parts of Europe. The effect of water temperature on membrane flux was reported to be 3% per 1 °C changes in water temperature (Crittrnden et al., 2005). Under constant pressure, the variation in water temperature affected the flux through the UF membrane and ultimately impacted the final MFI-UF measurements. In addition, the decrease in water temperature may cause shrinkage to the cake layer leading to a formation of denser cake with high specific cake resistance, thus, higher MFI-UF (Kertész et al., 2008). The fouling potential order of NOM

is comparable to that at different pressure conditions. ANOVA analysis (Appendix B, Table B2) shows that the MFI-UF_{exp} values estimated at different temperature conditions were significant ($p < 0.05$). Post ANOVA test illustrates that the difference within groups (e.g. mean of humic acid MFI-UF at 5 vs. 30 ºC, etc.) was also significant (p-values < 0.05), demonstrating that the MFI-UF_{exp} testing is dependent on the temperature condition.

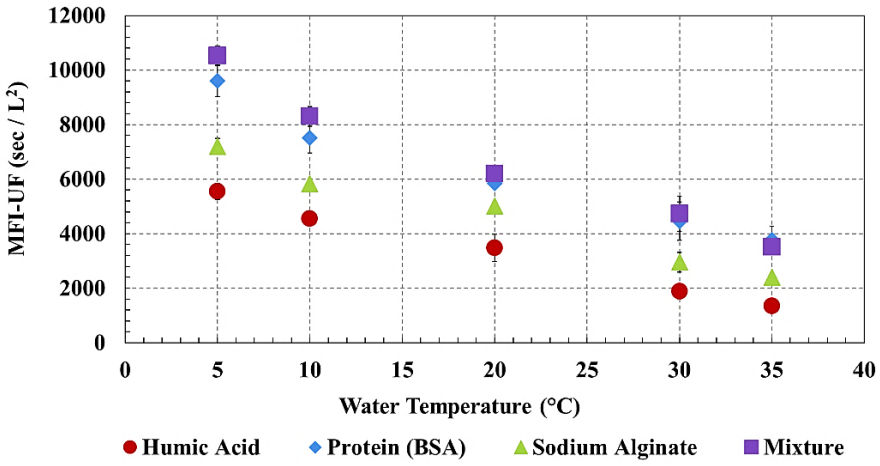

Figure 3.6 – MFI-UF_{exp} measured for various NOM fractions at different water temperature (P = 2 bar)

3.3.2.3 MFI-UF surface plots and TOC rejection

The MFI-UF_{pr}, using GLM (Equation 3.7), was used to establish the influence of the operating pressure and water temperature on the final MFI-UF values. GLM results indicated that both parameters were of significance (Appendix B Table B3). Equations 3.7A-3.7D are the GLM models for different NOM fractions. It should be noted that the β values are the standardized regression coefficients and thus, the relative importance of pressure and temperature can be compared regardless of their units. From Equations 3.7A-

3.7D, it can be clearly seen that for all model NOM, the MFI-UF value increases by 0.652-0.755 units with a unit increase in pressure, holding temperature as a constant. In contrast, the standardized regression coefficient for temperature indicates that for a unit increase in temperature, the MFI-UF decreases by 0.609-0.691 units, holding pressure as a constant. From these models, it is clear that the pressure and temperature both influence the MFI-UF value but in opposing directions.

$$\text{MFI-UF}_{pr} = (\beta_0 + \beta_1 \text{ Pressure} + \beta_2 \text{ Temperature}) \qquad \text{Equation (3.7)}$$

$$\text{MFI-UF}_{pr}\,(\text{Humic}) = (1589 + 0.652\ \text{P} - 0.623\ \text{T}) \qquad \text{Equation (3.7A)}$$

$$\text{MFI-UF}_{pr}\,(\text{Protein}) = (3352 + 0.721\ \text{P} - 0.691\ \text{T}) \qquad \text{Equation (3.7B)}$$

$$\text{MFI-UF}_{pr}\,(\text{Alginate}) = (1189 + 0.755\ \text{P} - 0.609\ \text{T}) \qquad \text{Equation (3.7C)}$$

$$\text{MFI-UF}_{pr}\,(\text{Mixture}) = (2599 + 0.739\ \text{P} - 0.653\text{T}) \qquad \text{Equation (3.7D)}$$

Figure 3.7 presents 3D surface plots of the MFI-UF simulations as a function of pressure and temperature. The plots illustrates that the MFI-UF value increases with increasing pressure and decreasing temperature. According to Darcy's law, membrane resistance is dependent on both the pressure and water viscosity. The increase in the MFI-UF with pressure increase or temperature decrease could be attributed to resistance increase of the fouling layer, thus, higher MFI-UF values. Proteins (BSA) were found to be particularly sensitivity to increases in pressure, as was the NOM mixture, however this is attributed to the protein component in the mixture as a dominant foulant.

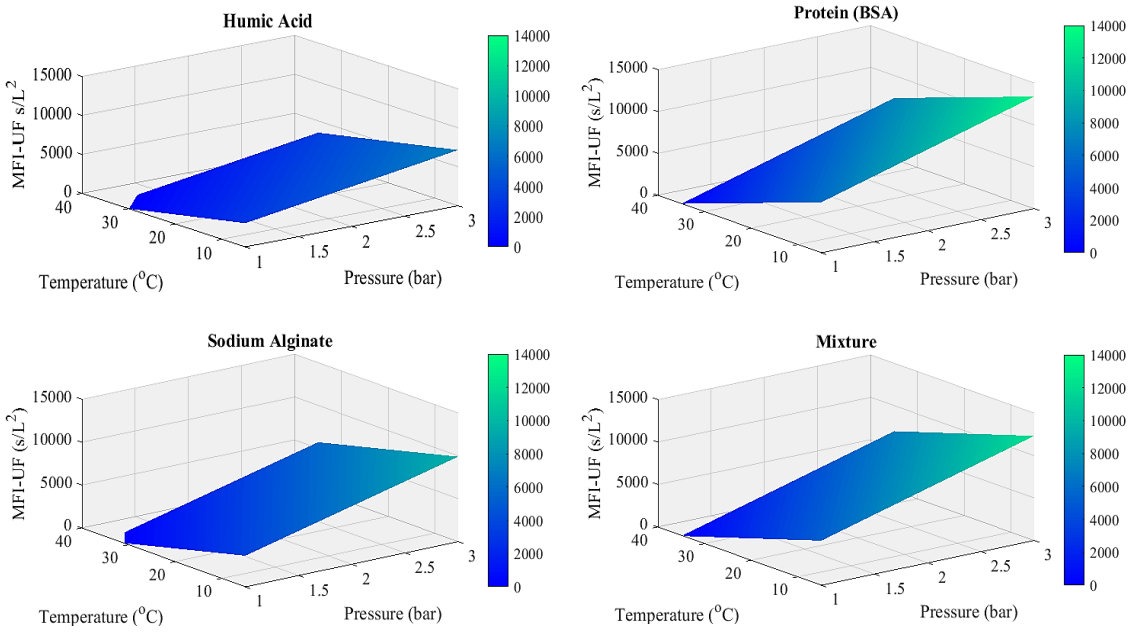

Figure 3.7 – 3D surface plots of the MFI-UF as a function of pressure and temperature

Figure 3.8 illustrates the TOC rejection by the 13kDa UF membrane versus the MFI-UF fouling index. The TOC measurements were utilized to assess the MFI-UF fouling prediction and to determine any direct correlations between the MFI-UF value determined and the TOC rejected by the UF membrane. This is particularly important as there is no research that has used the TOC measurement as a method of assessing the predictability of the MFI-UF testing.

The TOC rejection of different feed solutions was found to decrease with increasing temperature. At lower temperature (5 ºC), > 60% of TOC was rejected by the UF membrane for all model solutions whereas < 45% of TOC was rejected at 35 ºC. Under all temperature conditions, the highest rejection was for BSA and NOM mixture whereas lower rejection for humic acids and alginate. Therefore, the increase in the MFI-UF value at low

temperature was related to the high NOM rejection by the UF membrane whereas at high temperature, NOM were passing through the UF membrane to the filtrate side, thus, lower fouling and MFI-UF value.

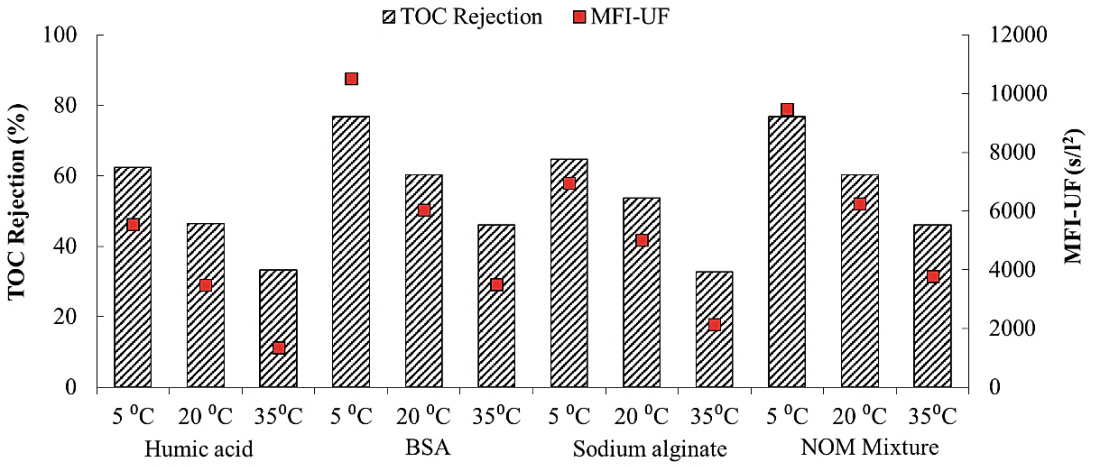

Figure 3.8 – MFI-UF and TOC rejection with water temperature conditions (P = 2 bar)

3.3.3 Modelling of MFI-UF measurements ($MFI\text{-}UF_{exp}$, $MFI\text{-}UF_{nor}$, $MFI\text{-}UF_{pr}$)

Operating pressure and water temperature change seasonally and over filtration cycle time periods in membrane systems, thus the current value of the MFI-UF test performed at the standard conditions of 2 bar and 20 ºC, while useful for comparing across studies, can overestimate or underestimate the fouling potential of NOM in site specific challenges. An empirical based model that can calculate MFI-UF values at non-standard operating conditions is proposed to help extend it's useful applicate range in terms of NOM fouling assessments.

The MFI-UF value is calculated from relationship between the inverse of the flow rate (t/V) and the permeate volume (V). The obserevd changes in the MFI-UF value at different

pressure and temperature conditions could be related to the changes in filtration characteristics (e.g., flow, viscosity, etc.) and/or fouling layer properties. Therefore, the next step was to plot the MFI-UF_{exp} values versus the final filtered water volume and determine if the filtered water volume reflects the fouling conditions observed during testing. Ideally, higher filtered water volume indicates lower MFI-UF value and vice versa. Figure 3.9 presents the filtered water volume as a function of MFI-UF_{exp} for different NOM solutions. Overall, it can be clearly seen that the water volume decreases with increasing MFI-UF_{exp} value (R^2 between 0.68-0.78) which indicates that both pressure and temperature conditions heavily influence results. The changes in the final filtered water volume is an indicator of the changes in filtration characteristics of NOM water at the different conditions examined.

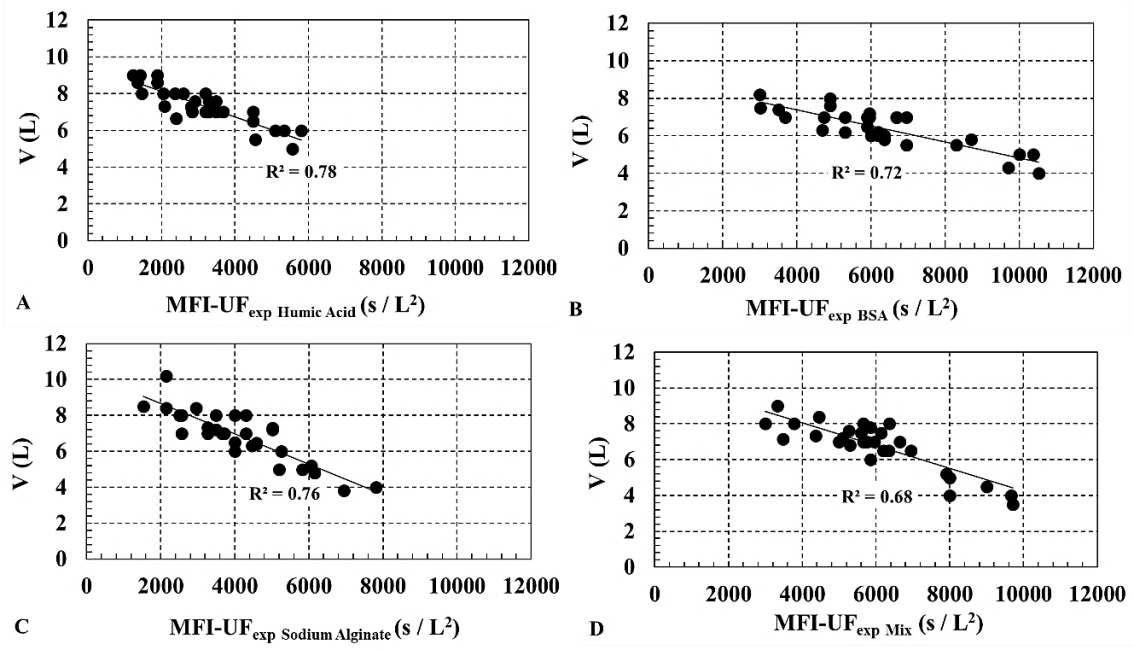

Figure 3.9 – MFI-UF as a function of filtered water volume for the 4 different synthetic solutions (A) Humic Acid, (B) BSA, (C) Sodium Alginate and (D) NOM Mixture

As both parameters (pressure and temperature) were found to be statistically significant, the next step was to use the model that incorporates water temperature and operating pressure, MFI-UF_{nor} (Equation 3.6) to assess the ability of the MFI-UF to predict NOM fouling conditions away from the standard reference conditions.

$$\text{MFI-UF}_{nor} = \frac{\mu_{20\,^{o}C}}{\mu_T} \text{x} \frac{P}{P_0} \text{ x MFI} - \text{UF}_{exp} \qquad \text{Equation (3.6)}$$

Figure 3.10 presents a comparison between the MFI-UF_{exp} (Equation 3.2), MFI-$UF_{nor,}$ (Equation 3.6), and the MFI-UF_{pr} (GLM, Equation 3.7). The MFI-UF_{nor} values in Figure 3.10 match the MFI-UF_{exp} at the referenced testing conditions (i.e. 2 bar, 20 ºC) but deviate by 10-15% at other non-referenced conditions. Therefore, the observed increase or decrease in the MFI-UF_{exp} values measured at different conditions was mainly attributed to the fouling tendency of water at specific filtration conditions. Thus, the MFI-UF_{exp} values measured at standard conditions can be altered to actual filtration conditions by adjusting the pressure and viscosity terms in the MFI-UF equation.

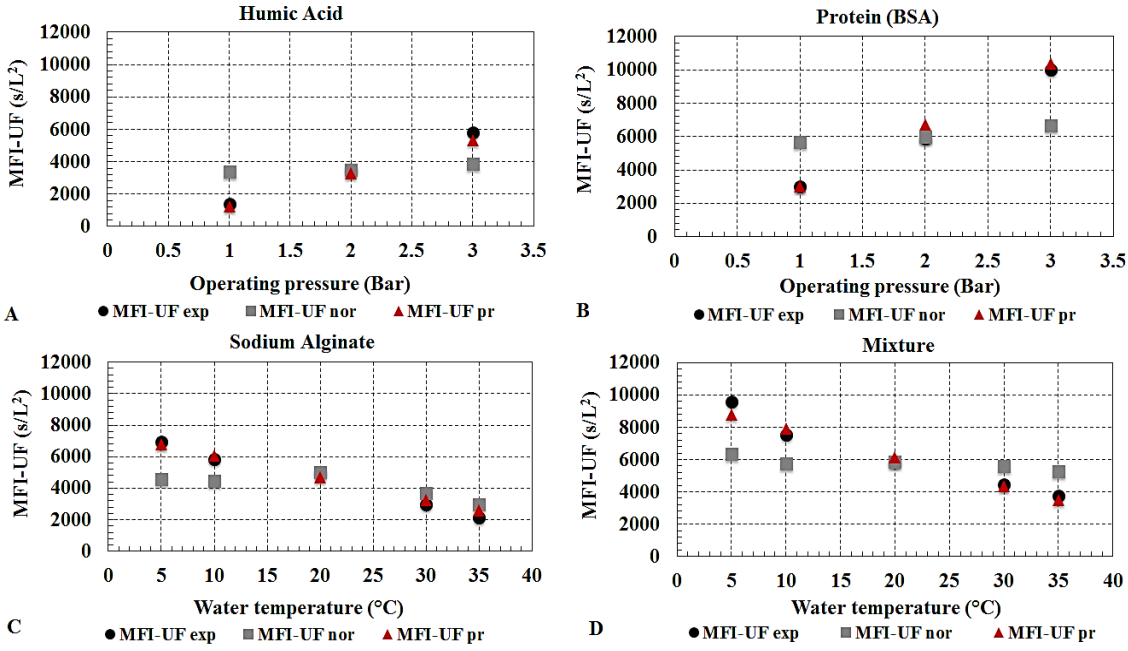

Figure 3.10 – MFI-$UF_{exp,}$ vs. MFI-UF_{nor} vs. MFI-UF_{pr} for different model solutions

Thus, from these results, instead of having to design an MFI-UF test for the changes in temperature and pressure, the GLM equations 3.7A-3.7D can be used as preliminary assessment of NOM fouling potential under changes in operational conditions. Future research should investigate the effect of water chemistry (i.e. pH, ionic strength, etc.) on the MFI-UF, as well as advancing the use of MFI-UF as a fouling prediction method for full scale membrane systems.

3.4 Conclusions

The presence of NOM in water poses major implications for membrane processes to maintain operational performance. This research investigated the application of the MFI-UF method to predict fouling of various NOM fractions under changes in pressure and temperature. The following points summarize the outcomes of this research:

- The NOM fouling potential order predicted by the MFI-UF_{exp} was NOM mixture, BSA, alginate, humic acid, respectively. The NOM mixture and BSA solutions exhibited a higher propensity for pore fouling relative to the alginate and humic acid test waters.
- The NOM mixture and BSA were more sensitive to changes in pressure and temperature, as determined by GLM and 3D surface plots, and exhibited higher fouling as temperature decreased and pressure increased.
- The normalization model presented was useful in estimating the MFI-UF values away from standard conditions for the different NOM fractions, which varied between 10-15% as pressure and temperature changed.
- The MFI-UF_{exp} values changed by > 30% as pressure and temperature were varied, likely due to changes in fouling layer characteristics by cake compression and/or shrinkage.

3.5 Acknowledgements

The authors would like to acknowledge the Saudi Arabia Ministry of Education (MOE) and Natural Sciences and Engineering Research Council of Canada (NSERC) for helping fund this research.

3.6 References

ASTM International, Designation: (D8002 – 15, 2015). Standard test method for modified fouling index (MFI-0.45) of Water.

Betancourt, W., Rose, J., 2004. Drinking water treatment processes for removal of Cryptosporidium and Giardia. Veterinary Parasitology 126, 219–234.

Boerlage, S., Kennedy, M., Aniye, M., Abogrean, E., Tarawneh, Z., Schippers, J., 2003. The MFI-UF as a water quality test and monitor. Journal of Membrane Science 211, 271–289.

Boerlage, S., Kennedy, M., Dickson, M., El-Hodali, D., Schippers, J., 2002. The modified fouling index using ultrafiltration membranes (MFI-UF): characterisation, filtration mechanisms and proposed reference membrane. Journal of Membrane Science 197, 1–21.

Boerlage, S., Kennedy, M., Tarawneh, Z., Faber, R., Schippers, J., 2004. Development of the MFI-UF in constant flux filtration. Desalination 16, 103-113.

Crittenden, J., Trussell, R., Hand, D., Howe, K., Tchobanoglous, G., 2005. Water treatment: principles and design, 2nd edition, Montgomery Watson Harza Ed, Wiley, New Jersey, USA.

Gao, W., Liang, H., Ma, J., Han, M., Chen, Z., Han, Z., Li, G., 2011. Membrane fouling control in ultrafiltration technology for drinking water production: a review. Desalination 272, 1–8.

Guo, W., Ngo, H., Li, J., 2012. A mini-review on membrane fouling. Bioresources Technology 122, 27–34.

Hashino, M., Hirami, K., Katagiri, M., Kubota, T., 2011. Effects of three natural organic matter types on cellulose acetate butyrate microfiltration membrane fouling. Journal of Membrane Science 379, 233– 238.

Ho, C., Zydney, A., 2000. A Combined pore blockage and cake filtration model for protein fouling during microfiltration. J. Colloid Interface Science 232, 389−399.

Jeong, S., Vigneswaran, S., 2015. Practical use of standard pore blocking index as an indicator of biofouling potential in seawater desalination. Desalination 365, 8–14.

Jermann, D., Pronk, W., Boller, M., 2008. Mutual influences between natural organic matter and inorganic particles and their combined effect on ultrafiltration membrane fouling. Environmental Science and Technology 42, 9129–9136.

Ju, I., Hong, S., 2015. Multiple MFI measurements for the evaluation of organic fouling in SWRO desalination. Desalination 365, 136–143.

Katsoufidou, K., Sioutopoulos, D., Yiantsios, S., Karabelas, A., 2010. UF membrane fouling by mixtures of humic acids and sodium alginate: Fouling mechanisms and reversibility. Desalination 264, 220-227.

Kertész, S., László, Z., Horváth, Z., Hodúr, C., 2008. Analysis of nanofiltration parameters of removal of an anionic detergent. Desalination 221, 303–311.

Kitis, M., Karanfil, T., Wigton, A., Kilduff, J., 2002. Probing reactivity of dissolved organic matter for disinfection by products formation using XAD-8 resin adsorption and UF fractionation. Water Research 36, 3834-3848.

Mosqueda-Jimenez, D., 2003. Impact of manufacturing conditions of Poly ethersulfone membranes on final characteristics and fouling reduction, PhD thesis, Department of Civil Engineering, University of Ottawa, Ottawa, ON.

Nagel, R., 1987. Seawater desalination with polyamide hollow fiber modules at DROP. Desalination 63, 225–246.

Peiris, R., Jaklewicz, M., 2013. Assessing the role of feed water constituents in irreversible membrane fouling of pilot-scale ultrafiltration drinking water treatment systems. Water Research 47, 3364 -3374.

Rodriguez, S., Amy, G., Schippers, J.C., Kennedy, M., 2015. The Modified Fouling Index Ultrafiltration constant flux for assessing particulate/colloidal fouling of RO systems. Desalination 365, 79–91.

Schippers, J., Verdouw, J., 1980. The modified fouling index: a method of determining the fouling characteristics of water. Desalination 32, 137-148.

Taheri, A., Sim, L., Haur, C., Alkhondi, E., Fane, A., 2013. The fouling potential of colloidal silica and humic acid and their mixtures. Journal of Membrane Science 433, 112–120.

Villacorte, L., Ekowati, Y., Winters, H., Amy, G., Schippers, J., Kennedy, M., 2015. MF/UF rejection and fouling potential of algal organic matter from bloom-forming marine and freshwater algae. Desalination 367, 1–10.

Zazouli, M., Nasseri, S., Ulbricht, M., 2010. Fouling effects of humic and alginic acids in nanofiltration and influence of solution composition. Desalination 250, 688-692.

Zularisam, A., Ahmad, A., Sakinah, M., Ismail, A., Matsuura, T., 2011. Role of natural organic matter (NOM), colloidal particles, and solution chemistry on ultrafiltration performance. Separation and Purification Technology 78(2), 189-20.

Chapter 4

Investigation into the Temperature Effect on NOM Fouling and Cleaning in Submerged Polymeric Membrane Systems

Mohammad T. Alresheedi* and Onita D. Basu*

*Department of Civil and Environmental Engineering, Carleton University, 1125 Colonel By Drive, Ottawa, ON, K1S 5B6, Canada.

Published: Journal of Desalination and Water Treatment

Abstract

Limited research on the influence of changing temperature conditions on reversible and irreversible NOM fouling has been conducted. Fouling and cleaning of a submerged polymeric ultrafiltration membrane with different NOM components (humic acids, proteins, polysaccharides, and their mixture) was examined at 5, 20, and 35 °C. Membrane fouling was evaluated using the MFI-UF and UMFI index methods, analysis of cake layer properties, and specific flux recovery. Results showed that fouling increased by 15-35% when water temperature decreased from 20 °C to 5 °C whereas fouling decreased by 15-25% when the temperature increased to 35 °C. The $UMFI_f$ fouling order was consistent across all temperature conditions with the NOM mixture and BSA fouling more severely than the alginate and humic acid. The UMFI and MFI-UF exhibited the same fouling order and can be used in complement to each other. BSA was found to be more sensitive to temperature changes and irreversibly foul more than humic acid and alginate. The ratio of irreversible to reversible fouling ($UMFI_{hir}/UMFI_{hr}$) increased by 15-25% from 35 °C to 20

°C and by 30-40% from 20 °C to 5 °C indicating the need for altered cleaning strategies at cold water conditions.

Keywords: Fouling indices; MFI-UF; NOM fouling; Temperature; UMFI

4.1 Introduction

Membrane processes are considered a reliable option for safe drinking water production. However, fouling by natural organic matter (NOM) (such as humic, protein, and polysaccharide like substances) creates significant challenges for membrane processes to maintain good performance during operation. Fouling can decrease membrane efficiency, increase operating costs, and ultimately decrease the lifetime of the membrane.

Water temperature is a key design parameter that influences membrane operation in terms of fouling and cleaning. However, studies that have examined temperature associated impacts with membranes are more commonly done with high pressure systems (nanofiltration (NF) and reverse osmosis (RO)) at temperatures greater than 20 °C. These studies tend to focus more on solution viscosity and solute diffusivity challenges with operation but not changes in fouling behavior (Zhao and Zhou, 2011; Jin et al., 2009). Other studies have investigated temperature impacts with wastewater MBR systems (Ma et al., 2013; Gao et al., 2012), whereas drinking water low pressure membrane studies with a focus on lower temperatures are very limited (Steinhauer et al., 2015). In particular, the effect of low water temperatures (e.g. 5 °C) have not been investigated in depth. Drinking water systems have in general neglected the interplay of water temperature and fouling on low pressure membrane systems. Although one study with low pressure membrane systems

found that current standards for membrane integrity testing overestimated safety design values by not taking into account temperatures below 5 °C (Farahbakhsh et al., 2006) highlighting the need for this type of research. Very little is known on the effect of water temperature on NOM fouling and cleaning of low pressure polymeric membranes which are critical for their design and operation for drinking water production.

Researchers have developed several methods to quantify fouling for membrane systems. Blocking laws quantify fouling location such as within the pores, pore blocking, and cake layer (Hermia et al., 1982). Fouling indices, which are considered simple and short filtration tests, are commonly used to predict the fouling potential of the membrane feed. The silt density index (SDI) and modified fouling index (MFI), using a 0.45μm pore size membranes, have been commonly used as fouling predictors for RO membranes (ASTM, 2014; Schippers and Verdouw, 1980). Boerlage et al. (2002) developed the MFI–UF, making use of ultrafiltration (UF) membranes to count for particles <0.45 μm. Feed water having an MFI-UF < 3000 s/L^2 is equivalent to SDI < 3 %/min, which is considered acceptable for membrane feed (Boerlage et al., 2003; Boerlage et al., 2002). Few studies applied the MFI-UF for assessing biofouling with RO systems (Jeong and Vigneswaran, 2015; Villacorte et al., 2015). Other studies investigated the influence of inorganic silica and calcium colloids on the MFI-UF fouling index with RO systems (Taheri et al., 2013). However, limited to no research exists that evaluates the use of the MFI-UF to predict NOM fouling for low pressure membrane systems under changes in water temperature condition.

The unified membrane fouling index (UMFI) model (Huang et al., 2008) has been applied to quantify fouling based on hydraulic and chemical reversibility and irreversibility components. Although different fouling types, i.e., reversible versus irreversible, are well defined in the literature, inconsistent bench scale results have been reported regarding membrane fouling by NOM, possibly due to different testing conditions, with many deviations from full-scale practice (Hashino et al., 2011; Katsoufidou et al., 2010; Xiao et al., 2009). These studies were often conducted for short durations at conditions that do not include hydraulic backwash cycles in the testing and use of different membrane materials. Moreover, correlations between MFI-UF and UMFI for assessing NOM fouling in polymeric membrane systems under changes in water temperature condition needs to be clarified. In this research, filtration performance, NOM fouling and chemical cleaning of a submerged polymeric UF membranes across a range of feed water temperatures (5, 20, and 35 °C) are examined. The UMFI method is utilized to assess for respective reversible and irreversible fouling; while the MFI-UF is used to assess its effectiveness for predicting NOM fouling in general and under changing temperature conditions. The temperature impact on chemical cleaning is investigated with respect to membrane resistance and permeability recoveries with the various NOM solutions.

4.2 Materials and Methods

4.2.1 Feed solutions

Four different synthetic feed water solutions were used in this study to cover the range of hydrophobic and hydrophilic NOM types typically found in surface water sources (Hashino et al., 2011; Katsoufidou et al., 2010; Jermann et al., 2008). Humic acids (2.5 mgC/L); a

protein (bovine serum albumin, BSA, 2.5 mgC/L); a polysaccharide (sodium alginate, 2.5 mgC/L); and a mixture of the three NOM models (0.83 mgC/L/each NOM model, total of 2.5 mgC/L), were used as model NOM foulants. All model substances were purchased from Sigma Aldrich. A moderate hardness and alkalinity of 75 mg/L calcium carbonate ($CaCO_3$) and a low level of turbidity (5 NTU) as kaolin clay particles were included in the synthetic water matric to represent the more complex conditions of a surface water source (Jermann et al., 2008).

Feed solutions were prepared using DI water and were mixed using a magnetic stirrer one-day prior any experiment to ensure that materials were dissolved completely. Feed water was continuously mixed using a VWR dual speed mixer to ensure homogeneous water conditions throughout the experiment. The feed tank was insulated to maintain constant temperature throughout the testing period. An immersion heater (Cole Parmer) and a compact chiller (LM series, Polyscience) were used to adjust the water temperature as required. Temperature and pH were monitored continuously using HACH (cat.no. 58258-00) HQd Field Case equipment. The pH of the feed was adjusted as needed to 7.5 with NaOH. The molecular weight distribution and zeta potential of the feed solutions, which are comprised of the respective NOM components, kaolin clay, and calcium, were measured using a UF fractionation method described by Kitis et al. (2002) (shown in Table 4.1). A Malvern Nano-sizer was used to determine the zeta potential of feed water solutions. Triplicate measurements were performed for each sample.

Table 4.1- Molecular weight fractionation and zeta potential of feed solutions

	Model Feed Solutions			
Molecular Weight	Humic acid	BSA	Alginate	Mixture
> 100 kDa	38%	51%	36%	55%
30 kDa - 100 kDa	42%	44%	48%	42%
10 kDa - 30 kDa	10%	2%	6%	2%
5 kDa - 10 kDa	6%	1%	3%	1%
1 kDa - 5 kDa	5%	2%	4%	1%
< 1 kDa	2%	1%	2%	1%
Zeta Potential (ζ)	-22 ± 5	-18 ± 4	-20 ± 5	-16 ± 7

4.2.2 Experimental setup and approach

4.2.2.1 Submerged polymeric membrane setup

Two submerged membrane systems were evaluated in parallel as shown in Figure 4.1. Zenon ZW-1 hollow fiber (UF) membranes made of polyvinylidene fluoride (PVDF), with a nominal pore size of 0.04 μm (surface area of 0.047 m^2) were used and operated under a vacuum pressure between 0 and -8.7 psi (0 and 0.6 bar). Filtration experiments were performed for 24 hrs under the operational conditions presented in Table 4.2. These operational conditions were applied based on previous work by De Souza and Basu (2013) and Alresheedi and Basu (2014). The flow rate and direction of permeate (i.e. forward and backward) were controlled using WinLN software. Pressure readings were recorded every 10 seconds using Operational Flux 2.0 program.

Table 4.2- Operational conditions of filtration experiments

Parameter	
Flux	38 LMH
Filtration Cycle	15 minutes
Filtration Mode	Dead-end
Backwash Duration	20 seconds
Air Scour	5 L/min (LPM)
Total Filtration Time	24 hours

To assess the potential seasonal impacts of water temperature on membrane fouling and cleaning, feed water temperature was varied between 5, 20, and 35 ºC. Equation 4.1 (Crittenden et al., 2005) was used to correct flux measured at different temperature to standard temperature of 20 °C. This is important as the flux greatly depends on water temperature.

$$J_{20\,^{o}C} = J_m\,(1.03)^{T_{20^{0}C} - T_m} \qquad \text{Equation (4.1)}$$

$J_{20\,^{o}C}$ and $T_{20\,^{o}C}$ are the flux and temperature at 20 ^{0}C, respectively. J_m and T_m are the measured flux and temperature, respectively.

Membranes were cleaned in place (CIP) between each experiment following manufacture specified recommendations. Cleaning of the membrane units was done in two steps: soaking in a 250 ppm of sodium hypochlorite (NaOCl) solution for 4 hours followed by soaking in citric acid solution for another 4 hours. Chemical cleaning was conducted at room temperature. DI water was then filtered through the membranes at permeate flux of 38 LMH and the membrane permeate flow was measured to ensure that the membranes were able to achieve the required flux before being placed back in operation.

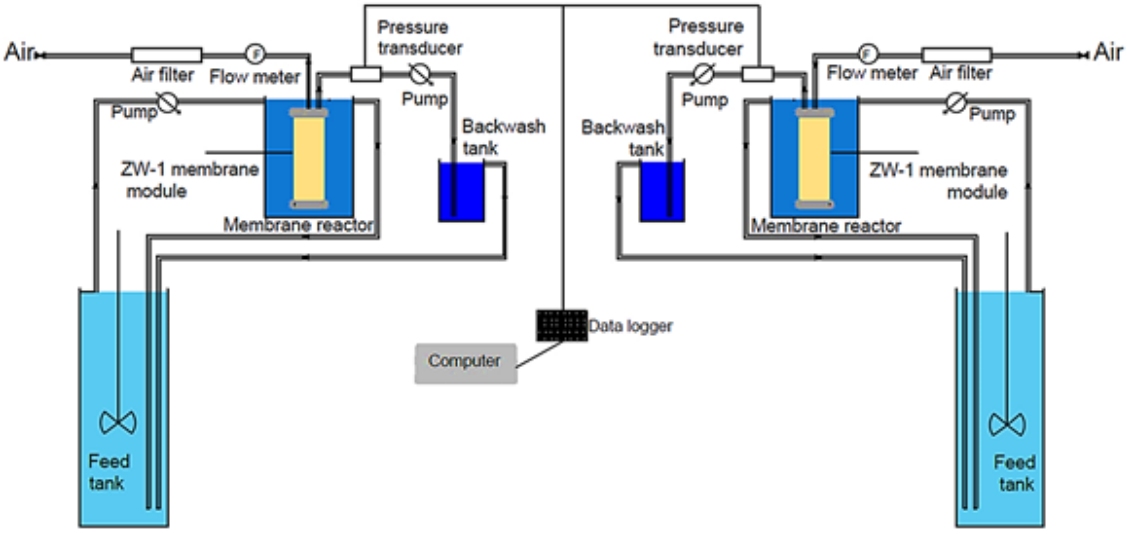

Figure 4.1- A schematic representation of the bench scale polymeric membrane setups

4.2.2.2 Fouling resistances using the unified membrane fouling index (UMFI) method

To assess polymeric membrane's fouling at different water temperature conditions, the UMFI model, Equation 4.2 (Huang et al., 2008) was applied to quantify each contributing fouling resistance.

$$\frac{1}{J_S'} = 1 + (\text{UMFI}) \text{x } V_S \qquad \text{Equation (4.2)}$$

Where J_S' is the normalized specific flux (unitless), UMFI is an estimate of the extent of fouling (m^{-1}), and V_S (m^3/m^2) is the specific permeate volume. UMFI can be calculated using Equation 4.3.

$$\text{UMFI}_f = \text{UMFI}_{hr} + \text{UMFI}_{hir} = \text{UMFI}_{hr} + \text{UMFI}_{cr} + \text{UMFI}_{cir} \qquad \text{Equation (4.3)}$$

Where UMFI_f is the total fouling resistance index; UMFI_{hr} is hydraulically reversible fouling resistance index (i.e. removed by backwash); UMFI_{hir} is hydraulically irreversible

fouling resistance index (i.e. remained after backwash). $UMFI_{hir}$ can be divided into $UMFI_{cr}$ and $UMFI_{cir}$. $UMFI_{cr}$ is chemically reversible fouling resistance index (i.e., removable by chemical cleaning); and $UMFI_{cir}$ is chemically irreversible fouling resistance index (i.e., remained after chemical cleaning).

Figure 4.2 illustrates the UMFI method used to calculate different fouling resistances. $UMFI_f$ was calculated by using filtration data from the start to end of filtration. $UMFI_{hir}$ represent the slope of the line after the start of each filtration cycle. $UMFI_{hr}$ is the difference between $UMFI_f$ and $UMFI_{hir}$. $UMFI_{cir}$ was calculated by collecting data after the chemical cleaning step. $UMFI_{cr}$ is the difference between $UMFI_{hir}$ and $UMFI_{cir}$.

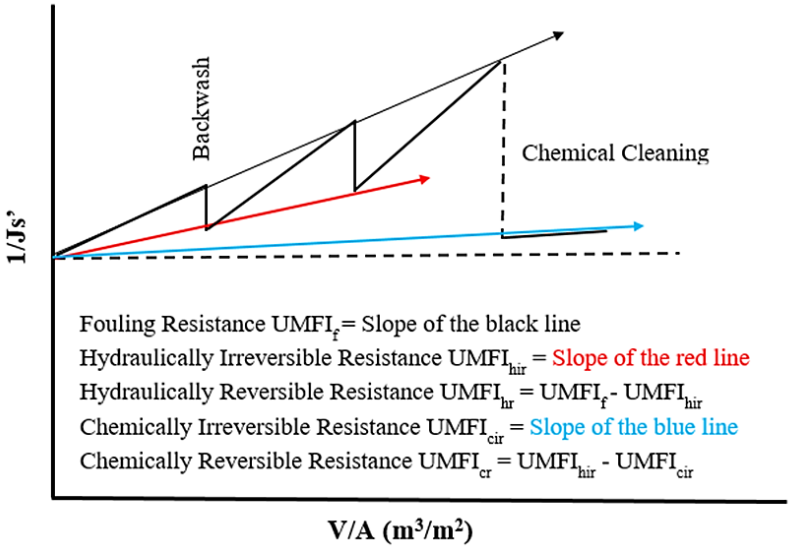

Figure 4.2 - Estimation of fouling resistances using the UMFI method (adapted from Alresheedi et al., 2017)

4.2.2.3 Specific cake resistance

According to Darcy's law, the flux through a clean membrane can be written as:

$$J = \frac{\Delta P_0}{\mu R_m} \qquad \text{Equation (4.4)}$$

J is the membrane flux ($m^3/m^2.s$); ΔP_0 is initial transmembrane pressure (kPa); R_m is the intrinsic membrane resistance (m^{-1}); and μ is the viscosity of the fluid (kPa s).

For fouled membrane, if all fouling is assumed to be a result of cake filtration, then Equation 4.4 can be rewritten as:

$$J = \frac{\Delta P}{\mu (R_c + R_m)} \qquad \text{Equation (4.5)}$$

ΔP is final transmembrane pressure (kPa); Rc is the cake layer resistance (m^{-1}).

The Rc can be expressed in terms of the specific cake resistance α_c (m/kg), the bulk concentration, C_b (kg/m^3), and the volume of filtered water per unit membrane area (V_s), as follows:

$$R_c = \alpha_c C_b V_s \qquad \text{Equation (4.6)}$$

Equations 4.4-4.6 can be combined to express the increase in transmembrane pressure at constant flux during cake filtration as shown in Equation 4.7 (Chellam and Wendong, 2006).

$$\Delta P = (J \mu)(\alpha_c C_b V_s + R_m) = \Delta P_0 + (J \mu C_b V_s)\alpha_c \qquad \text{Equation (4.7)}$$

The specific cake resistance α_c often increases according to a power law (Foley et al., 2006) as shown in Equation 4.8:

$$\alpha_c = \alpha_0 \Delta P^n \qquad \text{Equation (4.8)}$$

in which α_0 is a constant related primarily to the size and shape of the particles forming the cake, ΔP is final pressure, and n is the cake compressibility index, which ranges from zero (incompressible cake) to 1 or greater (for a highly compressible cake).

Scanning electron microscopy (SEM) analysis was conducted using 0.45 µm membrane filters fouled for 15 minutes at different feed water temperatures. SEM images were taken at 10.00 kx magnification using the Tescan Vega-II XMU equipment for more insights into the effect of temperature on the fouling layer of different NOM fractions.

4.2.2.4 MFI-UF fouling index

Fouling potential of feed water solutions from the submerged membrane experiments (i.e. humic acids, BSA, alginate, and NOM mixture), was assessed using the MFI-UF method (Boerlage et al., 2002). Fouling indices are used to measure and predict the fouling potential of membrane feedwater, diagnose fouling at the design stage, and/or monitor pretreatment performance during membrane operation. The MFI-UF setup is described in detail by Boerlage et al. (2002); Alresheedi et al. (2018). The characteristics of the MFI-UF membrane are presented in Table 4.3.

Table 4.3 - MFI-UF membrane characteristics

	MFI-UF Membrane
Membrane Type	UF - 13 kDa
Membrane Materials	PAN hollow fiber (Pall Corp.)
Configuration	Inside-out
Fiber ID	0.8 mm
Fiber OD	1.4 mm
Number of Fiber	400
Membrane Area	0.2 m^2
Module Length	347 mm
Module Diameter	42 mm

MFI-UF testing was determined according to method described by Boerlage et al. (2002). Feed water was filtered through the hollow fiber UF membrane under dead-end mode and pressure of 2 bars. Permeate was collected in a tank set on the electronic balance to acquire permeate volume (V) and filtration time (t) data from the balance. The $MFI\text{-}UF_{exp}$ was then calculated using Equation 4.9. d(t/V)/dV is the slope of two data points in the linear region of t/V versus V graph (described in detail by Boerlage et al. (2002).

$$MFI\text{-}UF_{exp} = \frac{d\left(\frac{t}{V}\right)}{dV} \qquad \text{Equation (4.9)}$$

The MFI-UF test was performed under the same water temperature conditions as the submerged polymeric membranes experiments (i.e. 5, 20, and 35 °C).

4.3 Results and Discussion

4.3.1 Effect of water temperature condition on NOM fouling

Figures 4.3A-4.3D show the inverse of the normalized specific flux ($1/J_s'$) versus filtered water volume per membrane area (V/A). Water temperature was found to impact NOM

fouling as follows: an increase in water temperature resulted in lower fouling rate for all NOM solutions. Overall, as temperature decreased from 20 ºC to 5 ºC, membrane fouling increased by 15-35% while fouling decreased by 15-25% when the temperature increased from 20 ºC to 35 °C. The changes in NOM fouling behavior with temperature could be attributed to the changes in fouling layer resistance and NOM retention (Kertész et al., 2008). Thus, changes in water temperature condition could be crucial factor for membrane systems to meet consistent performance targets.

Figure 4.3 also shows that different NOM fractions responded differently to temperature changes. BSA filtration is more sensitive to temperature changes in which fouling was observed to increase by 35% with decreasing temperature from 20 °C to 5°C compared to 15% and 20% for humic acid and alginate, respectively. In addition, fouling of the NOM mixture is approximately similar to BSA alone, indicating a higher effect from protein substances on fouling. The differences between fouling among the types of NOM could be partially attributed to the molecular weight distribution and zeta potential (as shown in Table 4.1). For humic acid and sodium alginate feedwater solutions, there were larger components with molecular weight in the range of 30-100 kDa which was smaller than the pore size of the membrane (0.04 μm) and may therefore adsorb on the pore surface and caused internal fouling or passed through the membrane to permeate side. On the other hand, BSA and NOM mixture feedwater solutions had a larger fraction of components with molecular weight > 100 kDa which may have caused pore blocking during the early stages of filtration and/or adsorbed on the pore surface leading to higher fouling compared to humic acid and sodium alginate.

Moreover, the zeta potential values of BSA and NOM mixture feed water (-18 mV and -16 mV respectively) were lower than that for humic acid and alginate feed water (-22 mV and -20 mV respectively) and would have a higher tendency to adsorb on the membrane surface or pores. Similar results were reported by Contreras et al. (2009) study in which BSA has a lower zeta potential (-20.7 mV) compared to sodium alginate (- 45.0 mV) and humic acid (-37.9) leading to lower electrostatic repulsion and higher hydrophobic interaction between BSA and thin-film composite NF membrane. Interestingly, sodium alginate (hydrophilic) resulted in higher fouling compared to humic acid (hydrophobic) indicating a strong influence from polysaccharides on membrane fouling compared to humic substances. These results are consistent with those reported by Hashino et al. (2011) in which the sodium alginate solution showed more severe flux decline than humic acid with MF membranes.

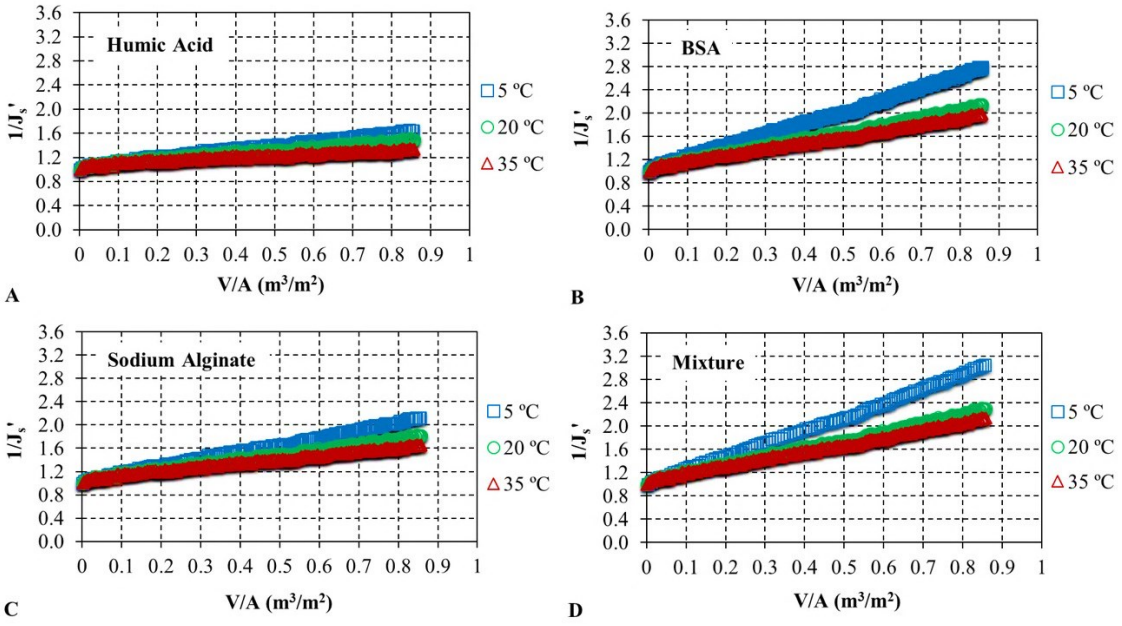

Figure 4.3 - NOM Fouling graphs **(A)** Humic Acid; **(B)** BSA; **(C)** Sodium Alginate; **(D)** Mixture. Js': normalized specific flux; V/A: filtered water volume per membrane area

Additionally, the specific cake resistance (α_c) and compressibility index (n) were calculated from the experimentally determined values of the filtration pressure, bulk concentration, and specific filtered water volume, considering cake filtration is the dominant fouling mechanism (Alresheedi et al., 2018), as described in Equations 4.4-4.8. Figures 4.4A shows that α_c value of all NOM models decreases as feed water temperature increases from 5 to 35 ºC, therefore, temperature influences the NOM cake structure. Jin et al. (2009) found that humic acid colloids decreased in size with increasing temperature of RO feed. As a result, smaller particles produced more porous deposits and influenced fouling. In this study, the decrease in α_c with increasing temperature could be attributed to the decrease in NOM size which may have changed the cake layers into more porous and open structures. Thus, lower fouling was obtained at higher temperature. Furthermore, Figures 4.4A and 4.4B show that BSA and NOM mixture cake resistances are significantly affected by temperature; changes in cake resistance with temperature indicate more compressible cake (n= 0.85 and 0.89 for BSA and NOM mixture, respectively). This is reflected in Figure 4.3, where the fouling trend for BSA and NOM mixture changes significantly, particularly between 5 °C and 20 °C. The compressibility indices for humic acid and sodium alginate are quite similar (0.57 and 0.59, respectively) which differ from those of Sioutopoulos et al. (2010) who found that humic acid deposits are more compressible (n = 0.70) compared with alginate deposits (n = 0.40) with UF membranes. The difference in the actual numerical value of n may be caused by the different membrane material and/or the high concentration of total dissolved solids in the solutions used by Sioutopoulos et al. (2010).

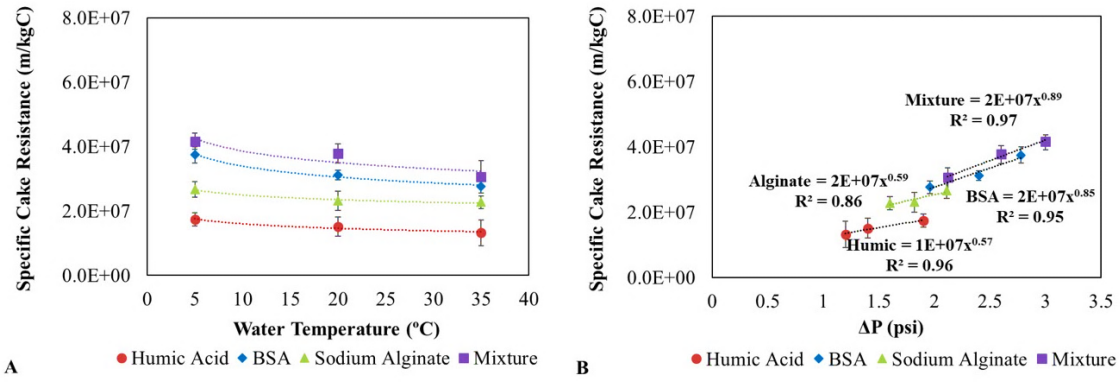

Figure 4.4 – (A) Changes in specific cake resistance with temperature; (B) estimated compressibility index values

To visualize the effect of temperature on NOM fouling layer properties, Figure 4.5 shows SEM images of humic acid, BSA, and sodium alginate fouling layers. The SEM analysis were conducted using 0.45 µm membrane filters fouled for 15 minutes at constant pressure of 1 bar and different feed water temperatures. From Figure 4.5, it can be clearly seen that the fouling layers differ between different NOM components. At 20 ºC, humic acid filled the pores partially and developed a layer of relatively open structure whereas protein and sodium alginate developed a rough gel layer and appeared to fill more pores compared to humic acid. This is reflected in Figure 4.3, where the fouling for BSA and alginate was higher than humic acid. Figure 4.5 also shows a decrease in water temperature from 20 ºC to 5 ºC resulted in more compact layer for all NOM components. More specifically, at 5 ºC, BSA completely blocked membrane pores and developed a fouling layer of high resistance. This can be supported by the findings from Figure 4.4 in which BSA has the highest specific fouling resistance and compressibility index values compared to alginate and humic acid.

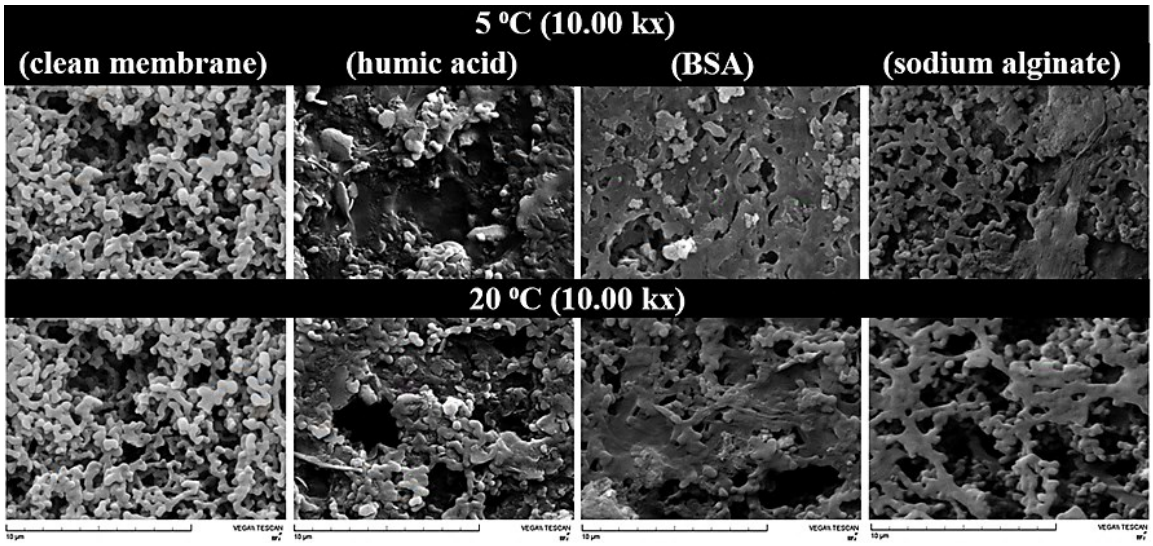

Figure 4.5 – SEM images of NOM fouling layers at 5 °C and 20 °C (P = 1 bar) using 0.45µm membrane filters.

4.3.2 Fouling indices assessment at different water temperature conditions

4.3.2.1 Reversible and irreversible fouling indices

To quantify membrane fouling during membrane filtration, fouling resistances using the unified membrane fouling index method (UMFI) were estimated. The lower the $UMFI_{hir}/UMFI_{hr}$ ratio the more effective the hydraulic backwashes, due to greater cake formation. While higher the $UMFI_{hir}/UMFI_{hr}$ ratio the greater the NOM adsorption and pore blockage and thus a greater need for chemical cleans as hydraulic backwashes are less effective. The hydraulically irreversible fouling index ($UMFI_{hir}$) can be categorized into the chemically reversible fouling ($UMFI_{cr}$) or the chemically irreversible fouling ($UMFI_{cir}$). $UMFI_{cr}/UMFI_{hir}$ quantifies the irreversible fouling ratio removed by a chemical clean while $UMFI_{cir}/UMFI_{hir}$ quantifies the fouling ratio that remains after a chemical clean. Minimizing chemical cleans is preferred to help control membrane aging which decreases the hydraulic resistance and hydrophobicity of membrane material (Puspitasari et al., 2010). Moreover, controlling the degree of chemical cleaning helps minimize chemical

waste production and maintain membrane productivity. Figure 4.6A-4.6C shows the UMFI values determined at different tested water temperature conditions. The $UMFI_f$ fouling index order was consistent at different temperature which was the highest for the NOM mixture followed by BSA, alginate, and lastly humic acid. The similar $UMFI_f$ values for the NOM mixture and the BSA solution indicate that protein-based NOM significantly contributes to fouling in membrane systems. Hashino et al. (2011) similarly reported a significant flux decline of cellulose acetate butyrate membrane caused by BSA adsorption compared to alginate. Moreover, BSA fouling, refer to Figure 4.6, is more sensitive to changes in water temperature condition in which BSA $UMFI_f$ increased by 35% with decreasing temperature from 20 °C to 5°C compared to 15% and 20% for humic acid and alginate, respectively.

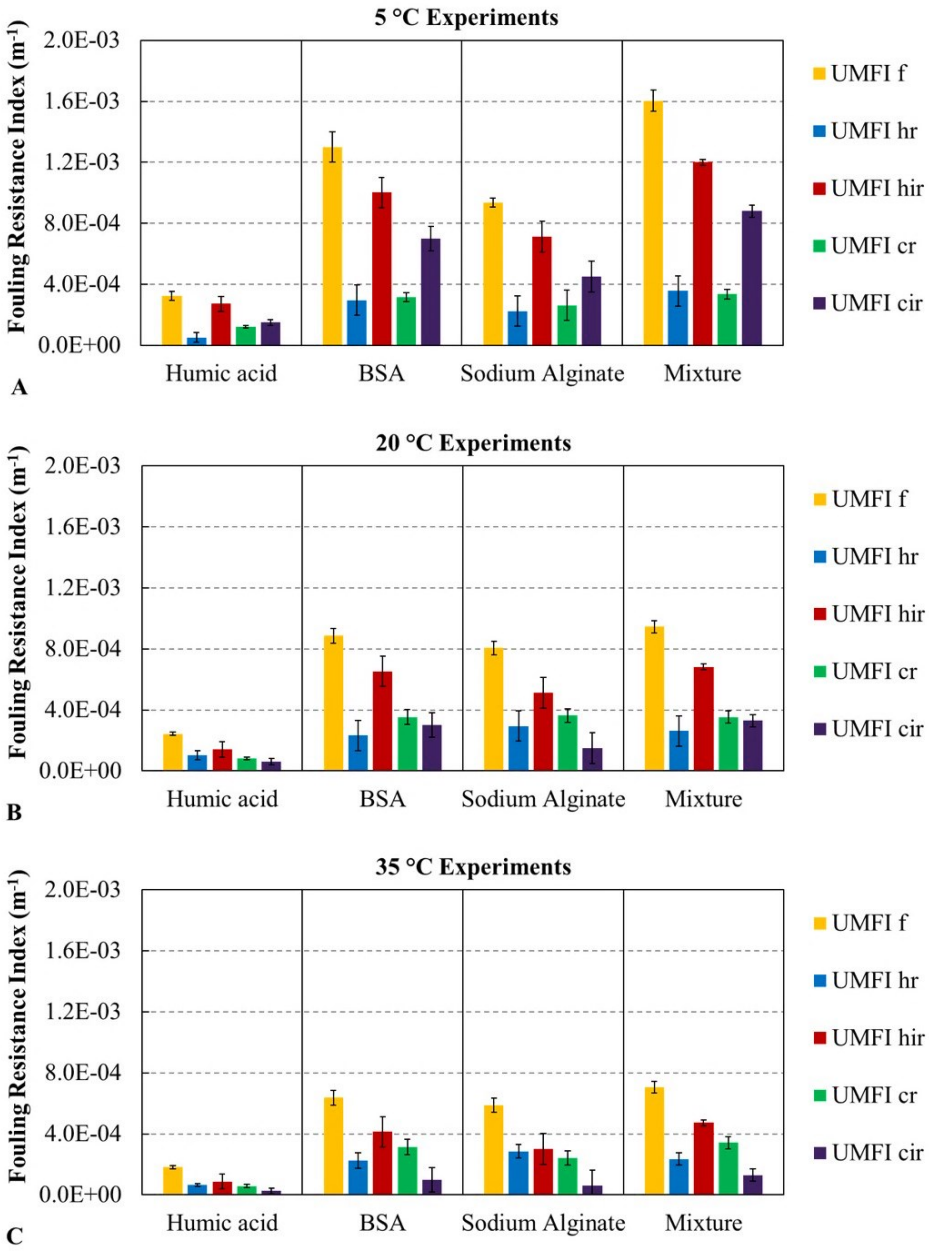

Figure 4.6 - Estimated UMFI values at different temperature conditions.

*Note: $UMFI_f$: unified total fouling index; $UMFI_{hr}$: unified hydraulically reversible fouling index; $UMFI_{hir}$: unified hydraulically irreversible fouling index; $UMFI_{cr}$: unified chemically reversible fouling index; $UMFI_{cir}$: unified chemically irreversible fouling index.

To quantify the effect of water temperature on NOM fouling behaviors, Figure 4.7 presents the changes in irreversible to reversible fouling index ratios ($UMFI_{hir}/UMFI_{hr}$) under all

tested water temperature conditions. The $UMFI_{hir}/UMFI_{hr}$ ratios of all NOM models was highest during the 5 °C operation, (1.8 to 3.3), compared to 20 °C, (0.95 to 1.9), and 35 °C, (0.7 to 1.3). The increase in the $UMFI_{hir}/UMFI_{hr}$ at lower temperature indicates lower hydraulic backwash efficiency, thus, higher NOM irreversibility. This is consistent with the increase in specific cake resistance observed in Figure 4.4A. The $UMFI_{hir}/UMFI_{hr}$ ratios decreased by about 30-40% as feed water temperature increased from 5 °C to 20 °C and by about 15-25% as the temperature increased from 20 °C to 35 °C. Therefore, hydraulic backwashing at warm water temperature (i.e. 20 and 35 °C) was more effective in removing the hydraulically irreversible fouling of NOM compared to cold water temperature, 5 °C. Irreversibility of the foulant layer is a major concern during membrane filtration, as it influences hydraulic or chemical cleaning requirements. Although hydraulic backwashing was efficient in mitigating a large percentage of NOM fouling at warm water temperature condition, the significant amount of irreversible fouling due to stronger adsorption of foulants actually poses a potential limitation to longer membrane operation.

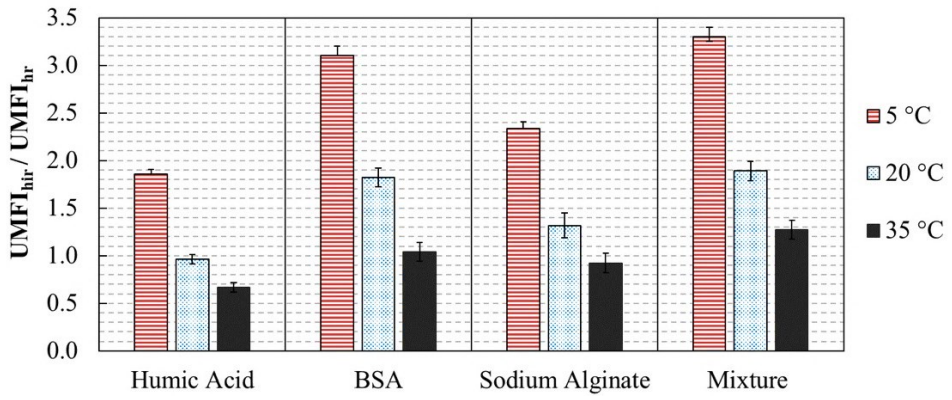

Figure 4.7 – Hydraulically irreversible to reversible fouling index ratios at different water temperature conditions*

*Note: $UMFI_{hir}/UMFI_{hr}$ ratio of 1 indicates 50% irreversible and 50% reversible fouling. Ratio > 1 indicates higher irreversible fouling.

4.3.2.2 Correlation of UMFI and MFI-UF indices

The MFI-UF method is used to assess the fouling tendency of a membrane feed whereas the UMFI provides information on the current fouling a membrane is subjected to. Thus, the MFI-UF is used to predict fouling while the UMFI is used to quantify fouling in an operating system. Feed water having an MFI-UF < 3000 s/L^2 (equivalent to an SDI < 3 %/min), is considered acceptable for membrane feed (Boerlage et al., 2002). However, the actual capacity of the MFI-UF to be used effectively as a prediction tool with NOM has yet to be evaluated in general and under changing water temperature conditions. Table 4.4 presents fouling index values predicted by the MFI-UF method. The results in Table 4.4 show an increased fouling potential across all NOM sources as the water temperature drops which is in agreement with the increased fouling tendency observed in Figure 4.7 using the UMFI method. The NOM fouling potential predicted by the MFI-UF was in the order of mixture > BSA > sodium alginate > humic acid which matches the fouling trend observed in the submerged polymeric UF system with the UMFI method.

Table 4.4 –MFI-UF index prediction of NOM fouling at different temperatures

	Humic Acid	**BSA**	**Sodium Alginate**	**Mixture**
		MFI-UF (s/L^2)		
5 ^{0}C	5559 ± 294	9880 ± 332	6948 ± 186	10122 ± 491
20 ^{0}C	3487 ± 300	6200 ± 220	5018 ± 222	6850 ± 495
35 ^{0}C	1350 ± 45	3511 ± 353	2144 ± 62	3774 ± 152

Figure 4.8 compares fouling resistances estimated by the UMFI method to the MFI-UF for various NOM foulants at different temperature conditions. From Figure 4.8, it can be observed that the MFI-UF values correlate well with the $UMFI_f$ (R^2 of 0.76) and $UMFI_{hir}$

(R^2 of 0.86). Since fouling irreversibility poses major implications during filtration with respect to membrane cleaning and life time, the MFI-UF testing method demonstrates a useful fit for predicting fouling before relying on operating data. Thus, a plant could use the MFI-UF to monitor and predict changes in irreversible fouling with temperature and make required alternations in membrane pretreatment and/or cleaning procedures.

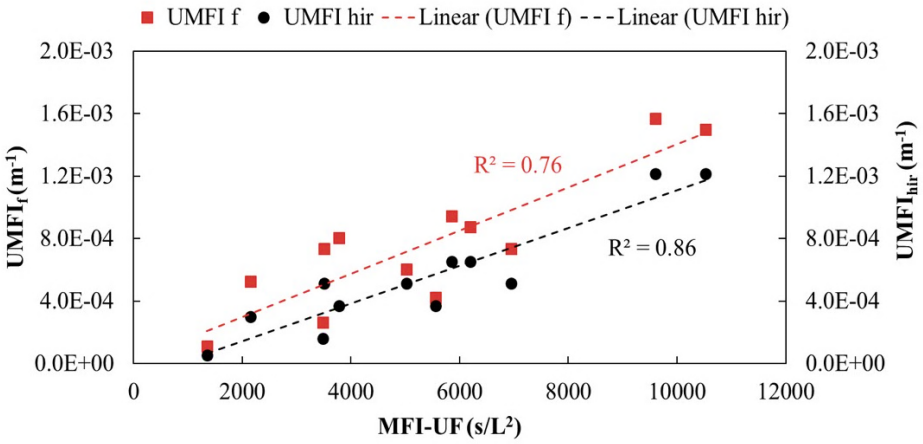

Figure 4.8 – Relationship between UMFI fouling resistances and MFI-UF fouling index

4.3.3 Impact of water temperature on chemical cleaning

As noted above, fouling with NOM across all model solutions increased as the water temperature decreased; additional tests were conducted to assess for changes in cleaning effectiveness with temperature as well. Figure 4.9 shows the ratio of chemically reversible fouling to hydraulically irreversible fouling indices, $UMFI_{cr}/UMFI_{hir}$, (Figure 4.9A), and specific flux recoveries (Figure 4.9B) at different water temperatures. From Figure 4.9A, it can be clearly seen that the $UMFI_{cr}/UMFI_{hir}$ ratios differ at different water temperatures. Under the operation at 5 °C, chemical cleaning efficiency was the lowest and increased by 10-40%, ($p < 0.05$), with increasing filtration temperature from 5 °C to 20 °C. Thus, the

initial chemical cleaning protocol recommended by the polymeric membrane's manufacturer (i.e. NaOCl followed by citric acid) was not sufficient in removing irreversible fouling at 5 °C compared to 20 °C. The decrease in the cleaning efficiency with temperature is attributed to the high irreversible fouling ratio at 5 °C as observed in Figure 4.7. Moreover, as water temperature increased from 20 °C to 35 °C, the $UMFI_{cr}/UMFI_{hir}$ ratios also increased but moderately by 10-15% ($p < 0.05$). The $UMFI_{cr}/UMFI_{hir}$ ratios of the NOM mixture and BSA were always lower than that for alginate and humic acids, indicating lower cleaning efficiency for the NOM mixture and BSA. This attributes to the higher irreversible fouling observed with the NOM mixture and BSA compared with the alginate and humic acid waters. Clearly, a more aggressive chemical cleaning strategy is required to better remove NOM mixture and BSA fouling at the lower temperature, highlighting the need to focus on both NOM type and water temperature to optimize chemical cleaning regimes.

The influence of filtration temperature on NOM chemical cleaning can also be observed in Figure 4.9B. The specific flux recoveries at 5 °C, after 1 cleaning cycle using NaOCl followed by citric acid, ranged from 85% to 95% which were significantly lower ($p < 0.05$) than those obtained at 20 °C (ranged from 95% to 98%). The difference in the specific flux recovery at 5 and 20 ºC conditions is attributed to the differences in the irreversible fouling ratios as shown in Figure 4.7. Thus, a more aggressive cleaning was needed to recover specific flux at 5 ºC compared to 20 ºC. This can be supported by the specific flux recovery values at 35 °C in which all NOM types were effectively removed and the specific flux recovery was > 95%. In addition, at 5 °C, the NOM mixture, BSA, and alginate required

an additional 1 hour cleaning using NaOCl (i.e. after the 1 recommended cleaning cycle using NaOCl followed by citric acid) to achieve > 95% of specific flux recovery (results not shown). On the other hand, at 20 °C and 35 °C, membranes were able to achieve > 95% after only 1 cleaning cycle. Humic acid cleaning was less impacted by temperature variation compared to the other NOM models (refer to Figures 4.9A-B). These results indicate the need to emphasize good pretreatment steps or modification of cleaning steps during membrane operation in cold climates to remove the majority of NOM from membrane feed in order to ensure higher specific flux recovery.

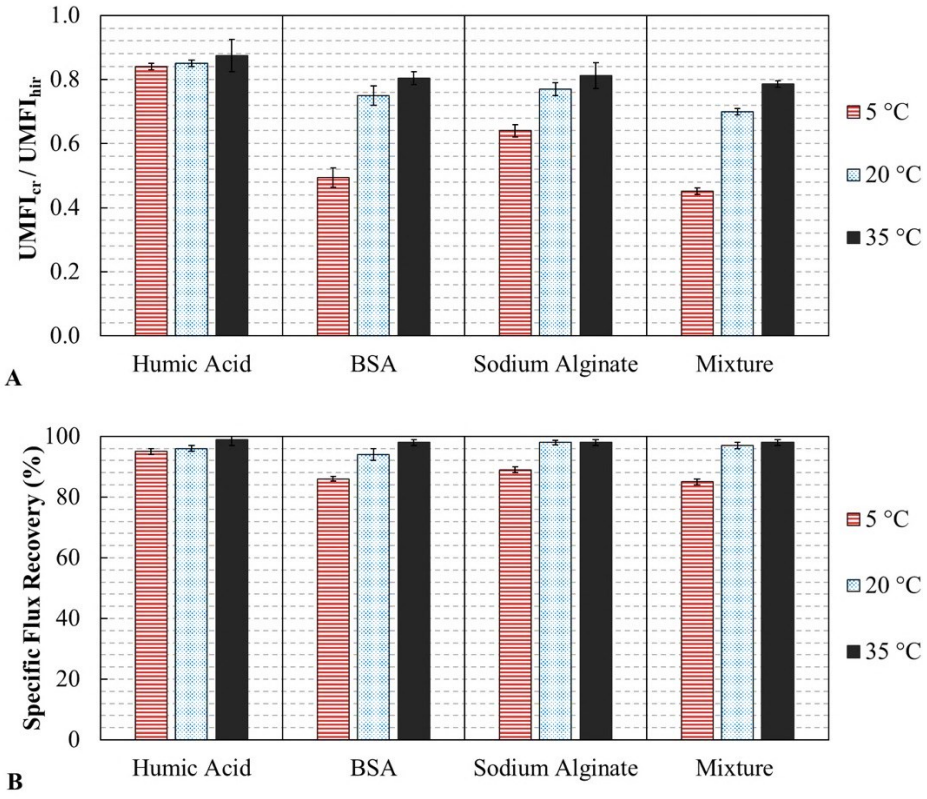

Figure 4.9 – Chemical cleaning efficiency at different filtration water temperature*. (A) $UMFI_{cr}/UMFI_{hir}$ ratios**; (B) Specific flux recovery.

*After 1 cleaning cycle using NaOCl followed by citric acid.

**Note: The higher the $UMFI_{cr}/UMFI_{hir}$ ratio the higher the chemical cleaning efficiency

4.4 Conclusions

Limited research has investigated changes in NOM fouling and cleaning with temperature. This research investigated the impact of water temperature at 5ºC, 20ºC and 35ºC on NOM fouling and cleaning using the UMFI and MFI-UF methods with the following key observations:

- Feed water temperature has a significant impact on submerged polymeric UF membrane fouling. Fouling increased by 15-35% when the water temperature decreased from 20 °C to 5 °C while the fouling decreased by 15-25% when the temperature increased to 35 °C. Thus, fouling analysis for plant subject to cold water conditions should be investigated more rigorously to help maintain membrane productivity.
- BSA was most sensitive to changes in water temperature whereas humic acid was least sensitive, highlighting the need to identify specific NOM fractions in water to better understand potential fouling changes.
- The MFI-UF fouling prediction trend was in strong agreement with UMFI indices for establishing NOM irreversible fouling, highlighting an advantage of the MFI-UF as a robust fouling prediction index for low pressure polymeric membranes.
- Aside from humic acid, chemical cleaning of all other NOM solutions was less efficient at the colder water temperature and thus indicate the need for alternative chemical cleaning strategies during lower water temperature conditions to recover membrane permeability.

4.5 Acknowledgements

The authors would like to acknowledge the Saudi Arabia Ministry of Education (MOE) and Natural Sciences and Engineering Research Council of Canada (NSERC) for helping fund this research. The authors would also like to thank summer student, Bia Pereira, for her hard work and help in the laboratory.

4.6 References

Alresheedi, M., Basu, O., 2014. Support media impacts on humic acid, cellulose, and kaolin clay in reducing fouling in a submerged hollow fiber membrane system. Journal of Membrane Science 450, 282–290.

Alresheedi, M., Basu, O., 2017. Fouling indices and resistance in series methods for quantification of NOM fouling in submerged polymeric membrane systems. IWA Membrane Technology Conference, Singapore.

Alresheedi, M., Basu, O., 2018. Application of MFI-UF Fouling Index with NOM Fouling under Various Operating Conditions. Desalination and Water Treatment 133, 45-54.

ASTM International, Designation: D4189 − 07 (Reapproved 2014). Standard test method for silt density index (SDI) of water.

Boerlage, S., Kennedy, M., Aniye, M., Abogrean, E., Tarawneh, Z., Schippers, J., 2003. The MFI-UF as a water quality test and monitor. Journal of Membrane Science 211, 271–289.

Boerlage, S., Kennedy, M., Dickson, M., El-Hodali, D., Schippers, J., 2002. The modified fouling index using ultrafiltration membranes (MFI-UF): characterisation, filtration mechanisms and proposed reference membrane. Journal of Membrane Science 197, 1–21.

Chellam, S., Wendong, X., 2006. Blocking laws analysis of dead-end constant flux microfiltration of compressible cakes. Journal Colloid Science 301, 248–257.

Contreras, A., Kim, A., Li, Q., 2009. Combined fouling of nanofiltration membranes: mechanisms and effect of organic matter. Journal of Membrane Science 327, 87–95.

Crittenden, J., Trussell, R., Hand, D., Howe, K., Tchobanoglous, G., 2005. Water treatment: principles and design, 2nd edition, Ed, Wiley, New Jersey, USA.

De Souza, N., Basu, O., 2013. Comparative analysis of physical cleaning operations for fouling control of hollow fiber membranes in drinking water treatment. Journal of Membrane Science 436, 28–35.

Farahbakhsh, K., Smith, D., 2006. Membrane filtration for cold regions – impact of cold water on membrane integrity testing. Journal of Environmental Engineering Science 5, 69-75.

Foley, G., 2006. A review of factors affecting filter cake properties in dead-end microfiltration of microbial suspensions. Journal of Membrane Science 274, 38-46.

Gao, W., Qu, X., Leung, K., Liao, B., 2012. Influence of temperature and temperature shock on sludge properties, cake layer structure, and membrane fouling in a submerged anaerobic membrane bioreactor. Journal of Membrane Science 421, 131-144.

Hashino, M., Hirami, K., Katagiri, M., Kubota, T., 2011. Effects of three natural organic matter types on cellulose acetate butyrate microfiltration membrane fouling. Journal of Membrane Science 379, 233– 238.

Hermia, J., 1982. Constant pressure blocking filtration laws application to power-law non-newtonian fluids. Institution of Chemical Engineers 60, 183-187.

Huang, H., Young, T., Jacangelo, J., 2008. Unified membrane fouling index for low pressure membrane filtration of natural waters: Principles and methodology. Environmental Science and Technology 42, 714–720.

Jeong, S., Vigneswaran, S., 2015. Practical use of standard pore blocking index as an indicator of biofouling potential in seawater desalination. Desalination 365, 8–14.

Jermann, D., Pronk, W., Boller, M., 2008. Mutual influences between natural organic matter and inorganic particles and their combined effect on ultrafiltration membrane fouling. Environmental Science and Technology 42, 9129–9136.

Jin, X., Jawor, A., Kim, S., Hoek, E., 2009. Effects of feed water temperature on separation performance and organic fouling of brackish water RO membranes. Desalination 239, 346–359.

Katsoufidou, K., Sioutopoulos, D., Yiantsios, S., Karabelas, A., 2010. UF membrane fouling by mixtures of humic acids and sodium alginate: Fouling mechanisms and reversibility. Desalination, 264, 220-227.

Kertész, S., László, Z., Horváth, Z., Hodúr, C., 2008. Analysis of nanofiltration parameters of removal of an anionic detergent. Desalination 221, 303–311.

Kitis, M., Karanfil, T., Wigton, A., Kilduff, J., 2002. Probing reactivity of dissolved organic matter for disinfection by products formation using XAD-8 resin adsorption and UF fractionation. Water Research 36, 3834-3848.

Ma, Z., Wen, X., Zhao, F., Xia, Y., Huang, X., Wait, D., Guan, J., 2013. Effect of

temperature variation on membrane fouling and microbial community structure in membrane bioreactor. Bioresources Technology 133, 462–468.

Puspitasari, V., Granville, A., Le-Clech, P., Chena, V., 2010. Cleaning and ageing effect of sodium hypochlorite on polyvinylidene fluoride (PVDF) membrane. Separation and Purification Technology 72, 301–308.

Schippers, J., Verdouw, J., 1980. The modified fouling index: a method of determining the fouling characteristics of water. Desalination 32, 137-148.

Sioutopoulos, D., Yiantsios, S., Karabelas, A., 2010. Relation between fouling characteristics of RO & UF membranes in experiments with colloidal organic and inorganic species. Journal of Membrane Science 350, 62-82.

Steinhauer, T., Hanely, S., Bogendorfer, K., Kulozik, U., 2015. Temperature dependent membrane fouling during filtration of whey and whey proteins. Journal of Membrane Science 492, 364–370.

Taheri, A., Sim, L., Haur, C., Alkhondi, E., Fane, A., 2013. The fouling potential of colloidal silica and humic acid and their mixtures. Journal of Membrane Sceince 433, 112–120.

Villacorte, L., Ekowati, Y., Winters, H., Amy, G., Schippers, J., Kennedy, M., 2015. MF/UF rejection and fouling potential of algal organic matter from bloom-forming marine and freshwater algae. Desalination 367, 1–10.

Xiao, K., Wang, X., Huang, X., Waite, T., Wen, X., 2009. Analysis of polysaccharide, protein and humic acid retention by microfiltration membranes using Thomas' dynamic adsorption model. Journal of Membrane Science 342, 22–34.

Zhao, S., Zou, L., 2011. Effects of working temperature on separation performance, membrane scaling and cleaning in forward osmosis desalination. Desalination 278, 157–164.

Chapter 5

Effects of Feed Water Temperature on Irreversible Fouling of Ceramic Ultrafiltration Membranes

Mohammad T. Alresheedi* and Onita D. Basu*

*Department of Civil and Environmental Engineering, Carleton University, 1125 Colonel By Drive, Ottawa, ON, K1S 5B6, Canada.

Submitted to: Journal of Separation and Purification Technology

Abstract

Temperature is known to influence the filtration performance of membrane systems through its direct impact on water viscosity. This research demonstrates that the changes in natural organic matter (NOM) fouling behavior with temperature are over and beyond simple viscosity changes in water. Constant flux experiments were performed in a tubular ceramic ultrafiltration (UF) system at 5, 20, and 35 ºC. The unified membrane fouling index (UMFI) was used to identify NOM reversible and irreversible fouling mechanisms; while the modified UF fouling index (MFI-UF) was used to predict the fouling potential of NOM. The results showed that after correcting for viscosity to standard 20 ºC compared to 5 ºC, UMFI values were higher than expected and reflected the higher fouling irreversibility observed at the lower temperature. The lower water temperature resulted in an increase in NOM retention along with decrease in backwash and chemical cleaning effectiveness as determined by the UMFI and FEEM analyses. However, increased water temperature did not adversely impact existing backwash or chemical cleaning protocols. In addition, The MFI-UF exhibited the same trend as UMFI for establishing NOM fouling and retention,

and therefore, the MFI-UF method is suitable for use as fouling predictor with ceramic membrane systems.

Keywords: Ceramic ultrafiltration; Fouling indices; Irreversible fouling; Temperature

5.1 Introduction

Ceramic membranes are drawing increasing attention in drinking water treatment sectors as a cost competitive alternative to polymeric membranes (Samaei et al., 2018; Lee et al., 2014; Vasanth et al., 2013). This emerging technology takes advantage of superior chemical resistance that enables aggressive chemical cleaning and structural rigidity that alleviates problems associated with repetitive testing, repair, and replacement. However, similar to polymerics, ceramic membranes face several challenging issues. The most important of these is loss of flux as the result of fouling, which can cause major limitations in the performance of membranes (Chang et al., 2015). Membrane fouling involves the cumulative aggregation of different foulants such as NOM, inorganic substances, colloidal species, and microorganisms on membrane surfaces or within their matrices, which can degrade their performance as well as decrease longevity (Cui et al., 2017). Among these foulants, the presence of NOM, such as humic, protein, and polysaccharide substances, is considered one of the major foulants that causes both reversible and irreversible fouling of membranes in water filtration (Chang et al., 2015; Hashino et al., 2011; Katsoufidou et al., 2007). Irreversible fouling is more problematic, necessitating chemical cleaning. However, limiting or avoiding chemical cleaning is recommended because of the detrimental effects of excess chemicals on membrane lifetime and the additional operational costs (Chang et al., 2015).

Many factors, including raw water characteristics, operational and environmental conditions (i.e., water temperature and pH), can negatively impact membrane performance and fouling (Cui et al., 2017; Lee et al., 2014). Among these factors, feed water temperature is an important operating parameter that has effects on membrane filtration, due to the nature of seasonal changes in the temperature of raw water. Temperature has a direct impact on water density and viscosity, which influence membrane flux. As viscosity and density increase, the transmembrane pressure (TMP) that is required to pass the water through the membrane also increases, which results in a decrease in membrane permeability. However, the effect of temperature on water properties is not sufficient to fully explain the drop in membrane flux and permeability and often overlooked in the study of membrane fouling.

Previous studies addressing the impacts of feed water temperature with membranes were commonly done with high pressure nanofiltration (NF) and reverse osmosis (RO) membrane systems (Roy et al., 2017; Zhao et al., 2011; Jin et al., 2009) or membrane bio reactor (MBR) systems (Ma et al., 2013; Van den Brink et al., 2011) and more focused on inorganic scaling and biofouling challenges with operation at temperatures greater than 20 °C but not changes in reversible and irreversible NOM fouling behavior. In fact, limited studies exist that examine the impact of temperature below 20 °C with low pressure membranes (Stade et al., 2015; Steinhauer et al., 2015; Farahbakhsh et al., 2006). Farahbakhsh et al. (2006) found that current standards for membrane integrity testing overestimated safety design values by not taking into account temperatures below 5 °C. Thus, thousands of dollars are wasted each year in membrane filtration plants to replace

damaged membranes, because the negative effects of cold water on membrane performance and fouling are often overlooked (Cui et al., 2017). Despite some studies that have showed the effect of different temperatures on membrane performance and permeability, to our best knowledge, no attention has been paid to the impacts on reversible and irreversible NOM fouling and cleaning mechanisms of low pressure membranes. In addition, while previous studies on temperature impact were focused on polymeric membranes, the emerging market of ceramic membranes for drinking water has received little attention in this area but is important for their implementation for drinking water treatment applications.

From a water quality testing perspective, fouling index methods are commonly used to quickly assess the fouling tendency of membrane feed water at the design stage and/or pretreatment requirements. The silt density index (SDI) and modified fouling index (MFI), using a 0.45μm membrane, are commonly utilized as fouling predictors and for quality control during membrane operation (ASTM 2014; Schippers et al., 1980). Boerlage et al. (2002) developed the MFI–UF, making use of a 13 kDa hollow fiber ultrafiltration (UF) membrane to count for particles < 0.45 μm. Feed water having an MFI-UF < 3000 s/L^2 is equivalent to SDI < 3 %/min, which is considered acceptable for membrane feed to control fouling (Boerlage et al., 2002). A number of studies applied the MFI-UF for assessing the fouling propensity with RO membrane systems (Taheri et al., 2013; Jeong et al. 2015; Villacorte et al., 2015). These studies have focused on particulate, inorganic scaling and biofouling with RO systems. Furthermore, in these studies, flat sheet UF membranes were used for the MFI-UF testing instead of hollow fiber membranes. In fact, the usability of the

MFI-UF with the hollow fiber membrane method for NOM fouling under changes in water temperature conditions and its applicability with ceramic membranes has yet to be examined.

The unified membrane fouling index (UMFI) model (Huang et al., 2008) is commonly used to quantify fouling based on reversibility and irreversibility components. Thus, unlike the MFI-UF, the UMFI provides information on the current fouling a membrane is subjected to. The actual capacity of the MFI-UF and UMFI to be effectively used as fouling assessment methods with ceramic membranes has yet to be evaluated in general and under changing water temperature conditions. In this research, the effect of feed water temperature (5, 20, and 35 °C) on the filtration performance, irreversible fouling and chemical cleaning of a ceramic UF membrane were examined. The MFI-UF method was used to assess its effectiveness for predicting NOM fouling while the UMFI method was utilized to assess for respective changes in reversible and irreversible fouling ratios under changing water temperature conditions.

5.2 Materials and Methods

5.2.1 Feed water solution

A synthetic feed water solution comprised of a mixture of three different NOM components: humic substances (humic acids), protein (bovine serum albumin, BSA); and polysaccharide (sodium alginate) was used for this study. These NOM model components are commonly found in surface water and have been previously used in membrane fouling studies (Chang et al., 2015; Hashino et al., 2011; Katsoufidou et al., 2007). The total

organic carbon (TOC) concentration in the feed water was 2.5 mg C/L (i.e. 0.83 mg C/L/ each NOM model) and was chosen to simulate the organic matter content in surface water (Chang et al., 2015). A moderate hardness of 75 mg/L calcium carbonate ($CaCO_3$) and a low level of turbidity (5 NTU) as kaolin clay particles were included in the synthetic water matric to represent the more complex conditions of a surface water source (Lee et al., 2014; Jermann et al., 2008). All chemicals were purchased from Sigma Aldrich. Feed water solutions were prepared in DI water and were mixed using a magnetic stirrer one-day prior any experiment to ensure that materials were dissolved completely. Feed water was continuously mixed using a VWR dual speed mixer to ensure homogeneous water conditions throughout the experiment. The pH of the feed was adjusted as needed to 7.5 with NaOH.

5.2.2 Ceramic UF fouling and cleaning experiments

Experiments were conducted under constant flux condition with an automated filtration system (Figure 5.1). Labview program code (National Instruments, NI) was created to operate the system automatically such as controlling the feed pump to have a constant flux, and automatically switches from filtration cycles to backwash cycles while recording flux and pressure data. Detailed information of the ceramic UF setup and equipment is described by Alresheedi et al. (2019). A tubular ceramic UF membrane (Ceramem^{TM}, Veolia) was used and its characteristics are as follows: monolithic module, SiC membrane material, inside-out channels (61), square channel (2 mm), pore size (0.01 μm), area (0.1 m^2), and module length (300 mm).

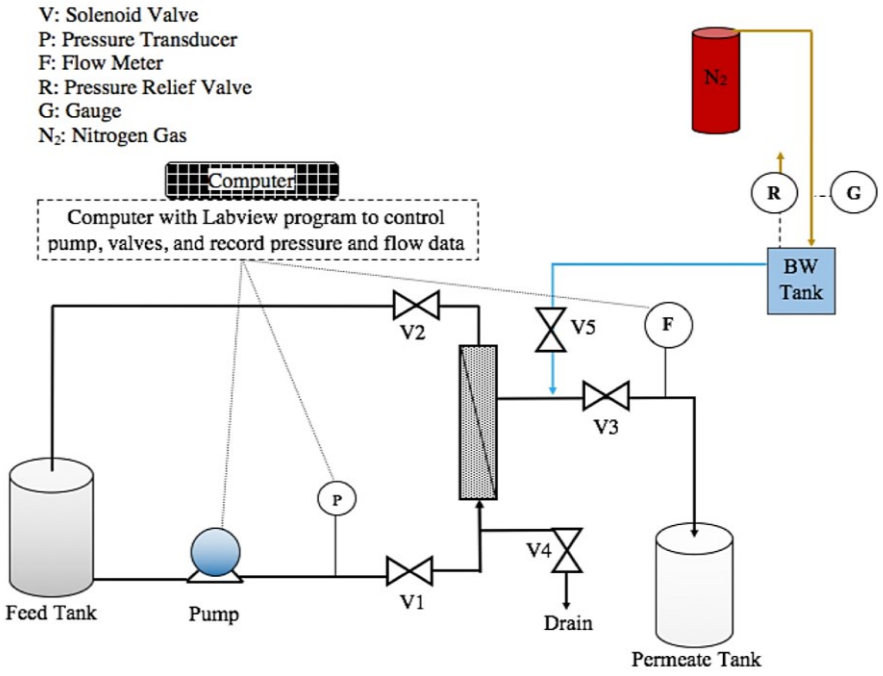

Figure 5.1 – A schematic representation of the ceramic UF setup

The ceramic membrane was fouled for 24 hours in dead-end filtration mode under constant flux of 100 LMH; backpulses were conducted for 20 seconds every 4 hours (0.4 m^3/m^2) using pressurized DI water at 2 bars (~30 psig) at room temperature. To assess the potential seasonal impacts of water temperature on ceramic UF fouling and cleaning, feed water temperature was assessed at 5, 20, and 35 ºC. Temperature was controlled either using an immersion heater (Cole Palmer) or a compact chiller (LM series, Polyscience). The feed tank was insulated to maintain constant temperature throughout the testing period. Temperature were monitored using HACH temperature probe (cat.no. 58258-00) HQd Field Case equipment. Equation 5.1 (Crittenden et al., 2005) was used to correct flux measured at different temperature to standard temperature of 20 °C. Experiments were performed in triplicates for each testing condition.

$$J_{20\,^{o}C} = J_m\,(1.03)^{T_{20^{o}C} - T_m} \qquad \text{Equation (5.1)}$$

$J_{20\,^{o}C}$ and $T_{20\,^{o}C}$ are the flux and temperature at 20 ºC, respectively. J_m and T_m are the measured flux and temperature respectively. After each fouling experiment, chemical cleaning (Clean in place, CIP) was performed according to the manufacturer recommendations using an oxidant, sodium hypochlorite (NaOCl, 500 mg Cl_2/L) followed by citric acid. Each cleaning step was performed for 4 hours. CIP wash water chemicals were prepared in 4 L of DI water and were recirculated for 1 hour followed by 3 hours soak. A clean water flux (CWF) test was then performed to determine the initial membrane resistance using the TMP versus flux relationship for a clean membrane.

5.2.3 Analysis

5.2.3.1 The unified membrane fouling index (UMFI)

To assess ceramic membrane fouling and cleaning performance, the UMFI model, Equation 5.2 (Huang et al., 2008) was applied to quantify each contributing fouling resistance.

$$\frac{1}{J_s'} = 1 + (\text{UMFI}) \text{x}\, V_S \qquad \text{Equation (5.2)}$$

Where J_s' is the normalized specific flux (i.e. measured specific flux (J_s) divided by initial specific flux (J_{s0}), (unitless), UMFI is an estimate of the extent of fouling (m^{-1}), and V_S (m^3/m^2) is the specific permeate volume. Total fouling index ($UMFI_f$) was calculated by using data from the entire filtration cycle (i.e., using the slope of the linear region of 1/ J_s'

versus V_s graph from the start to end of filtration. Using the procedure described in greater detail by Huang et al. (2008), hydraulically irreversible fouling index ($UMFI_{hir}$), that was remained after backwash, and chemically irreversible fouling index ($UMFI_{cir}$), that was remained after chemical cleaning, were also calculated using data collected after the hydraulic backwash and after the CIP procedure, respectively. Hydraulically reversible fouling index ($UMFI_{hr}$), that was removed by backwash, was calculated from the difference between $UMFI_f$ and $UMFI_{hir}$. Chemically reversible fouling index ($UMFI_{cr}$), that was removed by chemical cleaning, was calculated from the difference between $UMFI_{hir}$ and $UMFI_{cir}$. Consequently, $UMFI_f$ was fractionated to reversible and irreversible fouling as described in Equation 5.3.

$$\underbrace{UMFI_f}_{\textbf{Total}} = \underbrace{UMFI_f - UMFI_{hir}}_{\textbf{UMFI}_{hr}} + \underbrace{UMFI_{hir} - UMFI_{cir}}_{\textbf{UMFI}_{cr}} + \underbrace{UMFI_{cir}}_{\textbf{Chemically irreversible}} \qquad \text{Equation (5.3)}$$

Changes in the backwash and chemical cleaning efficiencies with temperature were assessed using the hydraulically reversible to irreversible ratios ($UMFI_{hr}/UMFI_{hir}$) and chemically reversible to hydraulically irreversible ratios ($UMFI_{cr}/UMFI_{hir}$), respectively.

5.2.3.2 Specific cake resistance

The intrinsic resistance (R_m) of a clean membrane was determined by filtering DI water through the ceramic membrane at a low flux (J) and after recording the pressure (ΔP_0) for 30 minutes, the flux was increased and the procedure continued in a stepwise fashion. Equation 5.4 was used to estimate R_m. μ is the water viscosity.

$$J = \frac{\Delta P_0}{\mu R_m} \qquad \text{Equation (5.4)}$$

For fouled membrane, assuming cake filtration is the dominant fouling mechanism, cake filtration mechanism can describe the pressure increase and membrane fouling. Equation 5.4 can be rewritten as:

$$J = \frac{\Delta P}{\mu (R_c + R_m)} \qquad \text{Equation (5.5)}$$

ΔP is final transmembrane pressure (kPa); R_c is the cake layer resistance (m^{-1}). The R_c can be expressed in terms of the specific cake resistance αc (m/kg), the bulk concentration, C_b (kg/m^3), and the specific permeate volume (V_s), as follows:

$$Rc = \alpha_c C_b V_s \qquad \text{Equation (5.6)}$$

Equation 5.7 (Chellam et al., 2006) can be used to express the increase in pressure at constant flux during cake filtration:

$$\Delta P = (J.\mu)(\alpha_c . C_b . V_s + R_m) = \Delta P_0 + (J . \mu . C_b . V_s)\alpha_c \qquad \text{Equation (5.7)}$$

5.2.3.3 Carbon and fluorescence excitation and emission matrix (FEEM) analyses

NOM retention at different water temperature conditions was determined by performing total organic carbon (TOC) analysis (using a Shimadzu TOC-VCPH/ CPN analyzer) on samples from feed and permeate water. NOM retention was then calculated using Equation 5.8.

$$\text{NOM Retention} = \left(\frac{Feed_C - Permeate_C}{Feed_C}\right) \text{x } 100 \qquad \text{Equation (5.8)}$$

Where $Feed_C$ is the carbon concentration in feed water; $Permeate_C$ is the carbon concentration in permeate water. Multiple TOC samples were taking during filtration time and the average TOC values were used to calculate the percentage NOM retention.

A carbon mass balance was performed to determine indirectly the carbon mass remaining on the membrane before and after backwashing and chemical cleaning. This was done by performing TOC analysis on feed, permeate, hydraulic backwash and chemical wash waters. The mass of hydraulically irreversible carbon, which refer to the foulants remained on the membrane after filtration and before chemical cleaning, was determined using Equations 5.9. The hydraulically irreversible carbon was further divided into chemically reversible and irreversible, which refer to the foulants removed by chemical cleaning and foulants remained on the membrane after chemical cleaning, respectively (as shown in Equation 5.10).

$$(C_{hir}.V_{hir}) = (C_f.V_f) - (C_p.V_p) - (C_{hr}.V_{hr}) \qquad \text{Equation (5.9)}$$

$$(C_{hir}.V_{hir}) = (C_{cr}.V_{cr}) + M_{cir} \qquad \text{Equation (5.10)}$$

Where: C (mg C/L) is the carbon concentration; V (L) is the water volume; f, p, hr, hir, cr, and M_{cir} denote feed water, permeate, hydraulically reversible (i.e. in backwash water), hydraulically irreversible (i.e. remained on membrane after backwash and before chemical cleaning), chemically reversible (i.e. in chemical wash water), and chemically irreversible (i.e. remained on membrane after chemical cleaning), respectively. The percentage error of the carbon measurements was calculated to ensure accurate mass balance at different

testing conditions. Backwash and chemical cleaning efficiencies were assessed using the hydraulically reversible to irreversible carbon mass ratios ($C_{hr}.V_{hr}$ / $C_{hir}.V_{hir}$) and chemically reversible to hydraulically irreversible carbon mass ratios ($C_{cr}.V_{cr}$ / $C_{hir}.V_{hir}$), respectively. Carbon data was then compared to the fouling indices data estimated by the UMFI method.

Additionally, FEEM analysis was performed on water samples from feed, permeate, backwash, and chemical wash waters for qualitative insights into NOM fouling and cleaning at different temperature conditions examined. For each sample, the fluorescence was measured by scanning the excitation wavelengths from 250 to 350 nm in 2 nm steps and detecting the emission intensity in 10 nm steps between 250 and 600 nm using Cary Eclipse Fluorescence Spectrophotometer (Varian, Surrey, UK). Excitation and emission slit widths were 5 nm. Each measurement was carried out in standard quartz cuvette (1.0 cm path length).

5.2.3.4 MFI-UF fouling index

Fouling potential of the NOM mixture solution from the ceramic UF membrane experiments was assessed using the MFI-UF method (Boerlage et al., 2002). The MFI-UF setup is described in detail by Boerlage et al. (2002) and Alresheedi et al. (2018). A hollow fiber polymeric UF membrane was used for the MFI-UF testing (proposed by Boerlage et al., 2002), with the following characteristics: molecular weight cut off (13 kDa); membrane materials (PAN); inside out; fiber inside diameter (0.8 mm); fiber outside diameter (1.4

mm); number of fibers (400); membrane area (0.2 m^2); module length (347 mm); module diameter (42 mm).

MFI-UF testing was determined by filtering feed water through the hollow fiber UF membrane under dead-end mode and constant pressure of 2 bars. Permeate water was collected in a tank set on an electronic balance to acquire permeate volume (V) and filtration time (t) data from the balance. The MFI-UF was then calculated using Equation 5.11 (rewritten in Equation 5.12) (Boerlage et al., 2002). Where t is the filtration time (s); V is permeate produced (m^3); ΔP is the pressure (bar); μ is the viscosity of water (kg/m s); A is the membrane area (m^2); R_m is the membrane resistance (m^{-1}); α_c is the specific cake resistance (m/kg); and C_b is the bulk concentration (kg/m^3). d(t/V)/dV is the slope of two data points in the linear region (cake filtration region) of t/V versus V graph (described in detail by Alresheedi et al. 2018; Boerlage et al. 2002). The MFI-UF test were performed under 5, 20, and 35 °C water temperature.

$$\frac{t}{V} = \frac{\mu R_m}{\Delta P A} + \left(\frac{\mu C_b \alpha_c}{2 \Delta P A^2}\right) V = \frac{\mu R_m}{\Delta P A} + \text{MFI} - \text{UF} \ (V) \qquad \text{Equation (5.11)}$$

Which can be rewritten as

$$\text{MFI-UF} = \left(\frac{\mu C_b \alpha_c}{2 \Delta P A^2}\right) = \frac{d\left(\frac{t}{V}\right)}{dV} \qquad \text{Equation (5.12)}$$

5.2.3.5 Statistical analysis

Fouling and cleaning data obtained at different water temperature conditions were analyzed with the statistical program SPSS 22.0. One-way ANOVA (using the F-test) was performed

on the data collected. The mean difference between conditions was considered to be significant at a p-value of ≤ 0.05.

5.3 Results and Discussion

5.3.1 Effect of feed water temperature on ceramic UF fouling

Figure 5.2 illustrates the effect of water temperature variation on ceramic UF fouling. The data shown in Figures 5.2A and 5.2B are the experimental $UMFI_f$ ($UMFI_f$ (exp)), which represents the $UMFI_f$ graph at temperature (T), and the normalized $UMFI_f$ ($UMFI_f$ (nor)), which represents the $UMFI_f$ graph normalized to 20 ºC to account for changes in water viscosity using Equation 5.1, respectively. Therefore, the difference in $UMFI_f$ (nor) values at different temperature is due to fouling. It can be clearly seen that with decreasing water temperature from 20 °C to 5 °C, the $UMFI_f$ (exp) of the NOM mixture (Figure 5.2A) increased from 6.9E-01 to 12.5E-01 m^{-1}; while $UMFI_f$ (exp) decreased from 6.9E-01 to 4.6E-01 m^{-1} when the temperature increased from 20 ºC to 35 °C. According to Darcy's law, the flux is a function of filtration pressure, membrane resistance, and the viscosity of water, therefore, water temperature has a great effect on flux because as both the membrane resistance and viscosity are temperature dependent. The increase in $UMFI_f$ (exp) with decreasing temperature at constant flux filtration could be partially attributed to the increase in solution viscosity combined with increase in resistance of the membrane material, which then resulted in higher $UMFI_f$ (exp) value (Cui et al., 2017; Lee et al., 2013). However, Figure 5.2B shows that the changes in NOM fouling with temperature are over and beyond simple viscosity changes of water. The $UMFI_f$ (nor) values (i.e. after correcting for viscosity) showed that at 5 °C, the fouling index was 10.5E-01 m^1 which was

significantly higher than that at 20 ºC ($UMFI_f$ (nor) of 6.9E-01 m^{-1}) ($p < 0.05$); while the $UMFI_f$ (nor) value at 35 °C decreased to 6.0 E-01 m^{-1}. Therefore, the increase or decrease in the $UMFI_f$ (exp) values with temperature was not solely attributed to changes in water viscosity.

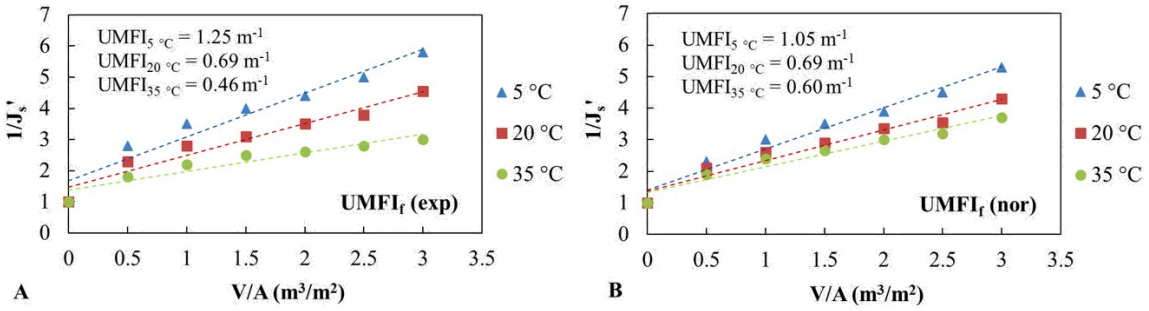

Figure 5.2 – Changes in the UMFI fouling index at different water temperature.
(A) $UMFI_f$ (exp): UMFI before viscosity correction; **(B)** UMFI (nor): UMFI after viscosity correction

Figure 5.3 shows the changes in the UMFI values due to viscosity changes versus fouling with temperature. The $UMFI_f$ (nor) values showed that at 5 °C, only 43% of the increased in fouling index was attributed to the high viscosity of water; whereas 57% was due to fouling. Also, at 35 °C, 64% of the decreased in fouling index was attributed to the low viscosity of water whereas 36% was due to fouling. Thus, it is evident that the increase or decrease in the UMFI with temperature is due to changes in fouling behavior of NOM combined with changes in water viscosity.

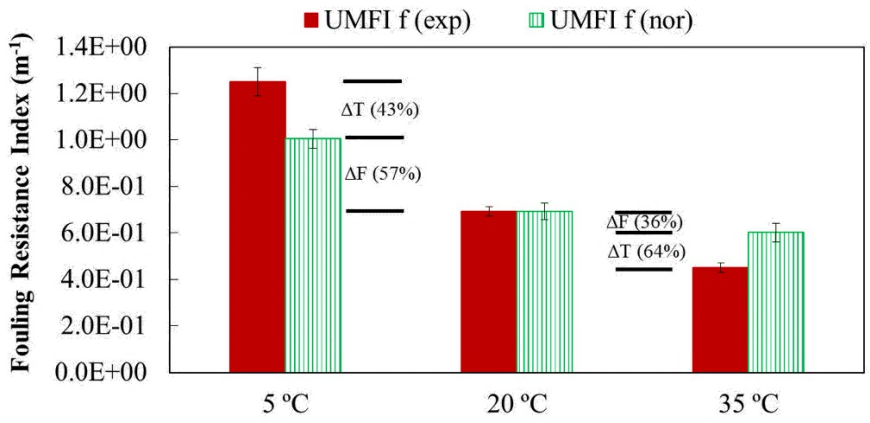

Figure 5.3 – Changes in $UMFI_f$ values due to changes in viscosity versus fouling with temperature*

*$UMFI_f$ (exp): experimental unified membrane fouling index; $UMFI_f$ (nor): normalized unified membrane fouling index. ΔT: changes in $UMFI_f$ due to viscosity changes; ΔF: changes in $UMFI_f$ due to fouling

Additionally, Table 5.1 shows that the specific cake resistance, α_c, value of the NOM mixture increased as feed water temperature decreased from 35 to 5 ºC. The higher α_c value at 5 ºC indicates an increase in foulant deposition on the ceramic membrane and the production of a cake layer with lower permeability and higher fouling resistance. The percentage NOM retained by the ceramic UF increased from 62% to 88% ($p < 0.05$) with decreasing temperature from 35 ºC to 5 ºC (refer to Table 5.1) and consistent with the α_c findings. The increase in NOM retention at lower temperature could be attributed to the changes in the fouling layer formed on the membrane and increase in NOM size, thus, more NOM were retained by the ceramic UF membrane and higher fouling occurred. Cui et al. (2017) study reported a decrease in polyvinylidene fluoride (PVDF) membrane diameter and membrane permeability and an increase in the intrinsic hydraulic resistance were observed for a membrane operated at cold water temperature (0.3 °C). Similarly, Jin

et al. (2009) reported higher NOM capture with RO systems in which the size of humic acid increased with decreasing water temperature. Therefore, temperature has an impact of both membrane properties and foulants.

Table 5.1– Estimated specific cake resistance and NOM retention values at different temperature (n=3)

Water Temperature	Specific Cake Resistance (α_c) ($x10^8$)	Retention (%)
5 ºC	17.21	88±2
20 ºC	14.62	78±6
35 ºC	13.08	62±4

FEEM analysis (Figure 5.4) was used to analyze samples from the ceramic UF permeate water at two different temperature conditions (5 ºC and 20 ºC). The FEEM analysis were used to provide qualitative information on NOM retention with temperature. Higher FEEM intensities indicate more NOM in the water, thus, lower permeate quality. The fluorescence peaks for humic-like substances are reported from 250-390 nm (range of excitation) and between 400-500 nm (range of emission). The fluorescence peaks for protein/polysaccharides-like substances are from 230-290 nm (range of excitation) and between 300-360 nm (range of emission) (Matilainen et al., 2011). In Figure 5.4, the fluorescence intensities/peaks of the NOM mixture permeate water at 5 ºC were 18.2 au for humic acid and 21.7 au for proteins/alginate. At 20 ºC, the FEEM intensities for humic acid in the permeate water increased to 25.6 au whereas much higher protein/alginate substances were found in the permeate water (38.6 au) indicating lower NOM retention at

20 ºC compared to 5 ºC. Van den Brink et al. (2011) study with MBR systems found that with decreasing temperature, a shift was found in polysaccharides particle size distribution which led to high retention and fast pore blocking, thus, higher fouling at lower temperature. The FEEM results correlate well with the $UMFI_f$ values (Figure 5.3) and NOM retention data (Table 5.1) demonstrating the effect of temperature on NOM retention by the ceramic UF membrane and the quality of permeate water.

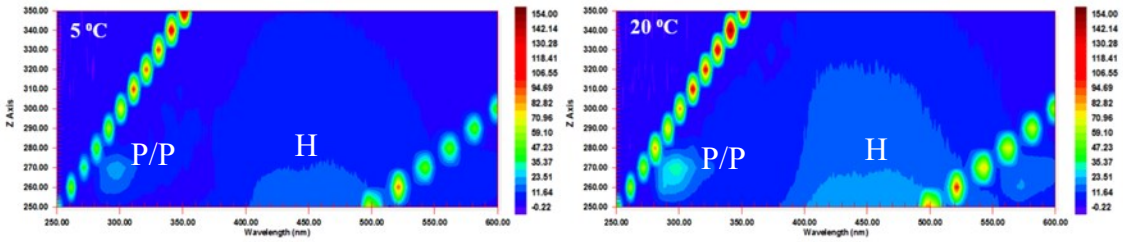

Figure 5.4 – FEEM images of the ceramic UF permeate of NOM mixture at 5 and 20 °C. P/P: (proteins, BSA/ polysaccharides); H: (humics)

5.3.2 Impact of feed water temperature on backwash and chemical cleaning effectiveness

The overall UMFI analysis showed an impact of water temperature on NOM fouling; this can be further categorized by the reversible and irreversible fouling fractions to help assess backwash and chemical cleaning effectiveness. Figure 5.5 demonstrates that with decreasing temperature from 20 ºC to 5 ºC, the hydraulically irreversible fouling index ($UMFI_{hir}$) increased by 35% ($p < 0.05$), whereas the $UMFI_{hir}$ decreased by 15% ($p < 0.05$), with increasing temperature from 20 ºC to 35 ºC. Thus, the increase in NOM fouling at lower temperature was due to the higher irreversible accumulation of NOM which resisted hydraulic backwashes. That is the temperature drop not only increases fouling due to

hydraulic resistance with the increased water viscosity; but also the very nature of the NOM alters with the drop in water temperature and some fraction of the NOM shifts from reversible at 20 C to irreversible at 5 C. This is reflected in the hydraulically reversible fouling index ($UMFI_{hr}$) data in which the backwash efficiency was lower at 5 ºC and increased as temperature increased from 5 to 35 ºC. The chemically irreversible fouling index ($UMFI_{cir}$) was the highest at 5 ºC indicating lower chemical cleaning efficiency at the lower temperature. Irreversibility of the foulant layer is a major concern during membrane filtration, as it influences physical and chemical cleaning requirements. The significant amount of hydraulically and chemically irreversible fouling at 5 ºC pose a potential limitation to longer membrane operation.

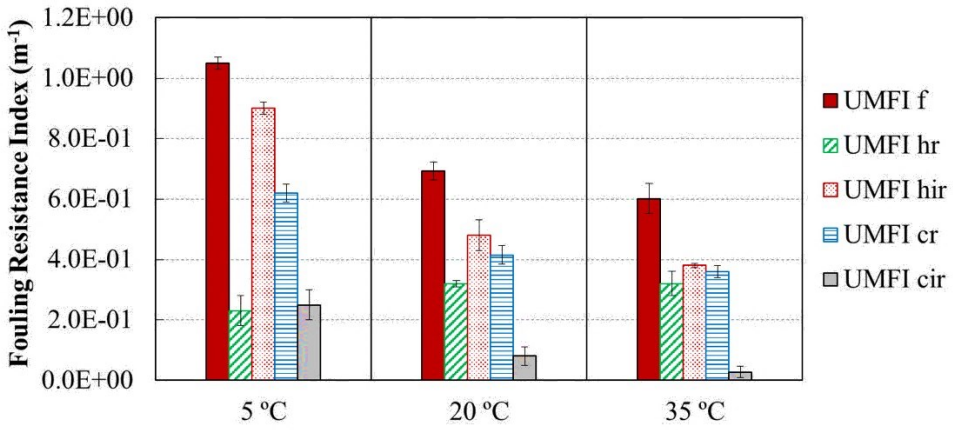

Figure 5.5 – UMFI fouling indices at different water temperature conditions*

*Note: $UMFI_{hr}$: unified hydraulically reversible fouling index; $UMFI_{hir}$: unified hydraulically irreversible fouling index $UMFI_{cr}$: unified chemically reversible fouling index; $UMFI_{cir}$: unified chemically irreversible fouling index

Figure 5.6 shows the hydraulically reversible to irreversible fouling ratios ($UMFI_{hr}/UMFI_{hir}$) and carbon ratios (C_{hr}/C_{hir}) at different temperature. With decreasing

water temperature from 20 °C to 5 °C, the $UMFI_{hr}/UMFI_{hir}$ ratio of the NOM mixture decreased from 0.62 to 0.35 ($p < 0.05$). The decreased in the $UMFI_{hr}/UMFI_{hir}$ at lower temperature indicated lower hydraulic backwash efficiency, thus, higher NOM hydraulically irreversible fouling. This can be supported by the carbon data in which the C_{hr}/C_{hir} ratio decreased from 0.45 to 0.31 with decreasing temperature from 20 °C to 5 °C. Thus, the backwash pressure applied to mitigate fouling at standard feed water temperature of 20 °C was not sufficient in removing NOM fouling deposits at 5 °C. This is consistent with the increase in specific cake resistance and NOM retention values at lower temperature (refer to Table 5.1). The $UMFI_{hr}/UMFI_{hir}$ and C_{hr}/C_{hir} ratios at 35 °C increased to 0.71 and 0.66, respectively, indicating more effective backwash at higher temperature. This could be partially attributed to the lower cake resistance and NOM retention at 35 °C (refer to Table 5.1), hence, better cleaning.

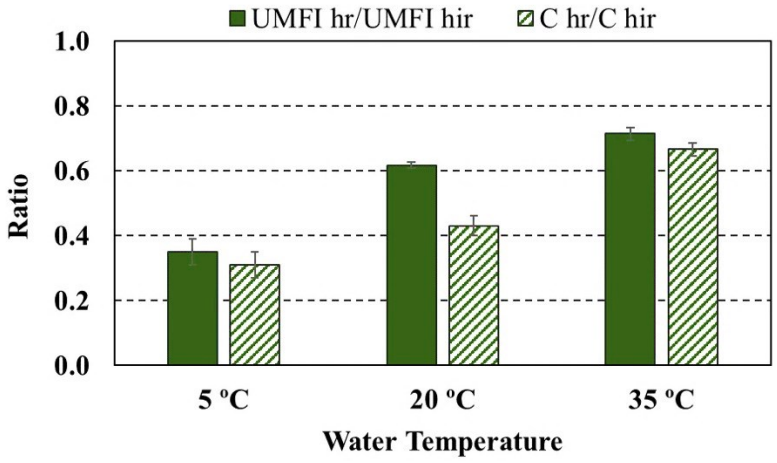

Figure 5.6 – Effect of water temperature on backwash efficiency*

$UMFI_{hr}/UMFI_{hir}$: hydraulically reversible to irreversible fouling ratios; C_{hr}/C_{hir}: hydraulically reversible to irreversible carbon ratios.

*Note: The higher the $UMFI_{hr}/UMFI_{hir}$ ratio, the higher the backwash efficiency; the higher the C_{hr}/C_{hir} ratio, the higher the removed carbon mass

The results from the UMFI analysis can be supported by the FEEM plots of the NOM mixture backwash water (Figure 5.7). At 20 ºC, the fluorescence intensities/peaks for humic acid and proteins/alginate were 27.6 au and 37.1 au, respectively; while at 5 ºC, the fluorescence intensities/peaks for humic acid in the backwash water was 24.2 au and surprisingly no proteins/alginate were found in the backwash water at 5 ºC. By comparing the FEEM plots of the permeate water (Figure 5.4) and the backwash water (Figure 5.7) at 5 ºC, it is clear that proteins/alginate substances resisted hydraulic backwash and caused irreversible fouling for the ceramic UF. Van den Brink et al. (2011) and Ma et al. (2013) studies found that lower temperature had negative impacts on proteins and polysaccharides substances and biofouling in MBR systems. Therefore, both proteins and polysaccharides are problematic for membrane systems and more impacted by water temperature condition than humic substances. The FEEM plots correlate well with the $UMFI_{hr}/UMFI_{hir}$ ratios (Figure 5.6) demonstrating the effect of temperature on the NOM reversibility and irreversibility. Therefore, it is recommended to alter membrane backwash procedure with temperature (i.e. by increasing backwash pressure, frequency, etc.,) to better control membrane fouling.

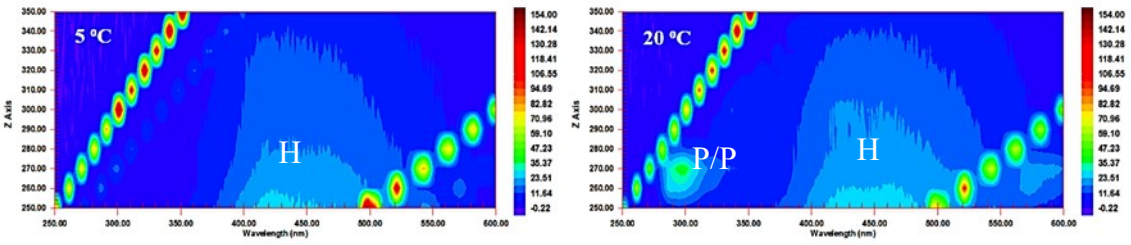

Figure 5.7 – FEEM images of the ceramic UF backwash water of NOM mixture at 5 and 20°C. P/P: (proteins, BSA/ polysaccharides); H: (humics)

Figure 5.8 shows the chemical cleaning CIP efficiency at different feed water temperature conditions. The $UMFI_{cr}/UMFI_{hir}$ and C_{cr}/C_{hir} ratios under the operation at 5 °C was 0.78 and 0.58, respectively; while the ratios at 20 °C were significantly higher, 0.92 and 0.81, respectively ($p < 0.05$). Thus, chemical cleaning was not effective in removing irreversible fouling at 5 °C whereas at 20 °C, the foulants were effectively removed. The decrease in the cleaning efficiency at 5 °C is attributed to the high irreversible fouling (refer to Figure 5.5). At 35 °C, cleaning of the ceramic membrane was easier than 5 °C and 20 °C conditions resulting in higher $UMFI_{cr}/UMFI_{hir}$ and C_{cr}/C_{hir} ratios of 0.96 and 0.87, respectively.

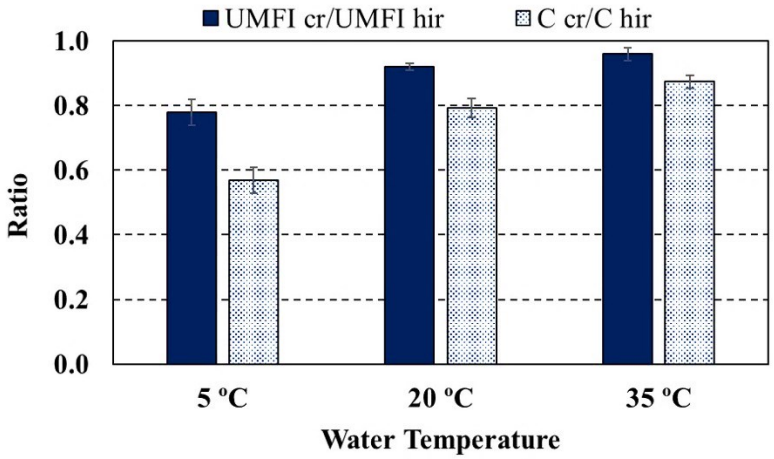

Figure 5.8 – Effect of water temperature on chemical cleaning efficiency*
$UMFI_{cr}/UMFI_{hir}$: chemically reversible to hydraulically irreversible fouling ratios; C_{cr}/C_{hir}: chemically reversible to hydraulically irreversible carbon ratios.
*Note: The higher the $UMFI_{cr}/UMFI_{hir}$ ratio, the higher the cleaning efficiency; the higher the C_{cr}/C_{hir} ratio, the higher the removed carbon mass

FEEM plots of the NaOCl chemical wash water (Figure 5.9), were used to qualitatively assess the cleaning efficiency at different temperature. At 5 °C condition, higher intensities of humic acid (32.6 au) but much lower intensities for BSA/alginate (18.4 au). FEEM

intensities at 20 °C for humic acid was 29.8 au which was approximately similar to that at 5 °C, while much higher FEEM intensities for BSA/alginate (38.1 au). These results indicate that the lower cleaning efficiency at 5 °C is attributed to the higher irreversible mass of BSA/alginate in the NOM mixture solution. Therefore, alteration of membrane chemical cleaning procedure at lower temperature is recommended to control chemically irreversible fouling and achieve higher permeability recovery. Chemical cleaning procedure was effective at both 20 °C and 35 °C ($p > 0.05$), refer to Figure 5.8, indicating that chemical cleaning procedure used at standard temperature (20 °C) should be sufficient at 35 °C when needed.

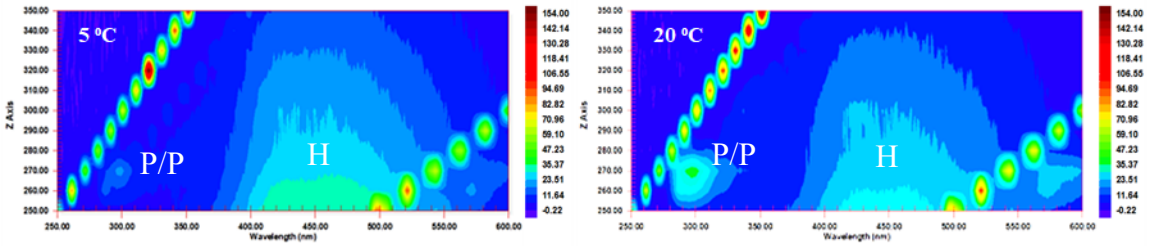

Figure 5.9– FEEM images of the ceramic UF NaOCl wash water of NOM mixture at 5 and 20 °C. P/P: (proteins, BSA/ polysaccharides); H: (humics)

5.3.3 Suitability of the MFI-UF index for fouling prediction with ceramic membranes

The MFI-UF and UMFI methods are used to evaluate membrane fouling, however, the different approaches in fouling assessment may suggest that direct comparison lack context. The MFI-UF provides an index value that indicates the fouling tendency of membrane feed whereas the UMFI provides information on the current fouling a membrane is subjected to (i.e. reversible vs. irreversible). Feed water having an MFI-UF < 3000 s/L^2 (equivalent to an SDI < 3 %/min), is considered acceptable for membrane feed (Boerlage

et al., 2002). However, the actual capacity of the MFI-UF to be used effectively as a prediction tool with NOM fouling for ceramic membranes has yet to be evaluated in general and under changing water temperature conditions.

Figure 5.10 shows the fouling index values (Figure 5.10A), specific cake resistances (Figure 5.10B), and NOM retention (Figure 5.10C) at different water temperature conditions as predicted by the MFI-UF testing. The MFI-UF values and specific cake resistances were calculated following the procedure described in section 5.2.3.4. The results in Figure 5.10A show that the MFI-UF value of the NOM mixture decreased significantly ($p < 0.05$) as the water temperature increased from 5 to 35 °C , indicating lower fouling potential at higher temperature. NOM in cold water temperatures (i.e. 5 °C) appears to have higher fouling potential (MFI-UF of 10122 s/L^2) compared to that at warmer temperatures (MFI-UF of 6850 s/L^2 and 3774 s/L^2 for 20 °C and 35 °C, respectively). This could be a critical issue in assessing NOM fouling specifically in regions where there is a large seasonal variation in water temperature, as in North America and some parts of Europe. The decrease in water temperature caused changes to the cake layer that was formed and the amount of NOM retained by the ceramic UF as shown in Figures 5.10B and 5.10C. The specific cake resistance (α_c) was found to increase with decreasing temperature from 20 °C to 5 °C (Figure 5.10B) along with an increase in NOM retention (Figure 5.10C). Therefore, the increase in the MFI-UF value at the lower temperature was related to the impact of temperature on BSA and alginate size (as shown in the FEEM images), resulting in high NOM retention by the UF membrane and an

increase in specific cake resistance whereas at high temperature, NOM were passing through the UF membrane to the filtrate side, thus, lower fouling and MFI-UF value.

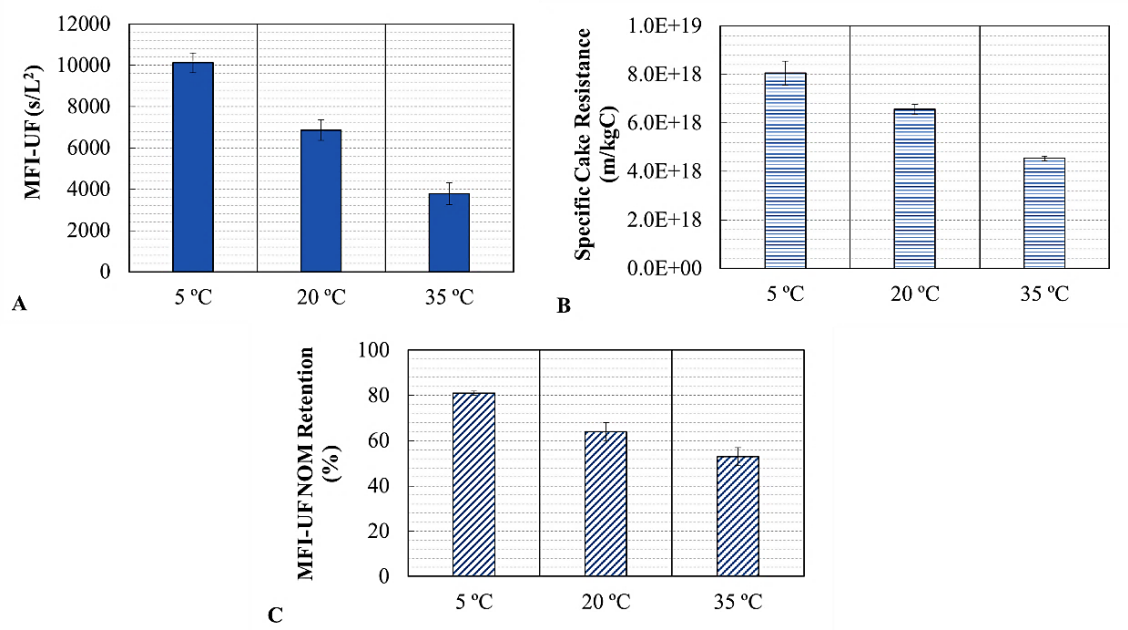

Figure 5.10 – (A) MFI-UF fouling index values at different temperature; **(B)** Changes in specific cake resistance with temperature based on the MFI-UF test; **(C)** NOM retention by the MFI-UF membrane at different temperature

Variation in water temperature demonstrated an impact on both the fouling potential of NOM (MFI-UF) and fouling mechanism (UMFI). Figure 5.11A shows that the MFI-UF fouling prediction trend is in agreement with the fouling tendency observed using the UMFI method. Moreover, Figures 5.11B and 5.11C show good correlations between specific cake resistance and NOM retention values obtained in the MFI-UF and ceramic UF systems, thus, the MFI-UF testing method demonstrates a useful fit for predicting NOM fouling and retention for ceramic membranes before relying on operating data (i.e. UMFI).

Although there are differences in the numerical values of specific cake resistances and NOM retentions which are attributed to the differences in membrane materials and characteristics, the MFI-UF is simple and short filtration test that can be used as a rapid assessment of NOM fouling compared to the UMFI analysis which normally requires long-term filtration data. Thus, a ceramic membrane plant could use the MFI-UF in addition to the UMFI to assess potential changes in NOM fouling with temperature and make required alternations in membrane pretreatment and/or cleaning procedures.

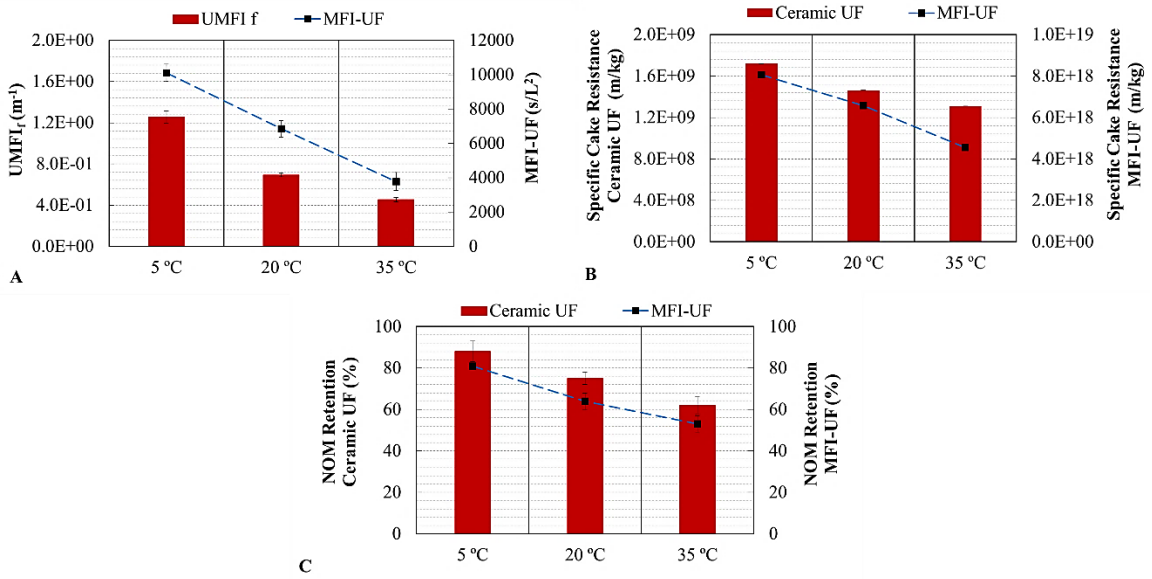

Figure 5.11 – (A) Relationship between $UMFI_f$ and MFI-UF fouling indices; **(B)** Specific cake resistance with temperature; **(C)** NOM retention by MFI-UF and ceramic UF membranes

5.4 Conclusions

Water temperature is an important design parameter for membrane systems. This research investigated the impact of water temperature on NOM fouling and cleaning of a tubular

ceramic UF membrane using the UMFI and MFI-UF fouling index methods. Key findings were:

- The effect of variation of feed water temperature on fouling of ceramic UF membranes was over and beyond simple viscosity changes of water. The $UMFI_f$ and NOM retention increased when the water temperature decreased from 35 °C to 5 °C due to changes in NOM fouling behavior and specific fouling resistance. Thus, fouling analysis performed at standard temperature (20 °C) will underestimate the impact of cold water condition on ceramic membranes performance.
- The reversible and irreversible fouling ratio ($UMFI_{hr}/UMFI_{hir}$) changed with temperature, thus, alteration of backwash procedure (i.e. increase or decrease in backwash pressure) with temperature is required to help control fouling and maintain membrane productivity.
- FEEM analysis demonstrated higher levels of protein removal with backwashing at 20 °C temperature versus 5 °C; and thus FEEM is useful in determining specific fouling components that can be addressed under site specific NOM and temperature changes.
- Changes in NOM fouling characteristics with temperature as predicted by the MFI-UF method demonstrated useful fit with the UMFI values and NOM retention data obtained in the ceramic UF system. Thus, the utilization of the MFI-UF proved to be useful for assessing the potential changes in NOM fouling behavior with temperature for ceramic membrane systems.

5.5 Acknowledgements

The authors would like to acknowledge the Saudi Arabia Ministry of Education (MOE) and Natural Sciences and Engineering Research Council of Canada (NSERC) for helping fund this research. We also wish to thank Geoff Seatter and Kerwin Lewis for their help with installation of the automated filtration system.

5.6 References

Alresheedi, M., Barbeau, B., Basu, O., 2019. Comparisons of NOM fouling and cleaning of ceramic and polymeric membranes during water treatment. Separation and Purification Technology 209, 452-460.

Alresheedi, M., Basu, O., 2018. Application of MFI-UF fouling index with NOM fouling under various operating conditions. Desalination and Water Treatment 133, 45-54.

ASTM International 2014. Standard test method for silt density index (SDI) of water. Designation: D4189 − 07.

Boerlage, S., Kennedy, M., Dickson, M., El-Hodali, D., Schippers, J., 2002. The modified fouling index using ultrafiltration membranes (MFI-UF): characterisation, filtration mechanisms and proposed reference membrane. Journal of Membrane Science 197, 1-21.

Chang, H., Qu, F., Liy, B., Yu, H., Li, K., Shao, S., Li, G., Liang, H., 2015. Hydraulic irreversibility of ultrafiltration membrane fouling by humic acid: Effects of membrane properties and backwash water composition. Journal of Membrane Science 493, 723-733.

Chellam, S., Wendong, X., 2006. Blocking laws analysis of dead-end constant flux microfiltration of compressible cakes. Journal of Colloid Interface Science 301, 248–257.

Crittenden J., Trussell R., Hand D., Howe K., Tchobanoglous G., 2005. Water Treatment: Principles and Design, 2nd edition, Ed, Wiley, New Jersey, USA.

Cui, L., Goodwin, C., Gao, W., Liao, B., 2017. Effect of cold water temperature on membrane structure and properties. Journal of Membrane Science 540, 19-26.

Farahbakhsh, K., Smith, D., 2006. Membrane filtration for cold regions – impact of cold water on membrane integrity testing. Journal of Environmental Engineering and Science 5, 69-75.

Foley, G., 2006. A review of factors affecting filter cake properties in dead-end microfiltration of microbial suspensions. Journal of Membrane Science 274, 38-46.

Hamad, J., Ha, C., Kennedy, M., Amy, G., 2013. Application of ceramic membranes for seawater reverse osmosis (SWRO) pre-treatment. Desalination and Water Treatment 51, 4881-489.

Hashino, M., Hirami, K., Ishigmi, T., Ohmukai, Y., Maruyama, T., Kubota, N., Matsuyama, H., 2011. Effect of kinds of membrane materials on membrane fouling with BSA. Journal of Membrane Science 384, 157-165.

Huang, H., Young, T.A., Jacangelo, J., 2008. Unified membrane fouling index for low pressure membrane filtration of natural waters: Principles and methodology, Environmental Science Technology 42 714–720.

Jeong, S., Vigneswaran, S., 2015. Practical use of standard pore blocking index as an indicator of biofouling potential in seawater desalination. Desalination 365, 8–14.

Jermann, D., Pronk, W., Boller, M., 2008. Mutual influences between natural organic matter and inorganic particles and their combined effect on ultrafiltration membrane fouling. Environmental Science and Technology 42, 9129-9136.

Jin, X., Jawor, A., Kim, S., Hoek, E., 2009. Effects of feed water temperature on separation performance and organic fouling of brackish water RO membranes. Desalination 239, 346–359.

Katsoufidou, K., Yiantsios, S.G., Karabelas, A.J., 2007. Experimental study of ultrafiltration membrane fouling by sodium alginate and flux recovery by backwashing. Journal of Membrane Science 300, 137-146.

Lee, H., Kim, S., Choi, J., Oh, H., Lee, W., 2013. Effects of water temperature on fouling and flux of ceramic membranes for wastewater reuse. Desalination and Water Treatment 51, 5222–5230.

Lee, S., Kim, J., 2014. Differential natural organic matter fouling of ceramic versus polymeric ultrafiltration membranes. Water Research 48, 43-51.

Ma, Z., Wen, X., Zhao, F., Xia, Y., Huang, X., Wait, D., Guan, J., 2013. Effect of temperature variation on membrane fouling and microbial community structure in membrane bioreactor. Bioresource Technology 133, 462–468.

Matilainen, A., Gjessing, E., Lathinen, T., Hed, L., Bhatnagar, A., Sillanpaa, M., 2011. An overview of the methods used in the characterisation of natural organic matter (NOM) in relation to drinking water treatment. Chemosphere 83, 1431–1442.

Roy, Y., Warsinger, D., Leinhard, J., 2017. Effect of temperature on ion transport in nanofiltration membranes: diffusion, convection and electro migration. Desalination, 420, 241–257.

Samaei, S., Gato-Trinidad, S., Altaee, A., 2018. The application of pressure-driven ceramic membrane technology for the treatment of industrial wastewaters – A review. Separation and Purification Technology 200, 198–220.

Schippers J., Verdouw J. 1980. the modified fouling index: a method of determining the fouling characteristics of water. Desalination 32, 137-148.

Stade, S., Kallioinen, M., Tuuva, T., Manttari, M., 2015. Compaction and its effect on retention of ultrafiltration membranes at different temperatures. Separation and Purification Technology 151, 211-217.

Steinhauer, T., Hanely, S., Bogendorfer, K., Kulozik, U., 2015. Temperature dependent membrane fouling during filtration of whey and whey proteins. Journal of Membrane Science 492, 364–370.

Taheri, A, Sim, L., Haur, C., Alkhondi, E., Fane, A., 2013. The fouling potential of colloidal silica and humic acid and their mixtures. Journal of Membrane Science 433, 112–120.

Van den Brink, P., Satpradit, O., Bentem, A., Zwijinenburg, A., Temmink, H., Loosdrecht, M., 2011. Effect of temperature shocks on membrane fouling in membrane bioreactors. Water Research 45, 4491-4500.

Vasanth, D., Pugazhenthi, G., Uppaluri, R., 2013. Cross-flow microfiltration of oil-in-water emulsions using low cost ceramic membranes. Desalination 320, 86-95.

Villacorte, L., Ekowati, Y., Winters, H., Amy, G., Schippers, J., Kennedy, M., 2015. MF/UF rejection and fouling potential of algal organic matter from bloom-forming marine and freshwater algae. Desalination 367, 1–10.

Zhao, S., Zou, L., 2011. Effects of working temperature on separation performance, membrane scaling and cleaning in forward osmosis desalination. Desalination 278, 157–164.

Chapter 6

Comparisons of NOM Fouling and Cleaning of Ceramic and Polymeric Membranes during Water Treatment

Mohammad T. Alresheedi[*], Benoit Barbeau[**], Onita D. Basu[*]

[*] Department of Civil and Environmental Engineering, Carleton University, 1125 Colonel By Drive, Ottawa, ON, K1S 5B6, Canada.

[**] Department of Civil, Geological and Mining Engineering, Polytechnique, C.P. 6079 Succursale Centre-Ville, Montreal, QC, H3C 3A7, Canada.

Published: Journal of Separation and Purification Technology

Abstract

This research examines the effect of various NOM fractions on ceramic and polymeric UF membranes performance in terms of fouling and cleaning. Fouling experiments were performed using five model solutions, humic acid, protein as bovine serum albumin (BSA), alginate with and without calcium, and a combined NOM mixture. Two chemical agents were selected: an oxidant (NaOCl) and caustic (NaOH). Fouling and cleaning behavior were assessed using the resistance in series (RIS) model, membrane permeability, carbon mass balance, and fluorescence excitation and emission matrix (FEEM) analysis. The results demonstrated that NOM fouling order of the ceramic UF was similar to polymeric UF with the following trend: NOM mixture ≈ BSA > alginate ± Ca^{+2} > humic acid. However, the backwash efficiency was 1.5x-2x higher for the ceramic UF in comparison to the polymeric UF, indicating a much higher hydraulic reversibility for the ceramic UF. A carbon mass balance in complement with FEEM plots determined that NOM removal

by the ceramic UF was ≈ 10% higher than the polymeric UF. Chemical cleaning was found to be effective for both membrane types. Thus, it was not possible to conclude, that the ceramic membrane demonstrated an advantage for chemical cleaning under the conditions studied.

Keywords: Ceramic UF; Polymeric UF; NOM fouling; Chemical cleaning; Carbon balance

6.1 Introduction

Membrane processes are considered a reliable option for drinking water production. However, fouling by NOM, such as humic acids, proteins and polysaccharide-like substances, is one of the greatest challenges in membrane-based drinking water processes (Hashino et al., 2011; Katsoufidou et al., 2010). Fouling includes the short and long term loss of membrane permeability. The short term fouling is the reversible accumulation of NOM and particulate matter that can be removed by hydraulic backwash and/or chemical cleaning. Long term fouling is the slower loss of permeability due to the irreversible sorption of materials that resists hydraulic backwash and/or chemical cleaning. Irreversible fouling, in particular, is an inevitable phenomenon that results in the deterioration of membrane performance, chemical cleaning and membrane replacements, and hence increases operational cost of membrane systems.

Over the past years, research efforts have been focused on understanding fouling with a goal of minimizing it while improving filtration performance. In order to do so, the role of membrane material (i.e. type, hydrophobicity, etc.) has been highlighted as an important

factor to minimize fouling (Hashino et al., 2011; Evans et al., 2008) with negatively charge/hydrophilic membranes being the preferred option for surface water treatment (Shao et al., 2011). In addition, the properties of NOM in water are considered an important factors that influences fouling. It was reported that hydrophobic NOM components, such as humic substances contributed to membrane fouling (Katsoufidou et al., 2005) while other studies found that polysaccharide-like substances, contributed to higher fouling than humic substances (Hashino et al., 2011; Katsoufidou et al., 2010). Synergy was also reported between different NOM fractions (Jamal et al., 2014; Katsoufidou et al., 2010) or NOM and inorganic matters (Jermann et al., 2008).

While the majority of past research was conducted using polymeric membranes, alternative ceramic membranes have received increasing attention in the drinking water industry. Ceramic membranes which are made of inorganic materials are superior to their polymeric counterpart in their mechanical and chemical characteristics allowing for higher fluxes and backwash pressures as well as aggressive cleaning approaches without risk of damaging membrane integrity (Lee and Kim, 2014; Pendergast and Hoek, 2011). These advantages can potentially increase the operational life expectancy of ceramic membranes and decrease the cleaning and replacement requirements. Moreover, ceramic membranes are expected to last 20 years compared to a typical 7-10 years with polymeric membranes leading to lower life-cycle costs than polymeric membranes (Wise, 2015). However, ceramic membranes currently impose higher initial capital costs compared to polymeric membranes which has thus far largely limited their use to industrial applications (e.g., food and beverage, oil and gas produced waters (Vasanth et al., 2013; Zhou et al., 2010).

However, due to their operational advantages, the implementation of ceramic membranes for drinking water production is increasing and expected to grow over the next years.

Although some of the operational advantages of ceramic membranes are reported in the literature, few quantitative data exists about NOM fouling and the associated chemical cleaning protocols of ceramic membranes compared to their polymeric counterpart during surface water treatment. Oxidants and caustics are typically used to clean membranes fouled by organic compounds through oxidation, hydrolysis, and solubilization (Regula et al., 2014). However, the primary choice of appropriate cleaning agent for NOM is difficult as site specific needs should be considered (i.e. specific feedwater and membrane materials). Moreover, as irreversible fouling is known to be influenced by membrane and NOM properties (Hashino et al., 2011; Shao et al., 2011), NOM is expected to be less reactive with ceramic membranes due to the hydrophilic nature of the membrane (Lee and Kim, 2014; Zhou et al., 2010). Thus, research which examines clean in place (CIP) methodologies with different NOM fractions is required to increase fundamental understanding of cleaning regimes that control reversible and irreversible fouling for the two different membrane types. Therefore, the objectives of this research are to elucidate differences in fouling fractions (reversible vs irreversible) and cleaning efficiency of ceramic and polymeric UF membranes with various NOM types. The RIS model, membrane permeability, NOM mass balance and fluorescent excitation emission matrix (FEEM) analysis of permeate, backwash and chemical wash waters were used to investigate reversible and irreversible fouling and chemical cleaning performance using sodium hydroxide (NaOH) and hypochlorite (NaOCl).

6.2 Materials and Methods

6.2.1 Model foulants

NOM model foulants used in this study were humic acids (Sigma Aldrich lot #BCBK5107V) (2.5 mg C/L); a protein (bovine serum albumin, BSA, 2.5 mg C/L); a polysaccharide (sodium alginate 2.5 mg C/L), average molecular weight between 30 kDa – 100 kDa (Katsoufidou et al., 2010); sodium alginate with Ca^{+2} addition (75 mg/L as $CaCO_3$) using calcium sulfate ($CaSO_4$); and a mixture of the three NOM models, 0.83 mgC/L/each model (2.5 mg C/L as final concentration). The humic acid model (Sigma Aldrich) has been previously used in numerous membrane fouling investigations because of its fouling propensity (to accelerate fouling) and known characteristics. The test with alginate/ Ca^{+2} was included in the experimental design due to the high fouling propensity of this combination (Jamal et al., 2014). All model substances were purchased from Sigma Aldrich. Model solutions were prepared using pure deionized (DI) water and were mixed using a magnetic stirrer one-day prior to experiments ensuring that materials were dissolved completely. In addition, turbidity (5 mg/L of kaolin clay, equivalent to 5 NTU), and alkalinity (75 mg/L as $CaCO_3$) using sodium bicarbonate ($NaHCO_3$) were added. The pH of the feed was maintained around 7.5. NOM molecular weight distributions of synthetic solutions and zeta potential (as shown in Table 6.1 were measured using a UF fractionation method described by Kitis et al., (2002) and a Malvern Nano-sizer.

Table 6.1 - Molecular weight fractionation and zeta potential of feed solutions

Model feed NOM solution					
Molecular Weight	Humic acids	BSA	Sodium alginate - Ca^{+2}	Sodium alginate + Ca^{+2}	Mixture
> 100 kDa	32%	25%	28%	36%	38%
30 kDa - 100 kDa	38%	61%	30%	48%	41%
10 kDa - 30 kDa	18%	5%	22%	6%	10%
5 kDa - 10 kDa	9%	5%	10%	3%	5%
1 kDa - 5 kDa	2%	2%	6%	4%	1%
< 1 kDa	1%	2%	4%	2%	3%
Zeta Potential (ζ) mV	-27 ± 5	-23 ± 4	-36 ± 7	-20 ± 5	-22 ± 7

6.2.2 Fouling experiments

Assays were conducted on an automated filtration system (Figure 6.1) consisting of a digital gear pump (Cole Parmer: Drive no. 75211-30, Head no. 07003-04), pressure transducer (Omega: model no. PX409-100G5V), flow meter (Cole Parmer: model no. 32703-52), solenoid valves (Macmaster: model no. 4711K731), and pressure vessel (Cole Parmer: model no. 29902-90) and nitrogen gas for backwash. Labview program code (National Instruments, NI, USA) was created to operate the system automatically such as controlling the feed pump to have a constant flux, and automatically switches from filtration cycles to backwash cycles while recording flux and pressure data.

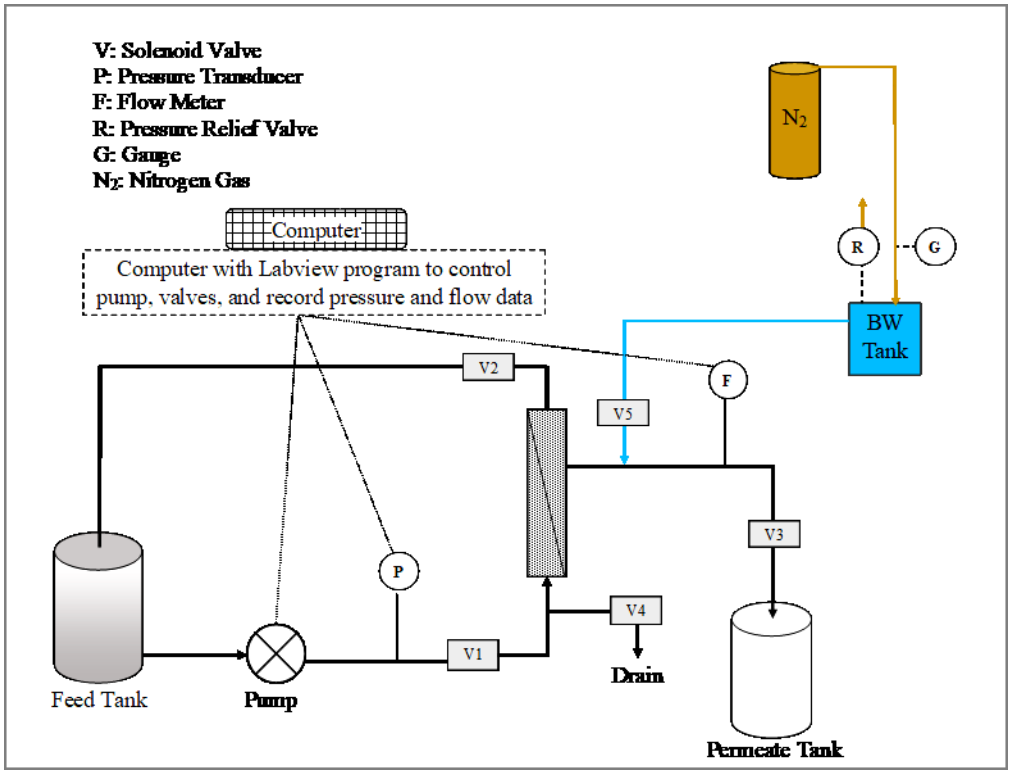

Figure 6.1- Automated membrane system

A ceramic UF (Ceramem^{TM}, Veolia) and polymeric UF (X-Flow^{TM}, Pentair) were used during this research and their characteristics are presented in Table 6.2. It should be noted that the characteristics of the two membranes (i.e. dimensions, area, and filtration configuration) were approximately similar to facilitate direct comparisons.

Table 6.2 – Ceramic and polymeric membranes characteristics*

Characteristics	Ceramic Membrane (Veolia)	Polymeric Membrane (Pentair)
Pore size	≈ 0.01 µm	≈ 0.01 µm
Configuration	Inside out	Inside out
Area	0.1 m^2	0.07 m^2
Length	300 mm	300 mm
Channel/fiber diameter	2 mm (61 square channels)	0.8 mm (93 hollow fibers)
Average Reynolds number (Re)	328 at 100 LMH	328 at 100 LMH
Cross-flow velocities	0.2 m/s	0.4 m/s

* Under an equivalent flux of 100 LMH and filtration cycle of 4 hrs/cycle, Ceramem ($A_{ceramic}$ = 0.1 m^2) and Pentair ($A_{polymeric}$ = 0.07 m^2) modules produce 40L/cycle and 28L/cycle, respectively. Thus, two Pentair modules are required to achieve similar productivity as one Ceramem membrane module.

Fouling experiments were performed for 24 hours under the following conditions: constant flux of 100 LMH; dead-end filtration mode; and backwash using pressurized water at 30 psi for 20 s every 4 hrs of filtration cycle (400 L/m^2). Clean water flux (CWF) was measured before and between experiments to determine the transmembrane pressure (TMP) versus flux relationship for a clean membrane and to estimate the intrinsic membrane resistance (R_m). This was done by filtering DI water through the membranes at a low flux and after recording the TMP for 30 minutes, the flux was increased and the procedure continued in a stepwise fashion. The initial membrane flux ($J_{initial}$), and TMP (ΔP) were used to estimate R_m at room temperature using Equation 6.1.

$$R_m = \frac{\Delta P}{\mu\, J_{initial}} \qquad \text{Equation (6.1)}$$

6.2.3 Chemical cleaning experiments

The goal of the chemical cleaning experiments was to provide direct comparisons of ceramic and polymeric membranes under equivalent cleaning protocols. CIP cleaning was performed using two common organic fouling cleaners: an oxidant, NaOCl or caustic cleaning, NaOH. Each cleaning was performed for 4 hours at a cleaning temperature of 35°C and pH of 11.0 for both cleaning solutions. Chemicals were recirculated at crossflow velocity of 0.1 m/s for 1 hour followed by 3 hours of soaking. For the NaOCl chemical wash, the free chlorine concentration was 500 mg Cl_2/L.

6.2.4 Analysis

6.2.4.1 Fouling resistances and specific flux recovery

To quantify membrane fouling during membrane filtration, total fouling resistance (R_f), hydraulically reversible fouling resistance (R_{hr}), hydraulically irreversible fouling resistance (R_{hir}), chemically reversible fouling resistance (R_{cr}), and chemically irreversible fouling resistance (R_{cir}) were estimated using the slope of the normalized pressure (P/P_0) and specific water volume (V/A) graph, (Figure 6.2) (Nguyen et al., 2011). The importance of each fouling resistance with respect to membrane operation is as follows; the greater the R_{hr}/R_f ratio, the more effective the hydraulic backwashes, possibly due to greater cake formation, the greater the R_{hir}/R_f ratio, the greater the NOM adsorption and pore blockage and thus greater the need for chemical cleans as hydraulic backwashes are ineffective. The R_{hir}/R_f ratio can be categorized into two ratios: the chemically reversible fouling ratio (R_{cr}/R_{hir}) and the chemically irreversible fouling (R_{cir}/R_{hir}). R_{cr}/R_{hir} quantifies the fouling

ratio removed by a chemical clean while R_{cir}/R_{hir} quantifies the fouling ratio that remains after a chemical clean.

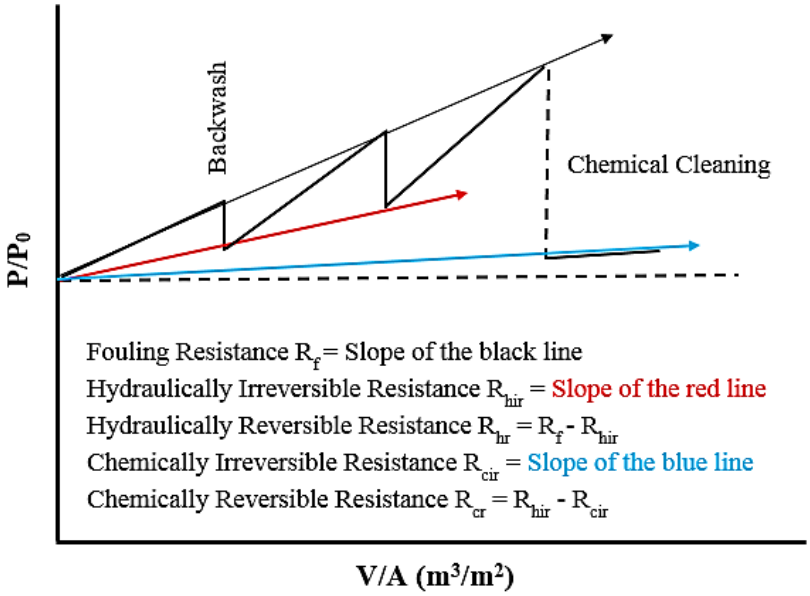

Figure 6.2- Resistances estimation using the slopes fouling graphs

The efficiency of chemical cleaning was assessed by comparing the chemically fouling resistance removal (R_{cr}) and specific flux recovery (SFR) using Equations 6.2 and 6.3.

$$\%\ R_{cr} = \frac{R_{cr}\ (\text{removed by each cleaning step})}{R_{hir}\ (\text{hydraulically irreversible fouling resistance})} \times 100 \qquad \text{Equation (6.2)}$$

$$\%\ SFR = \frac{\mathbf{Jsp}\ (\text{after cleaning})}{\mathbf{Jsp}_{initial}} \times 100 \qquad \text{Equation (6.3)}$$

6.2.4.2 Carbon mass balance

A carbon mass balance was performed to measure how much foulants were removed after each cleaning step and compare it to the fouling resistance removal data. This was done by

collecting samples from feed, permeate, backwash and chemical wash water and performing TOC analysis (using a Sievers^{TM} analyzer, GE Water) then converting the values to % mass for calculations (Equation 6.4).

$$\text{Mass}_{(\text{Feed})} = \text{Mass}_{(\text{Permeate})} + \text{Mass}_{(\text{hr})} + \text{Mass}_{(\text{cr, after NaOCl})} + \text{Mass}_{(\text{cr, after NaOH})} + \text{Mass}_{(\text{cir})}$$

Equation (6.4)

Where: hr (hydraulically reversible carbon); cr (chemically reversible carbon); cir (chemically irreversible carbon)

6.2.4.3 Fluorescence excitation and emission matrix (FEEM)

FEEM analysis was performed on water samples of the mixture solution for more insights into cleaning of different NOM compositions. Samples were collected from permeate, backwash and chemical wash waters. A spectrofluorophotometer, RF-5301 PC (Shimadzu), was used for the FEEM analysis. The excitation wavelength was set to 340 nm and the emission wavelength ranged from 300 nm to 600 nm. High sensitivity/slow scanning speed was used. Before analysis, a FEEM spectra of a blank was determined, then, the FEEM spectra of the analyzed sample was subtracted by the blank spectra. Python code, using Python xy, was used to plot the fluorescence data.

6.3 Results and Discussion

6.3.1 Ceramic versus polymeric UF performance comparison

6.3.1.1 NOM fouling and removal by ceramic and polymeric UF membranes

Figures 6.3A and 6.3B show the ceramic and polymeric UF fouling from different NOM solutions during each filtration cycle with respect to normalized pressure. NOM mixture exhibited the most severe fouling among the five model solutions. The presence of Ca^{+2} during the filtration of sodium alginate solution demonstrated a noticeable adverse effect on fouling. The zeta potential of the alginate solution was reduced from −36.7 mV to −20.5 mV when Ca^{+2} was added. The zeta potential reduction caused by Ca^{+2} addition could be attributed to the aggregation of Ca^{+2} and alginate molecules, thus, reduction of the electrostatic repulsion forces between alginate and membrane surface, thus increasing fouling rate (Jermann et al., 2008). The effect of Ca^{+2} addition on alginate fouling analogous to other reported results (Zularisam et al., 2011; Jermann et al., 2008) using polymeric membranes who found that flux decline by alginate and Ca^{+2} mixture increased significantly during filtration and resulted in alginate/ Ca^{+2} gel of a high specific resistance.

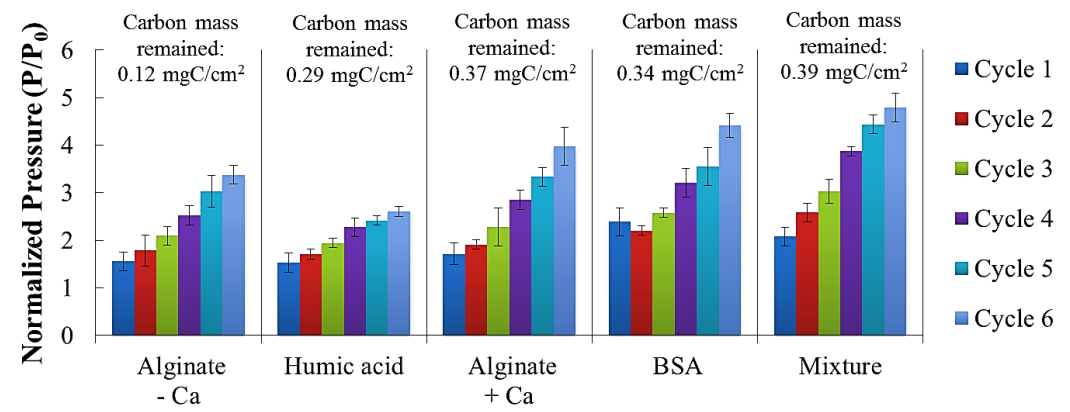

(A) Ceramic UF

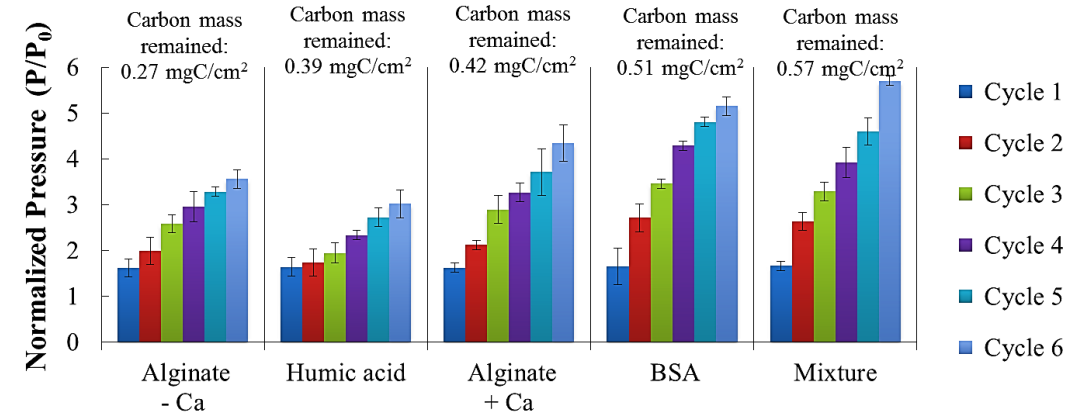

(B) Polymeric UF

Figure 6.3 – **(A)** Ceramic UF fouling by different NOM solutions (Flux: 100 LMH, BW: every 4 hours for 20s at 30 psi); **(B)** Polymeric UF fouling by different NOM solutions (Flux: 100 LMH, BW: every 4 hours for 20s at 30 psi).

Fouling of different NOM solutions of the ceramic UF was similar to the polymeric UF in terms of order; however, higher fouling was found with the polymeric UF. As backwash conditions were identical, we suggest that the difference in fouling can be attributed to the difference in material characteristics of both membranes. Previous studies suggested that membrane fouling was governed by membrane characteristics such as hydrophobicity and configuration. Lee et al. (2005) found that UF membrane with smoother surface had less fouling, while MF membrane with rough surface had severe flux decline due to deposition

of fouling materials in the valleys of the membrane surface. Polymeric membranes with lower surface porosity resulted in lower humic acid rejection and significant flux decline (Fu et al., 2008). Membranes with hydrophobic behavior was found to be more susceptible to membrane fouling than hydrophilic (Gray et al., 2007). In this study, the pore size of the two membranes is similar; however, the polymeric UF surface is hydrophobic, promoting a stronger interaction between foulants and membrane surface. In contrast, the ceramic UF surface is hydrophilic and can easily form bonds with water molecules which would reduce fouling. Another important factor is the surface charge of both membranes. SiC (ceramic) and PES (polymeric) membranes have reported point-of-zero charges of 2.5-3.5 and 4.5, respectively (Hofs et al., 2011). At our neutral pH of operation, both membranes were expected to exhibit negative charges and therefore repulsions were expected. However, due to the lower point of zero charge, higher electrostatic repulsion was therefore favoring the ceramic membrane. In summary, although the fouling order was similar, the ceramic UF demonstrated a better performance than polymeric UF in terms of lowering fouling rate which could either be due to more effective backwash or lower NOM retention by the ceramic membranes.

In order to validate the difference in NOM retention achieved by both membranes, NOM removals based on influent/effluent TOC concentrations are presented in Table 6.3. Removal results indicate that the highest TOC removal was for BSA and sodium alginate (+ Ca^{+2}) whereas lower removal for humic acids, sodium alginate (- Ca^{+2}) and the mixture solutions. However, although the removals for humic acid, sodium alginate (- Ca^{+2}) and the mixture solutions were approximately similar, it is unlikely that the removal mechanism

was the same since the mixture resulted in high levels of hydraulically irreversible fouling whereas sodium alginate (- Ca^{+2}) fouling was mostly reversible. The increase in alginate removal with Ca^{+2} addition could be attributed to the aggregation effect, thus increasing particle size and removal.

Table 6.3- NOM removals by the ceramic and polymeric UF (95% confidence interval)

NOM Solution	Ceramic UF	Polymeric UF
Humic Acid	67 % ± 2%	62 % ± 3%
BSA	84% ± 4%	77% ± 4%
Alginate + Ca^{+2}	80% ± 4%	76% ± 2%
Alginate - Ca^{+2}	66% ± 3%	71% ± 6%
Mixture	73% ± 2%	64% ± 3%

NOM removal by the ceramic and polymeric UF membranes were statistically analyzed using SPSS 22 by performing a Completely Randomized Block Design (CRBD) analysis. In CRBD, the experimental units are grouped into blocks according to known or suspected variation which is isolated by the blocks (Montgomery et al., 2013). The NOM solution is the known source of variation in the removal data and therefore, it was used as blocks while comparing the removal differences between the two membrane materials. CRBD analysis results (Appendix D) indicate that NOM removal was significantly influenced by membrane materials ($p = 0.008$), which could be attributed to the differences in the membrane structure and geometry. In other words, the overall higher level of removal of NOM between the ceramic and polymeric membranes can be attributed to the different membrane properties.

6.3.1.2 Hydraulic BW efficacy for ceramic and polymeric UF membranes

Table 6.4 presents the R_{hr} (hydraulically reversible resistance) and R_{hir} (hydraulically irreversible resistance) values estimated using the slope of fouling graphs. R_{hir} was the highest for the NOM mixture, 3.97E-3 and 6.76E-3, for the ceramic UF and polymeric UF respectively. Interestingly, the fouling resistances caused by the BSA solution alone was very close to that by mixture solution. This demonstrates the effect of BSA on membrane fouling. The R_{hr} values for the ceramic UF were always higher than that for the polymeric UF, which indicates that under identical filtration conditions, the interaction between NOM and ceramic membrane surface was weak, thus, high efficiency of backwashing with the ceramic UF than the polymeric UF. As a result, lower R_{hir} values were found with the ceramic UF compared to polymeric UF.

Table 6.4- R_{hr} and R_{hir} slope values of different feed NOM solutions

	Ceramic UF		Polymeric UF	
	R_{hr} ($x10^{-3}$) m^{-1}	R_{hir} ($x10^{-3}$) m^{-1}	R_{hr} ($x10^{-3}$) m^{-1}	R_{hir} ($x10^{-3}$) m^{-1}
Alginate - Ca^{+2}	5.60	1.36	4.30	2.78
Humic acid	4.20	1.05	2.90	2.46
Alginate + Ca^{+2}	4.10	2.89	1.70	5.60
BSA	3.31	3.72	1.80	6.55
Mixture	3.50	3.97	1.65	6.76

Figure 6.4 illustrates the backwash efficiency (represented by the R_{hr}/R_f ratios) for the ceramic and polymeric UF. Overall, hydraulically reversible fouling resistance contributed between ≈ 50-80% (20-50% irreversible fouling) and 20-60% (40-80% irreversible

fouling) for the ceramic and polymeric UF respectively. Importantly, under an equivalent backwash procedure, the R_{hr}/R_f ratios were 1.5x - 2x higher for the ceramic UF in comparison to the polymeric UF. Thus, the foulants were effectively removed more easily from the ceramic membrane through a simple backwash compared to the polymeric membrane. The superior backwash efficiency of the ceramic UF can potentially result in higher savings in ceramic membrane operational costs through the reduction of hydraulically irreversible fouling, and chemical cleaning frequency. Fouling of the alginate solution showed different trends with and without Ca^{+2} addition. Fouling was mostly irreversible during the filtration of the alginate (+ Ca^{+2}) solution, whereas it was reversible for the alginate (- Ca^{+2}) solution. This demonstrates the adverse impact of Ca^{+2} ions on alginate irreversibility which explain the difference in fouling behavior observed during filtration (Figure 6.3). Therefore, it is necessary to be aware of the interactions of water quality characteristics when utilizing membranes for NOM treatment.

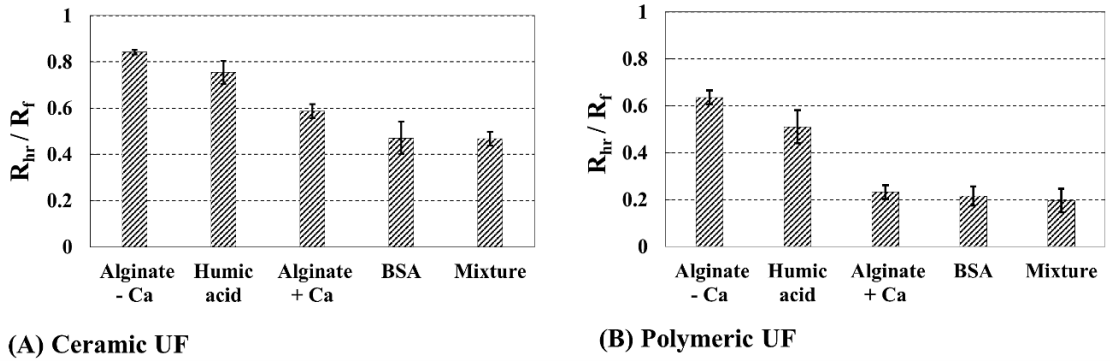

Figure 6.4 – Backwash efficiency (R_{hr}/R_f ratios). **(A)** Ceramic UF; **(B)** Polymeric UF. Higher ratios indicate higher BW efficiency and lower irreversibility.

6.3.1.3 Fouling analysis based on a carbon mass balance

Figure 6.5 shows the carbon mass balance found in the backwash water (hydraulically reversible), remained on the membrane (hydraulically irreversible) and in the permeate water. The results illustrate that for all model solutions, except the alginate ($– Ca^{+2}$), more than 50% of NOM was hydraulically irreversible. This demonstrates that NOM particles strongly adsorbed to the membrane surface or pores causing higher fouling irreversibility. During the filtration of alginate ($– Ca^{+2}$), ≈ 30-52% of NOM is found in the backwash water compared to 15-28% for alginate ($+Ca^{+2}$), which demonstrate the effect of Ca^{+2} on fouling reversibility/irreversibility of alginate. As observed earlier, the ceramic UF showed better removals of the hydraulically reversible carbon during backwashing demonstrating that under the same backwash procedure, the ceramic UF cleaning was more effective than the polymeric UF, highlighting an operational benefit of ceramic membranes over polymeric membranes. The carbon mass found in the permeate water was low: between 6-12% for the ceramic UF and 11-18% for the polymeric UF which indicate the higher NOM rejection and better permeate quality for the ceramic UF compared to the polymeric UF. The results of the carbon mass balance correlate well with the fouling resistance in series analysis and NOM removal data, and therefore, carbon mass balance could be a useful approach for fouling quantification in pilot and full-scale settings compared to RIS, which requires specific operator skill and experience and can also be time consuming and difficult to conduct on full-scale data.

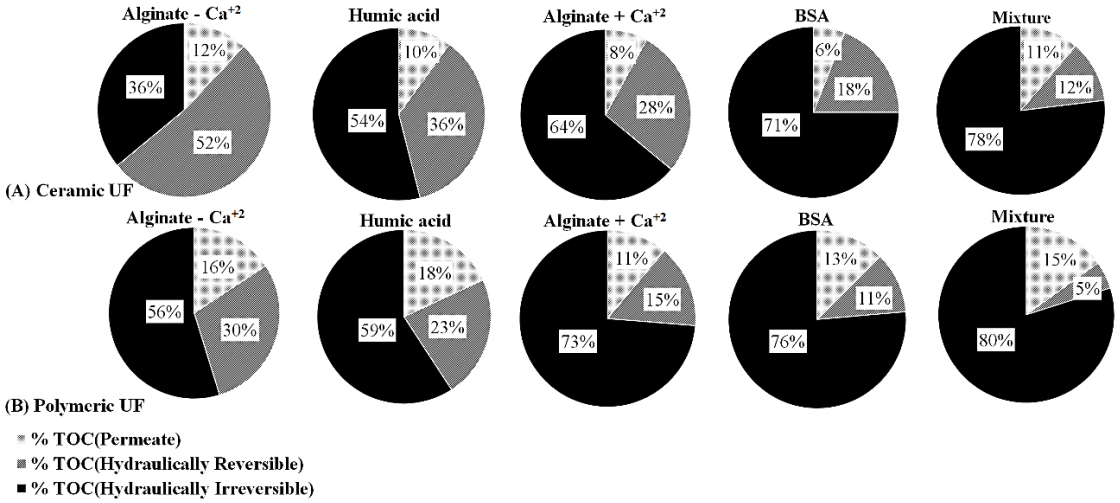

Figure 6.5 – Mass balance of carbon (expressed as % of the feed) found as hydraulically reversible (in the BW water), hydraulically irreversible (left on the membrane) or in the permeate water.

6.3.1.4 FEEM analysis of permeate and backwash waters

FEEM analysis was used to visualize the foulants in the ceramic and polymeric UF permeate and backwash water. Figure 6.6 shows fluorescence plots for the NOM mixture solution. The fluorescence peaks for humic-like substances are reported from 300-390 nm (range of excitation) and between 400-500 nm (range of emission). The fluorescence peaks for protein-like substances are around 230-280 nm (range of excitation) and between 310-360 nm (range of emission) (Matilainen et al., 2011). Backwash water samples from both membranes show high fluorescence intensity (≈ 900) in the region between Ex/Em 250-300/400-450 nm which indicates the presence of humic acids. BSA is also found in backwash water, however in less intensity than humic acids (≈ 300). Higher concentrations are found in the ceramic UF backwash water indicating better backwash efficiency than for the polymeric membrane. In addition, the ceramic UF permeate shows low FEEM intensities (≈ 250) than the polymeric UF permeate (≈ 400). These results are coherent

with the resistance-in-series and carbon mass analysis. Hydraulic BW are more effective on the ceramic membranes which leads to lower hydraulically irreversible fouling.

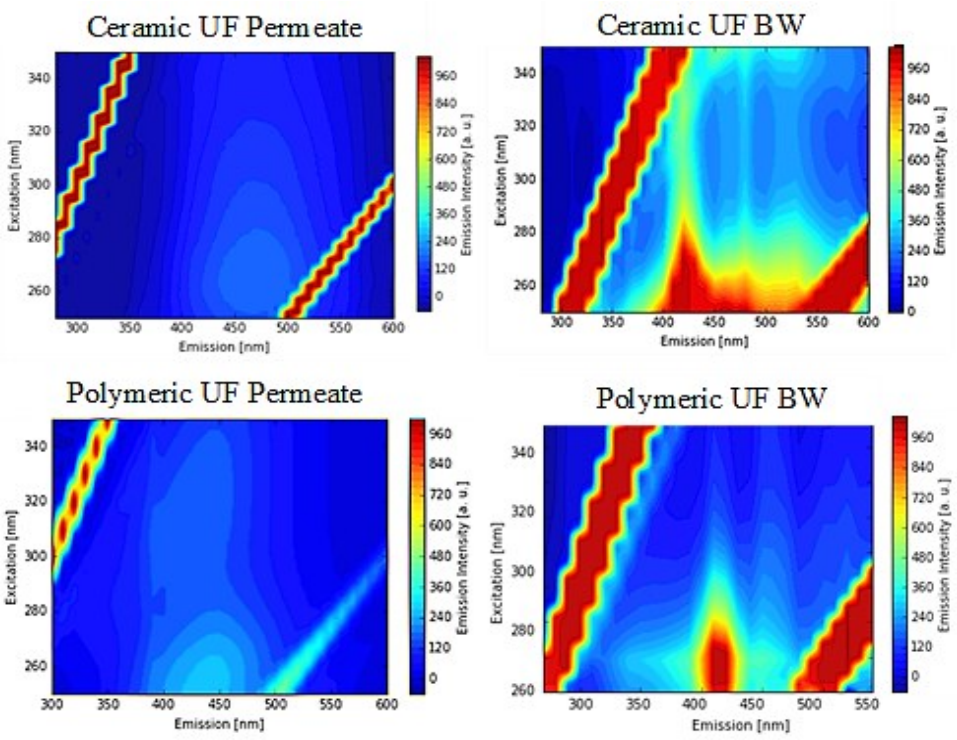

Figure 6.6 – FEEM plots of NOM mixture (permeate and backwash water)

6.3.2 Ceramic versus polymeric UF cleaning under equivalent cleaning protocols

6.3.2.1 Fouling resistance removal and specific flux recovery

After fouling experiments, both membranes were cleaned at pH 11.0 using NaOCl (500 mg Cl_2/L) or NaOH. Figures 6.7A-B show the chemical cleaning efficiency of different NOM foulants using the chemically reversible resistance (R_{cr}) for the two cleaning conditions. For the ceramic UF, $\%R_{cr}$ after NaOCl cleaning was around 80%, 60%, 74%, 62% and 58% (%SFR range was 65-85%) whereas after NaOH cleaning was around 90%, 85%, 90%, 88%, and 86% (%SFR was 95-97%) for humic acid, BSA, alginate (- Ca^{+2}),

alginate (+ Ca^{+2}) and mixture respectively. For the polymeric UF, % R_{cr} after NaOCl cleaning was around 72%, 55%, 65%, 58% and 50% (%SFR was 50-80%) whereas after NaOH cleaning was around 82%, 85%, 87%, 85% and 82% (%SFR was 88-92%) for humic acid, BSA, alginate (- Ca^{+2}), alginate (+ Ca^{+2}) and mixture respectively. Chemical cleanings of the polymeric UF showed similar %R_{cr} trends to that observed for the ceramic UF, however, the overall %R_{cr} removal was always lower for the polymeric UF. This illustrate that chemical cleaning of the ceramic membrane was easier and more efficient than the polymeric membrane.

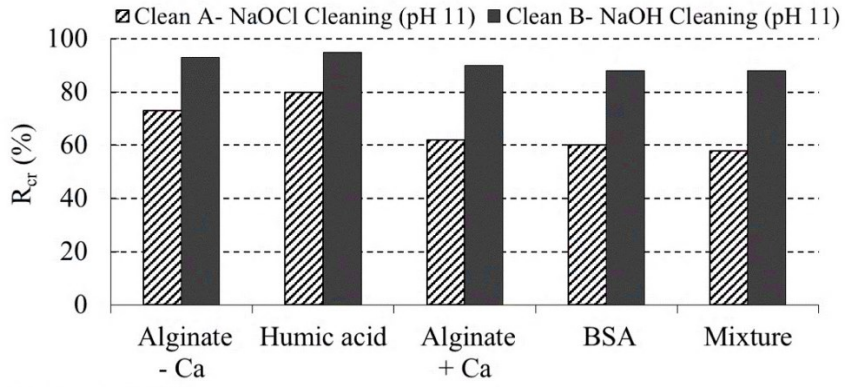

(A) Ceramic UF

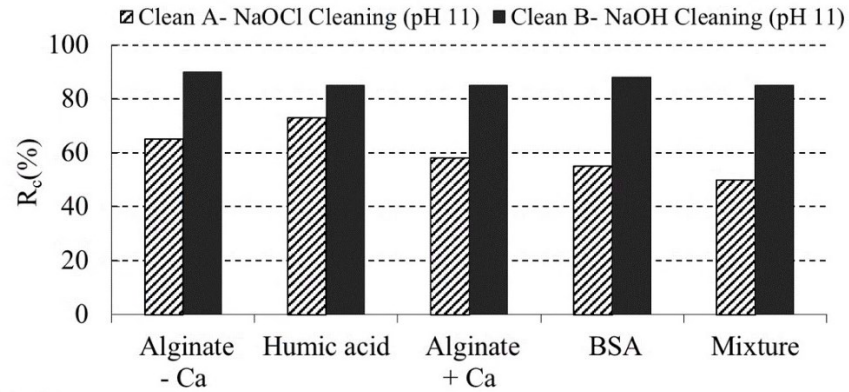

(B) Polymeric UF

Figure 6.7 – Cleaning efficiency based on the removal of chemically reversible resistance (R_{cr}) - pH 11; 35 ºC. **(A)** Ceramic UF; **(B)** polymeric UF

6.3.2.2 Chemically reversible and irreversible carbon mass balance in wash waters

Carbon mass (as percentages of total carbon) found in the NaOCl and NaOH wash waters (i.e. chemically reversible), and on the membrane after cleaning (i.e. chemically irreversible) are depicted in Figure 6.8. Surprisingly, it can be clearly seen that NaOH removed a higher carbon percentage of the BSA, alginate, and NOM mixture compared to NaOCl. On the other hand, both NaOCl and NaOH removed a higher carbon percentage of humic acids. NaOH can result in a hydrolysis reaction of the proteins and polysaccharides wherein a hydrogen group is removed from the molecules and replaced by a salt, hence, resulting in strong electrostatic repulsion between protein molecules and membrane surface (Kuzmenko et al., 2005). Moreover, Fukuzaki (2006) reported that, the addition of NaOCl and NaOH to water increases surface tension of the NaOCl solution. This increase in surface tension prevents the NaOCl solution from wetting solid surfaces and from penetrating into the deposit layer (Fukuzaki, 2006). Perhaps this is why in this study NaOH removed the BSA and alginate off the membrane surface better than NaOCl. More research is needed to better understand this unexpected difference in NaOH and NaOCl cleaning at the same pH. This indicates that the cleaning efficiency of different chemicals is highly dependent on the type of foulants in feed water. Thus, the selection and characterization of chemical cleaners for membranes should be based on the source of NOM fouling rather than fouling type (i.e. organic fouling). The chemically irreversible carbon percentages (refer to Figure 6.8), that is the carbon on the membrane that remained after cleaning, were lower for the ceramic UF, which explains the high cleaning efficiency observed in Figure 6.7. Thus, the high efficiency of chemical cleaning can ultimately decrease the replacement rate and increase the operational lifetime expectancy of ceramic membranes, through the

reduction of chemically irreversible fouling, compared to polymeric membranes. Future research is needed to estimate the long-term economic advantages of ceramic membranes compared to their polymeric counterpart.

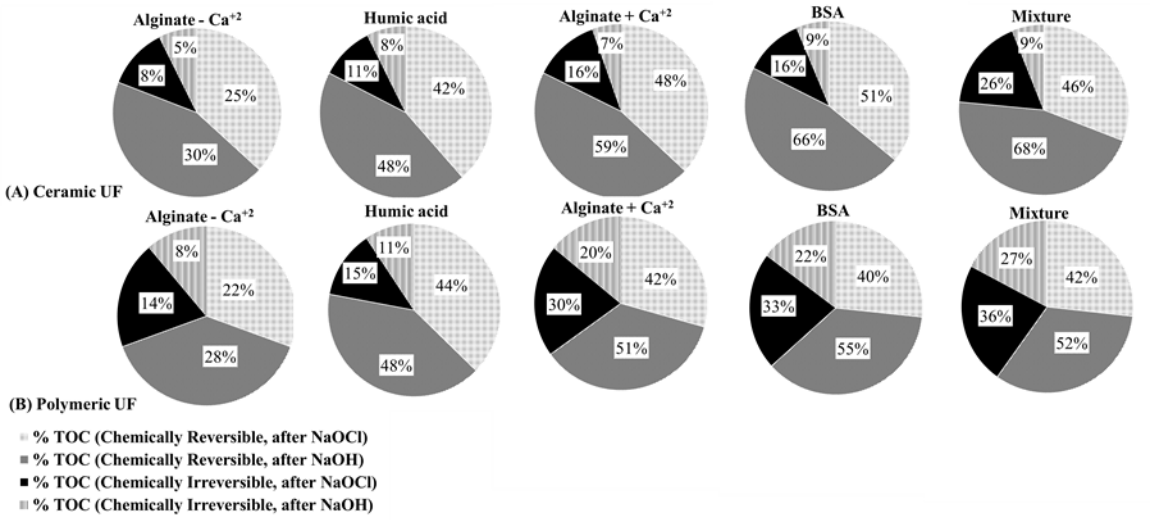

Figure 6.8 – Chemically reversible and irreversible % carbon (pH 11; 35 ºC)

FEEM plots for NaOCl and NaOH wash water for the solution with the NOM mixture are shown in Figure 6.9. The FEEM peaks found in the chemical wash water are quite similar, indicating that the type of NOM removed was similar under the two cleaning conditions. However, it can be observed that the fluorescent intensity is higher for the ceramic membrane, indicating that a larger portion of equivalent carbon was removed compared to the polymeric and indicates a better overall cleaning efficiency. The FEEM plots show similar results trend to that from RIS and carbon mass balance, demonstrating a useful approach for membrane fouling and cleaning evaluation when assessing removal of bulk organic constituents (i.e. humics and proteins).

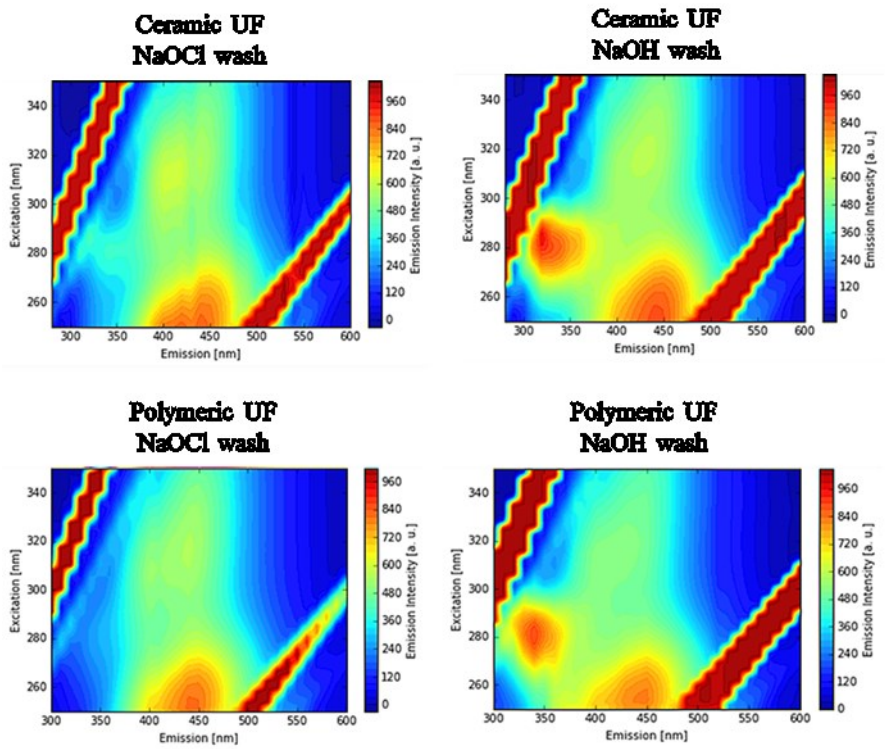

Figure 6.9 – FEEM plots of NOM mixture (NaOCl and NaOH wash water)

6.4 Conclusions

Information on NOM fouling and cleaning behavior with respect to ceramic membranes in comparison to polymeric membranes is limited with respect to drinking water applications. This research demonstrated that ceramic membranes had a higher degree of reversible fouling compared to polymeric membranes, indicating better hydraulic cleaning. In addition, this research clearly demonstrated that the fouling order between the two membranes were similar highlighting the ease of integration of ceramic membranes into drinking water applications. Key points from the research are summarized here:

- The backwash efficiency (R_{hr}/R_f ratios) was 1.5x-2x higher for the ceramic UF in comparison to the polymeric UF.

- Overall the hydraulic irreversibility was much higher for the polymeric membrane; where the NOM fouling resistance was 40-80% for the polymeric and only 20-50% for the ceramic membrane as determined by RIS.
- Fouling trends by RIS were confirmed by FEEM plots and the carbon content analysis in the ceramic UF backwash water was higher than the carbon content in the polymeric UF backwash water, which highlights an advantage of ceramic membranes with regards to hydraulic cleaning compared to polymeric membranes.
- More NOM was rejected by the ceramic membrane than the polymeric membrane although the fouling orders followed the same trend. The fouling was greatest with the NOM mixture ≈ BSA, alginate ($\pm Ca^{+2}$), and humic acid, respectively; indicating that both membranes are most susceptible to fouling by proteins.
- Chemical cleaning of ceramic and polymeric membranes was found to be effective for both membrane types. It was not possible to conclude that the ceramic membrane demonstrated an advantage for chemical cleaning. The FEEM plots demonstrate similar results trend to that from RIS and carbon mass balance, suggesting a useful approach for membrane fouling and cleaning evaluation when assessing removal of bulk organic constituents (i.e. humics and proteins).

6.5 Acknowledgements

The authors would like to acknowledge the Saudi Arabia Ministry of Education (MOE) and Natural Sciences and Engineering Research Council of Canada (NSERC) for helping fund this research. The authors wish to thank the CREDEAU laboratories at Polytechnique Montréal for providing the facilities to conduct this work as well as the collaboration of

Mireille Blais. We also wish to thank Geoff Seatter and Kerwin Lewis for their help with installation of the automated filtration system.

6.6 References

Evans, P., Bird, M., Pihlajamaki, A., Nystrom, M., 2008. The influence of hydrophobicity, roughness and charge upon ultrafiltration membranes for black tea liquor clarification. Journal of Membrane Science 313, 250-262.

Fu, X., Maruyama, T., Sotani, T., Matsuyama, H., 2008. Effect of surface morphology on membrane fouling by humic acid with the use of cellulose acetate butyrate hollow fiber membranes. Journal of Membrane Science 320, 483.

Fukuzaki, S., 2006. Mechanisms of actions of sodium hypochlorite in cleaning and disinfection processes. Biocontrol Science, Vol. 11, No. 4, 147-157.

Gray, S.R., Ritchie, C.B., Tran, T., Bolto, B.A., 2007. Effect of NOM characteristics and membrane type on microfiltration performance. Water Research 41, 3833-3841.

Hashino, M., Hirami, K., Ishigmi, T., Ohmukai, Y., Maruyama, T., Kubota, N., Matsuyama, H., 2011. Effect of kinds of membrane materials on membrane fouling with BSA. Journal of Membrane Science 384, 157-165.

Hashino, M., Hirami, K., Katagiri, M., Kubota, T., 2011. Effects of three natural organic matter types on cellulose acetate butyrate microfiltration membrane fouling. Journal of Membrane Science 379, 233-238.

Hofs, B., Ogier, J., Vries, D., Beerendonk, E., Cornelissen, E., 2011. Comparison of ceramic and polymeric membrane permeability and fouling using surface water. Separation and Purification Technology 79, 365– 374.

Jamal, S., Chang, S., Zhou, H., 2014. Filtration behaviour and mechanisms of polysaccharides. Membranes 4, 319-332.

Jermann, D., Pronk, W., Boller, M., 2008. Mutual influences between natural organic matter and inorganic particles and their combined effect on ultrafiltration membrane fouling. Environmental Science and Technology 42, 9129-9136.

Katsoufidou, K., Yiantsios, S., Karabelas, A., 2005. A study of ultrafiltration membrane fouling by humic acids and flux recovery by backwashing: experiments and modeling. Journal of Membrane Science 266, 40.

Katsoufidou, K.S., Sioutopoulos, D.C., Yiantsios, S.G., Karabelas, A.J., 2010. UF membrane fouling by mixtures of humic acids and sodium alginate: Fouling mechanisms and reversibility. Desalination 264, 220-227.

Kitis, M., Karanfil, T., Wigton, A., Kilduff, J., 2002. Probing reactivity of dissolved organic matter for disinfection by products formation using XAD-8 resin adsorption and UF fractionation. Water Research 36, 3834-3848.

Kuzmenko, D., Arkhangelsky, E., Belfer, S., Freger, V., Gitis, V., 2005. Chemical cleaning of UF membranes fouled by BSA. Desalination 179, 323-333.

Lee, N., Amy, G., Croûe, J.P., Buisson, H., 2005. Morphological analyses of natural organic matter (NOM) fouling of low-pressure membranes (MF/UF). Journal of Membrane Science 261, 7.

Lee, S., Kim, J., 2014. Differential natural organic matter fouling of ceramic versus polymeric ultrafiltration membranes. Water Research 48, 43-51.

Matilainen, A., Gjessing, E., Lathinen, T., Hed, L., Bhatnagar, A., Sillanpaa, M., 2011. An overview of the methods used in the characterisation of natural organic matter (NOM) in relation to drinking water treatment. Chemosphere 83, 1431–1442.

Montgomery, D., 2013. Design and analysis of experiments 8th edition, John Wiley & Sons, Inc. Tempe, Arizona.

Nguyen, A., Tobiason, J., Howe, K., 2011. Fouling indices for low pressure hollow fiber membrane performance assessment. Water Research 45, 2627-2637.

Pendergast, M., Hoek, E., 2011. A review of water treatment membrane nanotechnologies. Energy Environmental Science 4, 1946-1971.

Regula, C., Carretier, E., Wyart, Y., Gesan-Guiziou, G., Vincent, A. Boudot, D., Moulin, P., 2014. Chemical cleaning/disinfection and ageing of organic UF membranes: A review. Water Research 56, 325-365.

Shao, J., Hou, J., Song, H., 2011. Comparison of humic acid rejection and flux decline during filtration with negatively charged and uncharged ultrafiltration membranes. Water Research 45, 473-482.

Vasanth, D., Pugazhenthi, G., Uppaluri, R., 2013. Cross-flow microfiltration of oil-in-water emulsions using low cost ceramic membranes. Desalination 320, 86-95.

Wise, B., 2015. Comparative capital costs of ceramic and polymeric membranes. AWWA Membrane Technology Conference, Orlando, Florida.

Zhou, J.E., Chang, Q.B., Wang, Y.Q., Wang, J.M., Meng, G.Y., 2010. Separation of stable oil-water emulsion by the hydrophilic nano-sized ZrO_2 modified Al_2O_3 microfiltration membrane. Separation and Purification Technology 75 (3), 243-248.

Zularisam, A.W., Ahmad, A., Sakinah, M., Ismail, A.F., Matsuura, T., 2011. Role of natural organic matter (NOM), colloidal particles, and solution chemistry on ultrafiltration performance. Separation and Purification Technology 78, 189-20.

Chapter 7

Chemical Cleaning of Ceramic Ultrafiltration Membranes – Ozone versus Conventional Cleaning Chemicals

Mohammad T. Alresheedi[*], Onita D. Basu[*], Benoit Barbeau[**]

[*] Department of Civil and Environmental Engineering, Carleton University, 1125 Colonel By Drive, Ottawa, ON, K1S 5B6, Canada.

[**] Department of Civil, Geological and Mining Engineering, Polytechnique, C.P. 6079 Succursale Centre-Ville, Montreal, QC, H3C 3A7, Canada.

Submitted to: Journal of Chemosphere

Abstract

This study investigates chemical cleaning mechanisms of a tubular ceramic UF membrane. The effect of cleaner type (ozone (O_3), sodium hypochlorite (NaOCl) and sodium hydroxide (NaOH)), clean in place (CIP) pH (11 vs. 12), and cleaning sequence on the removal of irreversible fouling of hydrophobic (humic acids) and hydrophilic (alginate with and without calcium (Ca^{+2})) NOM fractions were investigated. Results showed that different NOM types responded differently to chemical cleaning. Alginate without Ca^{+2} and humic acids were equivalently removed by NaOCl or NaOH whereas a lower cleaning efficiency of alginate with Ca^{+2} was observed. Increasing the pH of NaOCl and NaOH CIP increased the removal of the chemically reversible fouling index ($UMFI_{cr}$). The efficiency of NaOCl was always lower than that of NaOH at the same pH, which was attributed to surface tension (λ) differences in the CIP water and potential differences in cleaning mechanism. The ceramic UF CIP cleaning using O_3 (0.50 mg O_3/mgC) for 1 hour

demonstrated higher cleaning efficiency for humic acids and alginate (with and without Ca^{+2}), (%$UMFI_{cr}$ > 98%), than NaOCl or NaOH alone (%$UMFI_{cr}$>80%). The O_3 CIP was as effective as 4 hours cleaning using a sequential NaOH/NaOCl or combined NaOCl+NaOH CIP.

Keywords: Carbon balance; Ceramic UF; Chemical cleaning; NOM fouling; Ozone CIP

7.1 Introduction

Membrane filtration with polymeric membranes has become increasingly common for drinking water treatment. More recently, ceramic membranes have attracted interest due to their hypothesized robustness to vigorous physical and chemical cleaning methods. However, fouling by natural organic matter (NOM) remains one of the major membrane challenges to maintain good membrane filtration performance (Hashino et al., 2011; Katsoufidou et al., 2010) and research on fouling and cleaning of NOM with ceramic membranes needs further investigation.

Membrane fouling is correlated to the ability of a membrane to reject NOM and the deposition of rejected organic constituents on its surface and/or in its pores (Kim et al., 2008). Reversible fouling can be removed by hydraulic backwash and/or chemical cleaning. Irreversible fouling resists hydraulic backwash and/or chemical cleaning. Irreversible fouling results in poor membrane performance by decreasing the permeate flux, and thus, increasing the need for chemical cleaning or even forcing membrane module replacement (Shi et al., 2014).

The main goal of chemical cleaning is to remove membrane fouling, particularly irreversible fouling. The selection of a cleaning agent depends on the characteristics of feed water and compatibility of membrane materials (Regula et al., 2014). Sodium hypochlorite (NaOCl) and sodium hydroxide (NaOH) are the most commonly used chemicals in the maintenance and recovery cleaning of membranes (Wang et al., 2018; Shi et al., 2014). They are used to remove NOM fouling through oxidation, hydrolysis and solubilization (Regula et al., 2014). Oxidation by NaOCl degrades the NOM functional groups to carboxyl and aldehyde groups, which make them more susceptible to removal (Wang et al., 2014). On the other hand, NaOH encourages dissolution of carboxylic and phenolic functional groups such as proteins and polysaccharides (Porcelli and Judd, 2011). Studies addressing the impacts of different cleaning parameters of NaOCl and NaOH for cleaning polymeric membranes have shown that chemical concentration and cleaning sequence are important factors that governs the cleaning efficiency (Puspitasari et al., 2010; Hilal et al., 2005) Wang X. et al. (2018) found that increasing chlorine concentration from 100 to 1000 mg Cl_2/L of NaOCl resulted in faster diffusion of chlorine within the fouling layer, thus, higher oxidizing capability and cleaning efficiency. Puspitasari et al. (2010) reported that the repeated cleaning of PVDF membranes with 0.5% NaOCl (5,000 mg Cl_2/L) was as effective as a single cleaning performed with 1%. However, it is commonly known that a high concentration of chemicals and frequent cleaning can oxidize membrane polymers and cause swelling of membrane fibers, thus, shortening the membrane lifetime (Puspitasari et al., 2010; Arkhangelsky et al., 2007). Moreover, frequent cleaning can cause changes in membrane functional groups, physical structure and surface properties (Wang et al., 2018; Zhang et al., 2017; Shi et al., 2014). Thus, polymeric membranes are typically

restricted to pH 11 or lower and chlorine concentration < 500 mg Cl_2/L (Regula et al., 2014; Porcelli et al., 2011).

Made of inorganic materials, ceramic membranes have many advantages over polymeric membranes as they are supposed to be mechanically, thermally, and chemically stable (Kim et al., 2008). Most importantly, ceramic membranes have superior chemical resistance allowing much more aggressive cleaning approaches (i.e. pH > 11 and high chemicals concentration) without risk of damaging membrane integrity (Lee et al., 2013). Utilization of high pH cleaning in a single or stepwise approach with the NaOCl and NaOH solutions can be beneficial for controlling irreversible fouling of ceramic membranes for drinking water treatment applications. However, to date there is little/no research in this area.

Ozone (O_3) cleaning adds in another dimension to cleaning of ceramic membranes that is not available to polymeric membranes. The use of O_3 with ceramic membranes for the treatment of natural waters has been shown to reduce membrane fouling (Zhang et al., 2013; Kim et al., 2008). O_3 can oxidize NOM through a direct molecular O_3 attack as well as by an indirect means: free radical formation resulting from O_3 decomposition in the bulk phase, O_3 oxidation of NOM or O_3 reaction with the ceramic membrane surface (Regula et al., 2014; Van Geluwe et al., 2011). Karnik et al. (2005) found that membrane flux improved by 65% - 90% when a crossflow-operated ceramic membrane was combined with ozonation. Other studies such as Zhang et al. (2013) and Sartor et al., (2008) reported that in situ ozonation transforms organics into smaller hydrophilic molecules, thus, less fouling. It should be noted that in the above studies, O_3 is dosed in a pre-ozonation mode,

with the backwash step or continuously injected into the membrane tank. However, limited to no research exists that investigate alternative ozone clean in place (O_3 CIP) cleaning regimes with respect to NOM fouling control for ceramic membranes.

Research which examines CIP methodologies with different NOM fractions is required to increase operational understanding of cleaning regimes that control irreversible fouling of ceramic membranes. Therefore, in this paper, we investigated various chemical cleaning conditions of a ceramic UF membrane fouled by hydrophilic (alginate) and hydrophobic (humic acids) NOM fractions. The NOM fouling behavior was characterized using the unified membrane fouling index (UMFI), NOM retention and carbon mass balance to assess for respective differences in reversible and irreversible fouling mechanisms. O_3 CIP performance was investigated for controlling irreversible alginate and humic acids fouling in comparisons to a single, stepwise, or combined chemical cleaning approach using NaOCl and NaOH.

7.2 Materials and Methods

7.2.1 Model foulants

NOM model foulants used in this study were a hydrophobic NOM, humic acids (Sigma Aldrich lot #BCBK5107V) (2.5 mg C/L) and a hydrophilic polysaccharide, sodium alginate, (Sigma Aldrich) (2.5 mg C/L); and sodium alginate with Ca^{+2} addition 75 mg/L as $CaCO_3$ (30 mg Ca^{+2}/L) using calcium sulfate ($CaSO_4$). Humic acids and alginate (Sigma Aldrich) have been previously used in numerous membrane fouling investigations because of their fouling propensity and known characteristics (Katsoufidou et al., 2010; Xiao et al.,

2009). The test with alginate/ Ca^{+2} was included in the experimental design due to the high fouling propensity of this combination (Jamal et al., 2014). Model solutions were prepared using pure deionized (DI) water and were mixed using a magnetic stirrer one-day prior to experiments ensuring that materials were dissolved completely. In addition, turbidity (5 mg/L of kaolin clay, equivalent to 5 NTU, with > 95% of particles in the 2-5 μm range), and alkalinity (75 mg/L as $CaCO_3$) using sodium bicarbonate ($NaHCO_3$) were added. The pH of the feed solution was maintained around 7.5. The zeta potential of humic acids and alginate feed solutions were measured using the Malvern Zetasizer-Nano.

7.2.2 Experimental setup and approach

An automated ceramic membrane system (Figure 7.1) was used for this research. The system consists of a digital gear pump (Cole Parmer: Drive no. 75211-30, Head no. 07003-04), pressure transducer (Omega), flow meter (Cole Parmer: model no. 32703-52), solenoid valves (MacMaster), and pressure vessel (Cole Parmer). Nitrogen gas was used to maintain pressure in the pressure vessel for backwash. Labview program (National Instruments, NI) code was created to operate the system automatically such as controlling the feed pump to have a constant flux, and automatically switches from filtration cycles to backwash cycles while recording flux and pressure data. A tubular ceramic UF membrane (Ceramem^{TM}, Veolia) was used and its characteristics are as follows: monolithic module, SiC membrane material, inside-out channels (61), square channel (2 mm), pore size (0.01 μm), area (0.1 m^2), and module length (300 mm). The ceramic membrane was fouled by humic acids or alginate for 24 hours in dead-end filtration mode under constant flux of 100 LMH; backpulses were conducted for 20 seconds every 4 hours using pressurized water at 2 bars

(~30 psig). Between cleaning experiments, a clean water flux (CWF) test was performed to determine the membrane resistance using the transmembrane pressure (TMP) versus flux relationship for a clean membrane. This was done by filtering water through the ceramic membrane at a low flux and recording the TMP after 30 minutes the flux was increased, and the procedure continued in a stepwise fashion. The initial membrane flux ($J_{initial}$), and TMP (ΔP) and kinematic viscosity (μ) were used to estimate membrane resistance (R_m) using the Equation 7.1.

$$R_m = \frac{\Delta P}{\mu J_{initial}} \qquad \text{Equation (7.1)}$$

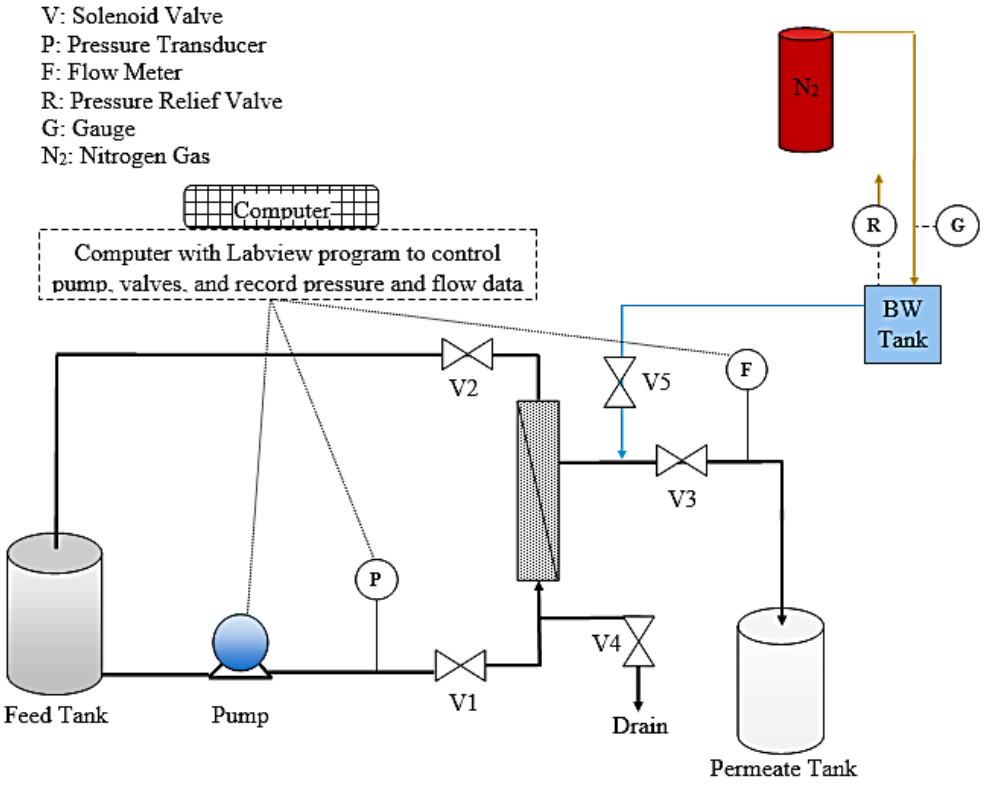

Figure 7.1- Automated ceramic membrane system

7.2.3 Chemical cleaning experiments

This research investigates pH 12 solutions in a single, stepwise, or combined approach with NaOCl and NaOH and O_3 CIP for increased irreversible fouling control on ceramic membranes for drinking water treatment applications. Both pH 12 and O_3 CIP are not recommended with polymeric membranes and could highlight an advantage to ceramic membranes in drinking water applications for irreversible fouling control.

7.2.3.1 Cleaning pH effect (pH 11 vs. pH 12)

Chemical cleaning (CIP) was performed using two common membrane cleaners: an oxidant, NaOCl (500 mg Cl_2/L, as free chlorine) or caustic, NaOH. NaOCl was purchased as a solution (6%). The concentration of free chlorine in the wash water was measured before testing using the HACH method (8021) and a digital colorimeter™ II. NaOCl and NaOH cleaning was examined at two different pH of 11 and 12. Cleaning was performed alternatively for 4 hours at a cleaning water temperature of 35 °C. Chemicals were prepared in 4 L of DI water and recirculated in a closed loop at a cross flow velocity of 0.1 m/s for 1 hour followed by 3 hours soak.

7.2.3.2 Chemicals cleaning sequence (NaOCl/NaOH, NaOH/NaOCl, combined NaOCl+NaOH)

The effect of chemical cleaning sequence of the ceramic UF was examined using three options. **Option A (NaOCl/NaOH):** cleaning with 500 mg Cl_2/L NaOCl (pH 12) for 2 hours followed by NaOH (pH 12) for 2 hours (total of 4 hours). **Option B (NaOH/NaOCl):** cleaning with NaOH (pH 12) for 2 hours followed by 500 mg Cl_2/L NaOCl (pH 12) for 2

hours (total of 4 hours). **Option C (NaOCl+NaOH):** NaOCl was simultaneously mixed with NaOH (pH 12) i.e. both chemicals were added concurrently at the same concentration as in their single solution (500 mg Cl_2/L NaOCl + 400 mg NaOH/L), and the cleaning duration was maintained at a 4 hours duration to ensure the same chemical contact time for direct comparisons with individual cleaning solutions. Cleaning was performed at 35°C water temperature.

7.2.3.3 Ceramic UF cleaning using O_3 CIP

O_3 cleaning efficiencies for hydrophilic NOM, alginate with and without Ca^{+2}, and hydrophobic NOM, humic acids, were examined. For each cleaning experiment, 4 L of ozonated water was first prepared by bubbling at 4 ºC a 6% ozone/oxygen gas (Ozone Solutions, USA) in DI water to saturation. Cleaning was performed by recirculating O_3 injected at either 0.25 mg O_3/mg C or 0.50 mg O_3/mg C, where mg C is the carbon mass accumulated on the membrane surface (i.e., O_3 concentration in the 4 L cleaning solution ranges from 15-30 mg O_3/L and 30-60 mg O_3/L for the 0.25 and 0.50 mg O_3/mg C ratios respectively). Recirculation of O_3 was performed in a closed loop for 1 hour at a cleaning water temperature of 15 °C. O_3 residuals were measured using the standard indigo trisulfonate method (Bader and Hoigin, 1981). Total organic carbon (TOC) analyses were performed during O_3 cleaning by collecting a sample at different time intervals (i.e. 1, 5, 10 minutes, etc.) to determine the cumulative O_3 demand and irreversible carbon removal as a function of cleaning time.

7.2.4 Analysis

7.2.4.1 The unified membrane fouling index (UMFI)

Fouling and cleaning were assessed using the UMFI model as shown in Equation 7.2 (Huang et al., 2008). Where J_s' is the normalized specific flux (i.e. measured specific flux (J_s) divided by initial specific flux (J_{s0}), (unitless), UMFI is an estimate of the extent of fouling (m^{-1}), and V_S (m^3/m^2) is the specific permeate volume.

$$\frac{1}{J_s'} = 1 + (\text{UMFI}) \text{x } Vs \qquad \text{Equation (7.2)}$$

Total fouling resistance index ($UMFI_f$) can be divided into the hydraulically reversible fouling resistance index ($UMFI_{hr}$) (i.e., removed by backwash), and hydraulically irreversible fouling resistance index ($UMFI_{hir}$), (i.e., remained after backwash), as shown in Equation 7.3. The $UMFI_{hir}$ can be divided into $UMFI_{cr}$ and $UMFI_{cir}$. $UMFI_{cr}$ is chemically reversible fouling resistance index (i.e., removed by chemical cleaning); and $UMFI_{cir}$ is chemically irreversible fouling resistance index (i.e. remained after chemical cleaning).

$$\text{UMFI}_f = \text{UMFI}_{hr} + \text{UMFI}_{hir} = \text{UMFI}_{hr} + \text{UMFI}_{cr} + \text{UMFI}_{cir} \qquad \text{Equation (7.3)}$$

$UMFI_f$ was calculated using the slope of the linear region of $1/J_s'$ versus V_s graph from the start to end of filtration. $UMFI_{hir}$ was calculated using the slope of $1/J_s'$ versus V_s graph using data points immediately after backwash. $UMFI_{hr}$ is the difference between $UMFI_f$ and $UMFI_{hir}$. $UMFI_{cir}$ was calculated using the slope of $1/J_s'$ versus V_s graph using data

points immediately after the chemical cleaning step. $UMFI_{cr}$ is the difference between $UMFI_{hir}$ and $UMFI_{cir}$.

7.2.4.2 Carbon mass balance

Carbon mass balance was performed to determine indirectly the carbon mass remaining on the membrane before and after each cleaning step. This was performed by TOC analysis on feed, permeate, hydraulic backwash and chemical wash waters. The mass of chemically irreversible carbon was deducted using Equation 7.4. The % error of the carbon measurements was calculated to ensure accurate mass balance at different testing conditions. Carbon data was then compared to the fouling resistance data estimated by the UMFI method.

$$\text{Mass}_{(cir)} = \text{Mass}_{(Feed)} - \text{Mass}_{(Permeate)} - \text{Mass}_{(hr)} - \text{Mass}_{(cr)} \qquad \text{Equation (7.4)}$$

Where: $Mass_{(cir)}$ (chemically irreversible carbon mass, i.e. remained on membrane); $Mass_{(hr)}$ (hydraulically reversible carbon mass, i.e. in backwash water); $Mass_{(cr)}$ (chemically reversible carbon mass, i.e. in chemical wash water).

7.2.4.3 Surface tension (λ) measurements

Surface tension measurements, using the capillary rise method, of NaOCl and NaOH CIP waters were conducted by immersing a capillary tube into the CIP water and measuring the liquid height in the tube. Jurin's law (Equation 7.5) was used to estimate the surface tension of CIP chemicals.

$$\lambda = \frac{h.\rho.g.r}{2\cos\theta} \qquad \text{Equation (7.5)}$$

Where λ is the surface tension (N/m); h is the height of the liquid in the capillary tube (m); ρ is the liquid density (kg/m^3); g is the gravitational acceleration (m/s^2); r is the tube radius (m); θ is the contact angle. The contact angle was determined by taking photos of a water/chemical droplets and using ImageJ software (an imaging processing software) to determine the contact angle. Photos were taken 1 minute after depositing the drop on the surface. Tests were conducted in triplicate for each CIP condition and the average of three measurements is reported. The λ of NaOCl and NaOH CIP waters at pH 11 was further measured with the addition of nonionic surfactants (500 mg/L of Tween 80) to assess the impact of surfactants addition on the wetting ability of NaOCl and NaOH.

7.3 Results and Discussion

7.3.1 Ceramic UF fouling by alginate and humic acids

Initial filtration experiments were conducted to establish the fouling behavior of hydrophobic (humic acid) and hydrophilic (sodium alginate) NOM with ceramic UF membrane. The UMFI (Huang et al., 2008) which represents the slope of the data in the linear zone, was used to quantify fouling of each NOM type. Figure 7.2 shows that the membrane fouling behaviors differed between the model NOM solutions. The alginate + Ca^{+2} solution resulted in the highest fouling ($UMFI_{alginate\ +Ca^{+2}}$ of 1.13 m^{-1}) followed by alginate - Ca^{+2} ($UMFI_{alginate\text{-}Ca^{+2}}$ of 0.89 m^{-1}), and humic acids ($UMFI_{humic\ acids}$ of 0.71 m^{-1}) respectively. The rate of fouling increased with each filtration cycle, demonstrating high

accumulation of NOM. The presences of Ca^{+2} in feed water showed negative impacts on alginate fouling. Specifically, after the first 8 hours filtration cycle, the alginate + Ca^{+2} solution demonstrated higher increase in fouling compared to alginate - Ca^{+2}. Ca^{+2} reduced the zeta potential of alginate from −36 mV to −20 mV due to double layer compression and reduction of the electrostatic repulsion forces between colloids and membrane surface, thus increasing the fouling rate. This can be supported by Katsoufidou et al. (2010) study on alginate fouling with polymeric membranes. It was found that the presence of calcium leads to reduced alginate inter-chain electrostatic repulsion, thus promoting formation of coiled alginate macro-molecular structures. Such coiled macro-molecules tend to form more compact and less permeable fouling layers. The results from the ceramic UF system analogous to those by Katsoufidou et al. (2010) and Hashino et al. (2011) using polymeric membranes, in which humic acid had a gradual flux decline and lower fouling rate compared to alginate.

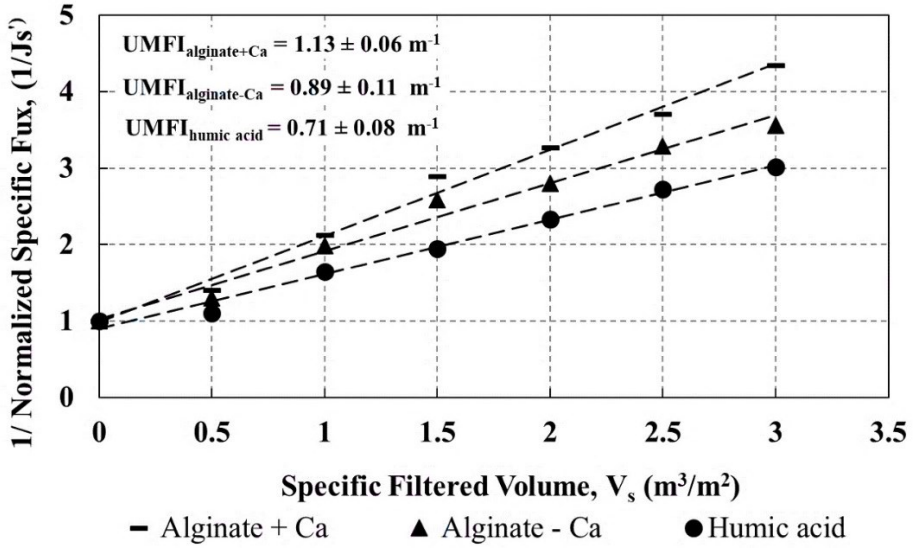

Figure 7.2 –Ceramic UF membrane fouling by different NOM solutions (Constant Flux: 100 LMH, BW: every 4 hours (0.4 m^3/m^2) for 20s at 30 psi. pH= 7.5. Total filtration time: 24 hours. UMFI: Unified membrane fouling index.

Figure 7.3 shows the hydraulically reversible and irreversible fouling ratios (i.e. $UMFI_{hr}/UMFI_f$ and $UMFI_{hir}/UMFI_f$) for the alginate ± Ca^{+2} and humic acids solutions. Overall, the $UMFI_{hir}/UMFI_f$ ratio of different NOM fractions ranged between 16%-41% of total fouling. The alginate solution showed different fouling behaviors with and without Ca^{+2} addition. Fouling was more reversible for the alginate - Ca^{+2} solution in which 76% was removed by backwash whereas in the case of alginate + Ca^{+2}, only 59% was removed. As a result, deposition of alginate onto the membrane surface increases and a more densely packed fouling layer of high hydraulic resistance was formed. Moreover, alginate (with and without Ca^{+2}) resulted in higher irreversible fouling compared to humic acids indicating a strong influence of polysaccharides on ceramic membrane fouling compared to humic substances. Katsoufidou et al. (2010) and Kimura et al. (2004) studies with polymeric UF membranes showed that polysaccharides caused irreversible fouling apparently due to pore blockage. It was reported that alginate resulted in a rapid irreversible fouling due to internal pore constriction which led to development of cake layer of high specific resistance (Katsoufidou et al., 2010; Kimura et al., 2004).

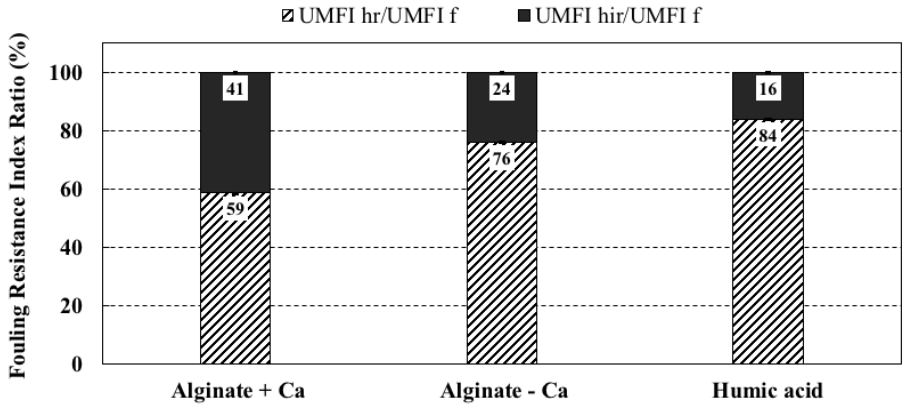

Figure 7.3 – Hydraulically reversible fouling index ($UMFI_{hr}$) and hydraulically irreversible fouling index ($UMFI_{hir}$) ratios*
*Higher $UMFI_{hr}$ / $UMFI_f$ percentage indicates higher backwash efficiency and lower irreversibility.

Table 7.1 presents the carbon mass found in the backwash water (hydraulically reversible), remaining on the membrane (hydraulically irreversible) and in the permeate water. During the filtration of alginate (– Ca^{+2}), 54% of feed carbon (0.22 mg C/cm^2) remained on the ceramic membrane compared to 64% (0.35 mg C/cm^2) for alginate (+ Ca^{+2}), which demonstrate the effect of Ca^{+2} on fouling reversibility/irreversibility of alginate. For humic acids, 36% of feed carbon (0.18 mg C/cm^2) remained on the membrane which was lower than carbon mass determined for alginate ± Ca^{+2}. Therefore, membrane backwash was more effective in removing humic acids fouling deposits compared to alginate (refer to Table 7.1). The results of the carbon masses are coherent with the UMFI data in Figure 7.3. The higher % of the hydraulically reversible carbon (i.e., carbon in the backwash water) for humic acids indicate higher backwash efficiency (i.e. high $UMFI_{hr}/UMFI_f$ ratio) and lower irreversibility compared to Alginate – Ca^{+2} (as reflected in Figure 7.3). Additionally, the high hydraulically irreversible carbon (i.e., carbon remained on the membrane) for the alginate with Ca^{+2} addition (i.e., Alginate + Ca^{+2}) indicates higher irreversible fouling and thus lower backwash efficiency (refer to Figure 7.3). Thus, carbon mass balance measurements demonstrated a simple and useful approach for fouling quantification in bench scale setting.

Table 7.1- Hydraulically reversible and irreversible carbon percentages (n = 3)*

Model NOM	Hydraulically Reversible Carbon (%)	Hydraulically Irreversible Carbon %**	Permeate Carbon (%)
Humic acids	52 ± 6	36 ± 8 (0.18)	12 ± 6
Alginate – Ca^{+2}	36 ± 4	54 ± 8 (0.22)	10 ± 5
Alginate + Ca^{+2}	28 ± 8	64 ± 6 (0.35)	8 ± 6

*Total organic carbon in the feed: 100%. n = 3: triplicate experiments.

**Values in parenthesis are giving the surface concentration of carbon in mg/cm^2

7.3.2 Ceramic UF cleaning: effect of cleaning pH and cleaning agent

The fouling experiments clearly demonstrated that alginate ± Ca^{+2} and humic acids contribute differently to irreversible fouling of a ceramic UF membrane. Therefore, the next step was to compare the cleaning efficiency of NaOCl, NaOH, and O_3 CIP for controlling irreversible fouling of alginate ± Ca^{+2} and humic acids. The effect of pH on the cleaning efficiency of NaOCl and NaOH is shown in Figure 7.4. The percentages of $UMFI_{cr}$ recovered by NaOCl CIP (500 mg Cl_2/L) at pH 11 were 62%, 74%, and 80% for alginate + Ca^{+2}, alginate – Ca^{+2}, and humic acids, respectively. On the other hand, NaOH showed much higher cleaning efficiency at pH 11 compared to NaOCl in which the $\%UMFI_{cr}$ recovered were 80%, 86%, and 88% for alginate + Ca^{+2}, alginate – Ca^{+2}, and humic acids respectively. The cleaning efficiency of NaOCl increased significantly ($p < 0.05$) by 10-20% with increasing pH from 11 to 12 while there was also a significant ($p < 0.05$) 10% improvement for NaOH at the higher pH of 12. Increasing pH can cause swelling of the fouling layer which results in an increase in the cake voidage, and thus results in a higher cleaning efficiency (Wang et al., 2018; Strugholtz et al., 2005). The increase in the cleaning ability of NaOCl and NaOH at pH 12 in this study resulted in a more effective oxidation and hydrolysis reactions between cleaning chemicals and NOM within the fouling layer (Shi et al., 2011). Consequently, the fouling layer was broken down relatively more easily at pH 12 compared to pH of 11 and resulted in a higher cleaning efficiency. Liang et al. (2008) study indicates that caustic promotes a more open fouling layer that allows the chlorine to reach the membrane surface, which explain the increased efficacy of NaOCl at higher pH of 12 compared to 11.

Figure 7.4 also shows the %$UMFI_{cr}$ recovered by ozone (O_3) cleaning compared to NaOCl and NaOH. It can be clearly seen that a 1 hour of O_3 CIP at a ratio of 0.50 mgO_3/mgC (~ 60 mg O_3/L) resulted in > 98% removal of the $UMFI_{cr}$ for alginate ± Ca^{+2} and humic acids. The higher cleaning efficiency of O_3 is attributed to higher oxidation reactions between O_3, free radicals and NOM. O_3 can react with humic acids and polysaccharides and breakup the aromatic rings and glycosidic linkages which transform NOM molecules into oxygenated functional groups (Van Geluwe et al., 2011; Song et al., 2010). The oxygenated functional groups are hydrophilic which have lower propensity for adsorption on membrane surface. In this study, O_3 oxidized humic acids and alginate substances on the ceramic membrane surface and transformed the fouling layer into more hydrophilic and porous structure which enhanced their removals from the membrane surface (Zhang et al., 2013; Sartor et al., 2008). This is supported by Song et al. (2010) who reported an O_3 dose of 0.50 mg O_3/mgC, applied for 10 minutes to surface water increased the hydrophilicity of NOM by 45% which reduced membrane fouling. Although the irreversible fouling masses of alginate + Ca^{+2}, alginate - Ca^{+2}, and humic acids on the membrane were different (0.35, 0.22, 0.18 mgC/cm^2, respectively), O_3 CIP for 1 hour at 15°C demonstrated equivalent reductions of hydrophilic alginate and hydrophobic humic acids fouling. Moreover, the % $UMFI_{cr}$ obtained by O_3 CIP at a ratio of 0.50 mg O_3/ mgC are higher than those obtained by NaOCl or NaOH at pH 11 and 12 ($p < 0.05$) despite the difference in characteristics of the tested NOM foulants. A lower ozone ratio of 0.25 mg O_3/mg C was found to be less effective at cleaning the membrane. For this condition, the %$UMFI_{cr}$ recovered decreased to 64%, 68% and 74% for alginate + Ca^{+2}, alginate – Ca^{+2}, and humic acids, respectively.

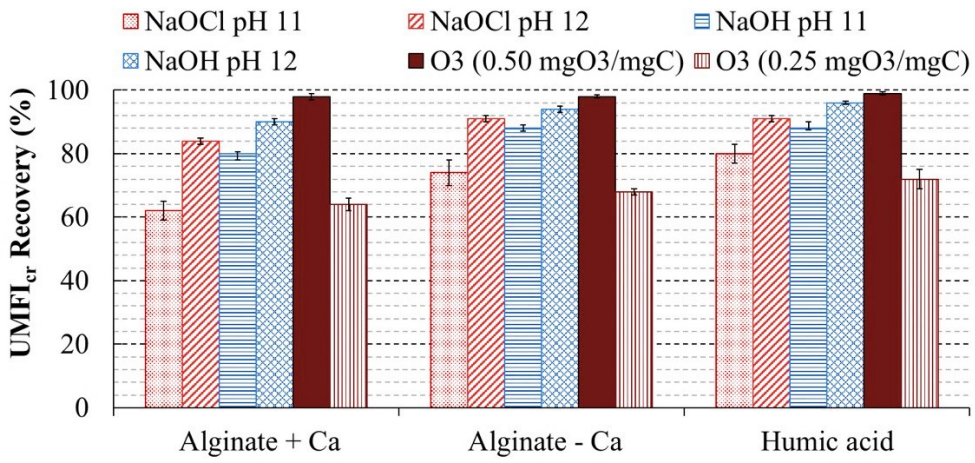

Figure 7.4- Effect of cleaning pH and cleaning agent on the removal of $UMFI_{cr}$ of ceramic UF*

*Cleaning time: NaOCl and NaOH CIP: 4 hrs; O_3 CIP: 1 hr.

* $UMFI_{cr}$: chemically reversible fouling index: $((UMFI_{hir} - UMFI_{cir}) / UMFI_{hir}) \times 100$

While O_3 CIP at ratio of 0.50 mg O_3/mg C was effective for the removal of alginate ± Ca^{+2} and humic acids, different NOM fractions responded differently to the NaOCl and NaOH cleaning (refer to Figure 7.4). NaOCl at pH 11 or 12 showed an equivalent cleaning of alginate - Ca^{+2} and humic acids ($p > 0.05$). The same can be said for NaOH at pH 11 or 12. On the other hand, in the case of alginate + Ca^{+2}, the $\%UMFI_{cr}$ values recovered by NaOCl at pH 11 and 12 were lower than those obtained with alginate - Ca^{+2} and humic acids. It is commonly known that NaOCl is important for cleaning organic substances (Shi et al., 2014; Porcelli et al., 2011; Arnal et al., 2009). It increases the repulsion between the negatively charged functional groups, which results in a stretched, linear configuration of NOM, thus loosening the fouling layer and enhancing the efficacy of cleaning (Shi et al., 2014). Nevertheless, the NaOCl cleaning did not prove to be efficient when alginate + Ca^{+2} was present; i.e., the $\%UMFI_{cr}$ recovered for alginate + Ca^{+2} with NaOCl at pH 11 and 12 were significantly lower than that for alginate - Ca^{+2} and humic acids ($p < 0.05$). This could

be attributed to the high irreversible mass of alginate + Ca^{+2} compared to alginate - Ca^{+2} and humic acids (refer to Table 7.1). While NaOCl is known to cause swelling to hydrophobic polymeric membranes, and this assists in flushing out foulant material within the pores (Wang et al., 2018; Zhang et al., 2017; Ferrer et al., 2016; Regula et al., 2014) the same cannot be said for ceramic membranes since they have solid structures and hydrophilic surfaces, thus, the swelling effect is not possible. Thus, in ceramic membrane the impact of NaOCl as a cleaning agent is reduced. Other factors such as the hydrophilic nature of the ceramic SiC membrane, and the surface tension (λ) differences of the CIP waters may had an impact on the cleaning mechanisms.

Table 7.2 presents the contact angle and λ values determined for NaOCl and NaOH CIP waters. The λ value for pure water was 70.8±0.5 mN/m at 35 °C. In the current literature, the mean values for water surface tension at 25 °C range from 70.0 mN/m to 72.7 mN/m (Beattie et al., 2014; Estrela et al., 2005) agreeing with the value obtained in this study. It can be clearly seen that the addition of NaOCl and/or NaOH increased the λ value of water (refer to Table 7.2). The λ value of NaOCl CIP water at pH 11 was 77.2±0.7 mN/m which had the highest measured contact angle of 58.7º. The contact angle and λ measured for NaOH CIP at pH 11 were 42.8º and 73.1±0.1 mN/m, respectively, which are much lower than the λ values for NaOCl CIP solution. At pH 12, the contact angle and λ values for NaOCl decreased to 52.1º and 74.1±0.5 mN/m whereas slight changes were noted in the contact angle and λ values for NaOH at pH 12, 41.6º and 72.6±0.5 mN/m respectively. The results of our study agree with the results of Estrela et al. (2005) and Beattie et al. (2014) who obtained 75.0 mN/m for NaOCl and 72.8 mN/m for NaOH, at pH of 12 respectively.

These results indicate that for NaOCl at pH 11, the high λ value supressed the NaOCl cleaning efficiency compared to NaOH alone. NaOH appears to have a lower effect on surface tension compared to NaOCl. This may explain why NaOH resulted in better fouling resistance recovery under the different pH conditions examined compared to NaOCl.

Moreover, the increased cleaning efficiency observed with NaOCl at pH 12 was related to the high concentration of NaOH in the wash water solution (i.e., more NaOH was added to bring the pH to 12) which enhanced the diffusion of chlorine at higher pH of 12 (Wang et al., 2018). In addition, Table 7.2 shows lower contact angle and the λ values of the combined NaOCl and NaOH mixture, 41.7º and 73.5±1.0 mN/m at pH 11, and 41.5º and 72.1±0.3 mN/m at pH 12 compared to NaOCl or NaOH alone. The wetting ability of NaOCl and NaOH at pH 11 can be enhanced with the addition of nonionic surfactants. For example, we tested the addition of 500 mg/L of Tween 80 which reduced the λ values of NaOCl and NaOH solutions to 42.0±0.9 mN/m and 33.0±0.5 mN/m, respectively.

Table 7.2- Average surface tension values of CIP water (n=3)

CIP Condition	Contact angle	Surface Tension (mN/m)
NaOCl pH 11	58.7º±3.3º	77.2±0.7
NaOCl pH 12	52.1º±1.8º	74.1±0.5
NaOH pH 11	42.8º±2.1º	73.1±0.1
NaOH pH 12	41.6º±3.6º	72.6±0.5
NaOCl+NaOH pH 11	41.7º±1.4º	73.5±1.0
NaOCl+NaOH pH 12	41.5º±2.5º	72.1±0.3

Figure 7.5 shows the % carbon removed by chemical cleaning (i.e. carbon in the NaOCl NaOH, and O_3 wash waters) versus the resistance recovery (represented by $\%UMFI_{cr}$). It can be clearly seen that the carbon data correlates well with the fouling resistance removal ($R^2 \approx 0.86 - 0.92$). On the other hand, O_3 CIP demonstrated higher removal of carbon compared to NaOCl or NaOH. Since fouling irreversibility poses major implications during filtration with respect to membrane life time, the use of O_3 CIP could be more beneficial than NaOCl and NaOH for controlling irreversible fouling of NOM when utilizing ceramic membranes for drinking water treatment.

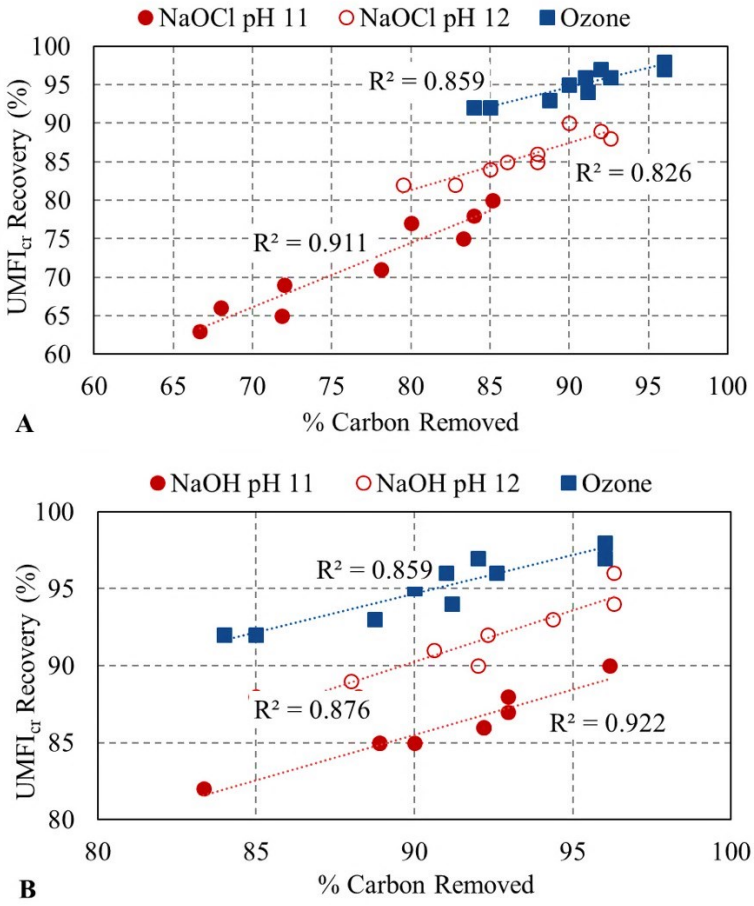

Figure 7.5- Correlations between chemically reversible fouling index recovery ($UMFI_{cr}$) and % carbon removed by various chemical cleaning: **(A)** NaOCl CIP vs. O_3 CIP; **(B)** NaOH CIP vs. O_3 CIP. Ozone CIP at a ratio of 0.50 mg O_3/mg C.

Measurements were made during the O_3 CIP in order to define the optimal duration of cleaning (as shown in Figures 7.6A-B). It can be seen that as the cumulative O_3 demand increased (Figure 7.6A), more carbon was removed for the different NOM types (Figure 7.6B). However, the carbon removal by O_3 with time was dependent on the type of NOM on the membrane. For alginate ± Ca^{+2}, the cumulative carbon removed (Figure 7.6B) increased slowly within the first 30 minutes of cleaning (i.e. 55% of total irreversible carbon mass was removed) and then increased sharply afterwards. On the other hand, humic acid carbon removal trend (Figure 7.6B) showed faster increase within the first 30 minutes of cleaning (i.e. 78% of total irreversible carbon mass was removed) followed by a moderate increase in carbon removal. This demonstrates that oxidation of hydrophilic alginate by O_3 was slower compared to hydrophobic NOM (i.e. humic acids). Moreover, this could be attributed to the differences in the irreversible carbon masses between the different NOM types. Overall, O_3 CIP cleaning using 0.50 mg O_3/mg C, for 1 hour at 15 ^oC, was effective in removing alginate and humic acids fouling.

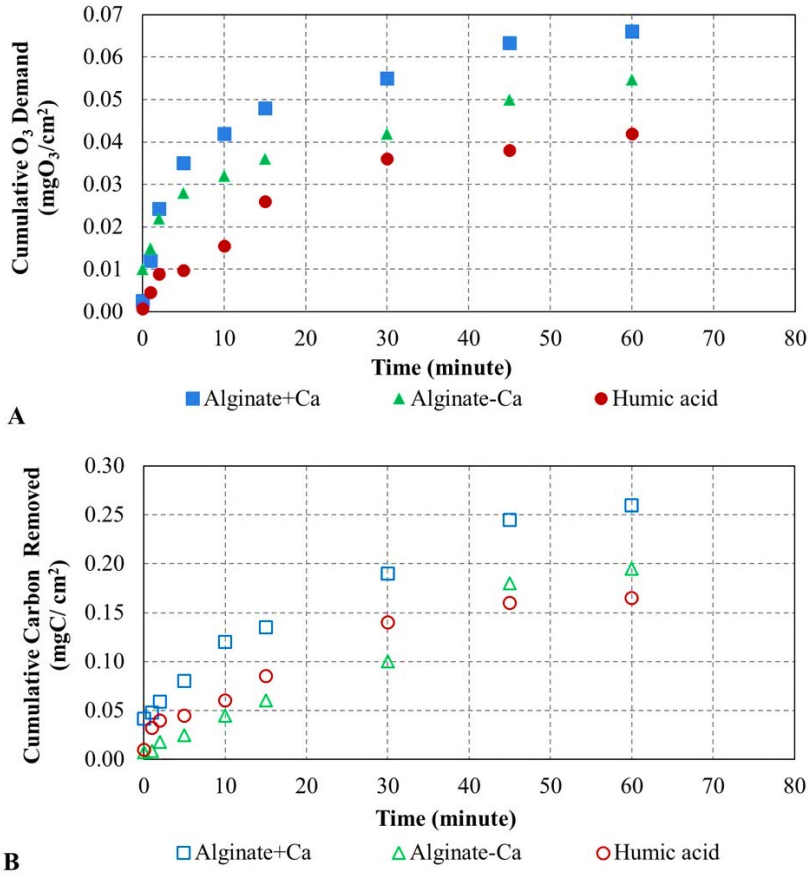

Figure 7.6– **(A)** Cumulative O_3 demand versus cleaning time; **(B)** Cumulative carbon removed versus cleaning time. O_3 CIP at a ratio of 0.50 mg O_3/mg C

7.3.3 Ceramic UF cleaning sequence: combined use of NaOCl and NaOH versus O_3

Irreversible membrane fouling is caused by the strong adsorption of NOM on the membrane surface or within its pores. The cleaning efficiency of NOM would varies depending on the characteristics of chemical reagent used for cleaning. The results in section 7.3.2 showed superior removal of alginate and humic acids foulants with O_3 CIP and an improved cleaning at pH of 12 when utilizing a single step approach to chemical cleaning with the NaOCl or NaOH solutions. Ceramic membranes have high chemical resistance, and therefore, a consecutive or combined use of NaOCl and NaOH cleaning

approach can be utilized which may be more effective than a two steps cleaning. However, to date there is little/no research in this area. Figure 7.7 shows that after NaOCl/NaOH cleaning sequence, the overall $\%UMFI_{cr}$ were 92%, 94% and 94% for alginate + Ca^{+2}, alginate – Ca^{+2}, and humic acid, respectively. The cleaning efficiency using sequential NaOCl/NaOH is equivalent to that using NaOH alone at pH 12 ($p > 0.05$). The cleaning efficiency increased significantly ($p < 0.05$) when NaOH was used before NaOCl (i.e., NaOH/NaOCl sequence), and resulted in $\%UMFI_{cr}$ of 98%, 99%, and 99% for alginate + Ca^{+2}, alginate – Ca^{+2}, and humic acid respectively. NaOH is known to increase the solubility of humic acid and polysaccharide substances by hydrolysis and solubilization, which can change the configuration of NOM and make the fouling layer into a looser and more open structure (Shi et al., 2014). This could provide an easier path for NaOCl reaching the foulant layer and oxidizing NOM. Similar results were reported by Kimura et al. (2004) study in which the flux recovery of a polymeric membrane fouled by NOM improved with cleaning using NaOH/NaOCl sequence compared to NaOH alone.

The combined use of NaOCl and NaOH refer to Figure 7.7, resulted in $\%UMFI_{cr}$ of > 98% for alginate ± Ca^{+2}, and humic acids. It is postulated that the NaOH provided an easier path for NaOCl to reach the foulant layer and oxidize NOM (Liang et al., 2008; Strugholtz et al., 2005). A previous study found that NaOH improved the capacity of H_2O_2 to remove and oxidize foulants similar to this work (Strugholtz et al., 2005). In addition, modifying surface tension while maintain pH has been demonstrated by others to improve cleaning (Wang et al., 2018; Ujihara et al., 2016; Levitsky et al., 2012). Thus, the lower surface tension of the combined NaOCl and NaOH CIP water at pH 12, 72.1±0.3 mN/m, (refer to

Table 7.2), may have improved the wetting ability of the CIP water and thus resulted in a higher cleaning efficiency. Therefore, not only the oxidation reactions, but also the mass transfer of chemicals and detached foulants need to be considered for efficient cleaning (Liu et al., 2001). The $\%UMFI_{cr}$ recovered by O_3 CIP at a ratio of 0.50 mgO_3/mgC are similar to $\%UMFI_{cr}$ recovered by the NaOH/NaOCl cleaning sequence and combined NaOCl+NaOH CIP ($p > 0.05$).

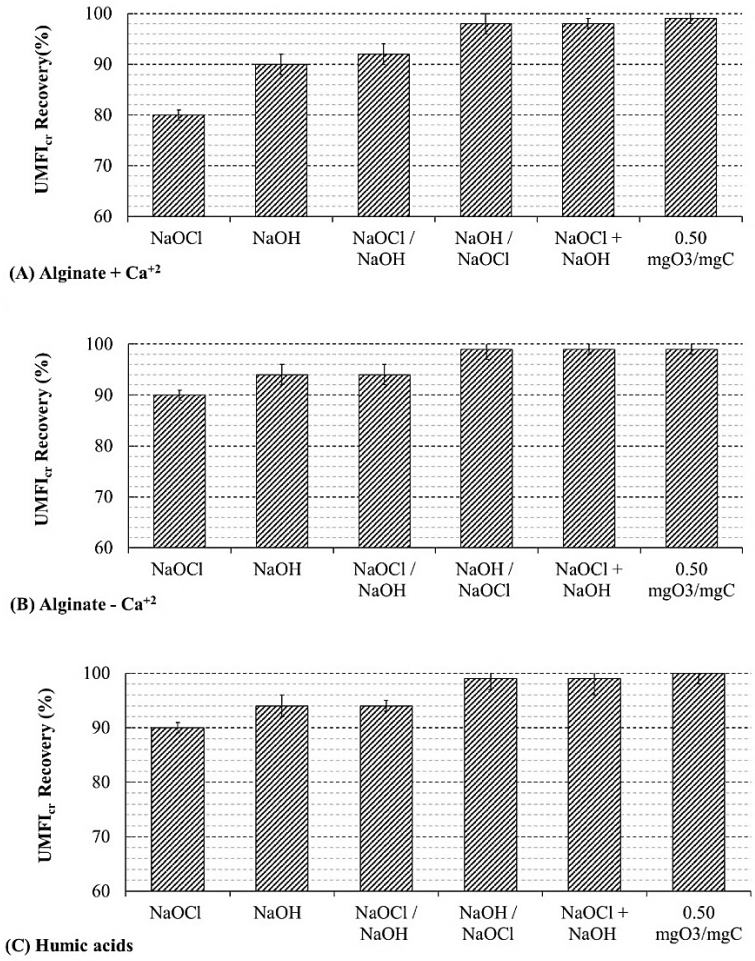

Figure 7.7– Recovery of UMFIcr following various ceramic UF cleaning sequence*. **(A)** Alginate+Ca^{+2}; **(B)** Alginate-Ca^{+2} **(C)** Humic acids.

* NaOCl and NaOH CIP: NaOCl 500 mg Cl_2/L; NaOH 0.01N, cleaning pH 12; cleaning time 4 hrs (total). NaOCl/NaOH: NaOCl followed by NaOH; NaOCl+NaOH: NaOCl mixed with NaOH.

Ozone CIP: 0.50 mgO_3/ mgC; cleaning time 1 hr. $UMFI_{cr}$: chemically reversible fouling index.

Table 7.3 presents cost comparisons of NaOCl, NaOH, and O_3 CIP. It can be clearly seen that based on the amount of chemicals used in this study, NaOCl has the highest cost (0.005 US$ per clean) followed by NaOH (0.002 US$ per clean) and O_3 (0.001 US$ per clean). Although O_3 investment costs were not considered, the amount of O_3 used in this study indicate that O_3 is the least expensive chemical compared to NaOCl and NaOH. Furthermore, O_3 CIP step requires a short cleaning duration (i.e., 1 hour), thus, less cleaning time compared to NaOCl and/or NaOH CIP (optimal cleaning time of 4 hours). These advantages suggest that the use of O_3 CIP with ceramic membranes provides an effective and economical cleaning option over conventional cleaning chemicals. Future investigations are recommended to determine the long-term capital/investment costs of O_3 CIP with ceramic membrane systems.

Table 7.3- Cost comparisons of NaOCl, NaOH, and O_3 (for one clean of the lab module)

	NaOCl (pH 12)	**NaOH (pH 12)**	**O_3**
Concentration	500 mg Cl_2/L + 60 mg/L NaOH	400 mg/L	60 mg/L
Cleaning Water Volume	4 L	4 L	4 L
Chemical Amount	2000 mg Cl_2 + 240 mg NaOH	1600 mg	240 mg
Cleaning Time	4 hrs	4 hrs	1 hr
Cost /kg	USD 2.3/kg Cl_2* + USD 1.2/kg NaOH	USD 1.2/kg	USD 2.52/kg O_3**
Cost / Clean	USD 0.005	USD 0.002	USD 0.001

*For 12% NaOCl

**0.085$/kW-h x 12 kw-h/kg$O_3$ + 0.15$/kg$O_2$ x 10kgO_2/kgO_3 = 2.52$/kg$O_3$

(Electricity cost x energy unit cost to produce) + (cost of Lox x quantity of Lox for an operation at 10% by wt.)

7.4 Conclusions

This research examined the utilization of O_3 CIP with ceramic UF membranes for controlling irreversible fouling of hydrophilic (alginate ± Ca^{+2}) and hydrophobic (humic acids) NOM compared to conventional cleaning chemicals (NaOCl and NaOH). Key points from the research are summarized here:

- O_3 (0.50 mgO_3 /mgC) was equally effective at removing alginate± Ca^{+2} and humic acids NOM foulants, while both NaOH and NaOCl were less effective with the alginate + Ca^{+2} condition, indicating a higher sensitivity of traditional cleaning chemical to water quality conditions for chemical cleaning and a more robust cleaning with O_3.
- For the conditions tested, a 1 hour of O_3 CIP at a ratio of 0.50 mgO_3/ mgC demonstrated an equivalent performance to 4 hours of cleaning using sequential NaOH/NaOCl or combined NaOCl+NaOH CIP (%$UMFI_{cr}$ > 98%). Future investigations should assess the optimal ozonation conditions (time vs. O_3 concentration) required to maximize O_3 CIP performance while minimizing costs.
- Cleaning efficiency of NaOCl and NaOH is governed by the pH of the CIP water. Future research should examine the effectiveness of surfactant addition versus pH adjustment for more economical and effective control of irreversible fouling of ceramic membranes.

7.5 Acknowledgements

The authors would like to acknowledge the Saudi Arabia Ministry of Education (MOE) and Natural Sciences and Engineering Research Council of Canada (NSERC) for helping

fund this research. The authors wish to thank the CREDEAU laboratories at Polytechnique Montréal for providing the facilities to conduct this work as well as the collaboration of Mireille Blais. We also wish to thank Geoff Seatter and Kerwin Lewis for their help with installation of the automated membrane filtration system.

7.6 References

Arkhangelsky, E., Kuzmenko, D., Gitis, V., 2007. Impact of chemical cleaning on properties and functioning of polyethersulfone membranes. Journal of Membrane Science, 305, 176–184.

Arnal, J.M., Garcia-Fayos, B., Sancho, G., Verdu, M., 2009. Ultrafiltration membrane cleaning with different chemical solutions after treating surface water, Desalination and Water Treatment 7, 198–205.

Bader, H., Hoigin, J., 1981. Determination of ozone in water by the indigo method. Water Research 449, 456.

Beattie, J., Djerdjev, A., Weale, A., Kallay, N., Lutzenkirchen, J., Preocanin, T., Selmani A., 2014. pH and the surface tension of water. Journal of Colloid and Interface Science 422, 54–57.

Estrela, C., Estrela, C., Guimaraes, L., Silva, R., Pecora, J., 2005. Surface tension of calcium hydroxide associated with different substances. Journal of Applied Science 13(2): 152-6.

Ferrer, O., Lefevre, B., Parts, G., Bernat, X., Gibret, O., Miquel, P., 2016. Reversibility of fouling on ultrafiltration membrane by backwashing and chemical cleaning: differences in organic fractions behaviour. Desalination and Water Treatment 57, 8593–8607.

Hashino, M., Hirami, K., Katagiri, K., Kubota, T., 2011. Effects of three natural organic matter types on cellulose acetate butyrate microfiltration membrane fouling. Journal of Membrane Science 379, 233– 238.

Hilal, N., Oluwaseun, O., Miles, N., Nigmatullin, R., 2005. Methods employed for control of fouling in MF and UF membranes: A Comprehensive Review. Separation Science and Technology, 40, 1957–2005.

Huang, H., Young, T., Jacangelo, J., 2008. Unified membrane fouling index for low pressure membrane filtration of natural waters: principles and methodology. Environmental Science Technology 42, 714–720.

Jamal, S., Chang, S., Zhou, H., 2014. Filtration behavior and mechanisms of polysaccharides. Membranes 4, 319-332.

Karnik, B., Davies, S., Chen, K.C., Jaglowski, D.R., Baumann, M.J., Masten, S.J., 2005. Effects of ozonation on the permeate flux of nano crystalline ceramic membranes. Water Research 39, 728–734.

Katsoufidou, K., Sioutopoulos, D., Yiantsios, S., Karabelas, A., 2010. UF membrane fouling by mixtures of humic acids and sodium alginate: Fouling mechanisms and reversibility. Desalination 264, 220-227.

Kim, J., Davies, S., Baumann, M., Tarabara, V., Masten, S., 2008. Effect of ozone dosage and hydrodynamic conditions on the permeate flux in a hybrid ozonation-ceramic ultrafiltration system treating natural waters. Journal of Membrane Science 311, 165- 172.

Kimura, K., Hane, Y., Watanabe, Y., Amy, G., Ohkuma, N., 2004. Irreversible membrane fouling during ultrafiltration of surface. Water Research 38, 3431–3441.

Lee, S., Dilaver, M., Park, P., Kim, J., 2013. Comparative analysis of fouling characteristics of ceramic and polymeric microfiltration membranes using filtration models. Journal of Membrane Science 432, 97-105.

Levitsky, I., Duek, A., Naim, R., Arkhangelsky, E., Gitis, V., 2012. Cleaning UF membranes with simple and formulated solutions. Chemical Engineering Science 69, 679–683.

Liang, H., Gong, W., Chen, J., Li, G., 2008. Cleaning of fouled ultrafiltration (UF) membrane by algae during reservoir water treatment. Desalination 220, 267–272.

Liu, C., Caothien, S., Hayes, J., Caothuy, T., Otoyo, T. and Ogawa, T., 2001. Membrane chemical cleaning: from art to science. Process membrane technology conference Port Washington, NY: 1-25.

Porcelli, N., Judd, S., 2011. Chemical cleaning of potable water membranes: A review. Separation and Purification Technology 71, 137-143.

Puspitasari, V., Granville, A., Le-Clech, P., Chena, V., 2010. Cleaning and ageing effect of sodium hypochlorite on polyvinylidene fluoride (PVDF) membrane. Separation and Purification Technology, 72, 301–308.

Regula, C., Carretier, E., Wyart, Y., Gesan-Guiziou, G., Vincent, A., Boudot, D., Moulin, P., 2014. Chemical cleaning/disinfection and ageing of organic UF membranes: A review. Water Research 56, 325-365.

Sartor, M., Gatjal, H., Mavrov, V., 2008. Demonstration of a new hybrid process for the decentralised drinking and service water production from surface water in Thailand. Desalination 222, 528–540.

Shi, X., Tal, G., Hankins, N.P., Gitis, V., 2014. Fouling and cleaning of ultrafiltration membranes: a review. Journal of Water Process Engineering 1, 121–138.

Song, Y., Dong, B., Gao, N., Xia, S., 2010. Huangpu River water treatment by microfiltration with ozone pretreatment. Desalination 250, 71-75.

Strugholtz, S., Sundaramoorthy, K., Panglisch, S., Lerch, A. BriJggef, A., Gimbe, R., 2005. Evaluation of the performance of different chemicals for cleaning capillary membranes. Desalination 179, 191-202.

Ujihara, R., Mino, Y., Takahashi, T., Shimizu, Y., Matasuyama, H., 2016. Effects of the ionic strength of sodium hypochlorite solution on membrane cleaning. Journal of Membrane Science 514, 566–573.

Van Geluwe, S., Braeken, L., Van der Bruggen, B., 2011. Ozone oxidation for the alleviation of membrane fouling by natural organic matter: A review. Water Research 45, 3551 -3570.

Wang, Q., Zeng H., Wua, Z., Cao, J., 2018. Impact of sodium hypochlorite cleaning on the surface properties and performance of PVDF membranes. Applied Surface Science 428, 289–295.

Wang, X., Ma, J., Wang, Z., Chen, H., Liu, M., Wu, Z., 2018. Re-investigation of membrane cleaning mechanisms using NaOCl: Role of reagent diffusion. Journal of Membrane Science 550, 278–285.

Wang, Z., Jinxing M., Chuyang, T., Katsuki, K., Wang, Q., Han., X., 2014. Membrane cleaning in membrane bioreactors: A review. Journal of Membrane Science 468, 276–307.

Xiao, K., Wang, X., Huang, X., Waite, T., Wen, X., 2009. Analysis of polysaccharide, protein and humic acid retention by microfiltration membranes using Thomas' dynamic adsorption model. Journal of Membrane Science 342, 22–34.

Zhang, X., Guo, J., Wang, L., Hu, J., Zhu, J., 2013. In situ ozonation to control ceramic membrane fouling in drinking water treatment. Desalination 328, 1-7.

Zhang, Y., Wang, J., Geo, F., Chen, Y., Zhang, H., 2017. A comparison study: The different impacts of sodium hypochlorite on PVDF and PSF ultrafiltration (UF) membranes. Water Research 109, 227-236.

Chapter 8

Summary, Conclusions and Recommendations

This chapter presents a summary of findings and conclusions from individual chapters followed by overall significant conclusions and contributions, and recommendations for future membrane work for drinking water treatment.

8.1 Summary of findings and conclusions

Stage 1: The applicability of the MFI-UF to predict fouling potential of different NOM fractions under changes in pressure and water temperature conditions was examined (Chapter 3). The following conclusions were made:

- The MFI-UF_{exp} method was sensitive to the type of NOM in feed water. A mixture of humic acid, BSA, and alginate resulted in the highest MFI-UF value compared to individual NOM solutions highlighting the need to identify specific NOM fractions in water to better understand potential fouling changes.
- All NOM types exhibited higher fouling propensity as water temperature decreased and pressure increased indicating the importance of assessing NOM fouling at expected conditions versus at standardized conditions alone. The developed MFI-UF normalization model (MFI-UF_{nor}) was useful in estimating the fouling potential away from standard testing conditions. Therefore, MFI-UF_{nor} model can be used to determine potential changes in NOM fouling behavior under changes in pressure and water temperature conditions.

Stage 2: Building upon stage 1, the impact of water temperature variation on irreversible NOM fouling of a submerged polymeric UF membrane was examined using the MFI-UF and UMFI fouling index methods (Chapter 4). The changes in backwash and cleaning effectiveness with temperature were investigated. The following conclusions were made:

- Water temperature demonstrated an impact on fouling and subsequent cleaning requirements for the submerged polymeric membrane. Irreversible fouling increased as temperature decreased from 35 to 5 ºC. As a results, backwash and chemical cleaning were less effective at lower temperature.
- Fouling and cleaning of the NOM mixture, BSA, and alginate solutions were sensitive to changes in water temperature whereas humic acid was least sensitive highlighting the need to identify specific NOM fractions in water to better understand potential changes in fouling and cleaning requirements.
- The MFI-UF fouling prediction demonstrated a useful fit with UMFI indices for establishing NOM irreversible fouling, highlighting an advantage of the MFI-UF as a robust fouling prediction index for low pressure polymeric membranes.

Stage 3: Building upon stages 1 and 2 of this research, the impact of water temperature variation on irreversible NOM fouling of a tubular ceramic UF membrane was examined using the MFI-UF and UMFI fouling index methods (Chapter 5). The changes in backwash and cleaning effectiveness with temperature were investigated. The following conclusions were made:

- The influence of feed water temperature on fouling of ceramic UF membranes is over and beyond simple water viscosity changes. The $UMFI_{nor}$ values (i.e. after correcting

for viscosity) showed that at 5 °C, only 43% of the increased in fouling was attributed to the high viscosity of water whereas 57% was due to fouling. Also, at 35 °C, 64% of the decreased in fouling was attributed to the low viscosity of water whereas 36% was due to fouling. Thus, fouling analysis performed at standard temperature (20 °C) will underestimate the impact of cold water condition on ceramic membranes performance.

- The irreversible fouling ratios increased at colder temperature (5 ºC), along with decreased in backwash and chemical cleaning effectiveness. Backwash and chemical cleaning were equally effective at 20 and 35 ºC compared to 5 ºC. Thus, modification of chemical cleaning procedure at cold water temperature condition is necessary to control irreversible fouling and recover membrane permeability.
- MFI-UF fouling indices and NOM retention were in agreement with the UMFI values and NOM retention data obtained in the ceramic UF system. Thus, the utilization of the MFI-UF is useful for assessing the potential changes in NOM fouling behavior with temperature for ceramic membrane systems. Moreover, the MFI-UF offers simple and short filtration test that can be used as a rapid assessment of NOM fouling compared to the UMFI testing which is normally performed on long-term filtration data.

Stage 4: Fouling and cleaning behaviors of different model NOM solutions were comparatively assessed for polymeric and ceramic UF membranes (Chapter 6). The following conclusions were made:

- The NOM fouling order was similar for both membranes which was greatest for the NOM mixture and BSA followed by alginate ($\pm Ca^{+2}$) and lastly humic acid, indicating that both membranes are most susceptible to fouling by proteins.

- Hydraulically irreversible fouling resistances of different NOM components were much higher for the polymeric UF compared to the ceramic UF highlighting an advantage of ceramic membranes with regards to physical cleaning compared to polymeric membranes.

- **Stage 5:** Builds on stage 4 to investigate the utilization of O_3 CIP with ceramic UF membranes for controlling irreversible fouling of hydrophilic and hydrophobic NOM compared to conventional cleaning chemicals (NaOCl and NaOH). The following conclusions were made:
- O_3 CIP at a ratio of 0.50 mgO_3 /mgC was effective in removing alginate ± Ca^{+2} and humic acids NOM foulants compared to single cleaning using NaOCl or NaOH CIP, highlighting an advantage of O_3 CIP with ceramic membranes for irreversible NOM fouling control.
- From the results achieved, a 1 hour of O_3 CIP at a ratio of 0.50 mgO_3/ mgC demonstrated an equivalent performance to 4 hours of cleaning using combined NaOCl and NaOH CIP.

8.2 Overall significant conclusions and contributions

Significant conclusions were made in the course of this research. The key contributions of this research are:

- Since it is essential to reduce membrane fouling by NOM, implementing the MFI-UF testing using a 13kDa hollow fiber polymeric membrane is useful for assessing the fouling potential of different NOM feed waters under changes in water temperature

conditions. A plant could perform the MFI-UF at standard temperature condition (i.e. 20 ºC) and then use the normalized model used in this research to adjust for water temperature changes to estimate the expected fouling in an operating polymeric and ceramic membrane systems.

- Changes in NOM fouling mechanisms for polymeric and ceramic membrane systems with temperature is over and beyond simple water viscosity changes. Irreversible NOM fouling is dominant at cold water condition, and therefore, utilizing the MFI-UF testing, implementing proper membrane pretreatment strategies and/or modifying cleaning procedures to reduce irreversible fouling of constituents having characteristics similar to that of humics, proteins, and polysaccharides are essential for long-term operational sustainability. Proteins particularly seem to be especially problematic for both polymeric and ceramic membranes.
- Although ceramic membranes are similar to their polymeric counterparts with regard to NOM fouling order, the robustness of ceramic membranes in terms of physical cleaning, highlight the ease of integration of ceramic membranes into drinking water applications.
- O_3 CIP proved effective for reducing humics and polysaccharides irreversible fouling compared to conventional cleaning chemicals. However, studies are required to determine the optimal ozonation conditions (time vs. O_3 concentration) for different types of water to maximize O_3 CIP performance while minimizing costs. Since the ceramic membrane is quite robust, it allows for some creativity regarding fouling mitigation techniques, particularly backwashes and chemical cleaning. Therefore, this opens the door to some more unique future investigations.

8.3 Recommendations for future work

Several results along the course of this research clearly indicate that further work on membrane fouling and cleaning is still needed. The MFI-UF method is useful to predict the fouling potential of various NOM feed waters under changing water temperature conditions with both polymeric and ceramic membrane systems. However, the MFI-UF, utilizing a hollow fiber membrane, is currently limited to academic lab based research and designing a commercial portable equipment of MFI-UF tester is important to facilitate the integration of the MFI-UF testing with polymeric and ceramic membrane systems.

Also, this research clearly demonstrated that membrane fouling can be underestimated at colder temperature. Northern areas, such as northern US and Canada, are the most sensitive to the effects of temperature change as water temperature can go below 5 °C in the winter and above 30 °C in the summer. Future studies should investigate the impacts of water temperature with actual source waters to better elucidate the complexities of real water systems and membrane fouling at low temperatures.

The ability of ceramic membranes to tolerate higher pressures and more challenging water qualities compared to polymeric membranes makes them ideal candidates for drinking water treatment. Ultimately, cost will always be a driving factor for membrane systems. Despite estimations that suggest that ceramic membranes are becoming cost competitive with polymeric membranes, the short-term, higher capital costs will often be an obstacle for ceramic membranes. However, with the higher costs of ceramic membranes does come higher quality and robustness. From the results achieved, under equivalent operational

conditions, ceramic membranes can be physically and chemically cleaned more easily compared to polymeric membranes. In addition, the robustness of ceramic membranes against rigorous chemical cleaning conditions (i.e. ozone) provides flexibility of the system. Future research should examine different cleaning techniques for irreversible fouling control with ceramic membranes. A creative investigation of different backwash and chemical cleaning procedures could be beneficial for sustainable membrane operation.

References

Alhadidi, A., Blankert, B., Kemperman, A.J.B., Schippers, J.C., Wessling, M., Van der Meer, W.G.J., 2011. Effect of testing conditions and filtration mechanisms on SDI, Journal of Membrane Science 381, 142–151.

Alhadidi, A., Kemperman, A.J.B., Schippers, J.C., Wessling, M., Van der Meer, W.G.J., 2011. The influence of membrane properties on the silt density index. Journal of Membrane Science 384, 205–218.

Ando, M., Ishihara, S., Iwahori H., Tada, N., 2003. Peculiar or unexpected behavior of silt density index of pretreated water for desalination.

Ang, W., Lee, S., Elimelech, M., 2006. Chemical and physical aspects of cleaning of organic-fouled reverse osmosis membranes. Journal of Membrane Science 272, 198–210.

Arkhangelsky, E., Kuzmenko, D., Gitis, V., 2007. Impact of chemical cleaning on properties and functioning of polyethersulfone membranes. Journal of Membrane Science 305, 176–184.

ASTM International, Designation: D8002 – 15 (Reapproved 2016). Standard test method for modified fouling index (MFI-0.45) of Water.

ASTM International, Designation: D4189 − 07 (Reapproved 2014). Standard test method for silt density index (SDI) of water.

Baghoth, S.A., Sharma, S.K., Amy, G.L., 2011. Tracking natural organic matter (NOM) in a drinking water treatment plant using fluorescence excitation-emission matrices and PARAFAC. Water Research 45, 797.

Betancourt, W., Rose, J., 2004. Drinking water treatment processes for removal of Cryptosporidium and Giardia. Veterinary Parasitology 126, 219–234.

Bieroza, M., Baker, A., Bridgeman, J., 2010. Fluorescence spectroscopy as a tool for determination of organic matter removal efficiency at water treatment works. Drinking Water Engineering Science 3, 63.

Bieroza, M., Baker, A., Bridgeman, J., 2011. Assessment of low pH coagulation performance using fluorescence spectroscopy. Journal of Environmental Engineering 137, 596.

Blankert, B., Betlem, B.H.L., and Roffel, B., 2006. Dynamic optimization of a dead-end filtration trajectory: Blocking filtration laws. Journal of Membrane Science 285, 90–95.

Boerlage, S., Kennedy, M., Aniye, M., Abogrean, E., Tarawneh, Z., Schippers, J., 2003. The MFI-UF as a water quality test and monitor. Journal of Membrane Science 211, 271–289.

Boerlage, S., Kennedy, M., Dickson, M., El-Hodali, D., Schippers, J., 2002. The modified fouling index using ultrafiltration membranes (MFI-UF): characterisation, filtration mechanisms and proposed reference membrane. Journal of Membrane Science 197, 1–21.

Boerlage, S., Kennedy, M., Tarawneh, Z., De Faber, R., Schippers, J., 2004. Development of the MFI-UF in constant flux filtration. Desalination 161,103-l 13.

Burashid, K. Hussain, A.R, 2004. Seawater RO plant operation and maintenance experience: Addur desalination plant operation assessment. Desalination 165, (1-3): p. 11-22.

Chang, E., Yang, S., Huang, C., Liang, C., Chiang, P., 2011. Assessing the fouling mechanisms of high-pressure nanofiltration membrane using the modified Hermia model and the resistance-in-series model. Separation and Purification Technology 79, 329– 336.

Crittenden, J., Trussell R., Hand D., Howe, K., Tchobanoglous, G., 2005. Water Treatment: Principles and Design, 2nd edition, Ed, Wiley, New Jersey, USA.

Cui, Z., Peng, W., Fan, Y., 2013. Ceramic membrane filtration as seawater RO pre-treatment: influencing factors on the ceramic membrane flux and quality. Desalination and Water Treatment 51, 2575–2583.

Dramas, L., Croue, J., 2013. Ceramic membrane as a pretreatment for reverse osmosis: interaction between marine organic matter and metal oxides. Desalination and Water Treatment 51, 1781–1789.

Fan, X., Tao, Y., Wang, L., Zhang, X., 2014. Performance of an integrated process combining ozonation with ceramic membrane ultra-filtration for advanced treatment of drinking water. Desalination 335, 47–54.

Farahbakhsh, K., Smith, D., 2006. Membrane filtration for cold regions – impact of cold water on membrane integrity testing. Journal of Environmental Engineering and Science 5, 69-75.

Fiksdal, L., Leiknes, T., 2006. The effect of coagulation with MF/UF membrane filtration for the removal of virus in drinking water. Journal of Membrane Science 279, 364–371.

Freeman, S., Shorney-Darby, H., 2011. What's the buzz about ceramic membranes? Journal of AWWA 103, 12-13.

Gone, D.L., Seidel, J.L., Batiot, C., Bamory, K., Ligban, R., Biemi, J., 2009. Using fluorescence spectroscopy EEM to evaluate the efficiency of organic matter removal during coagulation-flocculation of a tropical surface water (Agbo reservoir). Journals of Hazardous Materials 172, 693.

Guo, J., Wang, L., Zhu, J., 2013. Highly integrated hybrid process with ceramic ultrafiltration-membrane for advanced treatment of drinking water: A pilot study. Journal of Environmental Science and Health Part A 48, 1413–1419.

Guo, W., Ngo, H., Li, J., 2012. A mini-review on membrane fouling. Bioresource Technology 122, 27–34.

Habib, M., Unsia, H., Memon, A., Amin, U., Karim, Z., Khan A., Naveed, S., Ali, S, 2013. Predicting colloidal fouling of tap water by silt density index (SDI): Pore blocking in a membrane process. Journal of Environmental Chemical Engineering 1, 33–37.

Hamad, J., Ha, C., Kennedy, M., Amy, G., 2013. Application of ceramic membranes for seawater reverse osmosis (SWRO) pre-treatment. Desalination and Water Treatment 51, 4881-489.

Hao R., Ren H., Li, J., Ma, Z., Wan H., Zheng, X., Cheng, S., 2012. Use of three-dimensional excitation and emission matrix fluorescence spectroscopy for predicting

the disinfection by-product formation potential of reclaimed water. Water Research 46, 5765.

Harman, B.I., Koseoglu, H., Yigit, N.O., Sayilgan, E., Beyhan, M., Kitis, M., 2010. The removal of disinfection by-product precursors from water with ceramic membranes. Water Science and Technology 62 (3), 547-555.

Hashino, M., Hirami, K., Ishigami, T., 2011. Effect of kinds of membrane materials on membrane fouling with BSA. Journal of Membrane Science 384: 157– 165.

Hashino, M., Hirami, k., M., Katagiri, T., Kubota, N., 2011. Effects of three natural organic matter types on cellulose acetate butyrate microfiltration membrane fouling. Journal of Membrane Science 379, 233– 238.

Hashino, M., Katagiri, T., Kubota, N., 2011. Effect of membrane surface morphology on membrane fouling with sodium alginate. Journal of Membrane Science 366, 258–265.

Henderson, R., Baker, A., Parsons, S., Jefferson, B., 2008. Characterisation of algogenic organic matter extracted from cyanobacteria, green algae and diatoms. Water Research 42, 3435-3445.

Hermia J. 1982. Constant pressure blocking filtration laws application to power-law non-newtonian fluids. Transactions of the Institution of Chemical Engineers 60, 183-187.

Hilal, N., Oluwaseun, O., J. Miles, N., Nigmatullin, R., 2005. Methods employed for control of fouling in MF and UF membranes: A Comprehensive review. Separation Science and Technology 40 1957–2005.

Hofs, B., Ogier, J., Vries, D., 2011. Comparison of ceramic and polymeric membrane permeability and fouling using surface water. Separation and Purification Technology 79: 365– 374.

Huang, H., Lee, N., Young, T., Gary, A., Lozier, J.C., Jacangelo, J.G., 2007. Natural organic matter fouling of low-pressure, hollow-fibre membranes: effects of NOM source and hydrodynamic conditions. Water Research 41 (17) 3823–3832.

Huang, H., Young, T.A., Jacangelo, J.G., 2008 Unified membrane fouling index for low pressure membrane filtration of natural waters: Principles and methodology. Environmental Science Technology 42 714–720.

Jeong, S., Vigneswaran, S., 2015. Practical use of standard pore blocking index as an indicator of biofouling potential in seawater desalination. Desalination 365, 8–14.

Jin, X., Jawor, A., Kim, S., Hoek, E., 2009. Effects of feed water temperature on separation performance and organic fouling of brackish water RO membranes. Desalination 239, 346–359.

Ju, Y., Hong, I., Hong, S., 2015. Multiple MFI measurements for the evaluation of organic fouling in SWRO desalination. Desalination 365, 136–143.

Karnik, B., Davies, S., Chen, K.C., Jaglowski, D.R., Baumann, M.J., Masten, S.J., 2005. Effects of ozonation on the permeate flux of nano crystalline ceramic membranes. Water Research 39, 728–734.

Katsoufidou, K. S., Sioutopoulos, D. C., Yiantsios, S. G., Karabelas, A. J., 2010. UF membrane fouling by mixtures of humic acids and sodium alginate: Fouling mechanisms and reversibility. Desalination 264(3), 220-227.

Katsoufidou, K., Yiantsios, S. G., Karabelas, A. J., 2007. Experimental study of ultrafiltration membrane fouling by sodium alginate and flux recovery by backwashing. Journal of Membrane Science 300 (1–2), 137-146.

Kenari, S., Barbeau, B., 2016. Understanding ultrafiltration fouling of ceramic and polymeric membranes caused by oxidized iron and manganese in water treatment. Journal of Membrane Science 516, 1–12.

Kim, J., Davies, S., Baumann, M., Tarabara, V., 2008. Effect of ozone dosage and hydrodynamic conditions on the permeate flux in a hybrid ozonation–ceramic ultrafiltration system treating natural waters. Journal of Membrane Science 311, 165–172.

Kimura, K., Hane, Y., Watanabe, Y., Amy, G., Ohkuma, N., 2004. Irreversible membrane fouling during ultrafiltration of surface. Water Research 38, 3431–3441.

Konieczny, K., Bodzek, M., Rejca, M., 2006. A coagulation–MF system for water treatment using ceramic membranes. Desalination 198, 92–101.

Koo, C., Mohammad, A.W., Suja, F., Talib, M., 2012. Review of the effect of selected physicochemical factors on membrane fouling propensity based on fouling indices. Desalination 287, 167–177.

Koo, C., Mohammad, A.W., Suja, F., Talib, M., 2013. Use and development of fouling index in predicting membrane fouling. Separation and Purification Reviews, 42, 296–339.

Lee, S., Dilaver, M, Park, P., 2013. Comparative analysis of fouling characteristics of ceramic and polymeric microfiltration membranes using filtration models. Journal of Membrane Science 432, 97–105.

Lee, S., Kim, J., 2014. Differential natural organic matter fouling of ceramic versus polymeric ultrafiltration membranes. Water Research 48, 43-51.

Lehman, S., Adham, S., Liu, L., Fujuira, S., and Kanaya, S., 2007. Performance of new generation ceramic membranes using coagulation and ozonation pretreatment. American Water Works Association (AWWA) Membrane Technology Conference Tampa, Florida, USA.

Lehman, S.G., Liu, L., 2009 Application of ceramic membranes with preozonation for treatment of secondary wastewater effluent. Water Research 43, 2020-2028.

Li, W., Ling, G., Lei, F., Li, N., Peng, W., Li, K., Lu, H., Hang, F., Zhang, Y., 2018. Ceramic membrane fouling and cleaning during ultrafiltration of limed sugarcane juice. Separation and Purification Technology 190, 9–24.

Liang, H., Gong, W., Chen, J., Li, G., 2008. Cleaning of fouled ultrafiltration (UF) membrane by algae during reservoir water treatment. Desalination 220, 267–272.

Liu, L., Celik, E., Choi, H., 2011. Protein fouling behavior of carbon nanotube/polyethersulfone composite membranes during water filtration. Water Research 45, 5287-5294.

Loi-Brügger, A., Panglisch, S., Hattori, K., Yonekawa, H., Tomita, Y., and Gimbel, R., 2007. Open Up New Doors in Water Treatment with Ceramic Membranes. Membrane Technology Conference. American Water Works Association, Tampa, Florida, USA.

Lowe, J., Hossain, M., 2008. Application of ultrafiltration membranes for removal of humic acid from drinking water. Desalination 218 343–354.

Ma, Z., Wen, X., Zhao, F., Xia, Y., Huang, X., Wait, D., Guan, J., 2013. Effect of temperature variation on membrane fouling and microbial community structure in membrane bioreactor. Bioresource Technology 133, 462–468.

Markechova, D., Tomkova, M., Sadecka, J., 2013. Fluorecense excitation – emission matrix spectroscopy and parallel factor analysis in drinking water treatment: A review. Journal of Environmental Studies 22, 1289-1295.

Matilainen, A., Gjessing, E., Lathinen, T., Hed, L., Bhatnagar, A., Sillanpaa, M., 2011. An overview of the methods used in the characterisation of natural organic matter (NOM) in relation to drinking water treatment. Chemosphere 83, 1431–1442.

McAliley, I., D'Adamo, P., 2009. Advances in membrane treatment lead to more cost-effective options for drinking water providers. AWWA-WEA Annual Conference, Raleigh, NC.

Meyn, T., Altmann, J., Leiknes, T., 2012. In-line coagulation prior to ceramic microfi ltration for surface water treatment—minimisation of flocculation pre-treatment. Desalination and Water Treatment 42: 163–176.

Meyn, T., Bahn, A., Leiknes, T. O., 2008. Significance of flocculation for NOM removal by coagulation-ceramic membrane microfiltration. Water Science and Technology. Water Supply 8(6), 691–700.

Mo, H., Tay, K., Ng, H., 2008. Fouling of reverse osmosis membrane by protein (BSA): Effects of pH, calcium, magnesium, ionic strength and temperature. Journal of Membrane Science 315, 28–35.

Mosset, A., Bonnelye, V., Petry, M., and Sanz, M.A. 2008. The sensitivity of SDI analysis: from RO feed water to raw water. Desalination 222, 17–23.

Nguyen, A.H., Tobiason, J.E., Howe, K.J., 2011. Fouling indices for low pressure hollow fiber membrane performance assessment. Water Research 45, 2627-2637.

Nigam, M.O., Bansal, B., Chen, X.D., 2008. Fouling and cleaning of whey protein concentrate fouled ultrafiltration membranes. Desalination 218, 313–322.

Peldszus, S., Halle, C., Peiris, R., Hamouda, M., Jin, X., Legge, R, Budman, H., Moresoli, C, Huck, P., 2011. Reversible and irreversible low-pressure membrane

foulants in drinking water treatment: Identification by principal component analysis of fluorescence EEM and mitigation by biofiltration pretreatment. Water Research 45, 5161-5170.

Pendergast, M., Hoek, E., 2011. A review of water treatment membrane nanotechnologies. Energy Environmental Science 4, 1946-1971.

Pifer A.D., Fairey, J.L., 2012. Improving on SUVA254 using fluorescence-PARAFAC analysis and asymmetric flow field flow fractionation for assessing disinfection by product formation and control. Water Research 46, 2927.

Porcelli, N., Judd, S., 2010. Chemical cleaning of potable water membranes: the cost benefit of optimisation, Water Research 44, 1389–1398.

Puspitasari V., Granville A., Le-Clech P., Chena V., 2010. Cleaning and ageing effect of sodium hypochlorite on polyvinylidene fluoride (PVDF) membrane. Separation and Purification Technology 72, 301–308.

Rachman, R., 2011. Assessment of silt density index (SDI) as fouling propensity parameter in reverse osmosis desalination (MASc thesis). King Abdullah University of Science and Technology, Saudi Arabia.

Regula, C., Carretier, E., Wyart, Y., Gesan-Guiziou, G., Vincent, A., Boudot, D.,

Moulin, P., 2014. Chemical cleaning / disinfection and ageing of organic UF membranes: A review. Water Research 56, 325-365.

Rodriguez, S., Amy, G., Schippers, J.C., Kennedy, M., 2015. The Modified Fouling Index Ultrafiltration constant flux for assessing particulate/colloidal fouling of RO systems. Desalination 365, 79–91.

Rodriguez-Salinas, S., Al-Rabaani, B., Kennedy, M., Amy, G., Schippers, J., 2015. MFI–UF constant pressure at high ionic strength conditions. Desalination and Water Treatment 10, 64–72.

Rubia, A., Rodriguez, M., Prats, D., 2006. pH, Ionic strength and flow velocity effects on the NOM filtration with TiO2/ZrO2 membranes. Separation and Purification Technology 52, 325–331.

Sanchez-Polo, M., Rivera-Utrilla, J., von Gunten, U., 2006. Metal-doped carbon aerogels as catalysts during ozonation processes in aquatic solution. Water Research 40, 3375- 3384.

Sartor, M., Gatjal, H., Mavrov, V., 2008. Demonstration of a new hybrid process for the decentralised drinking and service water production from surface water in Thailand. Desalination 222, 528–540.

Schippers, J.C. and Verdouw, J. 1980. The modified fouling index, a method of determining the fouling characteristics of water. Desalination 32: 137–148.

Sentana, I., Puche, R., Sentana, E., Parts, D., 2011. Reduction of chlorination byproducts in surface water using ceramic nanofiltration membranes. Desalination 277 147–155.

Shao, J., Hou, J., Song, H., 2011. Comparison of humic acid rejection and flux decline during filtration with negatively charged and uncharged ultrafiltration membranes. Water Research 45, 473 -482.

Shi, X., Tal, G., Hankins, N., Gitis, V., 2014. Fouling and cleaning of ultrafiltration membranes: A review. Journal of Water Process Engineering 1, 121–138.

Sim, l., Ye, Y., Chen, V., Fane, A., 2010. Crossflow sampler modified fouling index ultrafiltration (CFS-MFI_{UF})—an alternative fouling index. Journal of Membrane Science 360, 174–184.

Sim, L.N., Ye, Y., Chen, V., and Fane, A.G., 2011 Comparison of MFI-UF constant pressure, MFI-UF constant flux and Crossflow Sampler-Modified Fouling. Water Research 45, 1639-1650.

Sioutopoulos, D., Karabelas, A., Yiantsios, S., 2010. Organic fouling of RO membranes: Investigating the correlation of RO and UF fouling resistances for predictive purposes. Desalination 261, 272–283.

Steinhauer, T., Hanely, S., Bogendorfer, K., Kulozik, U., 2015. Temperature dependent membrane fouling during filtration of whey and whey proteins. Journal of Membrane Science 492, 364–370.

Subhi, N., Leslie, G., Chen, V., Le-Clech, P., 2013. Organic fouling of ultrafiltration membrane: detailed characterization by liquid chromatography with organic carbon detection (LC-OCD). Separation Science and Technology 48, 199–207.

Taheri, A., Sim, L.N., Haur, C., Alkhondi, E., Fane, A., 2013. The fouling potential of colloidal silica and humic acid and their mixtures. Journal of Membrane Science 433, 112–120.

Tian, J., Ernst, M., Cui, F., & Jekel, M., 2013. Effect of different cations on UF membrane fouling by NOM fractions. Chemical Engineering Journal 223, 547-555.

Trang, V., Phuong, L., Dan, N., Thanh, B., Visvanathan, C., 2012. Assessment on the trihalomethanes formation potential of Tan Hiep Water Treatment Plant. Journal of Water Sustainability 2, 43-53.

Uyguner, C., Suphandag, S., Kerc, A., Bekbolet, M., 2007. Evaluation of adsorption and coagulation charachteristcs of humic acids proceded by alternative oxidation techniques. Desalination 210, 183-193.

Van de Ven, W, Sant K., Punt I., Zwijnenburg A., Kemperman A., Van der Meer, W., 2008. Hollow fiber dead-end ultrafiltration: Influence of ionic environment on filtration of alginates. Journal of Membrane Science 308, 218–229.

Van den Brink, P., Satpradit, O., Bentem, A., Zwijinenburg, A., Temmink, H., Loosdrecht, M., 2011. Effect of temperature shocks on membrane fouling in membrane bioreactors. Water Research 45, 4491-4500.

Van der Bruggen, B., Vandecasteele, C., Gestel, T., Doyen, W., Leysen, R., 2003. A Review of pressure-driven membrane processes in wastewater treatment and drinking water production. Environmental Progress (V01.22, No.1).

Van Geluwe, S., Braeken, L., Van der Bruggen, B., 2011. Ozone oxidation for the alleviation of membrane fouling by natural organic matter: A review. Water Research, 45, 3551 -3570.

Vasanth, D., Pugazhenthi, G., Uppaluri, R., 2013. Cross-flow microfiltration of oil-in-water emulsions using low cost ceramic membranes. Desalination 320, 86-95.

Villacorte, L., Ekowati, Y., Winters, H., Amy, G., Schippers, J., Kennedy, M., 2015. MF/UF rejection and fouling potential of algal organic matter from bloom-forming marine and freshwater algae. Desalination 367, 1–10.

Wang, Q., Zeng H., Wua, Z., Cao, J., 2018. Impact of sodium hypochlorite cleaning on the surface properties and performance of PVDF membranes. Applied Surface Science 428, 289–295.

Wang, X., Li, X., Huang, X., 2007. Membrane fouling in a submerged membrane bioreactor (SMBR): Characterisation of the sludge cake and its high filtration resistance. Separation and Purification Technology 52, 439–445.

Wang, X., Mab, J., Wang, Z., Chena, H., Liuc, M., Wu, Z., 2018. Re-investigation of membrane cleaning mechanisms using NaOCl: Role of reagent diffusion. Journal of Membrane Science 550, 278–285.

Wei, X., Wang, R., Li, Z., Fane, A.G., 2006. Development of a novel electrophoresis-UV grafting technique to modify PES UF membranes used for NOM removal. Journal of Membrane Science 273 (1-2), 47-57.

Xia, S., Zhou, Y., Ma, R., Xie, Y., 2013. Ultrafiltration of humic acid and surface water with tubular ceramic membrane. Desalination and Water Treatment 51, 5319–5326.

Xiao, K., Wang, X., Huang, X., Waite, T., Wen, X., 2009. Analysis of polysaccharide, protein and humic acid retention by microfiltration membranes using Thomas' dynamic adsorption model. Journal of Membrane Science 342, 22–34.

Xiao, P., Xiao, F., Wang, D., Qin, T., He, S., 2012. Investigation of organic foulants behavior on hollow-fiber UF membranes in a drinking water treatment plant. Separation and Purification Technology 95, 109–117.

Yiantsios, S.G., Sioutopoulos, D., and Karabelas, A.J. 2005. Colloidal fouling of RO membranes: an overview of key issues and efforts to develop improved prediction techniques. Desalination 183, 257–272.

Yin, N., Zhong, Z., Xing, W., 2013. Ceramic membrane fouling and cleaning in ultrafiltration of desulfurization wastewater. Desalination 319, 92–98.

Yuan, W., Zydney, A., 2000. Humic acid fouling during ultrafiltration. Environmental Science and Technology 34, 5043-5050.

Zepp, R., Sheldon, W., Moran, M., 2004. Dissolved organic fluorophores in southeastern US coastal waters: correction method for eliminating Rayleigh and Raman scattering peaks in excitation-emission matrices. Marine Chemistry 89, 15-36.

Zhang, T., Lu, J., Ma, J., Qiang, Z., 2008. Fluorescence spectroscopic characterization

of DOM fractions isolated from a filtered river water after ozonation and catalytic ozonation. Chemosphere 71, 911-921.

Zhang, X., Guo, J., Wang, L., Hu, J., Zhu, J., 2013. In situ ozonation to control ceramic membrane fouling in drinking water treatment. Desalination 328, 1-7.

Zhao, S., Zou, L., 2011. Effects of working temperature on separation performance, membrane scaling and cleaning in forward osmosis desalination. Desalination 278, 157–164.

Zhou, J., Chang, Q., Wang, Y., Wang, J., Meng, G., 2010. Separation of stable oil-water emulsion by the hydrophilic nano-sized ZrO_2 modified Al_2O_3 microfiltration membrane. Separation and Purification Technology 75 (3), 243-248.

Zularisam, A., Ahmad, A., Sakinah, M., Ismail, A. F., Matsuura, T., 2011. Role of natural organic matter (NOM), colloidal particles, and solution chemistry on ultrafiltration performance. Separation and Purification Technology 78(2), 189-20.

Zularisam, A., Ismail, A.F., Salim, R., 2006. Behaviours of natural organic matter in membrane filtration for surface water treatment — a review. Desalination 194-211–231.

Appendix (A)

Experimental Methods

A.1 Preparation of feed water solutions

Humic acids (2.5 mg C/L), a protein (bovine serum albumin, BSA, 2.5 mg C/L), a polysaccharide (sodium alginate, 2.5 mg C/L), and a mixture of the three NOM models (0.83 mg C/L/each NOM model, total of 2.5 mg C/L), were used as model NOM foulants. A moderate hardness and alkalinity of 75 mg/L calcium carbonate ($CaCO_3$) and a low level of turbidity (5 NTU) as kaolin clay particles were included in the synthetic water matric. All model substances were purchased from Sigma Aldrich. Feed solutions were prepared using DI water and were mixed using a magnetic stirrer one-day prior any experiment to ensure that materials were dissolved completely. During filtration experiments, feed water was continuously mixed using a VWR dual speed mixer to ensure homogeneous water conditions throughout the experiment. The pH of the feed was adjusted as needed to 7.5 with NaOH and monitored using the HACH (cat.no. 58258-00) HQd Field Case equipment.

A.2 Molecular weight fractionation and zeta potential (ζ) measurements

2 L of feed water solutions was prepared for the fractionation testing. The molecular weight distribution of different feed solutions was determined by ultrafiltration (UF) fractionation method using a 400 mL UF stirred cell (model 8400, Amicon Inc.) and five hydrophilic regenerated cellulose membranes (Millipore, Bradford MA) with different molecular weight cut offs (MWCOs) of 1,000, 5,000, 10,000, 30,000, and 100,000 Daltons (Figure A.1). The fractionation was performed sequentially by passing 400 mL of sample through the membrane with the highest MWCO to that with the lowest MWCO. Samples from

permeate and retentate of particular membrane were collected and total organic carbon (TOC) was analyzed using Tekmar Dohrmann, Phoenix 8000 TOC analyzer. Excess permeate produced by each fractionation step was used as the feed to the next membrane with a lesser MWCO. The TOC concentration of a particular molecular weight fraction was calculated by subtracting the TOC concentration of the filtrate from one membrane from the TOC concentration of the filtrate from the membrane of the next larger nominal MWCO. After fractionation experiments, membranes were rinsed with Milli-Q water for 60 minutes changing the water three times (i.e. every 20 minutes) and stored in 10% by volume ethanol/water solution and kept in refrigerator at 4 °C for later use. Prior to use, the membranes were rinsed several times after which Milli-Q water was allowed to filtered through them for three times.

Figure A.1- Molecular weight fractionation setup and UF membranes

A Malvern Zetasizer Nano was used to determine the zeta potential (ζ) of feed water solutions. In summary, an electric field is applied via electrodes immersed in a sample and this causes the charged particles to move towards the electrode of opposite polarity. Particle mobility is determined from the Smoluchowski model calculated by the Zetasizer equipment. Triplicate measurements were performed for each sample.

A.3 MFI-UF testing

The MFI-UF setup (Figure A.2) consisted of the following components: a digital gear pump (Cole Parmer: Drive No. 75211-30, Head No. 07003-04); a ball valve (Cole Parmer No. 01377-18); a pressure relief valve (Aquatrol No. 3ETU4), and a pressure regulator with gauge (Veolia No. LA512). PAN UF, hollow fiber, inside-out membrane module (Microza, Pall Corp.) with a MWCO of 13 kDa was used. High-capacity precision top loading balance (Adam Equipment NBL8201e) to measure the permeate volume. The MFI-UF testing was performed under constant pressure (variable temperature) or constant temperature (variable pressure). The pressure was regulated and monitored using the pressure regulator and the gauge while water temperature was controlled using either an immersion heater (Cole Parmer) or a compact chiller (LM series, Polyscience) as required. Feed water was filtered through the UF membrane under dead-end mode while monitoring flux decline during the test. Permeate was collected in a tank set on the electronic balance which has an RS 232 interface with a computer in order to acquire permeate volume (V) and filtration time (t) data from the balance. Data were recorded every 1 minute and imported into MS Excel spread sheet with data terminal software (TeraTerm). The MFI-UF was then calculated from the inverse of the flow rate (t/V) versus the permeate volume (V) recorded by the balance.

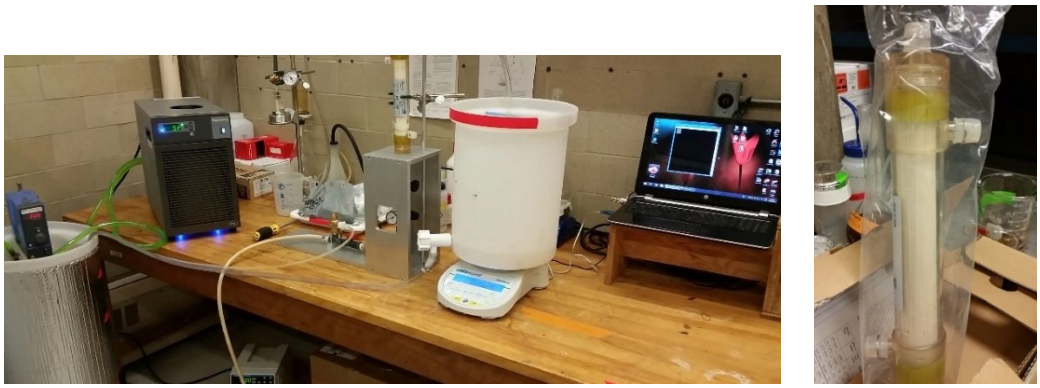

Figure A.2 - MFI-UF setup and 13 kDa UF membrane

A.4 Submerged Polymeric UF Membranes Testing

Two submerged membrane systems were used for the testing (Figure A.3). Zenon ZW-1 hollow fiber (UF) membranes made of polyvinylidene fluoride (PVDF), with a nominal pore size of 0.04 μm (surface area of 0.047 m^2) were used and operated under a vacuum pressure between 0 and -8.7 psi (0 and 0.6 bar). Filtration experiments were performed for 24 hrs under the following operational conditions presented: constant flux (38 LMH); backwash (38 LMH every 15 minutes for 20 seconds); air scour (5 L/minute). The flow rate and direction of permeate (i.e. forward and backward) were controlled using WinLN software. Pressure readings were recorded every 10 seconds using Operational Flux 2.0 program. A macro filter code (shown in Appendix C) was used to analyze filtration data (i.e. removing noisy data).

Membranes were cleaned in place (CIP) between each experiment following manufacturer specified recommendations. Cleaning of the membrane units was done in two steps: soaking in a 250 ppm of sodium hypochlorite (NaOCl) solution for 4 hours followed by soaking in 1% citric acid solution for another 4 hours. Chemical cleaning was conducted

at room temperature. DI water was filtered through the membrane after each cleaning until a permeate flux of 38 LMH was obtained; the permeate flux was determined manually by measuring the volume produced over 1 minute. Repeat cleanings were conducted until the flux 38±0.50 LMH was reached.

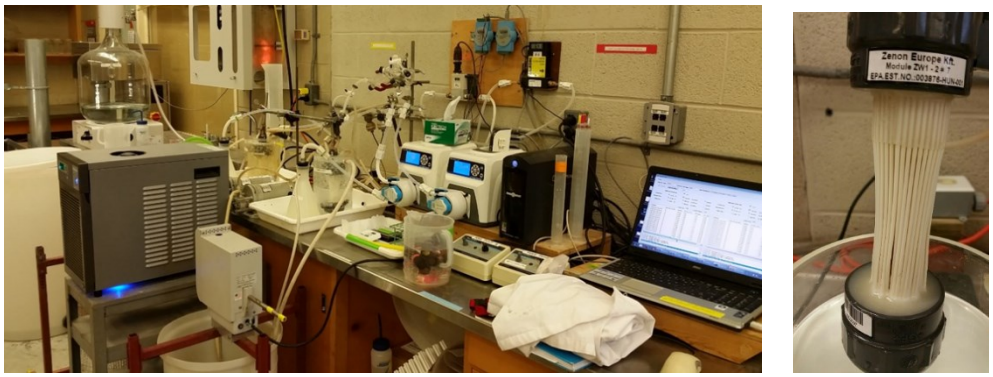

Figure A.3 - Automated submerged polymeric UF system and Zenon ZW-1 membrane

A.5 Ceramic and Polymeric UF Membranes Testing

Experiments were conducted on an automated filtration system (Figure A.4) consisting of a digital gear pump (Cole Parmer: Drive no. 75211-30, Head no. 07003-04), pressure transducer (Omega: model no. PX409-100G5V), flow meter (Cole Parmer: model no. 32703-52), solenoid valves (Macmaster: model no. 4711K731), and pressure vessel (Cole Parmer: model no. 29902-90) and nitrogen gas for backwash. Labview program code (National Instruments, NI, USA) was created to operate the system automatically such as controlling the feed pump to have a constant flux, and automatically switches from filtration cycles to backwash cycles while recording flux and pressure data. A ceramic UF (Ceramem^{TM}, Veolia) and polymeric UF (X-Flow^{TM}, Pentair) were used. Fouling experiments were performed for 24 hours under the following conditions: constant flux of

100 LMH; dead-end filtration mode; and backwash using pressurized water at 30 psi for 20s every 4 hrs. of filtration cycle (400 L/m^2). Clean water flux (CWF) was measured before and between experiments to determine the transmembrane pressure (TMP) versus flux relationship for a clean membrane and to estimate the intrinsic membrane resistance.

CIP cleaning was performed using two common organic fouling cleaners: an oxidant, NaOCl or caustic cleaning, NaOH. Each cleaning was performed for 4 hours at a cleaning temperature of 35°C and pH of 11.0 for both cleaning solutions. Chemicals were recirculated at crossflow velocity of 0.1 m/s for 1 hour followed by 3 hours of soaking. For the NaOCl chemical wash, the free chlorine concentration was 500 mg Cl_2/L which was measured before testing using the HACH method (8021) and a digital colorimeter™ II.

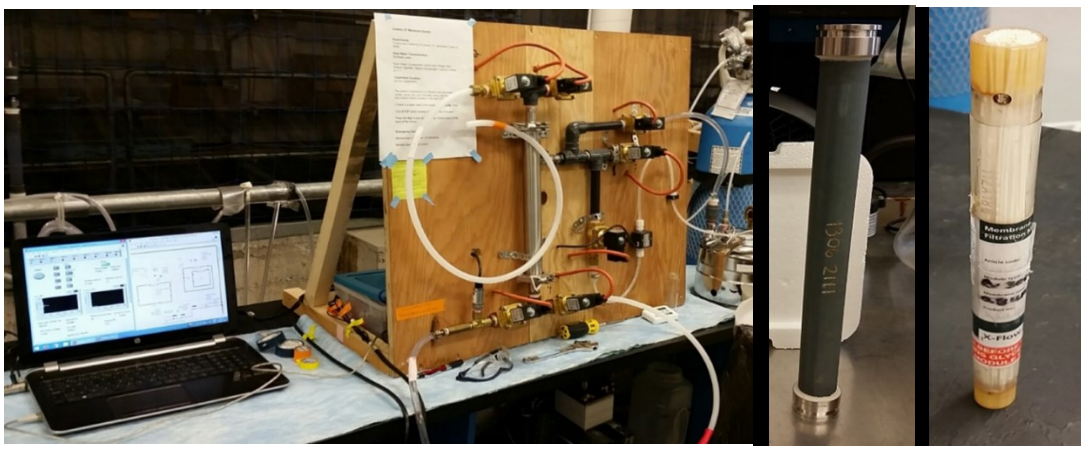

Figure A.4 - Automated ceramic UF system. Ceramem (Veolia) and X-Flow (Pentair) membranes.

A.6 Ceramic UF CIP Testing (NaOCl, NaOH, and O_3)

The cleaning efficiency of NaOCl and NaOH in a single, stepwise, and sequential cleaning was examined. NaOCl was purchased as a solution (6%). The concentration of free chlorine in the wash water (500 mg Cl_2/L, as free chlorine) was measured before testing using the HACH method (8021) and a digital colorimeter^{TM} II. Single cleaning using NaOCl or NaOH, (pH 11 or 12), was performed alternatively for 4 hours. NaOCl/NaOH sequential cleaning was performed with 500 mg Cl_2/L NaOCl (pH 12) for 2 hours followed by NaOH (pH 12) for 2 hours (total of 4 hours). NaOH/NaOCl sequential cleaning was performed with NaOH (pH 12) for 2 hours followed by 500 mg Cl_2/L NaOCl (pH 12) for 2 hours (total of 4 hours). For combined cleaning, (NaOCl+NaOH), NaOCl was simultaneously mixed with NaOH (pH 12), i.e. both chemicals were added concurrently at the same concentration as in their single solution, and the cleaning duration was maintained at a 4 hours duration to ensure the same chemical contact time for direct comparisons with individual cleaning solutions. Chemicals were prepared in 4 L of DI water and recirculated in a closed loop at a cross flow velocity of 0.1 m/s for 1 hour followed by 3 hours soak. Cleaning was performed at 35°C water temperature.

O_3 CIP cleaning efficiency was examined and compared to NaOCl and/or NaOH. For each O_3 cleaning experiment, 4 L of ozonated water was first prepared by bubbling at 4 ºC a 6% ozone/oxygen gas (Ozone Solutions, USA) in DI water to saturation (Figure A.5). Cleaning was performed by recirculating O_3 injected at either 0.25 mg O_3/mg C or 0.50 mg O_3/mg C, where mg C is the carbon mass accumulated on the membrane surface (i.e. O_3 concentration in the 4 L cleaning solution ranges from 15-30 mg O_3/L and 30-60 mg O_3/L

for the 0.25 and 0.50 mg O_3/mg C ratios respectively). Recirculation of O_3 was performed in a closed loop for 1 hour at a cleaning water temperature of 15 °C. O_3 residuals were measured using the standard indigo trisulfonate method (Bader and Hoigin, 1981). Total organic carbon (TOC) analyses were performed during O_3 cleaning by collecting a sample at different time intervals (i.e. 1, 5, 10 minutes, etc.) to determine the cumulative O_3 demand and irreversible carbon removal as a function of cleaning time.

Figure A.5 – Ozone and indigo solutions preparation

Appendix (B)

MFI-UF Statistical Analysis Summary

Table B1 – ANOVA and multiple Comparisons (Tukey HSD**)**
95% confidence interval)

Operating Pressure (Bar)	MFI-UF_{HA} p-value (0.002)*	MFI-UF_{BSA} p-value (0.001)*	MFI-UF_{SA} p-value (0.008)*	MFI-UF_{Mix} p-value (0.001)*
1 vs. 2	0.010	0.001	0.036	0.005
1 vs. 3	0.001	0.002	0.007	0.001
2 vs. 3	0.010	0.001	0.046	0.004

*p-value of all data set for each NOM model

Table B2 – ANOVA and multiple Comparisons (Tukey HSD)
(95% confidence interval)

Water Temperature (°C)	MFI-UF_{HA} p-value (0.001)*	MFI-UF_{BSA} p-value (0.002)*	MFI-UF_{SA} p-value (0.001)*	MFI-UF_{Mix} p-value (0.002)*
5 vs. 10	0.005	0.027	0.023	0.046
5 vs. 20	0.001	0.001	0.005	0.001
5 vs. 30	0.003	0.0003	0.001	0.002
5 vs. 35	0.002	0.002	0.001	0.001
10 vs. 20	0.042	0.012	0.031	0.009
10 vs. 30	0.007	0.003	0.004	0.002
10 vs. 35	0.006	0.001	0.004	0.001
20 vs. 30	0.030	0.036	0.041	0.037
20 vs. 35	0.044	0.041	0.035	0.040
30 vs. 35	0.042	0.038	0.050	0.045

*p-value of all data set for each NOM model

Table B3 – Regression coefficients for the predicted MFI-UF models

Model NOM	Regression Coefficients		
	Unstandardized β_0*	Unstandardized (Standardized) β_1*	Unstandardized (Standardized) β_2*
Humic Acid	1588.858	2058.965(0.652)	-121.343(-0.623)
Protein (BSA)	3351.687	3681.250(0.721)	-201.537(-0.691)
Sodium Alginate	1189.372	3139.250(0.755)	-140.453(-0.609)
Mixture	2598.917	3537.500(0.739)	-173.452(-0.653)

* β_0 : intercept; β_1: pressure effect; β_2 : temperature effect

MFI-UF GLM Models (SPSS Output)

ANOVA[a]

Model		Sum of Squares	df	Mean Square	F	Sig.
1	Regression	18049366.249	2	9024683.124	24.143	.003[b]
	Residual	1868968.591	5	373793.718		
	Total	19918334.839	7			

a. Dependent Variable: Humic acid MFIUF

b. Predictors: (Constant), Water Temperature (C), Operating Pressure (Bar)

Coefficients[a]

Model		Unstandardized Coefficients		Standardized Coefficients	Sig.	95.0% Confidence Interval for B	
		B	Std. Error	Beta		Lower Bound	Upper Bound
1	(Constant)	1588.858	1012.096		.177	-1012.818	4190.534
	Operating Pressure (Bar)	2058.965	432.316	.652	.005	947.662	3170.268
	Water Temperature (C)	-121.343	23.981	-.623	.004	-182.987	-59.699

a. Dependent Variable: Humic acid MFIUF

ANOVA[a]

Model		Sum of Squares	df	Mean Square	F	Sig.
1	Regression	53504398.972	2	26752199.486	77.078	.000[b]
	Residual	1735406.938	5	347081.388		
	Total	55239805.910	7			

a. Dependent Variable: Protein MFIUF

b. Predictors: (Constant), Water Temperature (C), Operating Pressure (Bar)

Coefficients[a]

Model		Unstandardized Coefficients		Standardized Coefficients	Sig.	95.0% Confidence Interval for B	
		B	Std. Error	Beta		Lower Bound	Upper Bound
1	(Constant)	3351.687	975.262		.019	844.695	5858.678
	Operating Pressure (Bar)	3681.250	416.582	.721	.000	2610.391	4752.109
	Water Temperature (C)	-201.537	23.108	-.691	.000	-260.938	-142.137

a. Dependent Variable: Protein MFIUF

ANOVA[a]

Model		Sum of Squares	df	Mean Square	F	Sig.
1	Regression	32532374.556	2	16266187.278	39.930	.001[b]
	Residual	2036821.058	5	407364.212		
	Total	34569195.614	7			

a. Dependent Variable: Sodium Alginate MFIUF

b. Predictors: (Constant), Water Temperature (C), Operating Pressure (Bar)

Coefficients[a]

Model		Unstandardized Coefficients		Standardized Coefficients		95.0% Confidence Interval for B	
		B	Std. Error	Beta	Sig.	Lower Bound	Upper Bound
1	(Constant)	1189.372	1056.567		.311	-1526.621	3905.364
	Operating Pressure (Bar)	3139.250	451.312	.755	.001	1979.117	4299.383
	Water Temperature (C)	-140.453	25.034	-.609	.002	-204.806	-76.100

a. Dependent Variable: Sodium Alginate MFIUF

ANOVA[a]

Model		Sum of Squares	df	Mean Square	F	Sig.
1	Regression	44583554.169	2	22291777.084	89.699	.000[b]
	Residual	1242585.249	5	248517.050		
	Total	45826139.418	7			

a. Dependent Variable: NOM Mixture MFIUF

b. Predictors: (Constant), Water Temperature (C), Operating Pressure (Bar)

Coefficients[a]

Model		Unstandardized Coefficients		Standardized Coefficients		95.0% Confidence Interval for B	
		B	Std. Error	Beta	Sig.	Lower Bound	Upper Bound
1	(Constant)	2598.917	825.247		.025	477.552	4720.281
	Operating Pressure (Bar)	3537.500	352.503	.739	.000	2631.362	4443.638
	Water Temperature (C)	-173.452	19.553	-.653	.000	-223.716	-123.189

a. Dependent Variable: NOM Mixture MFIUF

Appendix (C)

Macro Filter Code used in Fouling Data Analysis

(Created by Kelly Alder and Nigel De Souza**)**

```
Sub BWRfilt()

'
' BWRfilt Macro
' Authors: Kelly Alder and Nigel De Souza
' Keyboard Shortcut: Ctrl+n
'
    ' Create a variable to hold the column id
    Dim sColumn As String
    Dim sColumnHeader As String

    ' Create a new variable to hold the cell value
    Dim nValue As Double

   ' Create a new variable to hold percent difference
    Dim nPercentDiff As Double

    ' Create a new variable to hold previos value
    Dim nPrevValue As Double

    ' Create a string representation for the Column Id
    sColumn = Chr(ActiveCell.Column + 64) + "1"

    ' Go to the top of the selected column
    Range(sColumn).Select

    ' Get the text of the column header
    sColumnHeader = ActiveCell.Text

    ' Trim all leading and trailing whitespaces
    sColumnHeader = Trim(sColumnHeader)

    ' Make the Column HeEader uppercase
    ' for case-insensitive comparison
    sColumnHeader = UCase(sColumnHeader)

    ' Make sure we're looking at a Pressure Reasing Column
    If sColumnHeader = "PRESSURE_READING" Then

        ' Move the selected cell one row down
        ActiveCell.Offset(2, 0).Select

        ' Check that we haven't reached the end by checking that it's not blank
```

```
    While (ActiveCell.Text <> "")

      ' Get the cell value and previous cell value
      nValue = ActiveCell.Value

      ' Check to see if a row is positive
      If nValue > 0 Then

        ' Delete the positive row
        Rows(ActiveCell.Row).EntireRow.Delete

      Else

        ' Get the value of the previous cell
        nPrevValue = ActiveCell.Offset(-1, 0).Value

        ' Check to see if the cell value is greater than
        ' the previous value
        If nValue > nPrevValue Then

          'Calculate percent difference
          nPercentDiff = (nPrevValue - nValue) / nPrevValue * 100

          ' Check to see if percent difference is larger that our tolerance
          If nPercentDiff > 5 Then

            ' Delete this row, we dont want it
            Rows(ActiveCell.Row).EntireRow.Delete
          Else

            ' Move the selected cell one row down
            ActiveCell.Offset(1, 0).Select
          End If
        Else

          ' Move the selected cell one row down
          ActiveCell.Offset(1, 0).Select
        End If
      End If
    Wend
  Else

    ' Display Warning
    MsgBox ("Macro Must Be Run On a PRESSURE_READING Column!")
  End If
End Sub
```

Appendix (D)

Randomized Block Design (RBD) (SPSS Output)

Between-Subjects Factors

		Value Label	N
Treatment Membrane Type	10.00	Ceramic	5
	20.00	Polymeric	5
NOM Type	1.00	Humic	2
	2.00	BSA	2
	3.00	Alginate+Ca	2
	4.00	Alginate-Ca	2
	5.00	Mixture	2

Tests of Between-Subjects Effects

Dependent Variable: %Removal

Source	Type III Sum of Squares	df	Mean Square	F	Sig.
Corrected Model	495.500[a]	5	99.100	25.740	.004
Intercept	50268.100	1	50268.100	13056.649	.000
Block NOM Type	399.400	4	99.850	25.935	.004
Treatment Membrane Type	96.100	1	96.100	24.961	.008
Error	15.400	4	3.850		
Total	50779.000	10			
Corrected Total	510.900	9			

a. R Squared = .970 (Adjusted R Squared = .932)

Multiple Comparisons

Dependent Variable: %Removal

Tukey HSD

(I) NOM Type	(J) NOM Type	Mean Difference (I-J)	Std. Error	Sig.	95% Confidence Interval	
					Lower Bound	Upper Bound
Humic	BSA	-16.0000*	1.96214	.006	-24.7229	-7.2771
	Alginate+Ca	-11.5000*	1.96214	.019	-20.2229	-2.7771
	Alginate-Ca	-.5000	1.96214	.039	-9.2229	8.2229
	Mixture	-4.0000	1.96214	.046	-12.7229	4.7229
BSA	Humic	16.0000*	1.96214	.006	7.2771	24.7229
	Alginate+Ca	4.5000	1.96214	.047	-4.2229	13.2229
	Alginate-Ca	15.5000*	1.96214	.007	6.7771	24.2229
	Mixture	12.0000*	1.96214	.017	3.2771	20.7229
Alginate+Ca	Humic	11.5000*	1.96214	.019	2.7771	20.2229
	BSA	-4.5000	1.96214	.047	-13.2229	4.2229
	Alginate-Ca	11.0000*	1.96214	.023	2.2771	19.7229
	Mixture	7.5000	1.96214	.031	-1.2229	16.2229
Alginate-Ca	Humic	.5000	1.96214	.039	-8.2229	9.2229
	BSA	-15.5000*	1.96214	.007	-24.2229	-6.7771
	Alginate+Ca	-11.0000*	1.96214	.023	-19.7229	-2.2771
	Mixture	-3.5000	1.96214	.048	-12.2229	5.2229
Mixture	Humic	4.0000	1.96214	.046	-4.7229	12.7229
	BSA	-12.0000*	1.96214	.017	-20.7229	-3.2771
	Alginate+Ca	-7.5000	1.96214	.031	-16.2229	1.2229
	Alginate-Ca	3.5000	1.96214	.048	-5.2229	12.2229

*. The mean difference is significant at the .05 level.